

**Report No. K-TRAN: KU-97-1**  
**Final Report**

# **SEQUENCE STRATIGRAPHY OF THE LANE-ISLAND CREEK SHALES AND THE FARLEY LIMESTONE IN NORTHEASTERN KANSAS AND GEOLOGIC FACTORS AFFECTING THE QUALITY OF LIMESTONE AGGREGATES**

**J. McKirahan  
R. H. Goldstein  
E. K. Franseen  
University of Kansas  
Lawrence, Kansas**



**May 2000**

**K-TRAN**

**A COOPERATIVE TRANSPORTATION RESEARCH PROGRAM BETWEEN:  
KANSAS DEPARTMENT OF TRANSPORTATION  
THE KANSAS STATE UNIVERSITY  
THE UNIVERSITY OF KANSAS**

1. Report No. K-TRAN: KU-97-1		2. Government Accession No.		3. Recipient Catalog No.	
4. Title and Subtitle SEQUENCE STRATIGRAPHY OF THE LANE-ISLAND CREEK SHALES AND THE FARLEY LIMESTONE IN NORTHEASTERN KANSAS AND GEOLOGIC FACTORS AFFECTING THE QUALITY OF LIMESTONE AGGREGATES				5. Report Date May 2000	
				6. Performing Organization Code	
7. Author(s) J. McKirahan, R. H. Goldstein, and E. K. Franseen				8. Performing Organization Report No.	
9. Performing Organization Name and Address University of Kansas Department of Geology Lawrence, Kansas 66045				10. Work Unit No. (TRAIS)	
				11. Contract or Grant No. C-968	
12. Sponsoring Agency Name and Address Kansas Department of Transportation Docking State Office Bldg. Topeka, Kansas 66612				13. Type of Report and Period Covered Final Report December 1996 to May 2000	
				14. Sponsoring Agency Code 106-RE-0107-01	
15. Supplementary Notes					
16. Abstract Procedures should be implemented for rapidly evaluating durability of limestone aggregate to prevent use of substandard material in highway construction and to assure availability of highly durable aggregate. The objective of this study is to evaluate lithologic (rock type) variables that control durability of limestone aggregate. The Farley Limestone (Pennsylvanian, Missourian) is one of many limestone units quarried in Kansas for production of highly durable, Class 1 aggregate. By understanding the lithologic factors that control durability of aggregate from the Farley, an analog for other limestone units can be developed. The Farley Limestone was described from 17 localities to define associations of rock types (lithofacies) and to establish correlations to aggregate durability. Data on lithofacies characteristics, spar (coarse calcite or dolomite) percentage, spar size, and insoluble residue percentage exhibit no correlations to durability factor or expansion percentage. Data on total percentage of clay-rich rock, clay distribution, and mineralogy of insoluble residues are correlated to durability and expansion percentage. Limestones containing low percentages of diffuse or disseminated clay are more likely to produce aggregates of high durability. Aggregates containing multiple clay minerals exhibit reduced durability. Smectite, even in small quantities, negatively impacts durability, whereas illite apparently has little impact on durability. If changes in clay content deleterious to aggregate quality can be identified during lateral production of a ledge, then quarrying can be halted or can proceed in another direction while physical tests are run. Such a procedure could prevent use of substandard concrete in highway construction projects. Aggregate-producing phylloid-algal limestones of the lower Farley Limestone thicken into the local depositional lows. However, fine quartz-, feldspar-, and clay-rich sediments (siliciclastics) also seem to be deposited preferentially in paleotopographic lows. Thus, local paleotopographic low areas most distal from sources of siliciclastics can be predicted as the prime areas for location of durable aggregate.					
17. Key Words Aggregates, Limestone, Lithologic variables			18. Distribution Statement No restrictions. This document is available to the public through the National Technical Information Service, Springfield, Virginia 22161		
19. Security Classification (of this report) Unclassified		20. Security Classification (of this page) Unclassified		21. No. of pages 254	22. Price

**Sequence Stratigraphy of the Lane-Island Creek Shales  
and the Farley Limestone in Northeastern Kansas  
and  
Geologic Factors Affecting the Quality of  
Limestone Aggregates**

**By**

**J. McKirahan<sup>1</sup>, R.H. Goldstein<sup>1</sup> & E.K. Franseen<sup>2</sup>**

<sup>1</sup>University of Kansas, Department of Geology, Lawrence, KS 66045

<sup>2</sup>University of Kansas, Kansas Geological Survey, Lawrence, KS 66047

## **PREFACE**

**This research project was funded by the Kansas Department of Transportation K-TRAN research program. The Kansas Transportation Research and New-Developments (K-TRAN) Research Program is an ongoing, cooperative and comprehensive research program addressing transportation needs of the State of Kansas utilizing academic and research resources from the Kansas Department of Transportation, Kansas State University and the University of Kansas. The projects included in the research program are jointly developed by transportation professionals in KDOT and the universities.**

## **NOTICE**

**The authors and the State of Kansas do not endorse products or manufacturers. Trade and manufacturers names appear herein solely because they are considered essential to the object of this report.**

**This information is available in alternative accessible formats. To obtain an alternative format, contact the Kansas Department of Transportation, Office of Public Information, 7th Floor, Docking State Office Building, Topeka, Kansas, 66612-1568 or phone (785)296-3585 (Voice) (TDD). To obtain the pictures contained in this report in color, please contact Barbara Smith, Kansas Department of Transportation, Bureau of Material and Research, 2300 SW Van Buren, Topeka, Kansas, 66611-11195 or phone (785)291-3848.**

## **DISCLAIMER**

**The contents of this report reflect the views of the authors who are responsible for the facts and accuracy of the data presented herein. The contents do not necessarily reflect the views or the policies of the State of Kansas. This report does not constitute a standard, specification or regulation.**

## TABLE OF CONTENTS

<b>LIST OF FIGURES</b> .....	iv
<b>LIST OF TABLES</b> .....	viii
<b>Chapter 1: Introduction</b> .....	<b>1</b>
Purpose .....	2
Organization.....	4
<b>Chapter 2: Sequence Stratigraphy of the Lane-Island Creek Shales and the Farley Limestone .</b>	
Introduction.....	6
Area of Study .....	7
Stratigraphy.....	7
Argentine Limestone Member .....	11
Lane-Island Creek Shales.....	11
Farley Limestone Member .....	13
Bonner Springs Shale.....	13
Lithofacies & Depositional Environments of the Farley Limestone.....	14
Phylloid Algal Facies .....	14
Environmental Interpretation .....	18
Skeletal Wackestone-Packstone .....	22
Environmental Interpretation .....	24
Peloidal, Skeletal Packstone Facies.....	25
Environmental Interpretation .....	25
Sandy, Sketetal Grainstone-Packstone Facies.....	27
Environmental Interpretation .....	30
Oolite Facies.....	30
Environmental Interpretation .....	35
Osagia-Brachiopod Packstone Facies .....	35
Environmental Interpretation .....	36
Fossiliferous Siltstone .....	38
Environmental Interpretation .....	39
Lenticular Bedded-Laminated Siltstone and Fine Sandstone.....	39
Environmental Interpretation .....	41
Organic-rich Mudstone and Coal .....	43
Environmental Interpretation .....	43
Blocky Mudstone .....	44
Environmental Interpretation .....	45
Stratigraphic Correlations and Sequence-Stratigraphic Interpretations .....	48
Stratigraphic Datum .....	48
Argentine Limestone (Stratigraphic Surface A).....	54
Lane-Island Creek Interval.....	55
Upper Island Creek-Lower Farley Interval.....	57
Top of Lower Farley-Middle Farley Interval.....	62
Top of the Middle Farley-Upper Farley Interval .....	66
Conclusions.....	70
<b>Chapter 3: Geologic Factors Affecting the Quality of Limestone Construction Aggregate.....</b>	<b>75</b>

Introduction.....	76
Methodology.....	78
KDOT Physical Tests.....	79
Absorption.....	80
Modified Freeze-Thaw Test (Soundness) .....	80
L.A. Wear Test.....	81
Expansion.....	81
Durability Factor .....	81
Lithologic Parameters .....	82
Lithology.....	82
Spar Content.....	82
Bulk Spar Percentage .....	83
Average Spar Crystal Size and Crystal Form .....	83
Spar Percentage of Crushed Aggregates (Aggregate Spar).....	83
Clay Percentage and Type.....	85
Total Percentage of Clay-Rich Strata .....	85
Clay Distribution .....	86
Insoluble Residues .....	90
Percent Insoluble Residue .....	90
Insoluble Residue Grain Sizes & Aggregate Clay Percentage .....	90
Insoluble Residue Composition.....	91
Results.....	91
Lithology.....	93
Bulk Spar Percentage .....	96
Average Crystal Size.....	96
Aggregate Spar Percentage .....	98
Total Percentage of Clay-Rich Strata and Distribution of Clay .....	98
Percent Insoluble Residue.....	99
Insoluble Residue Composition & Aggregate Clay Percentage.....	103
Absorption.....	105
Discussion .....	105
Conclusions.....	109
<b>Chapter 4: Conclusions &amp; Implementation.....</b>	<b>111</b>
Sedimentology & Sequence Stratigraphy .....	112
Geologic Properties Affecting Quality of Limestone Aggregates .....	114
Predicting the Distribution of Class 1 Aggregate .....	115
Implementation .....	123
<b>References.....</b>	<b>126</b>
<b>Appendix 1: Measured Stratigraphic Sections.....</b>	<b>134</b>
Lithologic Symbols.....	136
Locality C1 .....	137
Locality C2 .....	142
Locality C3 .....	146
Locality C4 .....	149
Locality C5 .....	152
Locality C6 .....	155
Locality FRQ .....	159
Locality HM.....	163

Locality LQ.....	170
Locality MCI.....	174
Locality OAQ.....	178
Locality RQ.....	184
Locality SRBS.....	190
Locality SRO.....	197
Locality SRS.....	203
Locality WR.....	211
Locality 127.....	213

<b>Appendix 2: KDOT Physical Tests &amp; Other Laboratory Procedures .....</b>	<b>217</b>
KDOT Physical Test Procedures and Calculations.....	218
KDOT Modified Soundness Test for Aggregates.....	218
Description.....	218
Sample Preparation.....	218
Procedure.....	219
Calculation.....	219
KDOT Determination of Specific Gravity and Absorption.....	219
Description.....	219
Sample Preparation.....	220
Procedure.....	220
Calculation.....	221
ASTM C666: Standard Test Method for Resistance of Concrete to Rapid Freezing and Thawing: Procedure B.....	221
Scope.....	221
Significance and Use.....	221
Apparatus.....	222
Freezing-and-Thawing Cycle.....	223
Procedure.....	224
Calculation.....	225
ASTM C131: Standard Test Method for Resistance to Degradation of Small-Size Coarse Aggregate by Abrasion and Impact in the Los Angeles Machine.....	226
Scope.....	226
Summary of Test Method.....	226
Significance and Use.....	226
Procedure.....	227
Calculation.....	227
Determination of Percent Insoluble Residue.....	228
Sample Preparation of Insoluble Residues for X-Ray Diffraction Study.....	228
Preparation of Aggregate Thin Sections for Petrographic Examination.....	229
Insoluble Residue Grain Size Separations.....	230

## LIST OF FIGURES

<b>Figure 1.1.</b> Illustration of four common internal geometries and an example of lateral lithology change in cross-section.....	5
<b>Figure 2.1.</b> Index map of field area with locations of quarries, roadcuts and drill cores given.....	8
<b>Figure 2.2.</b> Stratigraphic sections showing traditional stratigraphic organization and also the revised stratigraphic organization used in this paper.....	10
<b>Figure 2.3.</b> Isopach map for the Argentine Limestone.....	12
<b>Figure 2.4.</b> Isopach map for the Lane-Island Creek shales.....	12
<b>Figure 2.5.</b> Photographs and photomicrographs illustrating the nature of the phylloid algal facies.....	15
<b>Figure 2.6.</b> Photomicrograph of <i>Archeolithophyllum</i> with well-preserved internal cellular structure.....	17
<b>Figure 2.7.</b> Photomicrographs of various micrite fabrics found in the phylloid algal facies.....	19
<b>Figure 2.8.</b> Photomicrograph of gastropod lined with early, fibrous cement.....	20
<b>Figure 2.9.</b> Hand samples of skeletal wackestone-packstone facies.....	23
<b>Figure 2.10.</b> Photomicrographs of skeletal wackestone-packstone fabrics.....	23
<b>Figure 2.11.</b> Photographs of hand samples of peloidal, skeletal packstone facies.....	26
<b>Figure 2.12.</b> Photomicrograph of peloidal, skeletal packstone facies.....	26
<b>Figure 2.13.</b> Photographs of hand samples of sandy, skeletal grainstone-packstone facies.....	28
<b>Figure 2.14.</b> Outcrop photos of sandy, skeletal grainstone-packstone facies.....	29
<b>Figure 2.15.</b> Photomicrograph of sandy, skeletal grainstone-packstone with abundant quartz grains.....	29
<b>Figure 2.16.</b> Photograph of oolite facies hand sample.....	32
<b>Figure 2.17.</b> Outcrop photograph of cross-bedded oolite grainstone from the lower Farley Limestone (locality MCI).....	32
<b>Figure 2.18.</b> (A) Rose diagram illustrating cross-bed paleocurrent directions from oolite at locality MCI. (B) Outcrop photograph of lower Farley oolite showing two distinct cross-bed directions.....	33
<b>Figure 2.19.</b> Photomicrograph of peloidal, oolite packstone with various cement fabrics.....	34



<b>Figure 2.20.</b> Photograph of hand sample illustrating fabric of <i>Osagia</i> , brachiopod packstone facies. ....	<b>37</b>
<b>Figure 2.21.</b> Photomicrograph of <i>Osagia</i> , brachiopod packstone facies. ....	<b>37</b>
<b>Figure 2.22.</b> Field photograph of burrow molds from the fossiliferous siltstone facies. ....	<b>40</b>
<b>Figure 2.23.</b> Field photograph of fossil fragments in fossiliferous siltstone facies. ....	<b>40</b>
<b>Figure 2.24.</b> Photograph of core section of fossiliferous siltstone facies. ....	<b>40</b>
<b>Figure 2.25.</b> Photographs of core sections showing nature of lenticular, laminated siltstone facies. ....	<b>42</b>
<b>Figure 2.26.</b> Outcrop photograph of lenticular, laminated siltstone facies. ....	<b>42</b>
<b>Figure 2.27.</b> Outcrop photograph of blocky mudstone facies. ....	<b>46</b>
<b>Figure 2.28.</b> Photograph of slickensided ped surface from blocky mudstone facies. ....	<b>47</b>
<b>Figure 2.29.</b> Cross-section of drill core showing abundance of plant fragments and root molds in blocky mudstone facies. ....	<b>47</b>
<b>Figure 2.30</b> Stratigraphic reconstruction along line A-AA (OAQ-MCI). ....	<b>49</b>
<b>Figure 2.31.</b> Stratigraphic reconstruction along line B-BB (LQ-C3). ....	<b>50</b>
<b>Figure 2.32.</b> Stratigraphic reconstruction along line C-CC (RQ-MCI). ....	<b>51</b>
<b>Figure 2.33.</b> Stratigraphic reconstruction along line D-DD (HM-MCI). ....	<b>52</b>
<b>Figure 2.34.</b> Fence diagram of stratigraphic reconstructions. ....	<b>53</b>
<b>Figure 2.35.</b> Isopach map of the lower Farley Limestone. ....	<b>63</b>
<b>Figure 2.36.</b> Isopach map of the middle Farley equivalent units showing the distribution of carbonates and siliciclastics within the interval. ....	<b>65</b>
<b>Figure 2.37.</b> Isopach map of the upper Farley interval. ....	<b>69</b>
<b>Figure 3.1.</b> Hand samples showing different types of spar accumulations. ....	<b>84</b>
<b>Figure 3.2.</b> Idealized drawing of clay distributions. ....	<b>87</b>
<b>Figure 3.3.</b> Photographs of shale beds and concentrated stylocumulates. ....	<b>88</b>
<b>Figure 3.4.</b> Photographs of diffuse stylocumulates. ....	<b>89</b>

<b>Figure 3.5.</b> Photograph of limestone bed with disseminated argillaceous material indicated by the bluish color of the rock.....	<b>89</b>
<b>Figure 3.6.</b> XY plot illustrating the relationship between durability factor and expansion percentage (n = 25).....	<b>92</b>
<b>Figure 3.7.</b> XY plot showing the relationship between durability factor and modified freeze-thaw (soundness) value (n = 30).....	<b>92</b>
<b>Figure 3.8.</b> Histogram showing the number of samples of phylloid-algal limestone within durability-factor categories.....	<b>95</b>
<b>Figure 3.9.</b> XY Plot showing relationship of durability factor to bulk spar percentage (n = 25). The weak relationship suggested is that as bulk spar percentage increases, durability increases.....	<b>95</b>
<b>Figure 3.10.</b> XY plot showing the relationship between average crystal size (in micrometers) and durability factor. Red data points represent spar-poor samples (n = 12) and black are spar-rich samples (n = 12). .....	<b>97</b>
<b>Figure 3.11.</b> XY Plot comparing the total aggregate spar percentage to durability factor (n = 9). The regression line suggests a weak relationship; the higher the aggregate spar percentage the higher the durability.....	<b>97</b>
<b>Figure 3.12.</b> XY plot comparing durability factor to total outcrop clay percentage (n = 25). This percentage includes concentrated stylocumulates, diffuse stylolites, and disseminated argillaceous material. ....	<b>100</b>
<b>Figure 3.13.</b> XY plot comparing expansion percentage to total outcrop clay percentage (n = 26). This percentage includes all three forms of clay. ....	<b>100</b>
<b>Figure 3.14.</b> XY plot comparing durability factor to the percentage of rock that contains only diffuse stylolites and disseminated argillaceous material (n = 25). ....	<b>101</b>
<b>Figure 3.15.</b> XY plot comparing expansion percentage to the percentage of rock that contains only diffuse stylolites or disseminated argillaceous material (n = 26).....	<b>101</b>
<b>Figure 3.16.</b> XY plot showing the relationship between durability factor and percent insoluble residue (n = 25).....	<b>102</b>
<b>Figure 3.17.</b> XY plot showing the relationship between expansion percentage and percent insoluble residue (n = 26).....	<b>102</b>
<b>Figure 3.18.</b> XY plot showing the relationship between durability factor and absorption percentage (n = 25). ....	<b>106</b>
<b>Figure 3.19.</b> XY plot showing the relationship between expansion percentage and absorption percentage (n = 26).....	<b>106</b>
<b>Figure 4.1.</b> Fence diagram showing known and predicted aggregate quality distribution.....	<b>116</b>

**Figure 4.2.** Cross-section along line A-AA (OAQ-MCI) showing known and predicted aggregate quality distribution.....117

**Figure 4.3.** Cross-section along line B-BB (LQ-C3) showing known and predicted aggregate quality distribution.....118

**Figure 4.4.** Cross-section along line C-CC (RQ-MCI) showing known and predicted aggregate quality distribution.....119

**Figure 4.5.** Cross-section along line D-DD (HM-MCI) showing known and predicted aggregate quality distribution.....120

## LIST OF TABLES

<b>Table 3.1.</b> Table of spar characteristics observed in the rocks of the Farley Limestone.....	<b>85</b>
<b>Table 3.2.</b> Lithology characteristics and durability factors of the 30 aggregates tested for this study.....	<b>94</b>
<b>Table 3.3.</b> Composition of each insoluble residue for which x-ray diffractometry data were obtained. Also shown are the calculated durability factors (NC = not calculated) and expansion percentages for each of the ten aggregates, as well as the calculated aggregate clay percentages. .	<b>104</b>

## ABSTRACT

Procedures should be implemented for rapidly evaluating durability of limestone aggregate to prevent use of substandard material in highway construction and to assure availability of highly durable aggregate. The objective of this study is to evaluate lithologic (rock type) variables that control durability of limestone aggregate. The Farley Limestone (Pennsylvanian, Missourian) is one of many limestone units quarried in Kansas for production of highly durable, Class 1 aggregate. By understanding the lithologic factors that control durability of aggregate from the Farley, an analog for other limestone units can be developed. The Farley Limestone was described from 17 localities to define associations of rock types (lithofacies) and to establish correlations to aggregate durability. Data on lithofacies characteristics, spar (coarse calcite or dolomite) percentage, spar size, and insoluble residue percentage exhibit no correlations to durability factor or expansion percentage. Data on total percentage of clay-rich rock, clay distribution, and mineralogy of insoluble residues are correlated to durability and expansion percentage. Limestones containing low percentages of diffuse or disseminated clay are more likely to produce aggregates of high durability. Aggregates containing multiple clay minerals exhibit reduced durability. Smectite, even in small quantities, negatively impacts durability, whereas illite apparently has little impact on durability. If changes in clay content deleterious to aggregate quality can be identified during lateral production of a ledge, then quarrying can be halted, or can proceed in another direction while physical tests are run. Such a procedure could prevent use of substandard concrete in highway construction projects. Aggregate-producing phylloid-algal limestones of the lower Farley Limestone thicken into the local depositional lows. However, fine quartz-, feldspar-, and clay-rich sediments (siliciclastics) also seem to be deposited preferentially in paleotopographic lows. Thus, local paleotopographic low areas most distal from sources of siliciclastics can be predicted as the prime areas for location of durable aggregate.

## ACKNOWLEDGMENTS

We are indebted to a number of people for their assistance and contacts. Our thanks to Robert Henthorne of the Kansas Department of Transportation for his help in setting up quarry access, providing needed KDOT materials and for lending us the services of James Burns and Dave Ely who patiently drilled eight invaluable cores for us. Our appreciation also goes to Frank Rockers of Shawnee Rock Company for his useful knowledge of the Class 1 aggregate testing process and for his patience and assistance in all the quarries he knows so well.

Thank you to the Kansas Department of Transportation for providing funding for this project and to Barbara Smith for serving as official contact with KDOT. The University of Kansas Department of Geology provided additional funds so that this report could be completed.

## EXECUTIVE SUMMARY

Identifying lithologies that produce highly durable (class 1) construction aggregates is of utmost importance to both aggregate producers and consumers. The high demand for class 1 aggregate by state, county and private agencies has increased the need for its efficient recognition. This study provides a geologic understanding of the controls on the distribution of highly durable aggregates and should be useful in locating and maintaining them as a resource. The major objective of this study is to reveal the possible sequence-stratigraphic controls on variability of aggregate quality and to evaluate lithologic variables that can be used to identify rock that is or is not suitable for use as class 1 aggregate.

The Farley Limestone (Pennsylvanian, Missourian) is one of many limestone units quarried in northeastern Kansas for production of class 1 aggregate and it is used as the test case for the study. By understanding how the lithologic factors interact to produce highly durable rock in the Farley, an analog for other similar limestone units in different locations can be developed. By monitoring lithologies and other geologic factors as quarrying progresses laterally, changes in quality may be detected and the aggregate reexamined, preventing the unintentional use of lower-quality aggregate.

This report is divided into two major papers in addition to an introductory section, conclusions and appendices. The first major paper, Chapter 2, discusses possible controls on the stratigraphy and sedimentation of the Farley Limestone in the study area as a way of developing a geologic understanding of its lithologic variation. The Farley Limestone was described from 17 core and outcrop localities to define lithofacies and to establish correlations. The observations indicate deposition during two cycles of relative sea-level fluctuation. Low relative sea-level was dominated by deposition of siliciclastics, whereas marine carbonate deposition dominated periods of high relative sea level. Detailed cross-sections and isopach maps show that local paleotopography controlled the distribution of many lithofacies, with deltaic siliciclastics and phylloid-algal limestones of the lower Farley preferentially deposited in depositional low areas. Likewise, in the middle Farley, lithofacies distribution appears to have been controlled by paleotopography. Laterally continuous distributions of lithofacies in the upper Farley indicate that the eventual filling of depositional low areas created subdued paleotopography. Paleotopography on the top of the Farley was caused by erosion that predated deposition of the Bonner Springs Shale.

The second major paper, Chapter 3, deals with the main factors thought to have a significant effect on quality of aggregate. Geologic parameters hypothesized to have had an impact on the durability of limestone construction aggregates include: (1) lithofacies characteristics, (2) bulk spar percentage, (3) average spar crystal size, (4) total percentage of clay-rich strata, (5) distribution of clays within the rock, (6) bulk percentage of insoluble residue and (7) mineralogy of insoluble residue. These parameters were measured in the Farley Limestone and compared to results of those physical tests used by the Kansas Department of Transportation to determine aggregate durability. Data on lithofacies characteristics, bulk spar percentage, average spar crystal size, and bulk insoluble residue percentage exhibit no convincing correlations. Data on total percentage of clay-rich strata, clay distribution, and mineralogy of insoluble residues produce useful correlations.

Limestones containing low percentages of diffuse or disseminated clay are more likely to produce aggregates of high durability. Aggregates containing multiple clay minerals exhibit reduced durability. Smectite, even in small quantities, negatively impacts durability, whereas illite apparently has little or no impact on durability.

The final section, Chapter 4, summarizes the conclusions of the previous chapters and integrates the two by presenting a prediction of the spatial distribution of aggregate quality in the Farley. This model can be used for more effective placement of quarries in the Farley limestone. The correlation between aggregate quality and clays in limestone aggregates can be used to monitor aggregate quality during the quarrying operation, useful as a rapid and inexpensive "first-cut" indication of a degradation in aggregate quality.



## **Implementation**

The location and maintenance of sources of Class 1 aggregate is an important problem to address. The use of the best, most durable aggregate in both state and local projects is economically important. This study represents one step in producing a set of geologic criteria that can be used to identify limestones that are likely to produce class 1 aggregates. Furthermore, this study has shown that by understanding the regional and local controls on the distribution of carbonate lithofacies, the chances of locating and maintaining sources of Class 1 aggregates are greatly enhanced. Future study will be needed not only in continuing to test these conclusions, but also in evaluating the application of the concepts developed to other similar limestone units from which Class 1 aggregates are produced.

### **Site Selection of Quarries in the Farley**

As development continues in the Kansas City area, it is essential that any new quarrying operations be located at sites most likely to produce a reliable source of Class 1 aggregate. Opening quarries in areas of poor sources of aggregate disrupts communities needlessly and does not assure Kansas Department of Transportation (KDOT) with a reliable source of Class 1 aggregate. To prevent needless disruption to communities and to assure a reliable source of Class 1 aggregate for KDOT, we have developed a geologic model whereby sources of Class 1 aggregate can be pre-sited, in the Farley Limestone of NE Kansas, before quarrying operations have begun.

As facies change laterally and vertically so do the geologic properties that have an impact on quality of aggregate. The property that seems to have the greatest impact on the lateral variability of carbonate facies is depositional topography. This topography, the relative sea-level history, and the location of the source area of the siliciclastics are the most important factors in controlling the distribution of fine siliciclastics within the Farley Limestone. Because the distribution of fine siliciclastic sediment has the most negative impact on aggregate quality, understanding the controls of fine-siliciclastic distribution results in the understanding of the distribution of durable aggregates.

To show the distribution of Class 1 aggregate and non-Class 1 aggregate in the Farley, the results of KDOT physical tests and known distribution of clay-rich limestone can be integrated with the stratigraphic cross-sections presented in Figures 2.30 to 2.34. The integrated cross-sections are presented in Figures 4.1 to 4.5. These cross-sections can be used as predictions of the distribution of Class 1 aggregate in the Farley, suitable for use in site selection for new quarries.

#### **Site Selection for Quarries in Other Units**

As new construction projects begin in various areas of Kansas, it is essential that KDOT be assured a reliable source of Class 1 aggregate in each area. Without such sources, costs of projects may be increased, delays in construction may be experienced, and inadvertent production of substandard aggregate and concrete is more likely. To assure KDOT with reliable sources of Class 1 aggregate for these new

projects, we recommend application of geologic models, which will allow location of the best new resources of Class 1 aggregate in each area.

Geologic reasons explain the distribution of Class 1 and non-Class 1 aggregate. We showed that the phylloid-algal limestones of the lower Farley Limestone thicken into the local depositional lows such as those found at localities SRBS, FRQ, WR, and C6 (Figures 4.1-4.5). We also concluded that phylloid-algal limestones commonly produce durable aggregates. However, siliciclastics also seem to be deposited preferentially in paleotopographic lows. Thus, local paleotopographic low areas most distal from sources of siliciclastics are the prime areas for location of Class 1 aggregate.

Therefore, locating high-quality aggregate requires more than simply locating thick successions of phylloid-algal limestone. Having an understanding of the conditions under which the rocks were originally deposited should aid in the location and maintenance of Class 1 aggregate resources. The most important conditions to understand seem to be paleotopography and source direction and distribution of siliciclastics. It seems likely that the implementation of these ideas to other limestone units of similar origin, such as the Argentine Limestone, the Spring Hill Limestone and other units of the Pennsylvanian of Kansas will assist in locating high-quality limestone construction aggregates.

In addition to phylloid-algal limestone, many facies deposited in higher energy depositional environments, such as oolite and peloidal, skeletal packstone,

produce Class 1 aggregate. This is likely related to the relatively low clay content in these high-energy facies. Some of these high-energy facies in the Farley Limestone are located on or immediately adjacent to paleo-highs, whereas others are located in subtle paleo-lows in the lower Farley. Clearly, more work remains to be done on the location and durability of high-energy facies in other units before any geologic concepts are implemented for development of this resource.

We propose that effective exploration for Class 1 aggregate should be enhanced by understanding the regional context and rock properties of each rock unit. Before new areas of quarry development are opened, KDOT geologists, geology students, consultants, or quarry personnel should conduct regional studies of the geologic environment into which the units were deposited. These studies should emphasize the geologic factors, learned from the Farley study, that are important in location of Class 1 aggregate. Lithofacies, abundance of clay-rich zones, spar content, percent insoluble residue, and mineralogy of the insoluble residues would be incorporated to develop a predictive 3-dimensional model of the likely distribution of class-1 aggregate for the new area. Although not foolproof, these models would provide a tool in making decisions regarding future quarry production and locations of new quarries.

#### **Monitoring Rock Properties During Quarrying**

Once production of Class 1 aggregate has begun, it is essential that aggregate quality remains Class 1 as limestone is quarried laterally. It is now well known,

however, that aggregate quality can change laterally and that substandard aggregate can inadvertently be used in highway construction projects. Currently, there is no way to assure aggregate quality without a time-consuming testing procedure that normally can take about six months. During this testing period, substandard aggregate can be produced, yielding highways susceptible to d-cracking. To avoid production of non-Class 1 aggregate, we propose that a “first cut” analysis be applied as ledges are quarried laterally. The analysis should be inexpensive, rapid, and simple to complete, and could be used as an indication of a negative change in aggregate quality that should precipitate further testing and a cessation of production in the location until KDOT physical tests can be run.

The data from our study indicate that the higher the total percentage of clay-rich strata present in the rocks, the lower the durability factor and the higher the expansion percentage. Furthermore, if three different clay minerals are present in the insoluble residues, durability is likely to decline. Smectite seems to have the most significant impact, which is likely due to its expansion properties upon absorption of water. Thus, even small amounts of smectite are likely to have a negative impact on aggregate durability. The critical threshold of smectite content is unknown at this time. Once quarrying has begun, it is important to maintain production of Class 1 aggregate and avoid use of substandard material. If changes in clay content can be identified during lateral production of a stratigraphic unit, then quarrying can be halted or can proceed in another direction while KDOT physical tests are run. We

propose that methods be developed for identification of such changes using inexpensive and rapid techniques. Once these methods have been developed, we propose training of KDOT and quarry personnel to identify such lithologic changes.

One applicable technique that could be applied for monitoring is the measurement of the total thickness of diffuse stylocumulate and clay-rich limestone. If this measurement increases laterally, then there is reason to recommend testing of aggregates, while quarrying is either halted or continued elsewhere. Initial testing would be accomplished rapidly, identifying the presence or absence of clays such as smectites in the samples. If such clays were identified, then KDOT physical tests should be run. Through short courses, KDOT and quarry personnel could be trained to recognize such changes. However, quality control with this approach may be difficult, as it relies on visual recognition of features in the field under variable environmental conditions.

Geophysical tools should prove to be more useful. One such tool is the gamma-ray log, which measures the natural gamma radiation of the rocks and can be used to discriminate between clay-rich limestones and clean limestones. Higher levels of natural radiation in clay-rich rocks are caused by the adsorption of thorium by clay minerals, the potassium content of clay minerals, and uranium fixed by associated organic material (Doveton, 1994). This is useful in the location of durable aggregates because gamma-ray logs give an indication of the amount of clay contained within a limestone unit. Furthermore, the measurement is relatively simple to obtain using

either a hand-held scintilometer at the outcrop, or a gamma-ray logging tool in a borehole. However, the standard gamma-ray tool provides little mineralogical information and may yield false positives for clay.

A more useful tool is spectral gamma-ray logging. This tool allows estimations of the separate contributions of the individual elements, which can then be used to estimate clay mineral volumes and types, and can eliminate false positives for clays (Doveton, 1994). If the spectral gamma ray indications of clay content increase laterally during aggregate production, then there is reason to recommend testing while quarrying is either halted or continued elsewhere. Initial testing would be accomplished rapidly, identifying the presence or absence of clays such as smectites in the samples using X-ray diffraction. If such clays were identified, then KDOT physical tests should be run. Through short courses, KDOT and quarry personnel could be trained to use the relatively inexpensive spectral gamma ray tool for evaluating lithologic variation that could indicate a decrease in aggregate durability.

## **Chapter 1: Introduction**



**Purpose**

Identifying lithologies that produce highly durable (class 1) construction aggregates is of utmost importance to both aggregate producers and consumers. As defined in Kansas, class 1 aggregate is construction-grade material that results from the processing of quarried rock that meets a minimum set of requirements concerning durability, freeze-thaw properties, and expansion percentages.

The Farley Limestone (Pennsylvanian, Missourian) is one of many units quarried in northeastern Kansas for production of class 1 aggregate. Many of the major, active quarries in the Kansas City area of northeastern Kansas currently are producing aggregate from the Farley Limestone. The high demand for class 1 aggregate by state, county and private agencies has increased the need for the efficient recognition of class 1 aggregate.

At present, the Kansas Department of Transportation (KDOT) uses a costly, six-month testing process to determine quality of aggregate. The major objective of this study is to reveal the possible sequence-stratigraphic controls on variability of aggregate quality and to evaluate lithologic variables that can be used to efficiently identify rock suitable for use as class 1 aggregate.

During the preliminary stages of the project we visited several quarries currently producing class 1 aggregate out of a variety of local limestone units. The units examined included the Tarkio Limestone, the Argentine Limestone, the Merriam and Spring Hill Limestones and the Farley Limestone. Based on preliminary observations, we found that some lithologic variables seemed to have an effect on whether a unit passes or fails class

1 aggregate testing. These lithologic variables allowed the development of several working hypotheses.

- (1) Micrite-rich, phylloid-algal lithologies consistently produce durable aggregates.
- (2) Distinct, sharp stylocumulates have little to no impact on durability, whereas diffuse stylocumulates have a negative impact.
- (3) Argillaceous limestone tends to fail testing; therefore the presence of clays in the insoluble residues has a negative impact.
- (4) Abundant, coarse, sparry calcite in the rock has a negative impact.
- (5) High microporosity (measured as absorption) does not have a negative impact.
- (6) Fine-grained, matrix-rich limestones tend to pass physical testing, whereas coarser carbonate grainstones with coarse cements tend not to pass.

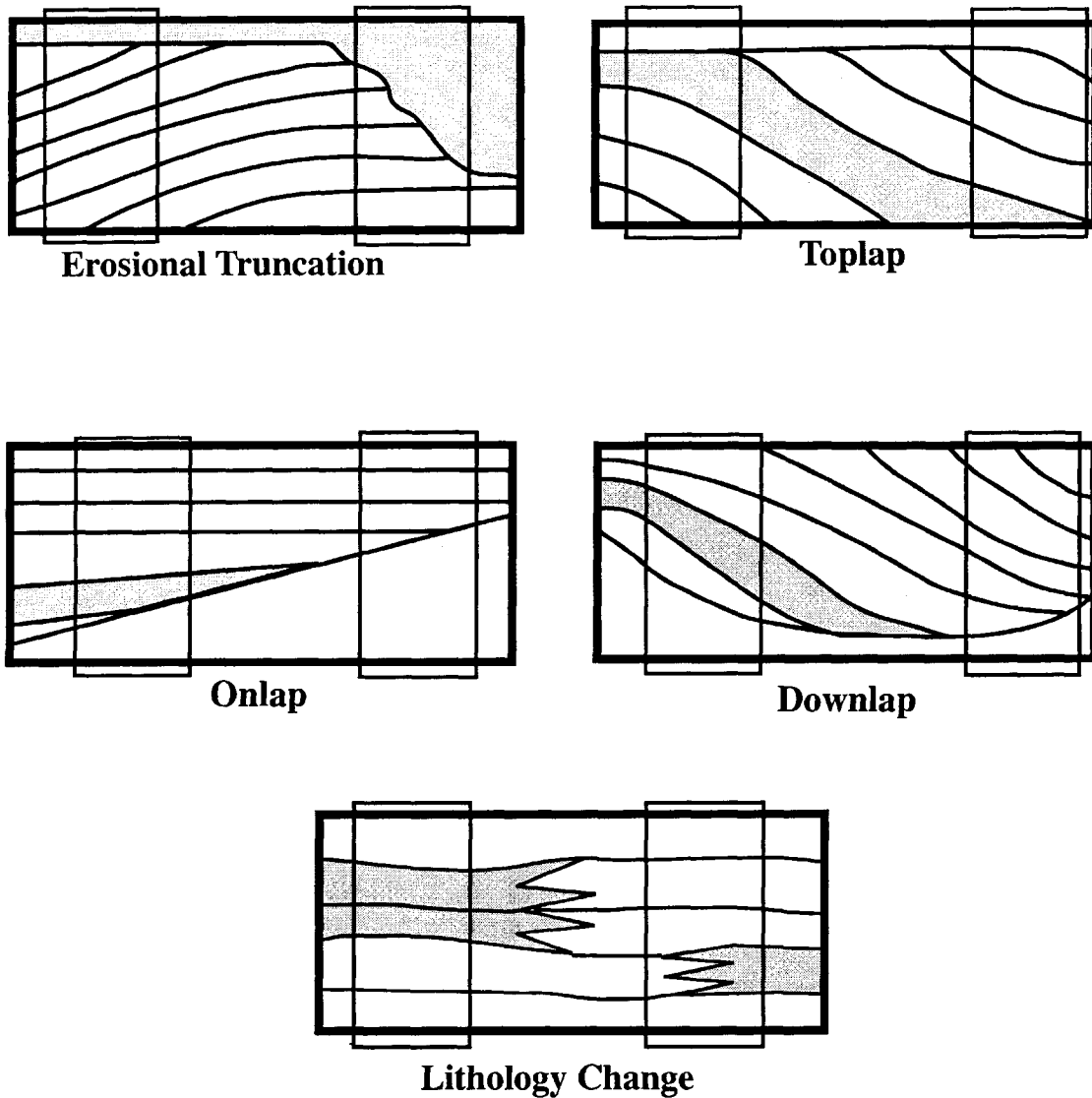
The Farley Limestone is used as the test case for the study because it exhibits significant lateral and vertical variation in quality of aggregate and allows initial examination of all of the above listed hypotheses. By understanding how the lithologic factors interact to produce highly durable rock in the Farley, an analog for other similar limestone units in different locations can be developed. Furthermore, better quality control can be established by realizing that stratigraphic units vary laterally in both geometry and lithology (Figure 1.1). By monitoring lithologies and other geologic factors as quarrying progresses laterally, changes in quality may be detected and the aggregate reexamined, preventing the unintentional use of lower-quality aggregate.

## **Organization**

This report is divided into two separate but related, stand-alone papers. The first paper, Chapter 2, discusses possible controls on the stratigraphy and sedimentation of the Farley Limestone in the study area as a way of developing a geologic understanding of the lithologic variation. Topics include a stratigraphic outline of the deposits of the Farley Limestone and surrounding units, description and environmental interpretation of the major lithofacies, and a discussion of stratigraphic correlations and factors responsible for the vertical and lateral distribution of lithofacies. These factors include relative sea level, paleotopography and source and distribution of siliciclastics.

The second paper, Chapter 3, deals with the main factors thought to have a significant effect on quality of aggregate. These factors include observations made on two levels. First, lithologies and the amounts of visible, coarse-calcite spar and diffuse or concentrated clay and stylocumulates were examined on outcrop and in hand sample. Second, the percentage and composition of the insoluble residues and the type, average crystal size and amount of calcite spar found in the crushed aggregates were examined petrographically and using x-ray diffraction. Correlations between these factors and KDOT physical tests are made in an attempt to simplify the identification of lithologies suitable or not suitable as class 1 aggregate.

The final section, Chapter 4, summarizes the conclusions of the previous chapters and integrates the two. The potential of using the Farley as a predictive model for aggregate distribution is discussed as are topics for future study concerning both the Farley Limestone and research on class 1 aggregate.



**Figure 1.1.** Illustration of four common internal geometries and an example of lithology change in cross-section. For each, hypothetical units of class 1 aggregate are shaded gray. Two boxes within each diagram represent quarry locations. Note how adjacent quarries may have differing stratigraphic successions and how geometric relationships and lithology changes can cause significant variation in the distribution of class 1 aggregates from one quarry to the next. The diagram illustrates the importance of understanding the lateral and vertical variability of stratigraphic units in relation to location and production of class 1 aggregates. Understanding the changes will allow aggregate producers to better maintain sources of class 1 aggregate.

**Chapter 2: Sequence Stratigraphy of the Lane-Island Creek Shales  
and the Farley Limestone**

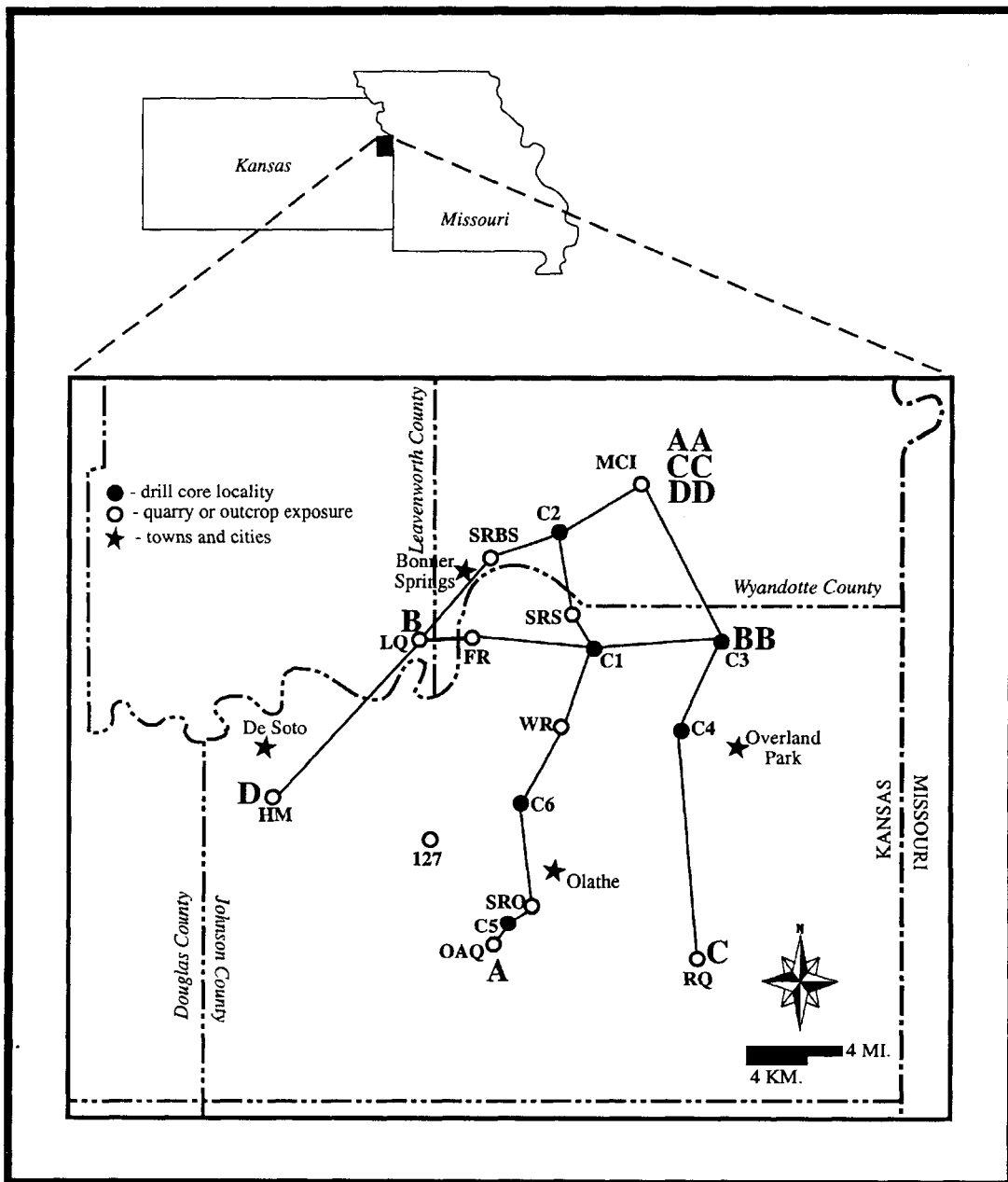
## **Introduction**

Historically, Pennsylvanian carbonate units of Kansas such as the Farley Limestone generally have been thought of as continuous layers. Upon close inspection, however, they reveal significant lateral and vertical variability of facies and geometry. The objective of this paper is to describe the stratigraphy and sedimentology of the Farley Limestone in northeastern Kansas with emphasis on evaluating the controls of the lateral and vertical distribution of both facies and stratal geometries. We hypothesize that the Farley was affected by depositional topography, source and distribution of siliciclastics, and changes in relative sea level. The development of a high-resolution sequence-stratigraphic framework for the Farley Limestone allows better understanding of how these factors controlled heterogeneity of facies.

A firm understanding of the sequence-stratigraphic framework of a unit such as the Farley Limestone provides a better understanding of the interaction of factors that control lithologic heterogeneity and provides predictive capabilities that are applicable to other Pennsylvanian limestone units similar to the Farley. Because many Pennsylvanian carbonate units similar to the Farley are petroleum reservoirs, these predictive capabilities are potentially useful for locating potential petroleum reservoirs in addition to identification of high-quality limestone aggregate resources.

## **Area of Study**

The field area in this study includes a combination of 18 quarry exposures, roadcuts, and drill cores in Johnson, Wyandotte, and Leavenworth counties in the Kansas City area of northeastern Kansas (Figure 2.1). Appendix 1 is a list of legal descriptions of all field localities and contains locality maps, photographs, and



**Figure 2.1:** Index map showing location and type of field localities and major towns for reference. Reconstructed cross-sections along lines A-AA, B-BB, C-CC, and D-DD are illustrated in Figures 2.30, 2.31, 2.32, and 2.33.

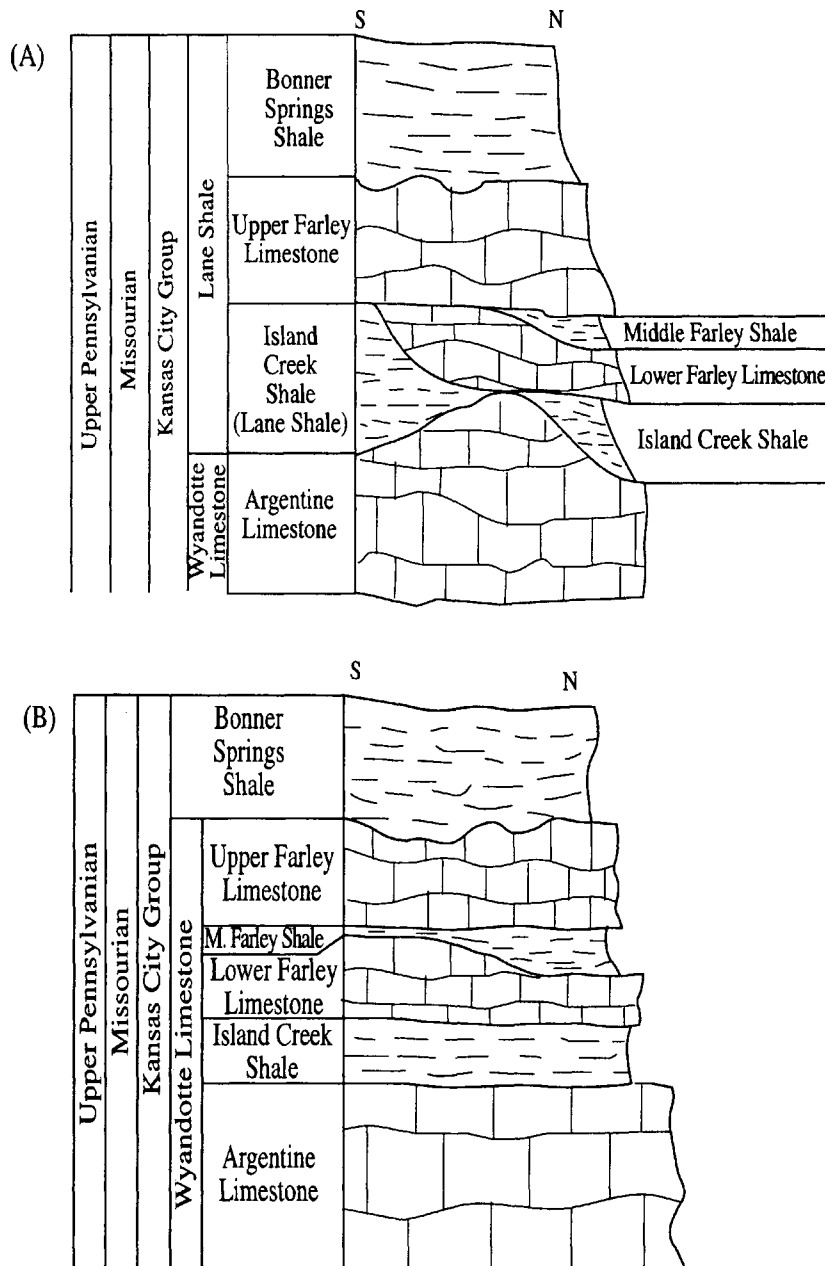
measured stratigraphic sections of each. Access to quarries was arranged through the quarry operator, and cores were drilled by the Kansas Department of Transportation and are repositied at the Kansas Geological Survey, Lawrence, Kansas.

### **Stratigraphy**

Described first in Missouri by Hinds and Green (1915), the Farley Limestone was defined as a thin limestone lying between the Argentine and Plattsburg Limestones and was placed as the middle member of the Lane Shale (Watney and Heckel, 1994). Moore (1932) and Newell (1935) later identified the Farley in northeastern Kansas (Johnson County) as two lithologically similar limestones separated by a shale unit and placed it as the upper member of the Wyandotte Limestone. Still later, Moore (1949) showed that in Kansas, north of Miami County, the Farley occurs as an extremely variable assemblage of limestone and shale beds above the more laterally persistent Argentine Limestone.

The stratigraphic nomenclature presented in this paper (Fig. 2.2A) reflects recent changes made by Arvidson (1990) and Watney and Heckel (1994), to the traditional stratigraphic classification (Figure 2.2B). The new stratigraphic nomenclature corrects a miscorrelation made by Moore (1936) who placed the Lane Shale below the Argentine Limestone rather than above it. The Farley is located above one of three different units depending on location within the field area. In the north and northeast the Farley is located immediately above the Island Creek Shale. In the southwest it overlies the Lane Shale and in the areas where these shale units are absent the Farley is found directly overlying the Argentine Limestone. The unit located directly over the Farley Limestone in all localities is the Bonner Springs Shale. A brief introduction to each of these units is presented below.





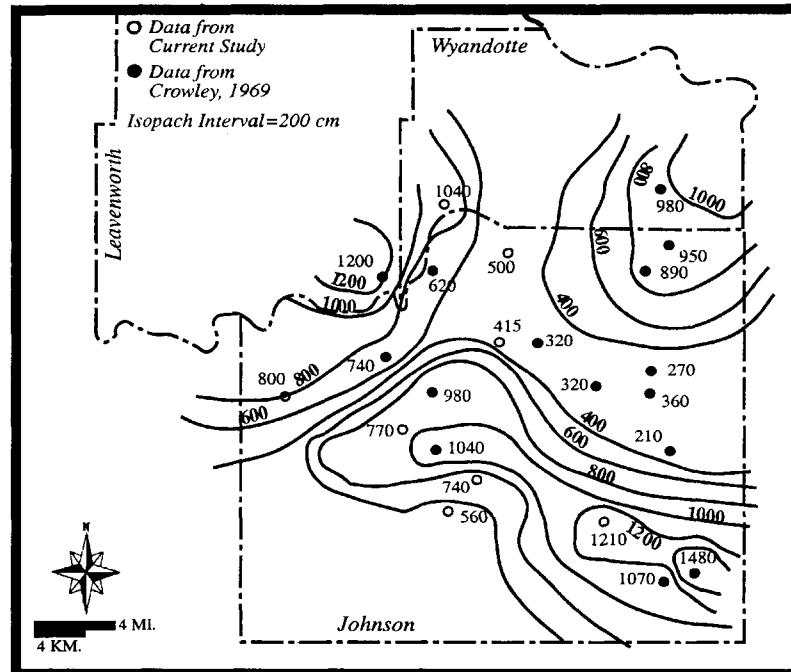
**Figure 2.2.** Generalized stratigraphic sections showing general relationships and lithologies of the units examined for this study. (A) Section showing revised stratigraphic nomenclature based on the work of Arvidson (1990) and Watney & Heckel, (1994). Major revisions include splitting the Farley Limestone and the Bonner Springs Shale out of the Wyandotte Limestone and regrouping them as part of the Lane Shale. This reflects the correlation of type Lane Shale to lie between Argentine and Farley Limestones in southeastern Kansas (southwest Johnson County, Miami and Anderson counties). See the text for further discussion of revisions. (B) Generalized stratigraphic section showing the traditional stratigraphic classification into which the Farley Limestone fits (after Arvidson, 1990).

### *Argentine Limestone Member*

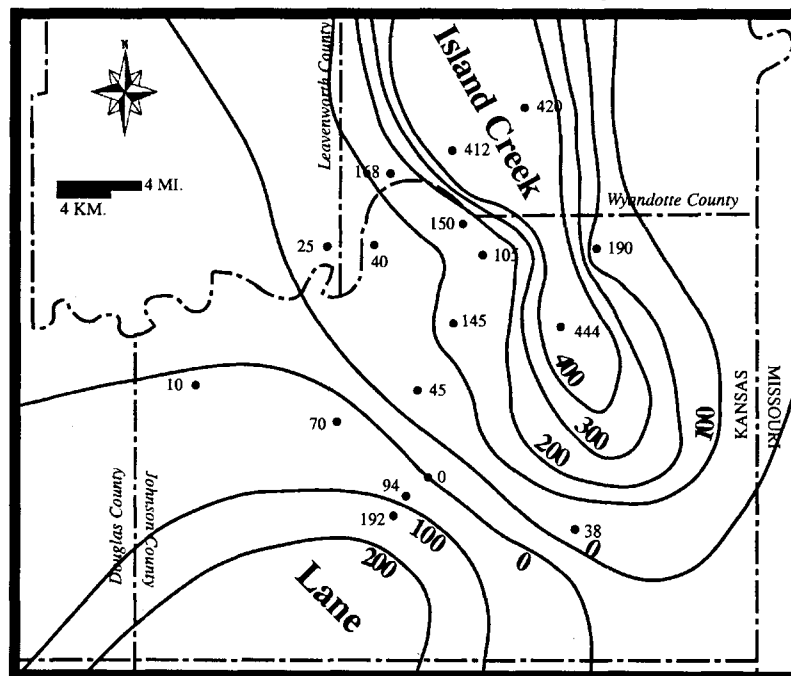
The Argentine Limestone is the uppermost member of the Wyandotte Limestone (Fig. 2.2A) and shows great variation in thickness throughout the area (Crowley, 1969; Arvidson, 1990; this study). Crowley (1969) attributed these thickness variations to the presence of a series of phylloid algal banks that attained thicknesses as great as 50 feet (Figure 2.3). In developing the sequence-stratigraphic framework of the Farley Limestone in this study, the paleotopography on the top of the Argentine Limestone is important because it could have influenced deposition of the Lane-Island Creek shales and Farley Limestone. Arvidson (1990) demonstrated the topographic influence of the Argentine and stated that the Lane Shale is confined to areas where the underlying Argentine Limestone member is thin. Crowley (1969) also demonstrated this topographic influence and stated that the Island Creek Shale extends southward from northern Wyandotte County between areas of thickened Argentine. For these reasons, the top of the Argentine Limestone is included in the correlations and cross-sections developed for this study discussed later.

### *Lane-Island Creek Shales*

Work by Arvidson (1990) indicated that the shales located below the Farley Limestone represent two distinct units and source directions. The isopach maps of Crowley (1969) and this study show that the Island Creek Shale had a northern source and extended southward in a thickened lobe into Johnson County (Fig. 2.4). Arvidson (1990) confirmed this source direction but showed that Crowley miscorrelated the Lane Shale, placing it below the Argentine instead of above. The new correlations of Arvidson (1990), however, also showed that the stratigraphic position of the type Lane Shale between Argentine and Farley Limestones demonstrates its equivalency with the



**Figure 2.3.** Isopach map showing thickness of the Argentine Limestone within the field area. Data taken from current study and from Crowley, 1969.



**Figure 2.4.** Isopach map showing the thickness of the Lane-Island Creek Shale. Note how thickness of these shale compliments thickness of Argentine Limestone illustrated above. Where the Lane-Island Creek shales are thin the Argentine is thick, and where the Lane-Island Creek is thick the Argentine is thin. Data taken from current study and Crowley, 1969. Isopach interval=100 cm.

Island Creek Shale. Furthermore, Arvidson (1990) argued that the siliciclastic interval separating the Argentine from the Farley in southern Johnson County represents material supplied primarily from southern sources, whereas siliciclastics with a northern source were not deposited here. The work done in the current study confirms that the Island Creek Shale member of the Lane Shale (Fig. 2.2A) does in fact represent two distinct shale units with little to no shale in the areas between them. This distinction of time-equivalent siliciclastics with different source directions is important to make. These siliciclastics are therefore referred to as Lane-Island Creek shales in order to establish that they are time-equivalent but in fact need to be thought of as separate units within the sequence-stratigraphic framework; this distinction is not made in the stratigraphic nomenclature presented in Figure 2.2A.

### ***Farley Limestone Member***

In the area of this study, the Farley Limestone is a mixed siliciclastic-carbonate unit typically composed of three individual submembers (Fig. 2.2A) of varying thickness and lithology; the lower, middle and upper Farley. The lower Farley is a carbonate unit and shows the greatest degree of lithologic and thickness variability. The middle Farley is dominantly siltstone but contains local accumulations of carbonate within it. In the southwest portion of the field area, the middle Farley is composed of a thick accumulation of skeletal carbonate with little to no shale. The upper Farley is exclusively carbonate and is the most lithologically consistent submember. Thickness variability in these units will be discussed in the later parts of this paper.

### ***Bonner Springs Shale***

The unit immediately overlying the Farley Limestone at all localities is the Bonner Springs Shale. The uppermost member of the Lane Shale, the Bonner Springs Shale, contains variable lithologies and thickness (90 cm to 9 m). Lithologies typically observed include

mudstone, siltstone, and sandstone (Enos *et al.*, 1989; Crowley, 1969; Arvidson, 1990; this study). Erosional scouring and backfilling as well as the development of a paleosol in the upper few feet of the Bonner Springs Shale indicates widespread subaerial conditions near the end of Bonner Springs deposition (Enos *et al.*, 1989).

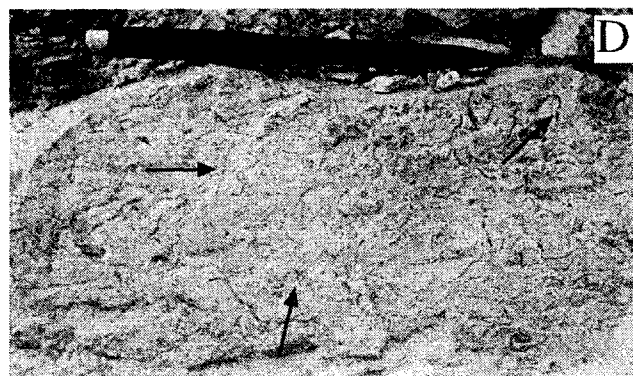
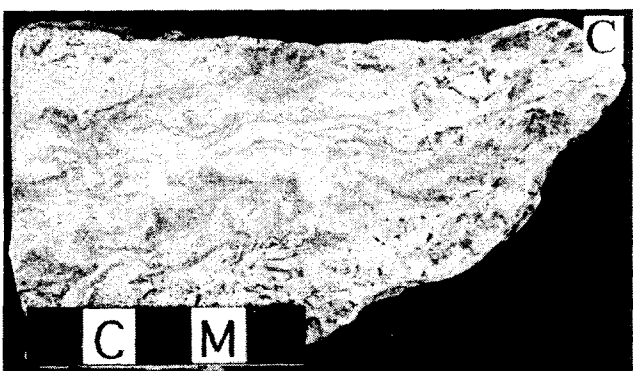
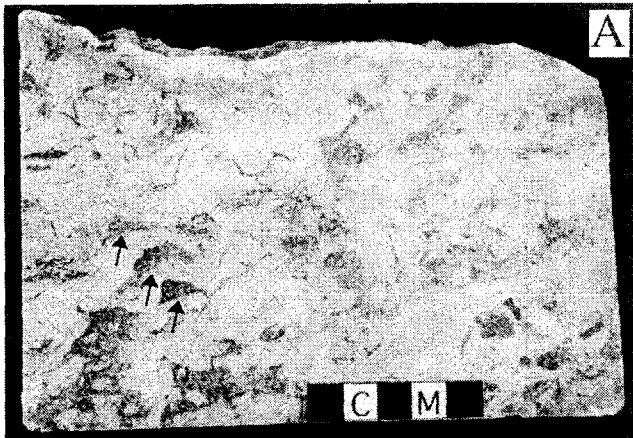
### **Lithofacies & Depositional Environments of the Farley Limestone**

The Farley Limestone is divisible into ten distinct lithofacies. All facies were established based on details observed at outcrops, in cores, and in thin sections.

#### ***Phylloid Algal Facies***

The most common facies in the Farley Limestone is the phylloid-algal facies (Fig. 2.5) that occurs as both boundstone and packstone. Present in all measured sections and cores, this facies is light to medium gray (N5-N7) on fresh exposures and weathered exposures are light brown to grayish-orange (5YR 5/6-10YR 7/4). Where the facies contains large percentages of disseminated argillaceous material (Fig. 2.5d) the rocks have a bluish hue (5B 7/1, 5B 5/1).

Bedding is thin to thick (25 to 100 cm) in scale and is accentuated by thin shale partings. These shale partings commonly contain abundant crinoidal and bryozoan material and are commonly diffused into overlying limestone beds and can account for as much as 30 percent of the rock mass. The main skeletal constituents are phylloid-algal blades, which account for more than 50 percent of the fossils and are present to the exclusion of other fossils in some areas. The phylloid algae have a variety of sizes but typically are wavy veinlets of calcite spar at least 3 cm in length and with lengths up to 12 cm.



**Figure 2.5** (A) Polished slab illustrating the appearance of the phylloid algal facies. Note the coarse calcite spar filling shelter pores beneath phylloid algal blades (arrows) (sample WR-1).

(B) Photomicrograph of phylloid algal blade with dense micrite above and spar filled shelter pore below (transmitted light; scale = 1mm; sample S-7).

(C) Hand sample showing denser packing of lamellar phylloid algal blades (sample RQ-11).

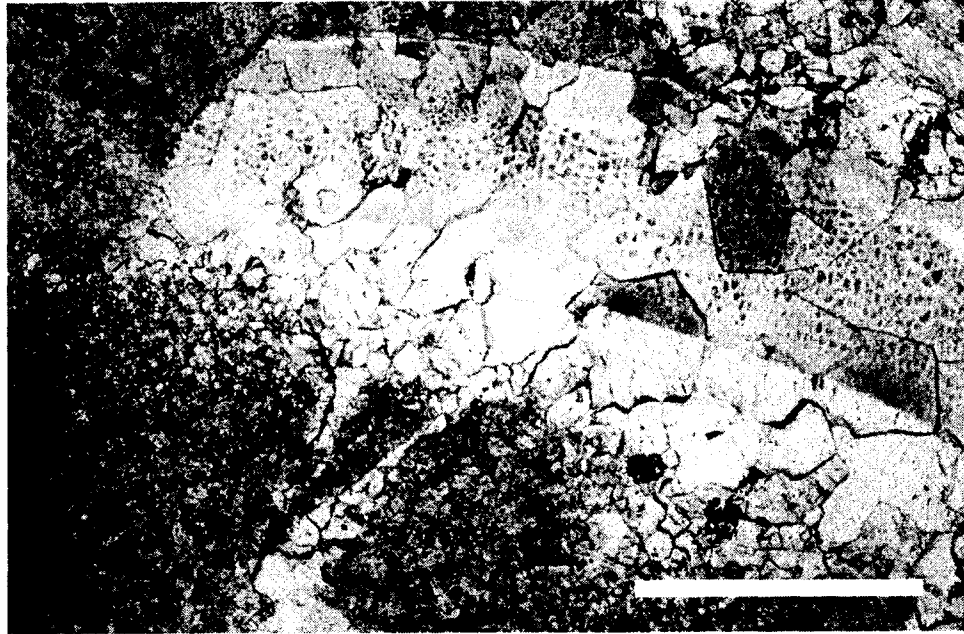
(D) Nature of phylloid algal facies as seen on outcrop. Small wavy veins are phylloid algal blades. (arrows) Bluish color in this particular outcrop is the result of a high percentage of finely disseminated argillaceous material (locality LQ).

The most commonly identified genus of phylloid algae in the Farley Limestone is *Archeolithophyllum* (Figure 2.6). Other phylloid algae such as *Eugonophyllum* and *Anchicodium* have been identified in the Farley in the past (Crowley, 1969; Harbaugh, 1960; Heckel & Cocke, 1969; Johnson, 1946, 1963; Konishi & Wray, 1961; Wray, 1968) and may be present but unrecognizable due to obliteration of the original structure. The associated fauna is dominated by brachiopods, bryozoans, and crinoids, whereas bivalves, gastropods, small rugose corals, ostracodes, and trilobites are present but much less common.

Shelter pores beneath algal blades (Figure 2.5 a, b) and phylloid algal molds contain coarse, blocky calcite spar. Fractures are typically filled with blocky calcite spar or in some cases coarse baroque dolomite. The facies generally shows little or no extant, large-scale porosity. In a few locations, however, phylloid-algal blades and other fossils have been leached leaving molds that are lined with light to moderate brown (5YR 5/6-5YR 4/4) residue.

On outcrop and in hand sample, the matrix appears to be homogeneous micrite. Petrographic examination, however, reveals a variety of micrite fabrics dominated by clotted or peloidal micrite. The clots of micrite are approximately 50 to 75 micrometers in size and occur in two forms. The most abundant form is a peloidal micrite sediment that occurs in interparticle and intraparticle spaces. (Figure 2.7a). The other dominant form is a growth framework that fills interparticle spaces and binds grains together (Figure 2.6 b, c). Other types of micrite occur as encrustations and micrite envelopes on many skeletal grains (Fig. 2.6d), especially phylloid-algal fragments. Micrite is also present as matrix that has been altered to microspar and pseudospar. These latter three types of micrite are less common than the clotted and peloidal forms.

The dominant types of spar within the phylloid-algal facies are interparticle



**Figure 2.6** Photomicrograph of *Archeolithophyllum* thalli. Note neomorphic calcite that overprints fabric and preserves the cellular, internal structure (Sample RW-7; transmitted light; scale bar = 1 mm).



cement and neomorphic calcite. Coarse, sparry calcite cement ( $\geq 0.5$  mm) is common in shelter pores and fractures whereas neomorphic spar replaces fossil grains (Fig. 2.6) and is present as an aggrading neomorphic replacement of micrite. Early, fibrous to bladed cements typically line the inside of such fossils as brachiopods and gastropods and are generally overprinted with blocky neomorphic spar (Figure 2.8). Associated with these early cements is a later partial infilling of micrite or peloidal micrite sediment with a final blocky calcite spar filling the rest of the pore space.

### Environmental Interpretation

Wray (1964) interpreted the growth habit of *Archeolithophyllum* as encrusting, locally attached, or free forms that formed semirigid crusts capable of providing a self-supporting skeletal framework and a sediment-binding function in the depositional environment. Furthermore, Wray (1964) compared *Archeolithophyllum* to the modern genus *Lithophyllum*, which is exclusively marine and extensively developed in shallow regions down to approximately 30 meters. By this comparison, and because algae depend on sunlight for important metabolic processes, it is reasonable to infer that the phylloid-algal facies was most extensively developed in shallow water, well within the photic zone. Additionally, other phylloid algae such as *Eugonophyllum* and *Anchicodium* also have been interpreted to live most abundantly in shallow water and effectively baffle and trap carbonate mud as well as to make direct contributions to sediment accumulation in the form of blades, crusts and fragments (Heckel & Cocke, 1969).

The phylloid algae were not likely to have been the only organism trapping and binding sediment. Tsien (1985) discussed possible microbial or bacterial origins of



**Figure 2.7** Photomicrographs of dominant micrite fabrics in phylloid algal facies.

(A) Peloidal micrite sediment fills inter- and intraparticle pore spaces and forms geopetal fabrics (Sample BS-7; transmitted light; scale bar = 1 mm).

(B) Peloidal micrite sediment filling interparticle pore spaces (Sample S-7; transmitted light; scale bar = 1 mm).

(C) Micrite encrustation on phylloid algal fragments (arrows) (Sample BS-6; transmitted light; scale bar = 1 mm).

(D) Clotted micrite growth fabrics protrude from grains and in many cases fill interparticle pore spaces, and bind grains together (Sample S-7; transmitted light; Scale bar = 1 mm).



**Figure 2.8** Photomicrograph of gastropod mold lined with early fibrous cement that is overprinted by neomorphic calcite. Original micritic matrix is recrystallized to microspar and some pseudospar. (Sample RW-9; transmitted light; scale bar = 400 micrometers)

micrites stating that patchy, clotted, or irregularly shaped masses may have been associated with decaying organic bodies, forming cryptalgal matlike structures that trapped, stabilized, and supported lime mud. The patchy micritic growth framework with a clotted appearance in the phylloid algal facies forms micrite masses that connect skeletal and phylloid fragments and fill interparticle pore spaces. Therefore, it is reasonable to assume that much of the micrite framework found in the phylloid algal facies is the result of microbial action that facilitated the precipitation and binding of carbonate mud and other carbonate grains.

The inferred growth habits outlined above are often cited in interpretations of depositional environments. The binding and encrusting nature of the algae is cited as evidence that the algae were responsible for the construction of algal mounds or banks. These banks resulted from the growth and proliferation of phylloid algae on and around topographic prominences. Harbaugh (1964) stated that, initially, algal mounds may have been localized by waves and currents that caused both argillaceous and calcareous material to be heaped into submerged bars. These bars then became nucleation sites for growth of phylloid algae. Heckel and Cocks (1969) supported this idea, saying that local sedimentary highs on an irregular sea floor provided favorable locations for growth of phylloid algae because sunlight was favorable for algal growth. Once established, the growth and proliferation of the algal community built up local phylloid algal mounds or banks.

Ball *et al.* (1977) offered an alternate interpretation and argued strongly against the concept of phylloid algae as mound or bank builders. They stated that phylloid algae were not builders of depositional topography but rather were only a source of building material. They went on to say that there is no evidence for the ideas that phylloid algae were commonly significant sediment bafflers or that they were ever important bank or mound builders in

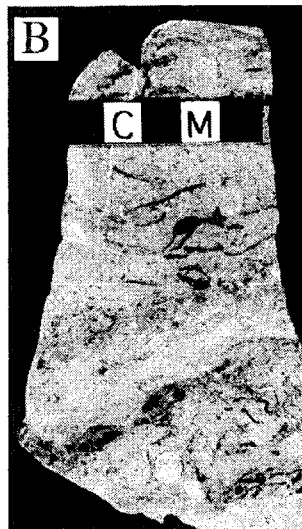
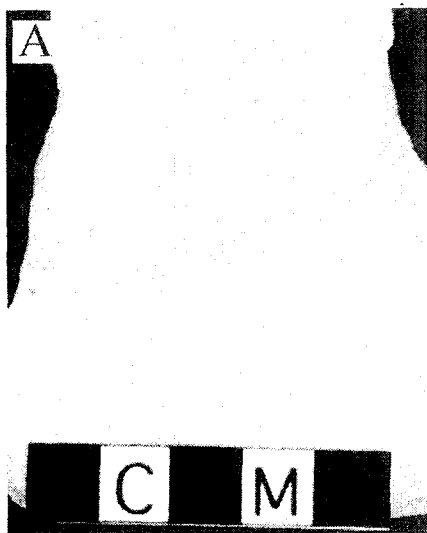
Pennsylvanian and Early Permian seas. In fact, the proliferation of phylloid algae or at least the environment where the greatest quantities of their transported remains occur, apparently was in broad, shallow embayments between contemporaneous deltaic depocenters (Ball *et al.*, 1977).

Although those on both sides of the argument are able to present evidence to support their conclusions, a combination of the two interpretations best serves to explain the distribution of phylloid-algal facies found in the Farley Limestone. Evidence for both models will be presented later in this paper.

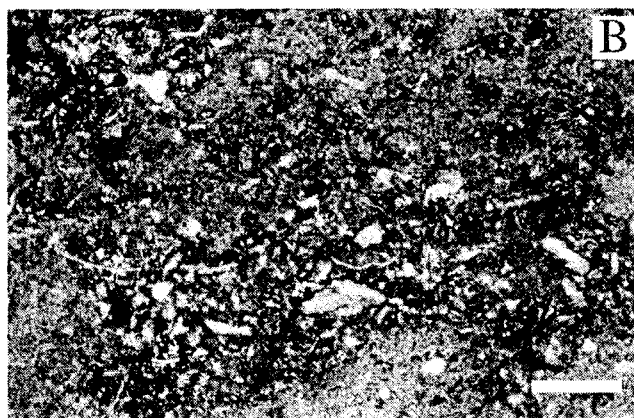
### ***Skeletal Wackestone-Packstone***

The skeletal wackestone-packstone facies (Fig. 2.9) consists of thin to medium-bedded (25 to 50 cm) medium- to light-gray (N5-N7) deposits. This facies is differentiated from the phylloid algal facies by a much lower percentage of phylloid-algal remains, typically around 15 to 20 percent of the total fauna, and a higher density of associated fauna. The skeletal wackestone-packstones also exhibit thinner average bedding (35 cm) than the phylloid algal facies. The most common skeletal constituents include both whole and fragmental brachiopods, bryozoans, crinoids, fusulinids, and gastropods as well as other unidentified skeletal fragments. Phylloid algae are present but typically occur as fragments of 5 cm or less and show no cellular preservation. Instead, the phylloid algal fragments occur as molds of algal thalli that have been filled with blocky calcite spar.

The dominant depositional fabric observed in hand samples is packstone. Patches of densely packed skeletal remains are often observed within individual thin sections (Figure 2.10). The accumulations range in size from 2-3 mm to 3-5 cm in both length and width.



**Figure 2.9.** Hand samples showing skeletal wackestone-packstone facies. (A) This sample contains dominantly fine-grained skeletal material and so appears to be a mudstone in hand sample. See Figure 2.10b for photomicrograph showing true fabric (sample BS-4); (B) This sample demonstrates the more typical expression of the facies with coarser skeletal material and fragmental phylloid algal remains (sample RW-2).



**Figure 2.10.** Photomicrographs showing various skeletal wackestone-packstone fabrics. (A) This sample exhibits depositional micrite matrix with densely accumulated skeletal material in a linear arrangement. This likely represents a burrow filled with skeletal material (sample RW-5; transmitted light; scale bar = 2 mm). (B) Skeletal wackestone with depositional micrite matrix and fine grained skeletal material. Photomicrograph taken from hand sample shown in Figure 2.9a (transmitted light; sample BS-4; scale bar = 1 mm).

Although present in a few thin sections, the clotted micrite fabric, which dominates the phylloid-algal facies, is much less common in the skeletal wackestone-packstone facies. Instead, the matrix is dominantly depositional micrite that has been recrystallized to microspar (Figure 2.10). Coarse spar is found filling fractures and geopetal cavities, but overall the facies contains a much smaller percentage of coarse spar than does the phylloid algal facies (15 to 25 percent in the skeletal wackestone-packstone facies versus 25 to 50 percent in the phylloid algal facies). The skeletal wackestone-packstone facies is similar to the phylloid-algal facies in terms of its distribution of amount of argillaceous debris.

#### Environmental Interpretation

The matrix of the skeletal wackestone-packstone facies is dominantly depositional micrite. The facies lacks abundant phylloid algae or abundant microbial micritic framework that would have trapped and bound carbonate mud. Therefore, the skeletal wackestone must have been deposited in a low-energy environment that allowed the deposition of fine carbonate matrix.

The diverse, unabraded fauna provides further evidence of a quiet, open-marine environment. The presence of organisms such as bryozoans, brachiopods, echinoderms, and corals indicates a marine environment of normal salinity (Heckel, 1972b). Additionally, the irregular patches of skeletal packstone in the facies are evidence of bioturbation with patches of dense skeletal material that probably represent the accumulation of skeletal material in burrows. It has been shown that these irregular patches of packstone-grainstone in modern settings may be produced by storm infilling of excavated burrow systems (Tedesco & Wanless, 1989).

### ***Peloidal, Skeletal Packstone Facies***

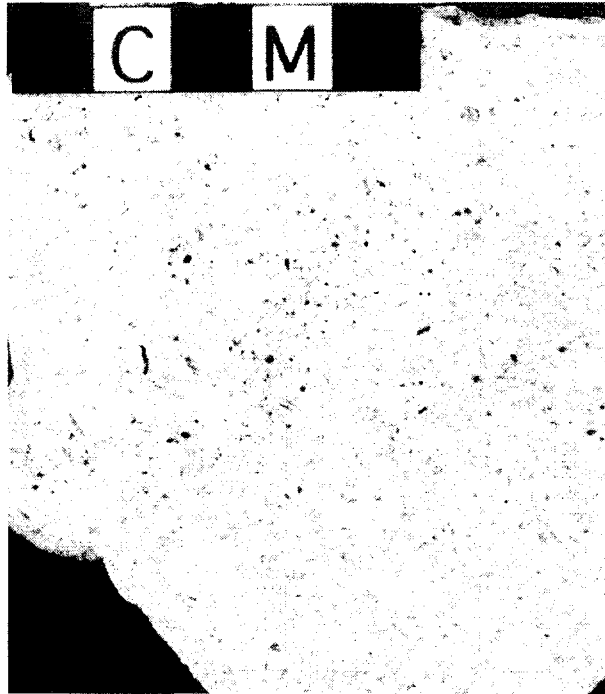
The peloidal, skeletal packstone facies (Fig. 2.11) exhibits a wide range of thicknesses (10 to 210 cm). On outcrop the bedding is thin to medium in scale ranging from 20 to 80 cm. The peloidal, skeletal packstone typically is yellowish to light gray (5Y 8/1-N8) both on fresh outcrops and in cores. The peloidal, skeletal packstone facies typically contains less than 3 percent silt and clay. The main constituents are peloids and skeletal fragments of brachiopods, bivalves, gastropods, bryozoans, crinoids, phylloid algae, and corals. Micrite matrix is present in all occurrences but most are matrix poor (approximately 3 to 5 percent matrix). Grain sizes are variable (100 microns to centimeters) but within each occurrence the constituents tend to be well sorted and show no preserved, physical sedimentary structures. Nearly all grains show some level of micritization from a thin envelope to complete replacement (Figure 2.12).

This facies contains a small percentage of extant interparticle and intraparticle porosity (3 to 5 percent) but most original porosity has been filled with blocky calcite spar or micrite. Early cements are bladed to fibrous spar found mainly in brachiopods and gastropods. The majority of the spar in this facies is equant blocky calcite cement that fills nearly all interparticle and intraparticle porosity. Because nearly all interparticle and intraparticle porosity has been filled with cement, the total percentage of the rock composed of spar is approximately 60 to 75 percent. The average crystal size, however, is small at approximately 0.5 mm.

### **Environmental Interpretation**

The relatively small amount of micrite matrix suggests that energy levels were too high to allow deposition of fine carbonate sediment. Therefore, this facies represents a higher-energy environment than that found in the skeletal wackestone-





**Figure 2.11.** Hand sample showing fabric of peloidal, skeletal packstone facies (sample BS-19).



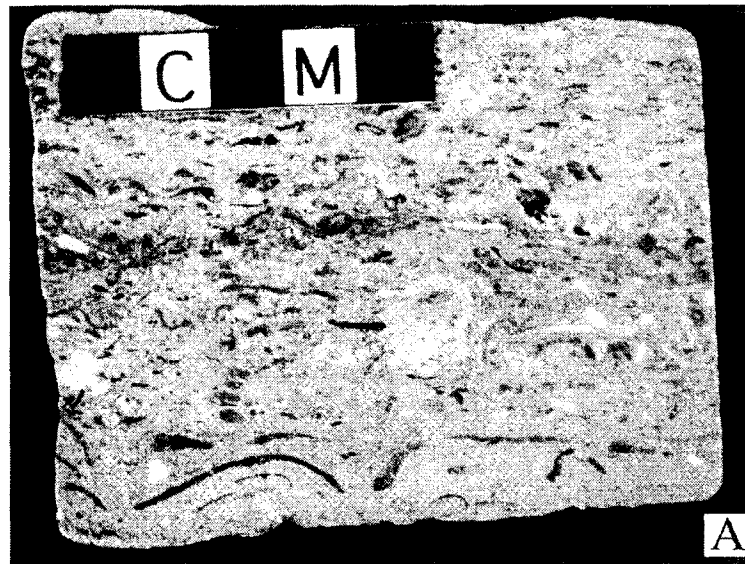
**Figure 2.12.** Photomicrograph of peloidal, skeletal packstone facies. Note the micritization in various stages of development from thin envelopes to complete replacement. Interparticle porosity is filled with equant, blocky cement (sample BS-19; transmitted light; scale bar = 500 micrometers).

packstone facies or phylloid-algal facies. The presence of abundant, well-developed micrite envelopes on nearly all grains also suggests a shallow-water, protected environment where intensive boring by microorganisms was common (Golubic *et al.*, 1975). The lack of physical sedimentary structures in the peloidal, skeletal packstone facies indicates energy high enough to transport and wash sediment but perhaps not continuous enough to prevent sedimentary structures present from being destroyed by bioturbation.

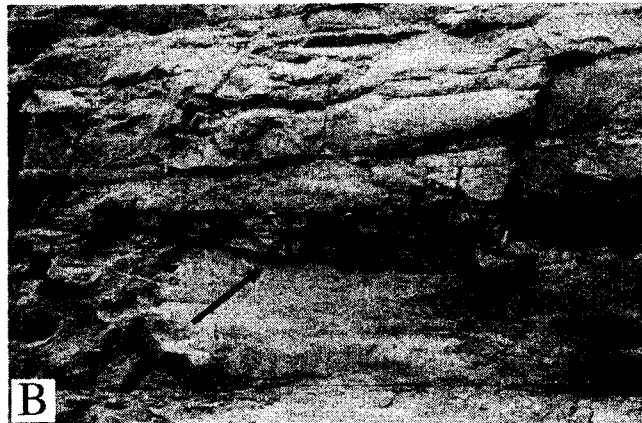
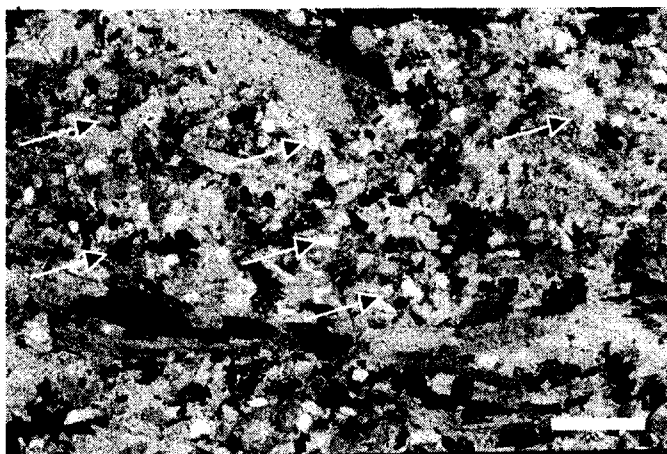
### ***Sandy, Skeletal Grainstone-Packstone Facies***

Found at only a few localities in the study area, the sandy, skeletal grainstone-packstone facies (Fig. 2.13) has several distinctive features. Bedding varies from horizontal beds to medium-scale cross bedding (Figure 2.14). The cross beds (Fig. 2.14a) are typically 15 to 30 cm thick and have variable apparent dips from 8 to 35°. Where the beds are horizontal, they are approximately 30 to 50 cm thick. The sandy, skeletal grainstone-packstone facies typically occurs as medium to medium-dark gray (N5-N4), silty to sandy beds that contain abundant, coarse fossil debris. The cross-beds are concave upward and in places truncate the beds below them. Where bedding is horizontal, there is a higher abundance of micrite and fine sand and silt.

The main skeletal constituents include brachiopod, bivalve, gastropod, algae, bryozoan, and crinoid fragments. Some nonfragmental fossils and whole fossil molds are present and typically are gastropods. In hand samples and in thin sections most elongate skeletal particles, such as brachiopod and bryozoan fragments tend to be oriented parallel (Figure 2.13). Also visible in some hand samples is grading with concentrations of coarser particles near the base of beds (Figure 2.13). In addition to the skeletal fragments, silt- and sand-sized quartz grains, peloids, and plant fragments



**Figure 2.13.** Hand samples showing nature and details of sandy, skeletal grainstone-packstone facies. (A) Hand sample showing general parallel orientation of elongate skeletal grains (sample S-10). (B) Hand sample that exhibits slight grading with coarsest grains concentrated at the base and finer particles distributed throughout the upper part of a bed (sample HM-7).



**Figure 2.14.** Outcrop photos of sandy, skeletal grainstone-packstone facies. (A) Cross-bedded sandy, skeletal grainstone-packstone as observed at locality HM (See figure 2.1 for locality map). Staff is 1.5 m. (B) Horizontal bedding in sandy, skeletal grainstone-packstone facies as observed at locality SRO (see figure 2.1 for locality map). Some trough cross bedding is present (arrow) but is truncated by overlying horizontal beds.

**Figure 2.15.** Photomicrograph of typical fabric of sandy, skeletal grainstone-packstone facies. Note abundance of coarse skeletal fragments. Also note the abundant fine sand-silt sized quartz grains (arrows) (sample S-7; plane polarized light; scale bar = 1 mm).

of various types and sizes are common. Plant fragments are typically oriented parallel to bedding planes in thin layers. Micritized grains are present but much less common than in the peloidal, skeletal packstone facies (Figure 2.15). The above described features allow the sandy, skeletal grainstone-packstone facies to be differentiated from the peloidal, skeletal packstone facies.

### Environmental Interpretation

The association of terrigenous material such as detrital quartz and plant material with marine skeletal debris in the sandy, skeletal grainstone-packstone suggests the close proximity of a terrigenous source to a marine environment. Because of this relationship, it seems most reasonable to interpret the sandy, skeletal grainstones and packstones found in the Farley as either distributary channel or distributary mouth bar deposits.

Deposition within tidal channels is one scenario. Medium-scale cross-beds like those found in the sandy, skeletal grainstone-packstone facies are characteristic of tidal channels in nearshore environments (Wilson & Jordan, 1985). Another possibility is deposition as a distributary mouthbar. Reineck and Singh (1975) stated that distributary mouth bars are sandy shoals formed near the seaward limit of distributary channels. Deposits of distributary mouth bars are made up of sand and silt, commonly with thin laminations of plant debris. The most common sedimentary structure is trough cross-bedding (Reineck & Singh, 1975).

### ***Oolite Facies***

Oolite (Fig. 2.16) occurs in several localities throughout the Farley Limestone. There are two types of oolite in the Farley Limestone, and they each comprise an oolite subfacies. The first type is ooid grainstone. The greatest accumulation of this subfacies is towards the north where the lower Farley is composed of a single bed of cross-bedded

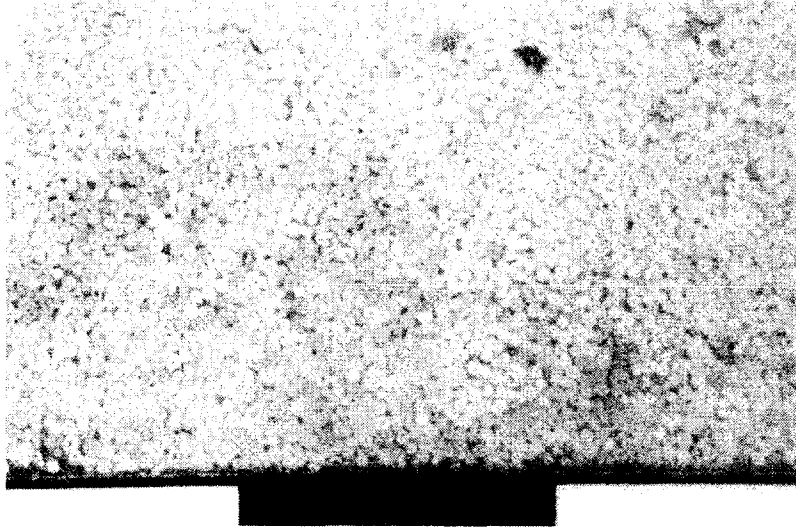
oolite (Figure 2.17 & 2.18b). This weathered outcrop is light to yellowish gray (N7-5Y 7/2). Other oolites to the south and southwest are composed of single, thin (15 to 55 cm) beds that show no cross-bedding. Cross-bed measurements taken in the north, indicate two dominant paleocurrent directions, one to the southeast and the other to the northwest (Figure 2.18). Ooid grainstones are also present as thin accumulations that are not cross-bedded.

Ooid sizes in ooid grainstone subfacies range from 0.5-1.5 mm. The deposits are well sorted and overpacked with slight grain suturing in places. Ooid cortices are dominantly fine quartz grains and skeletal fragments. Coarse-grained fossil material is rare to absent within the oolite grainstones. Fossil fragments, commonly encrusted by algae, are common. Cements are composed of equant, blocky calcite, and there is slight micritization of ooids and other grains. Oomoldic porosity is well developed in the northernmost ooid grainstones where ooid cortices have been leached away.

The oolitic, peloidal packstone subfacies are massively bedded accumulations that show no preserved sedimentary structures. Ooid and peloid sizes range from 150 to 1,000 microns and sorting is generally poor to moderate. Ooid cortices are unidentifiable due to replacement by blocky, equant calcite spar. Micrite envelopes on ooids are common and commonly completely micritize the grains (Figure 2.19).

Keystone vugs are common in the oolite, peloid packstone facies. These fenestrate and other interparticle pore spaces are lined with micrite cement that shows meniscus fabrics and fabrics similar to pendant cement. There is also a later isopachous fringe of bladed calcite cement around the grains and lining vugs. The final pore fill is coarse calcite spar or in some cases coarse baroque dolomite (Figure 2.19).

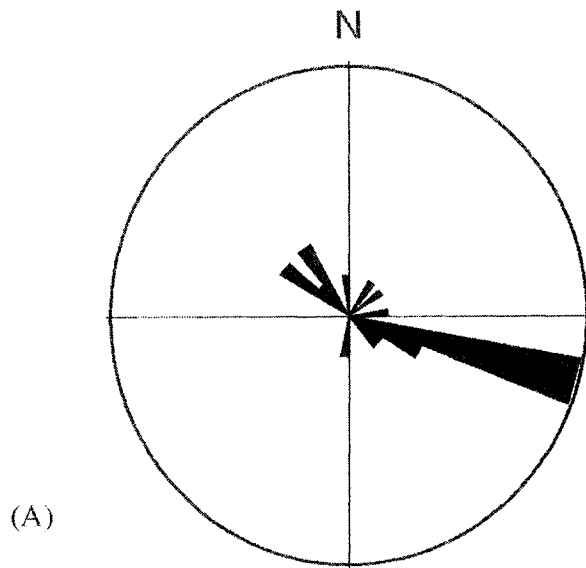
All occurrences of oolite are virtually free of shale or fine siliciclastic material. There are no shale partings between bedding planes and no diffuse argillaceous material.



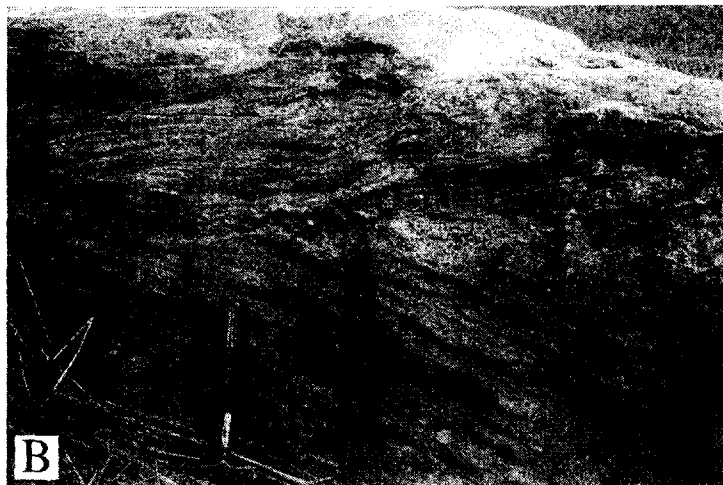
**Figure 2.16.** Detail of ooid grainstone from locality C6. Ooids in this locality (see Figure 2.1 for locality map) are well sorted and smaller relative to ooids found to the north. Scale bars are 1 cm each.



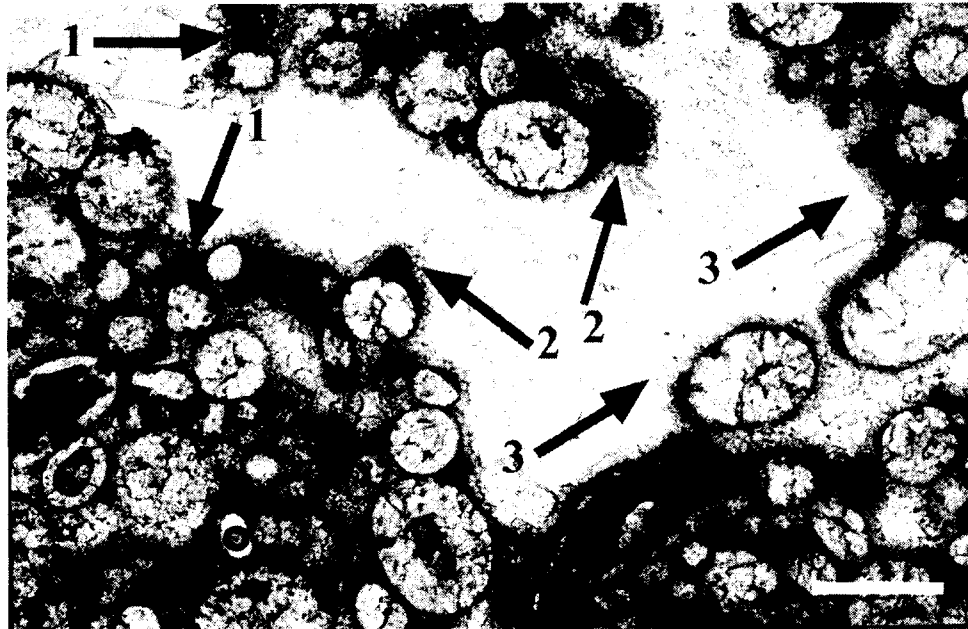
**Figure 2.17.** Outcrop of cross-bedded ooid grainstone in lower Farley at locality MCI (see Figure 2.1 for locality map).



**Figure 2.18.** (A) Rose diagram illustrating paleocurrent directions as measured from cross-bed orientation data. Based on 20 measurements collected from the lower Farley oolite at locality MCI. (B) Outcrop photo of cross-bedded oolite at locality MCI (see figure 2.1 for locality map). Note the variable cross-bed directions.







**Figure 2.19.** Photomicrograph of ooid, peloid packstone with large keystone vug. Note the micritic cement showing meniscus (1) and an asymmetric fabric similar to pendant cement (2). Also note the later isopachous fringe of bladed calcite cement (3). Final pore fill is coarse baroque dolomite and calcite spar (transmitted light; sample BS-3; scale bar = 500 micrometers).

## Environmental Interpretation

Harris (1984) described modern accumulations of several oolite facies around Joulters Cay on the Great Bahama Bank, including oolite grainstone and fine-peloid packstone that contains peloids, micritized ooids, and skeletal fragments. These two modern facies are similar to the oolite subfacies described from the Farley Limestone. Harris (1984) reported that fine-peloid packstones containing ooids accumulated in protected lows and that ooid grainstones formed on bedrock highs where bottom agitation was focused.

Although slight differences exist, an analogy between these modern oolites and oolites in the Farley Limestone is supportable. The micrite-free oolite grainstones are cross-bedded and represent deposition in the highest energy waters. Alternatively, the ooid, peloid packstones represent deposition in protected areas or deeper-water areas that had lower energy levels. Diagnostic indications of shallow water for the ooid, peloid packstone subfacies include the presence of keystone vugs and meniscus fabrics as well as, asymmetric pendant-like fabrics. These fabrics indicate cementation in the presence of water and air such as occurs in the marine or phreatic vadose zones (Tucker, 1991).

### ***Osagia-Brachiopod Packstone Facies***

Located within a single bed (30 to 95 cm thick) at the base of the upper Farley, the *Osagia*-brachiopod packstone facies (Fig. 2.20) is a marker bed and is useful for correlation. It is medium to medium-light gray (N5-N6) at the base and commonly has a color change to lighter gray toward the top (N7). This facies is distinguished by a zone of skeletal material and whole brachiopods, typically *Composita*. Other than the *Composita* there is little to no other coarse skeletal material. The brachiopods are typically encrusted

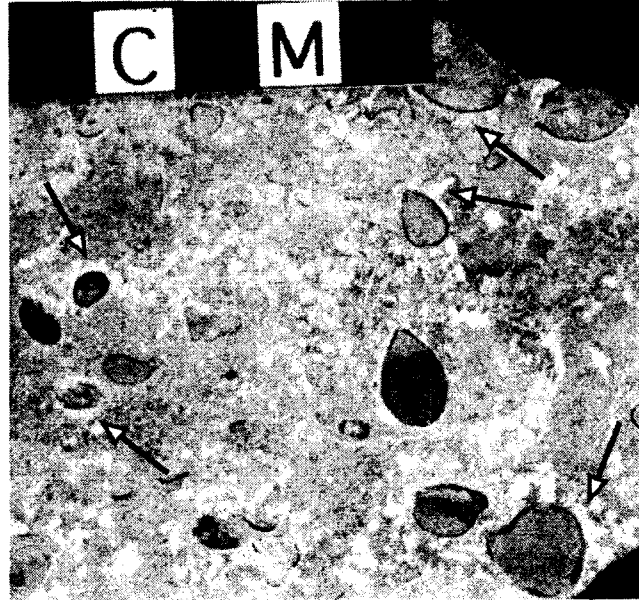
by *Osagia* (Figure 2.20, 2.21). Johnson (1963) described *Osagia* as colonies that consist of twisted tubes of varying sizes that form a laminated encrustation around a nucleus of fossil fragment or other foreign substance. The smaller tubes have dark walls and, in some examples, cross partitions. *Osagia* has been found to consist of an intergrowth of small tubular algae, similar to *Girvanella*, and the encrusting foraminifer *Nubecularia* (Johnson, 1963).

In the Farley, these encrusting masses completely or partially encrust grains of all types but seem to be most commonly found on whole brachiopods, brachiopod fragments, and phylloid-algal fragments. The coatings have a wide range of morphologies. In some samples they are irregular, thick, asymmetrical coatings, whereas in other occurrences they are symmetrical, thinly laminated coatings. The *Osagia* coated grains can be found throughout the bed but typically occur in the middle to upper half of the bed.

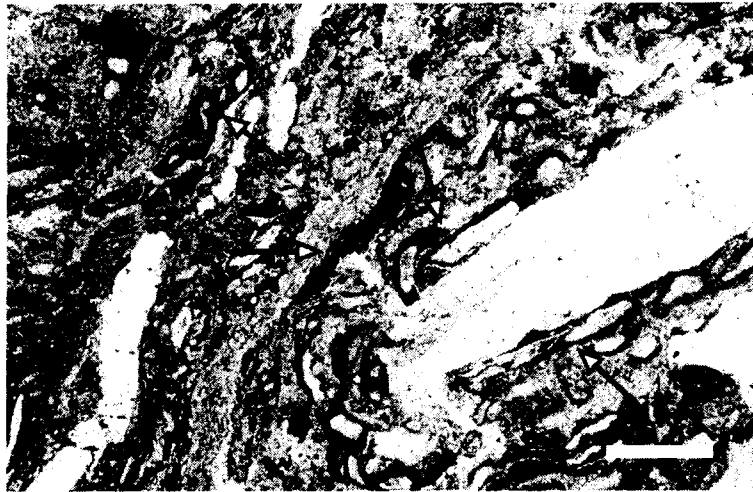
#### Environmental Interpretation

The wide distribution and consistent stratigraphic location and facies character of the *Osagia*-brachiopod packstone facies suggests that at the time of its deposition the environment was similar throughout the study area. Ginsburg (1960) reported that modern oncolites are formed in low intertidal and shallow subtidal zones and interpreted a similar environment for *Osagia*. Wilson (1975) indicated that oncolitic coatings commonly form in restricted marine bays and lagoons. Asymmetrical coatings of *Osagia* develop when the nucleus on which the coating is growing is occasionally overturned by wave action allowing growth to continue on a new surface (Ginsburg, 1960).

In the current study, the presence of *Osagia* coatings on all sides of a skeletal grain indicates an energy level just strong enough to overturn occasionally the grains



**Figure 2.20.** Hand sample of *Osagia*, brachiopod packstone facies. *Osagia* coatings are easily visible as white coatings on skeletal fragments and whole fossils (arrows). Also note the abundance of dense micritic matrix (sample BS-5).



**Figure 2.21.** Photomicrograph of *Osagia*, brachiopod packstone facies. Note the large brachiopod fragment with a coating of *Osagia* (arrows) recognized by the chambers (typically spar-filled) surrounded by dense (black) algal growth (transmitted light; sample SH-8; scale bar = 1 mm).

supporting the algal coatings. In many cases the *Osagia*-coated grains are skeletal fragments and small brachiopods that would not have required significant wave energies to move them. Furthermore, the abundance of micrite matrix suggests a moderate to low-energy environment as does the preservation of brachiopods articulated valves. Furthermore the presence of a low-diversity fauna dominated by *Composita* brachiopods indicates a somewhat restricted environment (Ramsbottom, 1978).

### ***Fossiliferous Siltstone***

Richly fossiliferous siltstones occur in the Farley and Lane-Island Creek shales throughout the study area. The fossiliferous siltstones represent the thinnest (20 to 150 cm thick) overall accumulations of siltstone in the Lane-Island Creek and middle Farley. They have a platy to blocky texture and a light bluish-gray to medium-gray color (5B 7/1-N5) on outcrops and in cores. The siltstones are highly calcareous and slightly micaceous and have no sedimentary structures, although burrow molds are present in some outcrops (Figure 2.22).

Most fossil material is fragmental although there are whole brachiopods, gastropods, and bivalves in some localities and the fossiliferous texture shows up best in weathered sections (Figure 2.23). In cores the fossiliferous siltstones are blocky to massive and contain variable amounts of fossil material (Figure 2.24). In the Lane-Island Creek, these fossiliferous siltstones are dominated by crinoid ossicles and calyx plates as well as articulated crinoid columnals, with brachiopods and fenestrate and ramose bryozoans also abundant. Fusulinid foraminifera are also present in minor amounts in two sections in the Island Creek. In the middle Farley siltstones, the fossil assemblage is dominated by fenestrate bryozoans and brachiopods with crinoids, bivalves, and gastropods present but less abundant.

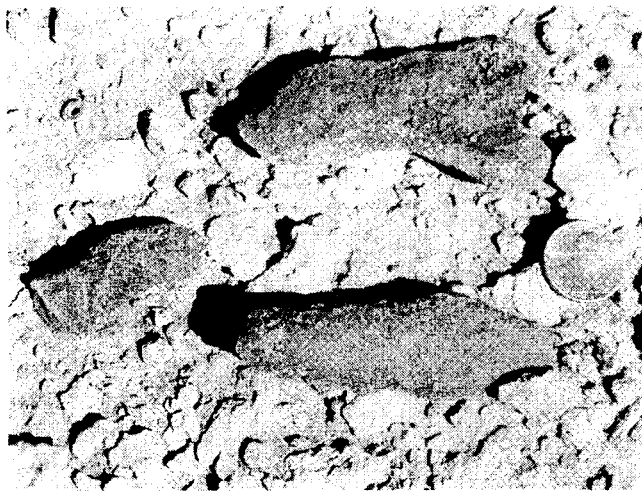
## Environmental Interpretation

Crinoids and other echinoderms are stenohaline, and their remains are originate in sediments of fully marine origin (Clarkson, 1993). Brachiopods are also normal-marine organisms, whereas bryozoans are able to survive in restricted conditions; but they prefer normal-marine environments (Heckel, 1972b).

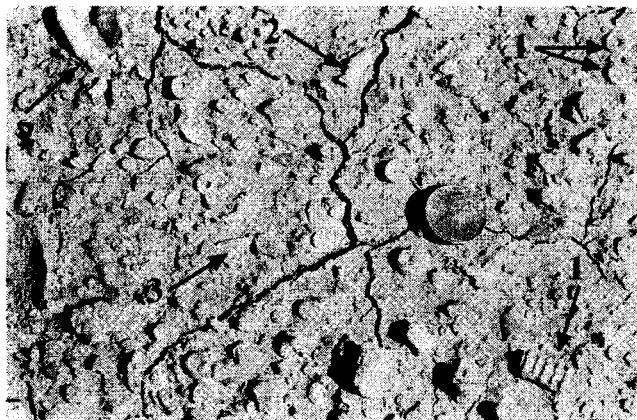
We interpret the environment of the fossiliferous siltstones as one of normal marine salinity and low energy levels. The most likely situation that gave rise to the fossiliferous siltstone facies is deposition in areas between the Lane and Island Creek deltas and in areas distal to the middle Farley delta. In these deeper areas between or distal to thickened delta lobes, water was clearer and calmer; and a normal-marine fauna could exist. Occasionally, influxes of large quantities of silty material from the deltas swamped and buried the organisms. Following this, the fauna recovered and bioturbation destroyed sedimentary structures and disrupted and disarticulated the buried fossils.

### ***Lenticular Bedded-Laminated Siltstone and Fine Sandstone***

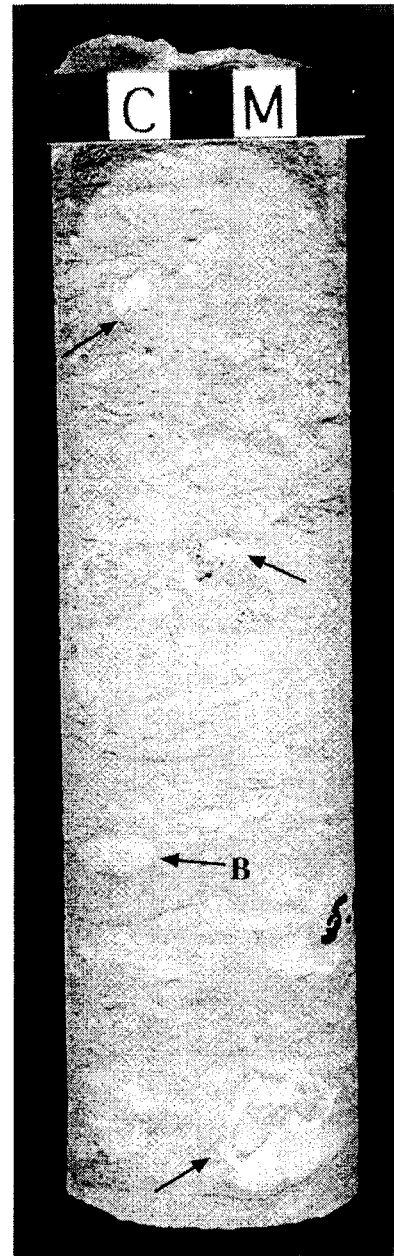
Siltstones with millimeter- to centimeter-scale lamination and lenticular bedding occur in both the middle Farley and Lane-Island Creek shales. The nature of this facies is most visible in cores (Fig. 2.25) and on very fresh outcrops. On weathered outcrops this facies appears as a platy to fissile, fine sandstone to siltstone (Figure 2.26). Colors vary with grain size with the siltstone being medium-light to medium gray (N6-N5) and the sandstone very light gray to light gray (N8-N7). The siltstone is noncalcareous, but the sandstone lenses and laminations are slightly calcareous. Fine sand-sized and coarser mica grains are abundant in this facies and are most visible in cores and on very fresh outcrops.



**Figure 2.22.** Burrow molds taken from fossiliferous siltstone facies. Burrows are distinguished by their circular to ellipsoid cross-section and are typically filled with fine sand and have silt and sand accreted to the outer surfaces (locality WR). Penny for scale.



**Figure 2.23.** Outcrop surface of fossiliferous shale. Note abundant fossil material including crinoid ossicles (1), ramose bryozoans (2), and brachiopod (3) fragments (locality WR). Penny for scale.



**Figure 2.24.** Core section showing nature of fossiliferous siltstone facies. Fossil fragments are white (arrows) in core and the siltstone is blocky to massive. Also visible are horizontal burrows (B); (locality C5).

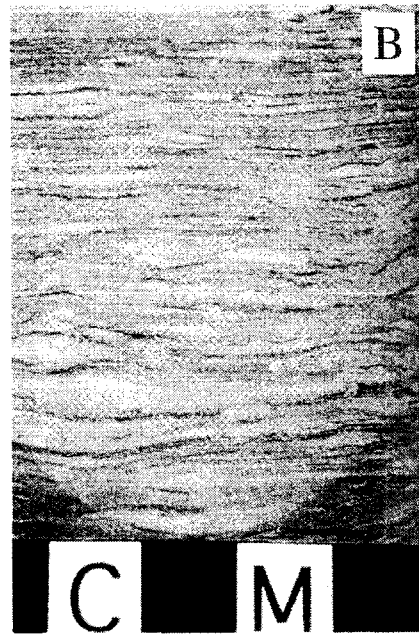
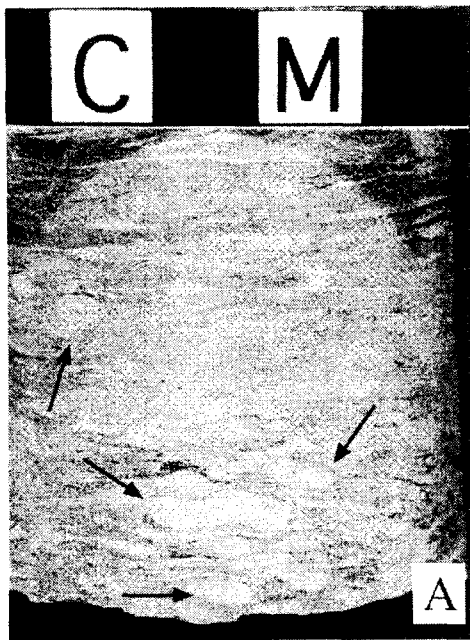
The lenticular bedding observed in cores and on fresh outcrops is the result of millimeter- to centimeter-scale laminations and lenses of fine sandstone within the finer siltstone. Faint, millimeter-scale ripple cross-laminations occur in the sand lenses in core and on fresh outcrop. Although no body fossils are present in this facies, horizontal burrow molds occur in most sections (Figure 2.25). The burrows are most visible in core and appear as circular to ellipsoid sandstone lenses in cross-section. These burrow forms typically distort and cross-cut laminations and lenticular bedding. The abundance of burrows is greater in the Island Creek siltstones, whereas the middle Farley siltstones have fewer burrows and much finer laminations (2 to 8 mm in the middle Farley v. 5 to 15 mm in the Island Creek) and lenticular bedding (Figure 2.25).

#### Environmental Interpretation

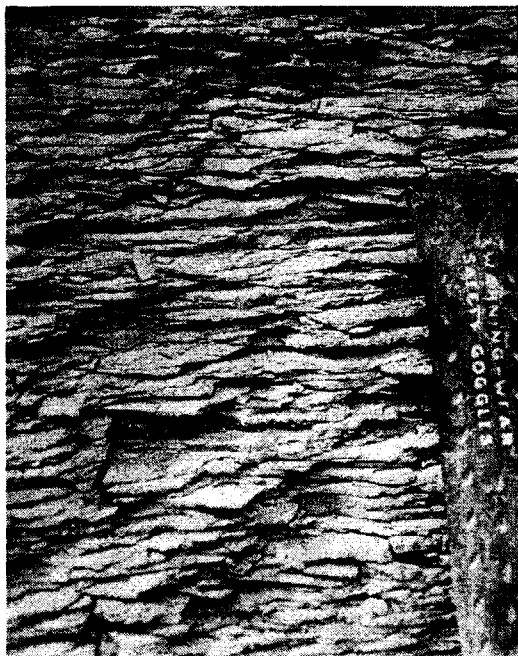
Reineck and Singh (1980) stated that lenticular bedding requires conditions of current or wave action depositing sand, alternating with slack-water conditions when mud is deposited. Furthermore, they concluded that it occurs primarily in subtidal zones and intertidal zones. Lenticular bedding is also a common feature of delta-front environments where sediment supply and flow strength fluctuate (Tucker, 1991).

Sedimentary structures similar to those observed in the middle Farley and Lane-Island Creek are found in the modern Mississippi delta. Moore and Scruton (1957) noted the presence of laminated to lenticular bedded sediments (their regular to irregular layers) in the Mississippi delta and they noted that these structures were present in two bands of sediments surrounding the delta in waters 6 to 300 feet deep. Additionally, they noted that such fine sedimentary structures as laminations and lenticular bedding are highly vulnerable to destruction and are most likely to be preserved in an environment which has rapid deposition or very few organisms (Moore and Scruton, 1957).





**Figure 2.25.** Core sections showing the fabric of the laminated to lenticular bedded siltstone and fine sandstone facies. (A) This core section from the Island Creek Shale contains abundant horizontal burrow molds (arrows) that disrupt laminations and lenticular bedding. (Core #3)  
 (B) This core section from the middle Farley shows finer laminations and contains fewer burrows. (Core # 3)



**Figure 2.26.** Photo showing nature of laminated to lenticular bedded siltstone to fine sandstone facies as it appears on weathered outcrop. Typical expression is as a platy to slightly fissile siltstone to fine sandstone. Ripple cross-laminations are rarely visible except on very fresh outcrops.

Shepard (1964) also discussed the presence of well-laminated sediments in the delta front of the Mississippi and stated that delta facies can be recognized by the abundance of lamination and the scarcity of marine organisms. Whereas the presence of burrows, especially in the Island Creek-Lane, indicates some bioturbation, the abundance of preserved sedimentary structures suggests rapid deposition that outpaced bioturbation. Therefore, it is most likely that the laminated to lenticular bedded siltstones and fine sandstones present in the middle Farley and Lane-Island Creek represent accumulations of marine, tidally dominated delta front to prodelta sediments rapidly deposited in shallow water or perhaps in depths to approximately 80 meters.

### ***Organic-rich Mudstone and Coal***

Darkly colored mudstones with high concentrations of plant debris, rootlets and organic matter occur in the southern part of the field area. These thin mudstones (15 to 50 cm thick) range in color from olive gray to grayish black (5Y 4/1-N2). The deposits are blocky to massive and not fissile. Also, there is a thin coal (2 to 5 cm thick) which may grade upward to typical dark mudstone. In addition to the abundant plant debris and rootlets, there is a fauna of very small (1 cm or less) bivalves. These fossils are rare and are the only body fossils observed.

### **Environmental Interpretation**

Dark gray to black shales of the Midcontinent are typically attributed to deposition in deep, anoxic waters far offshore (Heckel, 1977). These deep-water black shales are typically fissile and contain phosphate, pyrite, and an abundance of such pelagic fossils as conodonts and ammonoids (Heckel, 1977). The dark organic-rich mudstones described in the current study, however, are not fissile and do not contain phosphate or pelagic fossils.

It appears more likely that the dark organic-rich mudstones described herein were deposited in a brackish marsh or lagoonal environment. Lagoonal bottom sediments are muddy and black with hardly any traces of primary bedding visible due to bioturbation (Reineck & Singh, 1975). Reducing conditions within lagoonal environments are characterized by abundant well-preserved plant debris (Reineck & Singh, 1975) such as is preserved in the organic-rich mudstone and coal facies of this study. The thin coal seam in this facies further supports the interpretation of a lagoonal environment as does the absence of abundant and diverse fauna. The rare body fossils are small and probably are a restricted, dwarfed fauna.

### ***Blocky Mudstone***

Blocky mudstones (Fig. 2.27) are present in the middle Farley and the Island Creek Shale. In all occurrences the blocky mudstones are noncalcareous and comprise fine silt to clay with abundant mica. Colors typically range from medium, light gray (N6) to light olive gray (5Y 6/1) on fresh outcrops and in cores. Weathered outcrops have a large variety of colors with mottling common. Additional colors observed include shades of brown, olive green, and bluish gray.

The mudstones of the middle Farley are massively bedded and exhibit irregular curved fractures on outcrops. Hand samples and core sections break into irregular blocky masses 2 to 10 cm in longest dimension, with irregular to curved, slightly glossy fracture surfaces. In middle Farley outcrops and cores, striations are common on the glossy fracture surfaces (Figure 2.28). Body fossils are absent from all occurrences, but plant debris is abundant both on outcrops and in cores (Figure 2.29). Additionally, small tubular structures filled with light brown (5YR 5/6) residues are also common in the middle Farley.

The blocky mudstones of the Island Creek are of a slightly different nature than those found in the middle Farley. The Island Creek blocky mudstones are also massive bedded but have much more consistent coloration. The Island Creek blocky mudstones contain rare body fossils, typically small bivalves. The other main difference is that the blocky mudstones of the Island Creek have no glossy, striated fracture surfaces.

### Environmental Interpretation

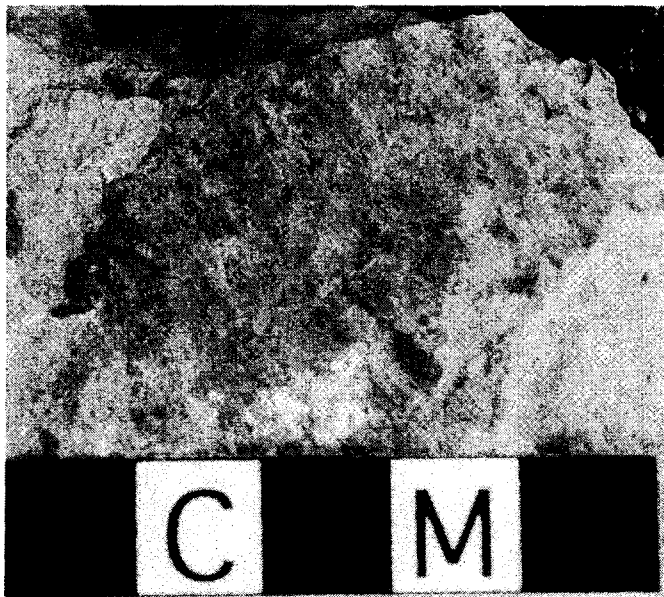
The blocky mudstones of the middle Farley exhibit features common to ancient soils. Watney *et al.* (1989) indicated diagnostic features used to identify paleosols including: (1) rhizoliths (rootlets), (2) ped surfaces in blocky mudstones, and (3) color mottling or isolated horizons of color. The blocky mudstones of the middle Farley and Island Creek have all of these features.

The blocky or brecciated nature of the mudstones results from the relict ped structure of the soil. Ped surfaces in the middle Farley are recognizable by their irregular to slightly curved surfaces with glossy striated coatings. The slightly glossy, surfaces of the blocky mudstones represent cutans and the striations are slickensides. Slickensides form in clayey soils where peds are repeatedly heaved past one another by swelling and shrinking during episodes of wetting and drying (Retallack, 1990).

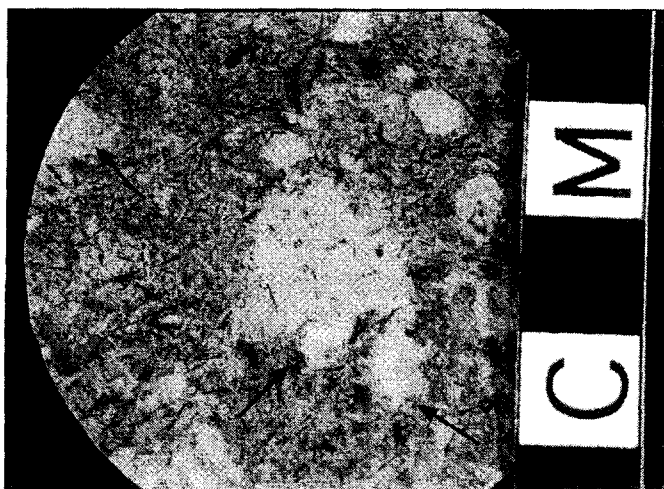
The mottled coloration of the middle Farley blocky mudstones is also characteristic of paleosols. Color mottling is typically a result of differential oxidation of iron and redistribution and formation of clay minerals (illuviation) (Watney *et al.*, 1989). Further evidence of paleosol development are the small tubular structures that represent rootlets. Based on these several characteristics common to paleosols, the blocky mudstones of the middle Farley are confidently identified as ancient soil horizons.



**Figure 2.27.** Blocky mudstone in the middle Farley as it appears on weathered outcrop. Note the blocky texture and color variations. (locality MCI)



**Figure 2.28.** Detail photograph of ped surface from the blocky mudstone facies. Note the glossy appearance and the striations on the surface. The glossy coating is the soil cutan and the striations are soil slickensides (sample from middle Farley, locality SRS).



**Figure 2.29.** Cross-section of core section with abundant plant material. Plant material (leaf, root and twig fragments) is very abundant in the blocky mudstone facies and is typically well preserved. Also note vertical root tubes visible in the core (arrows) (Core #4-Island Creek).

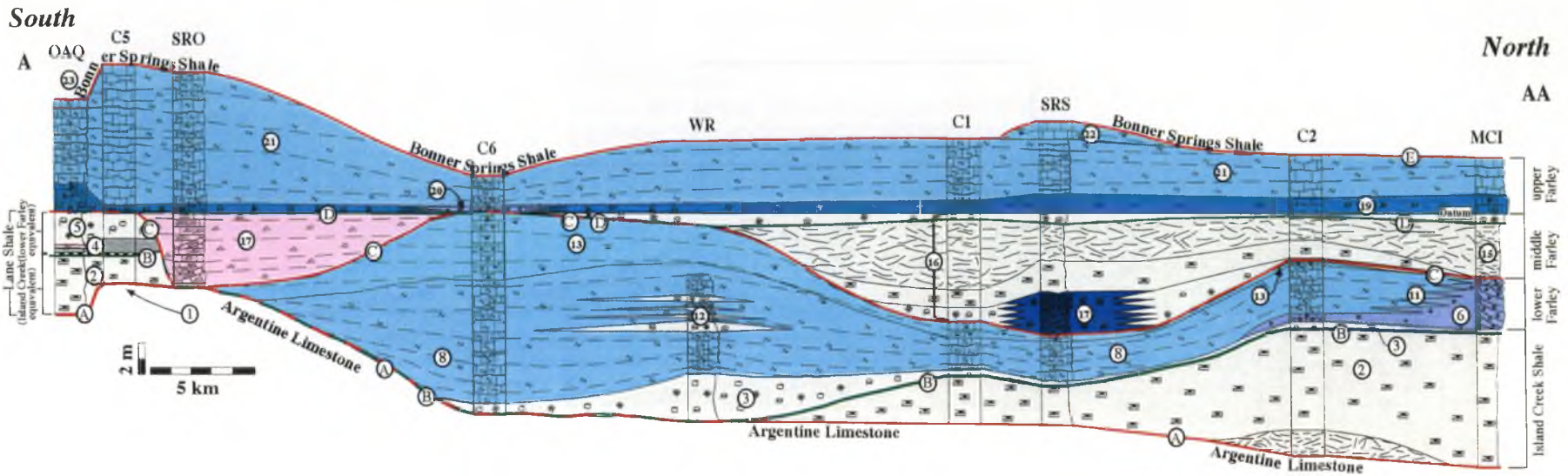
The lack of paleosol features and the presence of small body fossils indicates a different origin for the blocky mudstones of the Island Creek. The blocky mudstones of the Island Creek are interpreted as prodelta deposits. Prodelta deposits are characteristically fine-grained muddy sediments often containing shell remains and plant and wood debris (Reineck & Singh, 1975). Shepard (1957) described prodeltaic deposits of the modern Mississippi as homogeneous, structureless fine-grained clays and silty clays deposited in water depths greater than about 120 feet.

### **Stratigraphic Correlations and Sequence-Stratigraphic Interpretations**

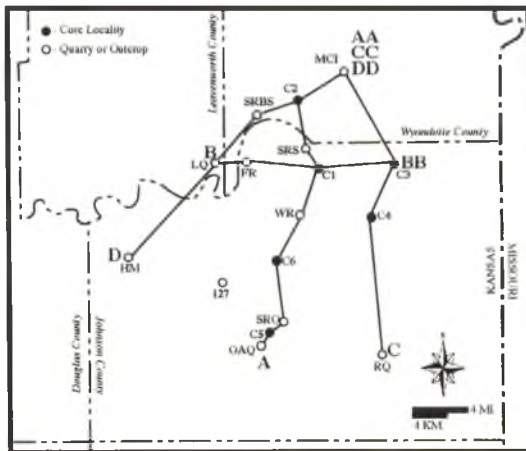
The stratigraphic correlations discussed below are illustrated in Figures 2.30 to 2.34. These figures are cross-sections and a fence diagram that present information gathered from stratigraphic description of outcrops, quarry exposures, and drill cores. Detailed measured stratigraphic sections of all localities are in Appendix 1. The goal of these correlations is to establish a sequence-stratigraphic framework that identifies sequence boundaries that indicate rise and fall of sea level as well as other significant stratigraphic surfaces on a regional scale (e.g., flooding surfaces). The establishment of such a framework in which sea-level history is known allows the examination of other influences on deposition such as depositional topography and distribution of siliciclastics. The following sections present the regional and stratigraphic distribution of lithofacies and uses their interpreted depositional environments and further detailed observations relevant to their sequence-stratigraphic interpretation to evaluate the controls on regional distribution of lithofacies.

### ***Stratigraphic Datum***

The basal bed of the upper Farley (30 to 90 cm thick) contains the only *Osagia*-brachiopod packstone facies found. This bed has consistent lithologic character and



**Figure 2.30.** Reconstructed cross-section along line A-AA. Index map shows localities used all stratigraphic reconstructions. Legend outlines lithologic symbols and color codes used for this figure and Figures 2.31-2.33.

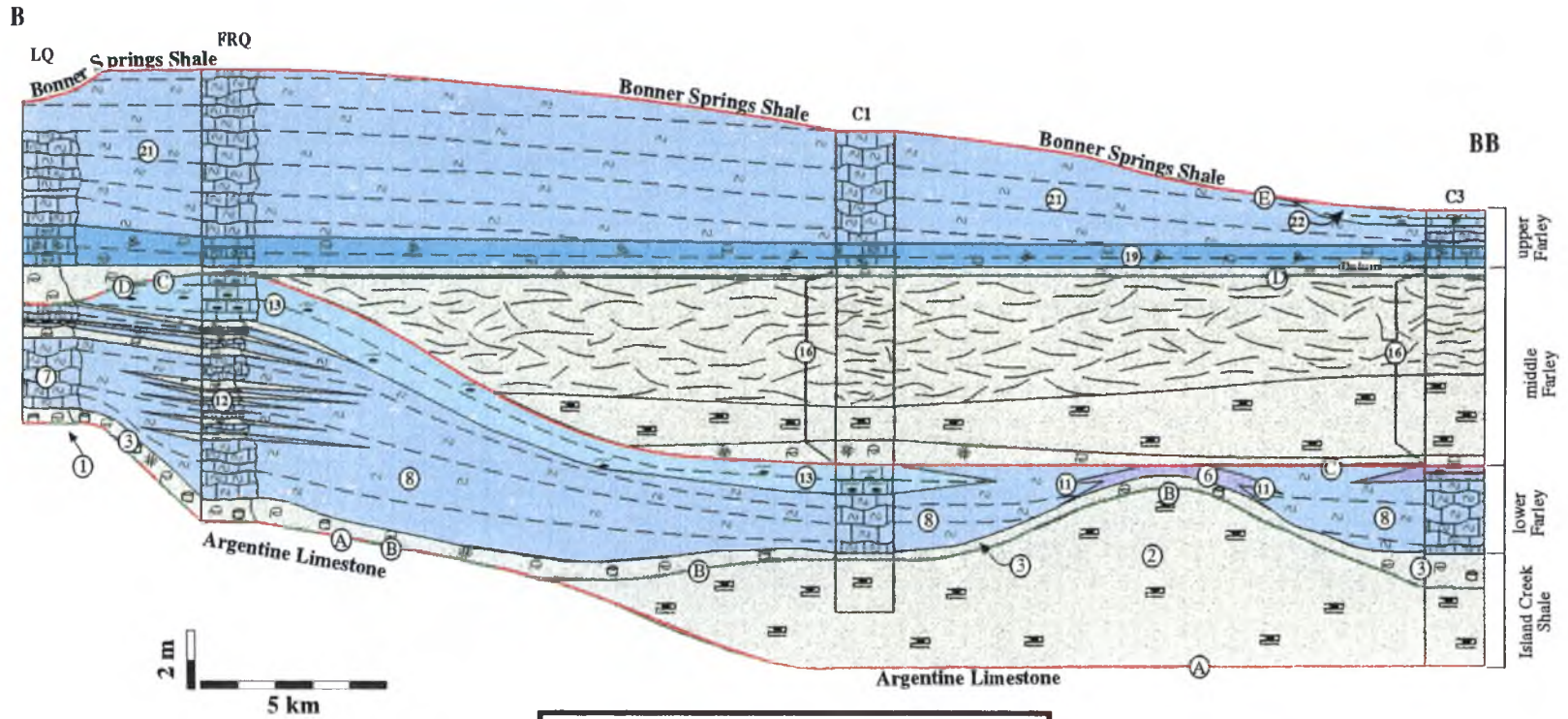


- |  |                                       |  |   |
|--|---------------------------------------|--|---|
|  | Phylloid Algal Facies                 |  | Coal  |
|  | Skeletal Wackestone                   |  | Dark, Organic-rich Mudstone                     |
|  | Peloidal, Skeletal Packstone          |  | Fossiliferous Siltstone                         |
|  | <i>Osagia</i> , Brachiopod Wackestone |  | Lenticular, Laminated Siltstone                 |
|  | Oolite                                |  | Blocky Mudstone                                 |
|  | Sandy, Skeletal Grainstone-Packstone  |  | Feature Number/ Surface Letter                  |
|  |                                       |  | Sequence Boundary                               |
|  |                                       |  | Marine Flooding Surface                         |
|  |                                       |  | Coincident Flooding Surface & Sequence Boundary |



West

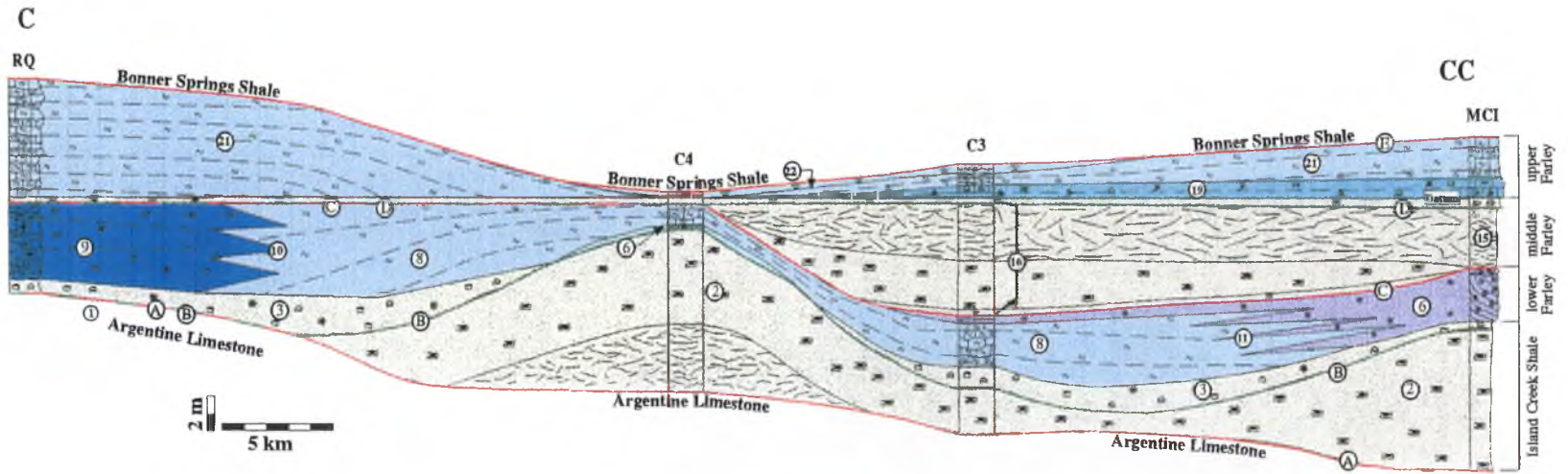
East



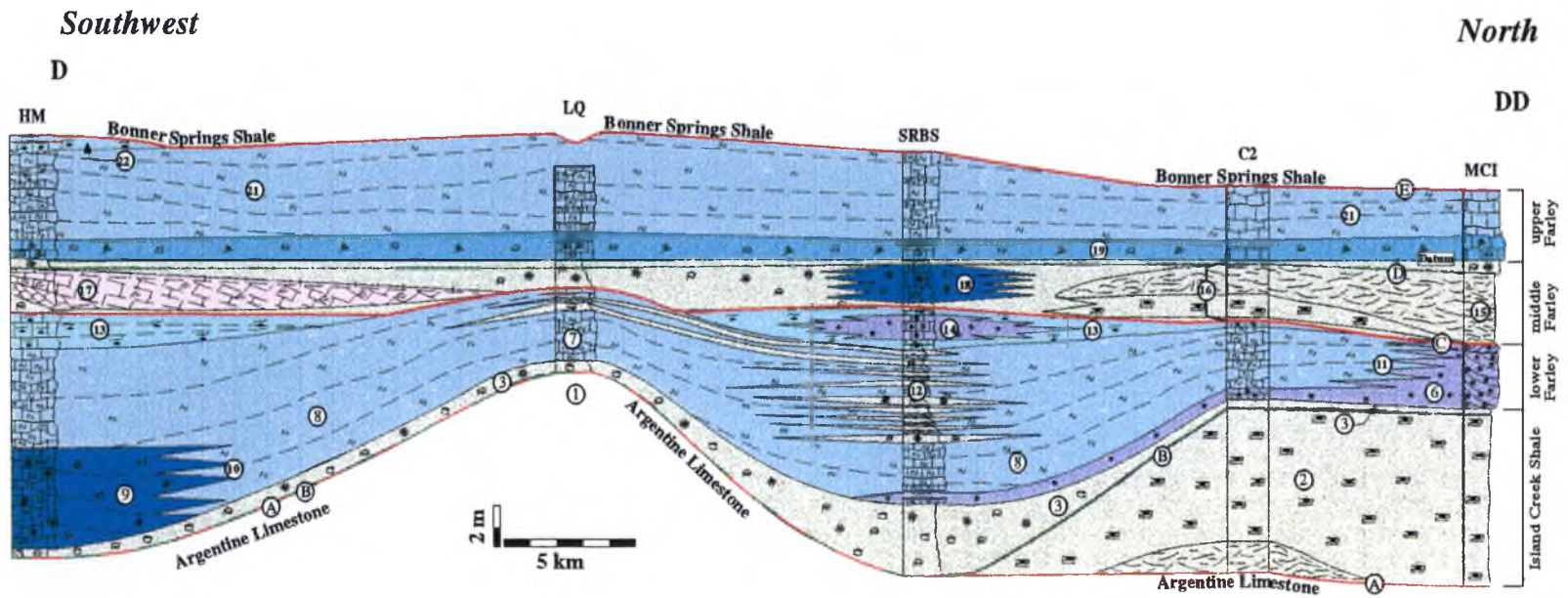
**Figure 2.31.** Reconstructed cross-sections along line B-BB. See figure 2.30 for legend and index map.

Southeast

North

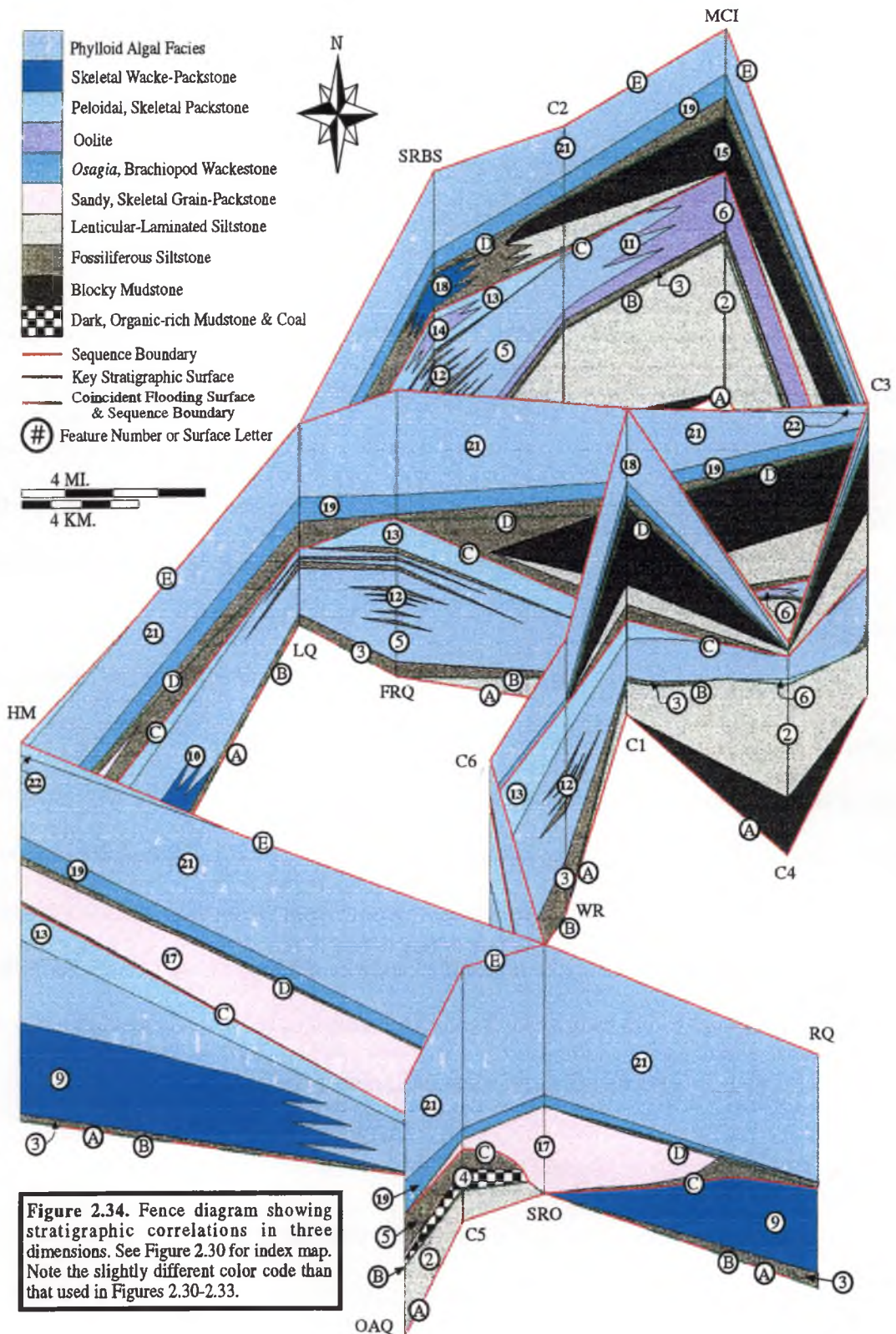


**Figure 2.32.** Reconstructed cross-sections along line C-CC. See Figure 2.30 for index map and legend.



**Figure 2.33.** Reconstructed cross-section along line D-DD. See Figure 2.30 for locality map and legend.





**Figure 2.34.** Fence diagram showing stratigraphic correlations in three dimensions. See Figure 2.30 for index map. Note the slightly different color code than that used in Figures 2.30-2.33.

stratigraphic location throughout the field area. The bed is recognized by a zone of whole brachiopods, brachiopod fragments, and other skeletal fragments that are encrusted with *Osagia*. The lithologic consistency of this thin bed suggests a similar environment throughout the area and is interpreted to have been deposited on a relatively flat depositional surface. For these reasons, the basal bed of the upper Farley makes an excellent marker bed and is the datum for the stratigraphic reconstructions (Figures 2.30 to 2.33). Use of this datum allows the closest possible reconstruction of actual depositional topography.

Isopach mapping based on data from Crowley (1969) and this study (Fig. 2.3) shows thickened areas of Argentine Limestone in the northeast, northwest, and southeast corners with an additional, slightly thickened area near the center of the field area. These topographic highs in the Argentine are also apparent in the reconstructed cross-sections (Figs. 2.30-2.33: Feature 1), which further indicates that the basal bed of the upper Farley is a reasonable datum to use for the stratigraphic reconstructions.

The stratigraphic reconstructions offered do not depict exact depositional topography for two main reasons. First, other regional work by Watney *et al.* (1989) suggests that the area may have had a slight south-southwestward dip that cannot be shown in the cross-sections. Second, compaction of shale and silt following deposition can alter thicknesses of a stratigraphic succession by as much as 40-50 percent (Tucker, 1991). These factors provide additional difficulties when attempting to accurately depict depositional topography. The following discussion separates the correlated strata into three stratigraphic intervals with related surfaces and discusses their origin.

#### ***Argentine Limestone (Stratigraphic Surface A)***

The Argentine Limestone is the carbonate unit located directly under the Lane-Island Creek shales or the Farley Limestone at all localities (Figures 2.30-2.33). The

Argentine Limestone has been interpreted as a fully marine unit with such facies as phylloid algal packstones, oolite, and skeletal packstone (Crowley, 1969; Watney *et al.*, 1989; Arvidson, 1990; this study)

Throughout the field area the Argentine Limestone has an irregular surface near its top that has been interpreted as a marine hardground or firmground (Watney *et al.*, 1989). This surface is most prominently developed in the west, center, and south (Localities HM, RQ, WR) where it is overlain by a thin fossiliferous siltstone. These areas received little to no siliciclastic influx, and this surface near the top of the Argentine represents the first significant surface in the sequence-stratigraphic framework of the Lane-Island Creek shales and the Farley Limestone (Figures 2.30-2.34: Surface A). This surface appears to be a surface of nondeposition that coincides with the time period between termination of Argentine carbonate deposition and the influx of the siliciclastics of the Lane-Island Creek shales discussed below.

### ***Lane-Island Creek Interval***

Directly overlying the Argentine Limestone in the north (localities MCI, C2), east (locality C4), and the south (localities OAQ, C5) are thick siltstones that are somewhat thinner in the east and west-central areas (localities SRS, C1 & C3) (Figures 2.30-2.34: Feature 2). These siltstones comprise the Lane-Island Creek shales, and the facies present are dominantly laminated to lenticular bedded siltstones but also include local accumulations of blocky mudstone. As discussed previously, these siltstone facies are interpreted as delta front to prodelta deposits. It is important to consider what controlled the distribution of these deposits.

Isopach mapping of the Lane-Island Creek interval (Fig. 2.4) suggests that the siliciclastics form two separate deltaic units with source in different directions. The Island Creek appears to have a northern source, whereas the Lane has a southern source.

Comparison of isopach maps for the Argentine Limestone and the Lane-Island Creek shales (Figs 2.3 & 2.4) suggest that the distribution of the deltaic siliciclastics was closely controlled by the subtle depositional topography of the Argentine Limestone. There are paleotopographic highs (thicks) in the Argentine Limestone in the northwest and northeast corners of the field area, and the Island Creek appears to fill a channel-shaped depositional low between these two topographic highs. Furthermore, the Island Creek delta thins into and terminates against a topographic high in the Argentine in the southeast corner of the area (Figures 2.3 & 2.4). This distribution of siliciclastics suggests that the deltaic deposits of the Island Creek did not form a topographically positive lobe or wedge as suggested by earlier authors (Crowley, 1969; Arvidson, 1990). Instead, these deltaic siliciclastics seemed to have behaved more as valley fills by filling depositional lows in the underlying limestone.

Distribution of the Lane deltaic sediments in the southern part of the field area also appears to have been controlled by the paleotopography of the Argentine Limestone (Figures 2.3 & 2.4). The lower part of the Lane delta extends into the area from the southwest and covers a broad area. This broad distribution could have been because there were fewer topographic restrictions on the underlying Argentine Limestone (Figure 2.4). The same isopach maps (Figs. 2.3 & 2.4) suggest that the siliciclastics of the Lane-Island Creek deltas in part overlapped highs in the Argentine Limestone.

The presence of deltaic siliciclastics immediately overlying the marine Argentine Limestone is interpreted as the result of a relative fall in sea level. This relative sea-level fall allowed the influx of deltaic siliciclastics from the north (Island Creek) and the south (Lane), which terminated deposition of Argentine carbonates. Interpretation of a relative sea-level fall is supported by the presence of two separate deltaic units that encroached into the area from different directions at the same time. Although the presence of deltaic

sediments overlying Argentine carbonates could have resulted from autogenic delta-lobe switching, the presence of two deltas entering the area from different directions at the same time would be unexpected; their migration is more likely the result of a relative sea-level fall. Thus, the boundary separating the underlying Argentine Limestone from the overlying siliciclastics of the Lane-Island Creek shales is interpreted as a sequence boundary (Figures 2.30 to 2.34: Surface A).

A lack of evidence of subaerial exposure in the Lane-Island Creek or along the top of the Argentine Limestone indicates that the relative sea-level fall was not extensive enough to expose the upper surface of the Argentine within the study area. It was, however, great enough to allow deltas to enter the area from both the north and south. This increase in siliciclastic input effectively shut down carbonate production. In areas receiving no deltaic siliciclastic influx, a marine hardground developed in the upper portion of the Argentine Limestone.

#### ***Upper Island Creek-Lower Farley Interval***

The lower Farley interval consists of a variety of siltstone and carbonate facies throughout the field area. The initial deposits of this interval are fossiliferous siltstones that are interpreted as accumulations of marine, prodeltaic sediments. These deposits overlie the deltaic siliciclastics of the Island Creek in the north and occur immediately over the Argentine Limestone in the western, southwestern, and central portions of the area where there are no deltaic siliciclastics (Figures 2.30 to 2.34: Feature 3). The fossiliferous siltstones are not present over the deltaic siliciclastics to the south in the area of the Lane delta. Instead, in this area the deposits immediately overlying the deltaic siliciclastics are composed of coal and dark, organic-rich shale with a local accumulation of sandy, skeletal grainstone-packstone (Figures 2.30, 2.34: Feature 4).



The fossiliferous siltstones to the north and west are correlated with the coal and dark, organic-rich mudstones and sandy, skeletal grainstone-packstones in the middle portion of the Lane delta to the south because the fossiliferous siltstones and the coal and dark, organic-rich mudstones and grainy skeletal bed all provide evidence of a marine flooding unit. These lithologies are similar to those described for flooding units in other similar Pennsylvanian units by Watney *et al.*, (1989), who stated that lithologies such as thin, fossiliferous siltstones as well as coals capped by invertebrate skeletal lags, are typically flooding units in Pennsylvanian depositional sequences. Furthermore, the widespread, regional extent of these marine lithologies suggests a major flooding event. Thus, the fossiliferous siltstones and the coal and dark, organic-rich mudstone capped by the sandy, skeletal grainstone-packstone are a single flooding unit expressed as different lithologies. Because flooding surfaces are important in interpreting the sequence stratigraphy, the base of this flooding unit is identified as the next key stratigraphic surface (Figures 2.30 to 2.34: Surface B).

Based on its lithofacies, the environments represented by the flooding unit have been interpreted as marine (fossiliferous siltstone) or restricted marine (dark, organic-rich mudstone). This switch to more marine facies suggests that siliciclastic sources had become more distal, and waters were more normal marine in salinity. Therefore, the transition from deltaic clastics to marine or restricted marine clastics probably resulted from a relative rise in sea level. In areas that received little to no deltaic influx, the marine flooding surface coincides with surface A, so that surfaces A and B are coincident in places.

Following the relative rise of sea level, carbonate production was established in all areas except the area of the Lane delta in the south, where fossiliferous siltstones continued to accumulate as prodelta deposits of the Lane delta while the lower Farley carbonates were being deposited (Figures 2.30, 2.34: Feature 5). Oolites and peloidal,

skeletal packstones accumulated in the north and east along topographic highs formed by the thick complex of the Island Creek siliciclastics (Figures 2.30 to 2.34: Feature 6). The thickness of the deltaic deposits produced a slight topographic prominence along which elevated energies prevailed due to shallower water depths. Phylloid algal facies are located in lows and directly over topographic highs (Figs. 2.31, 2.33: Feature 7) in the west, indicating deeper water depths to the west. Such an increase in depth was likely to have been due to original depositional slope which was approximately  $0.6 \text{ m}/\text{km}$  to the west-southwest (Watney et al, 1989).

The greatest accumulations of phylloid-algal limestones in the lower Farley interval are generally located in topographic lows adjacent to topographic prominences on either the Argentine Limestone or the Island Creek delta. (Figures 2.30 to 2.33: Feature 8). Therefore, it appears most likely that the phylloid algae of the lower Farley Limestone did not contribute to the construction of depositional topography as suggested by previous authors (Heckel & Cocke, 1969; Harbaugh, 1959, 1960; Arvidson, 1990). Although interpretation of phylloid algae located in depositional lows is contrary to the normal interpretation of topography construction for such facies, it is not new. Matheny and Longman (1996) showed that some of the phylloid-algal facies of the Paradox Basin are concentrated in depositional lows caused by salt solution. Ball *et al.* (1977) suggested that phylloid algae did not construct topography but were instead only a source of sediment that typically collected in depositional lows between deltaic depocenters. The situation in the lower Farley Limestone is likely to have been a combination of these two interpretations. Much of the phylloid algal material is fragmental and apparently not in growth position, which suggests that it may have been transported into the depositional lows. There are, however, also occurrences of phylloid-algal boundstone that may have

grown in the lows and not been transported. At this time the exact controls on the distribution of the phylloid algal facies are unknown.

In the southeast and southwest, in areas of deeper water farthest from deltaic siliciclastics, the quiet-water, skeletal wackestone-packstone facies was deposited (Figures 2.32 to 2.34: Feature 9). A more open-marine environment, promoted the deposition of the skeletal wackestone-packstone facies, was present in deeper, clear waters distal to the deltas and farther down the regional slope. Up the depositional slope to the north, there was a facies transition to phylloid-algal facies as water shallowed slightly (Figures 2.32 to 2.34: Feature 10). Farther to the north, the phylloid-algal facies grades to oolites where the shallowest water occurred (Figures 2.30, 2.31, 2.33, 2.34: Feature 11).

In one north-northwest to south-southeast trend, the lower Farley limestones are interbedded with marine shales and siliciclastics, becoming more abundant and coarser to the north-northwest (Figures 2.30-2.34: Feature 12). This suggests a shifted source of deltaic siliciclastics from the north-northwest with siliciclastics more abundant over underlying topographic lows. This supports the interpretation of Harris (1985) who suggested that the thin accumulations of siltstone in the Farley resulted from periodic influxes from the still active Island Creek delta to the northwest.

This shift in influx of siliciclastics is predictable given filling of the topography on the top of the Argentine Limestone by the Island Creek delta. The suggestion is that the siliciclastics in the lower Farley behaved in a manner similar to those of the Island Creek and preferentially filled depositional lows rather than constructing positive lobes or wedges. Because the valley in which the Island Creek siliciclastics were deposited was full or because sea-level rose above it, deposition of siliciclastics in the lower Farley shifted and found new low areas to fill.

In the western and central portions of the field area the lower Farley is capped by peloidal, skeletal packstone with local accumulations of oolitic, peloidal packstone (Figures 2.30, 2.31, 2.33, 2.34: Feature 13). These lithofacies indicate slightly elevated energy levels in which currents washed fine carbonate mud. An oolitic, peloidal packstone (locality SRBS) is sandwiched between beds of peloidal skeletal packstone (Figures 2.33, 2.34: Feature 14). This oolitic, peloidal packstone contains meniscus cement fabrics and keystone vugs, evidence for subaerial exposure of this facies prior to deposition of the immediately overlying peloidal, skeletal packstone.

The distribution of the peloidal, skeletal packstone facies is problematic. Peloidal, skeletal packstones and oolitic, peloidal packstones are located on and adjacent to topographic prominences in the lower Farley but not on the highest prominences. It is unknown what caused this distribution. One might have expected the highest energies to have been present on the paleotopographic highs and that packstones were generated there. But high energy present over the topographic highs may have swept carbonate sands off the highs into adjacent topographic depressions. Alternatively, currents may have been concentrated in paleotopographic low areas generating packstones in place.

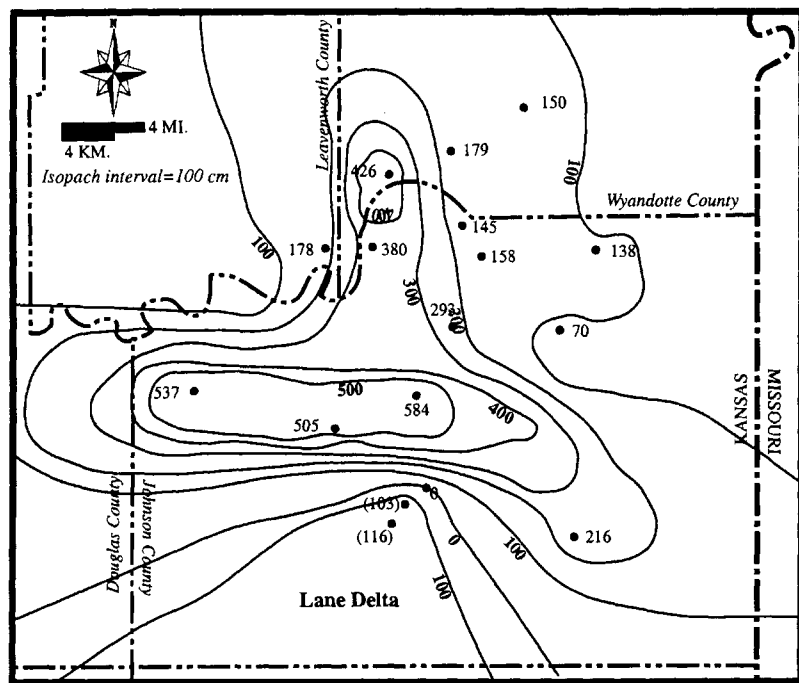
The evidence of subaerial exposure within the deposits at locality SRBS suggests that deposition of the peloidal, skeletal packstones at the top of the lower Farley resulted from a relative fall in sea level. This would explain why the facies is present in the topographically lower areas and not found on the highest highs. If sea level fell, the topographic prominences may have been exposed subaerially and received no carbonate deposition. The presence of marine siltstone directly above these deposits, however, suggests that sea level may have risen again slightly following the deposition of the oolitic, peloidal packstone facies before continuing the drop that formed the sequence boundary located along the top of the lower Farley discussed below. This subtle fluctuation in sea level may help to explain the unusual

distribution of peloidal, skeletal packstone facies within the lower Farley, with a minor relative sea-level fall bringing shallow waters and concentrating currents in paleotopographic lows.

Comparison of isopach maps for the lower Farley interval (Fig. 2.35) to those for the Argentine Limestone (Fig. 2.3) and the Lane-Island Creek shales (Fig. 2.4) illustrates that where the Argentine is thin the Lane-Island Creek is thick. Furthermore, where the lower Farley is thickest the Argentine Limestone is thin. Thus, the combined affect of Lane-Island Creek deposition followed by lower Farley Limestone deposition was to greatly reduce, but not completely eliminate, depositional topography. This is contrary to trends outlined by earlier authors (Heckel & Cocke, 1969; Crowley, 1969; Harbaugh, 1959, 1960; Arvidson, 1990) who suggested that thick accumulations of carbonates show a pronounced stacking pattern in which the thickest accumulations of one limestone directly overlie the thickest accumulations of the previous limestone unit thereby perpetuating topography upward in the stratigraphic section.

#### ***Top of Lower Farley-Middle Farley Interval***

A prominent surface (Figs. 2.30-2.34: Surface C) separates the lower Farley from the middle Farley. Along this surface, nonmarine blocky mudstones with paleosols directly overlie marine limestones in the north (Figs. 2.30, 2.32-2.34: Feature 15) suggesting subaerial exposure and possible erosion. The presence of nonmarine, blocky mudstones immediately over lower Farley limestones indicates a sequence boundary between the two units (Figures 2.30-2.34: Surface C). Elsewhere, these blocky mudstones are underlain by fossiliferous siltstones and lenticular, laminated siltstones that sit atop the limestones of the lower Farley (Figures 2.30-2.33: Feature 16). Clearly, there must be some complex internal geometries within the siliciclastics of the middle Farley, the structure of which is as yet unknown. The

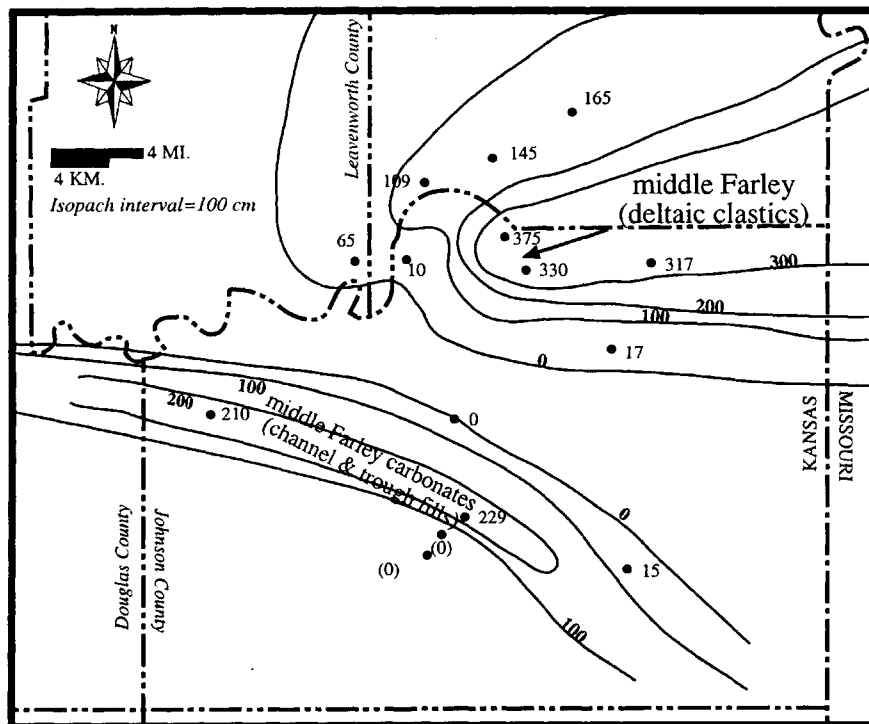


**Figure 2.35.** Isopach map of lower Farley limestone and equivalent shales to the south in the area of the Lane delta that was still active during deposition of the lower Farley. Note how the lower Farley thickness compliments the underlying Lane-Island Creek thickness variations illustrated in Figure 2.4. In areas where the Lane-Island Creek is thick, the lower Farley is thin and where the Lane-Island Creek shales are thin, the lower Farley is thick. The lower Farley limestone farther to the south is absent and instead is represented by a portion of the time-equivalent Lane Shale. Data from current study.

evidence for shallowing upward to nonmarine deposits in the middle Farley siliciclastics further supports the interpretation of a relative fall in sea level.

In addition to the siliciclastics discussed above, the middle Farley also contains deposits of sandy, skeletal grainstone and packstone (Figures 2.30, 2.33, 2.34: Feature 17). In the southwest, this facies is cross-bedded and located between beds of siliciclastics (Figures 2.33, 2.34: locality HM). This stratigraphic observation supports its correlation to other deposits of the middle Farley. In the south (localities SRO, C5), the sandy, skeletal grainstone-packstone is located in a trough-shaped low between the Lane delta to the south and a topographic high in the lower Farley to the north (Figures 2.30, 2.34-2.36).

This sandy, skeletal, cross-bedded grainstone-packstone lithofacies must have been deposited in a high-energy environment that was influenced by both marine and terrigenous input. The depositional lows into which it was deposited may have resulted from erosional channeling or by deposition in trough-shaped areas between constructional topography. For the southern example, the terrigenous material may represent material eroded from the Lane delta to the south, which perhaps was redeposited in depositional lows where tidal energy was focused. This interpretation of erosion of the Lane delta also is consistent with the absence of the middle Farley interval along the top of the delta. The example from the southwest (locality HM) is somewhat similar to the Pennsylvanian strata at Hamilton Quarry described by Feldman *et al.* (1990) in which a conglomerate was deposited in a system of relatively high-energy barriers and tidal inlets, mainly as part of an estuarine and lagoonal complex. In the Farley, the association of fossiliferous siltstones and cross-bedded facies suggest a similar setting to that of Hamilton Quarry. The example from the south (localities SRO, C5) is similar to that described by Cunningham and Franseen (1992) for a unit possibly equivalent to the Captain Creek Limestone. They suggested that such grainy units were



**Figure 2.36.** Isopach map showing thickness variations of the middle Farley Shale. The main delta lobe extends into the area from the northeast (arrow). The southern portion of the middle Farley is interpreted to represent a barrier bar and distributary channel system located off the distal end of the delta. Data from current study.



deposited in tidally influenced, topographic lows between algal build-ups where elevated energies resulted from constriction and focusing of tidal energies.

Local accumulations of skeletal wackestone-packstone also occur within the middle Farley at SRS and SRBS (Figures 2.30, 2.33, 2.34: Feature 18). At locality SRS, this facies is highly argillaceous and represents accumulation of argillaceous carbonate as a facies of the middle Farley. This argillaceous carbonate accumulated in what may have been a slight topographic low adjacent to the distal end of middle Farley deltaic deposition. The origin of the skeletal wackestone-packstone at SRBS is more problematic. This accumulation of skeletal wackestone-packstone is not argillaceous and contains only fine, fragmental skeletal material. It is also likely to be a facies of the middle Farley deltaic deposits but is less argillaceous due to a slightly more distal setting. The distribution of these facies are difficult to explain and with only two occurrences in the Farley no obvious control on their distribution is clear.

Isopach mapping for the middle Farley interval indicates that the underlying topography had an impact on the distribution of middle Farley deposits. Judging from the thicknesses, the deltaic siliciclastics of the middle Farley had a northeastern source (Fig. 2.36) and seem to have terminated against the thickened portions of the lower Farley (Figures 2.35 and 2.36).

#### ***Top of the Middle Farley-Upper Farley Interval***

The lithofacies at the top of the middle Farley interval (Figs. 2.30 to 2.34: Feature 16) suggests that deposition of the upper Farley carbonates was initiated following a relative rise in sea level. This relative sea-level rise is indicated by the thin layer of fossiliferous siltstone that overlies the nonmarine blocky mudstones (Figures 2.30 to 2.33: top of Feature 16). This layer represents a marine flooding unit, and the base of this fossiliferous siltstone bed represents the fourth significant surface in the sequence

stratigraphic framework (Figure 2.30-2.34: Surface D). This siltstone lithofacies was deposited only in parts of the field area closest to the source of middle Farley siliciclastics.

The *Osagia* marker bed (Figs. 2.30 to 2.34: Feature 19) generally marks the next event of the flooding. This marker bed is found in most of the field area and is recognized by the presence of *Osagia*-brachiopod packstone near the base that grades up to phylloid-algal facies. This widespread consistency of facies indicates that there may have been little to no depositional topography that would have compartmentalized environments and lithofacies as occurred in the lower Farley interval.

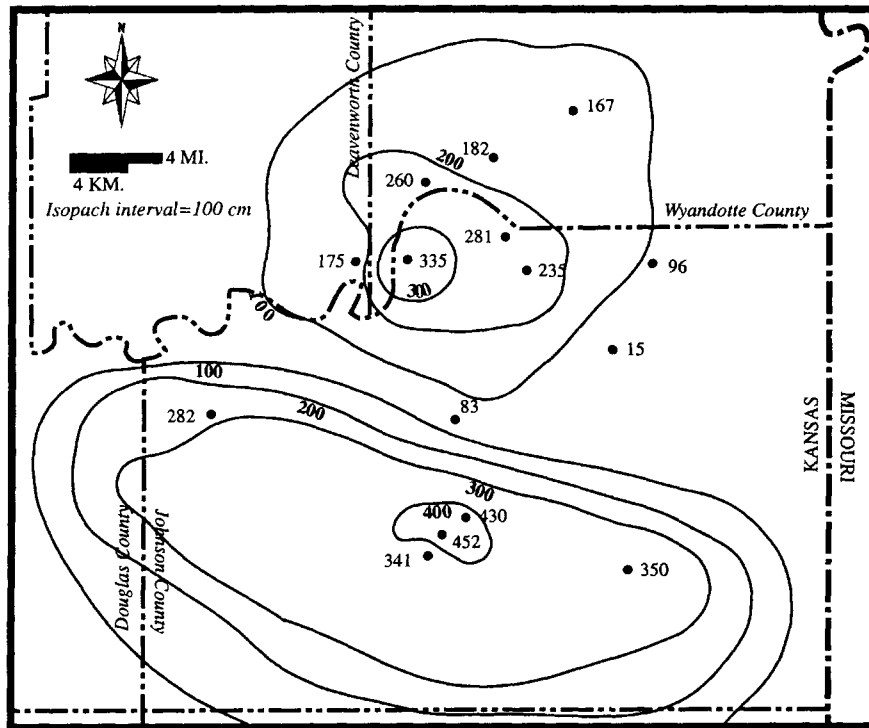
There are, however, some places in which the marker bed is missing. One locality (C6) in the center of the field area, from which the distinct marker bed is absent and which contains no middle Farley siliciclastics, provides a potential correlation problem. A thin oolite bed (Fig. 2.30: Feature 20) is present, however, that is correlated with the marker bed. Evidence that this correlation is correct is found to the south at OAQ and the southwest at HM. The marker bed at both of these localities contains abundant ooids that were likely to have been transported from the accumulation of oolite located on a slight topographic high located in the center of the field area (C6). The marker bed is also missing towards the southeast (locality RQ), which is possibly due to deeper water caused by regional dip, which was not conducive to formation of the *Osagia*-brachiopod packstone facies.

The dominant facies of the upper Farley is the phylloid-algal facies, which is present in all localities except one (C4) (Figures 2.30-2.34: Feature 21). This facies is consistent in character throughout the area and shows only gradual thickness change (Figs. 2.30 to 2.34, 2.37) and less facies variation relative to the deposits of the lower and middle Farley. This relatively gradual thickness variation and lateral consistency in facies may be a result of subdued depositional topography. By this stage of Farley deposition, most

most depositional topography had been reduced by filling with the deposits of the Lane-Island Creek as well as the lower and middle Farley. Therefore, the upper Farley exhibits much greater consistency in both thickness (Fig. 2.37) and lithofacies (Figures 2.30 to 2.34).

Localized accumulations of peloidal, skeletal packstone occur along the top of the upper Farley (Figures 2.30-2.34: Feature 22). This lithofacies indicates higher energy was present in some areas near the end of upper Farley deposition. Similar to occurrences of this facies in the lower Farley, the distribution of these peloidal, skeletal packstones in the upper Farley is somewhat enigmatic. Those located in the east (Figure 2.32: localities C3 & C4) are thin and located between areas of thickened phylloid-algal limestones. Here, even the *Osagia* marker bed is missing, suggesting erosion. It is possible that the peloidal, skeletal packstone was deposited in this area due to higher energy levels that resulted from concentration of currents between thickened accumulations of phylloid algal facies. This higher energy level then resulted in the erosion of some of the underlying facies, such as the *Osagia* marker bed, at C4.

At localities farther to the west (SRS and HM) the peloidal, skeletal packstone facies resembles the upper part of the Argentine Limestone, where it had been interpreted as a possible hardground. This is especially true at locality HM in the southwest, where there is an undulating but razor-sharp contact with the phylloid-algal facies below and where the peloidal facies also has a distinctly reddish color. The peloidal, skeletal packstone facies varies from approximately 20 to 100 cm in thickness in this locality. At locality SRS it is similar in appearance to that at HM but constitutes a single massive bed approximately 1.5 m thick along the top of the upper Farley. This bed is very even in thickness and flat-topped throughout the quarry and contains abundant, large bivalve fossils along the upper surface that suggest that this surface may have been encrusted with bivalves. These occurrences of peloidal, skeletal facies



**Figure 2.37.** Isopach map showing thickness variation of upper Farley interval. The thickness variations of this interval are more gradual than those found in underlying units (Figs. 2.3, 2.4, 2.35, 2.36). This is likely due to subdued depositional topography that followed deposition of the Lane-Island Creek and the lower-middle Farley intervals. This subdued topography allowed for more even facies and thickness distribution in the upper Farley.

are likely to have been the result of the development of a hardground along the top of the upper Farley which is missing in surrounding localities due either to nondevelopment or to erosion prior to the deposition of the overlying Bonner Springs Shale. Evidence of Bonner Springs erosion is further discussed below.

Deposition of the Farley Limestone was terminated by the next influx of siliciclastics. The overlying Bonner Springs Shale is a thick sequence of marine and nonmarine siliciclastics that contains evidence of widespread subaerial exposure and erosion (Enos *et al.*, 1989; Watney *et al.*, 1989; Arvidson, 1990; this study). For example, at locality OAQ in the south (Fig. 2.30: Feature 23) the lower part of the Bonner Springs Shale comprises a coarse-grained conglomerate that contains large (centimeter scale) clasts of what appear to be upper Farley phylloid algal facies. Other evidence of erosion previous to deposition of the Bonner Springs Shale is found in the Hunt-Midwest Sunflower quarry (locality HM) to the southwest. In this quarry, the upper Farley could be seen to start to pinch out apparently from erosion prior to deposition of the overlying Bonner Springs Shale. For this reason, the final significant stratigraphic surface in the framework of the Farley Limestone (Figs. 2.30 to 2.34: Surface E) is drawn as a sequence boundary along the upper surface of the Farley Limestone.

### **Conclusions**

The lateral and vertical variability observed in the Lane-Island Creek Shales and the Farley Limestone is the result of the interaction of fluctuating relative sea level, depositional topography, and the source direction and distribution of siliciclastics. Fluctuating relative sea level acted on a regional scale to cause large-scale changes in deposition such as the influx of deltaic siliciclastics or subaerial exposure of certain units.

On a more localized scale, depositional topography had the greatest control on the lateral and vertical distribution of lithofacies by influencing depositional environments.

The presence of two thick deltaic sequences overlying the marine Argentine Limestone indicates a relative fall in sea level between Argentine Limestone deposition and the deltaic Lane-Island Creek shales. Although delta lobe switching could explain the deltaic influxes, the presence of two separate deltas that entered the area from different directions during the same time would be unexpected with delta lobe switching. A lack of evidence of subaerial exposure in the Lane-Island Creek or along the top of the Argentine Limestone indicates that the fall was not extensive enough to expose the upper surface of the Argentine within the study area. The interpretation therefore, is that the upper surface of the Argentine represents the correlative conformity of an unconformity that was likely to have been located further to the north. The relative sea-level fall was, however, great enough to allow deltaic sediments to enter the area from both the north and south.

The lateral distribution of these deltaic sediments was closely controlled by the depositional topography of the underlying Argentine Limestone. The Island Creek deltaic deposits extended into the area from the north through a trough-shaped depositional low between two highs in the Argentine Limestone. In this manner, the Island Creek delta behaved as a valley fill rather than as a traditional delta lobe. The distribution of the southern Lane delta was also controlled by Argentine topography. The Lane shows a broader distribution due to fewer topographic restrictions in the Argentine Limestone to the south. In areas between the two deltas that received no influx of deltaic siliciclastics, a marine hardground developed along the upper surface of the Argentine Limestone.

The presence of a flooding unit and fully marine deposits along the top of the thickened Island Creek delta in the north indicates the termination of deltaic deposition in

the Island Creek delta. The change to carbonate deposition could have resulted from a relative rise in sea level or by a delta switch with no accompanying sea-level rise. The presence of a marine, carbonate-rich unit along the top of the Island Creek delta, however, indicates a relative rise in sea level.

Siliciclastic influxes remained somewhat active through lower Farley deposition, however, and its effects are represented by successions of alternating argillaceous phylloid-algal limestones and fossiliferous siltstones at several localities in the northwestern and central portions of the field area. As with the previous Island Creek siliciclastics, these pulses of deltaic siliciclastics were deposited in topographically low areas.

Following the relative sea-level rise, carbonate production was established throughout the northern and central area and depositional topography played a major role in the lateral and vertical distribution of lithofacies. High energy facies such as oolite and peloidal, skeletal packstone accumulated across topographic highs along the thickened Island Creek delta, whereas more quiet-water facies like phylloid algal boundstone and packstone and skeletal wackestone-packstone accumulated in the topographic lows where current energies were weaker.

Near the end of the lower Farley interval, higher energies were present, and as a result peloidal, skeletal packstones and oolitic, peloidal packstones accumulated along the top of the lower Farley in many places. These facies are found over and adjacent to some topographic prominences but are not found over the highest highs. Furthermore, there is evidence for subaerial exposure in the oolitic, peloidal packstones which are immediately overlain by additional marine facies. This relationship suggests that sea-level dropped then rose briefly before continuing to fall again. This could help account for the odd distribution of peloidal, skeletal packstones along the top of the lower Farley.

Lower Farley carbonate deposition was terminated by the influx of middle Farley siliciclastics into the area from the east-northeast. Like the deltaic influx of the Lane-Island Creek, the middle Farley delta influx followed a relative fall in sea level. This fall, however, was great enough to expose much of the delta in the study area and paleosols developed leading to the interpretation of a second sequence boundary. Associated with this deltaic influx was the deposition of the sandy, skeletal grainstone-packstone facies. This facies represents a high-energy environment located in tidally influenced channels or in trough-shaped topographic lows through which current energies were focused.

A second relative rise in sea level is indicated by a second marine flooding unit (fossiliferous siltstone) found along the top of the subaerially exposed middle Farley delta. This flooding unit is overlain by the fully marine upper Farley, which is relatively consistent in thickness and facies throughout the area. This consistency in facies is likely to be due to a relative lack in existing depositional topography. By this point in the deposition of the Farley Limestone, most depositional topography present starting with the Argentine Limestone had been filled with the deposits of the Lane-Island Creek shales as well as the lower and middle Farley limestones.

Finally, carbonate deposition of the Farley Limestone was terminated by a major relative sea-level fall that resulted in the accumulation of the Bonner Springs Shale and widespread exposure, erosion and paleosol development.

The complex distributions of carbonate and siliciclastic lithofacies described in the Lane-Island Creek and Farley Limestone illustrate the profound effect of paleotopography on the rock record. It was shown that carbonate and siliciclastic deposition responds to factors related to energy and accommodation, which in turn are greatly influenced by depositional topography. Siliciclastics are commonly focused into paleotopographic lows



of various origins; and, unlike what would be commonly expected, phylloid-algal facies of this interval seem to have a tendency to also fill lows rather than to accumulate on the highs.

**Chapter 3: Geologic Factors Affecting the Quality of  
Limestone Construction Aggregate**

## Introduction

The goal of this study is to evaluate geologic and physical properties of limestone aggregates in an attempt to find criteria that can be used to quickly and efficiently identify highly durable aggregates and those subject to decay over time. Most past concrete aggregate-related research in Kansas has concentrated on a type of deterioration known as d-cracking. D-cracking is characterized by fine, closely spaced, parallel cracks that have blue, black, gray, or white deposits in the crack at the pavement surface. It typically develops parallel to joints or cracks in the pavement. (Crumpton *et al.*, 1994).

An early study related to d-cracking was conducted by the Kansas Department of Transportation (KDOT) in 1944 and suggested a significant relationship between coarse aggregates and d-cracking. As a result, the sizes of aggregate used in pavement concrete were reduced, resulting in improved pavement performance. In 1973 Bukovatz *et al.* presented the results of another study on d-cracking and again concluded that coarse aggregates and specifically coarse limestone aggregates were a main cause of d-cracking. They stated that pavements that contained more than 35 percent coarse limestone aggregates were more likely to be d-cracked than pavements with less than 35 percent coarse limestone aggregates. Most pavements without limestone coarse aggregate were rated as good.

Best (1974) reported the results of a seven-year study with the goal of finding a specific cause for d-cracking. Although this study concluded that the exact cause of d-cracking still remained a mystery, it was suggested that the freezing and thawing of water within the pavements was a main contributor. This study also supported the previous suggestion that coarse, limestone aggregates were a cause of the problem.

Based on the results of the early studies and those reported by Bukovatz and Crumpton (1981), KDOT adopted new requirements for selecting limestone aggregates. The plan adopted was to evaluate each quarry, subdivided into beds, and to approve or reject each individual bed based upon the results of laboratory freeze-thaw testing of concrete beams containing the coarse limestone aggregate from each bed (Wallace & Hamilton, 1982). Those aggregates that meet a minimum set of requirements concerning durability, freeze-thaw resistance and expansion are considered class 1 aggregates and are approved for use as construction grade material. The testing system outlined by the 1982 report is used today, and the use of aggregates meeting the established criteria has reduced occurrences of d-cracking. The tests are costly and time consuming, however, taking a minimum of six months to perform.

This paper reports attempts to identify geologic parameters that can be used to identify quality aggregates more easily. During the preliminary stages of the project several quarries currently producing class 1 limestone aggregate in eastern Kansas were visited. The units examined included the Tarkio Limestone, the Merriam and Spring Hill Limestones, the Argentine Limestone, and the Farley Limestone. Based on preliminary observations of outcrops and hand samples at the start of this study, specific geologic variables to be discussed seem to affect whether a unit passes or fails the class 1 aggregate physical tests. These variables allowed the development of several general working hypotheses testable in the Farley Limestone.

- (1) Micrite-rich, phylloid-algal lithologies consistently produce durable aggregates.
- (2) Fine-grained, matrix-rich limestones tend to pass, whereas coarser carbonate grainstones with coarse cements tend not to pass.
- (3) High amounts of acid-insoluble residue in the rock has a negative impact.

(4) Distinct, sharp stylocumulates and shale beds have little or no impact on durability, whereas diffuse stylocumulates have a negative impact.

(5) Argillaceous limestones tend to fail testing; therefore the presence of clay minerals in the insoluble residues has a negative impact.

(6) Abundant, coarse, sparry calcites in the rock have a negative impact.

This study uses the Farley Limestone as a test case because it varies significantly both laterally and vertically in aggregate quality and allows initial testing of all of the hypotheses. If an understanding of how geologic factors interact to produce high-quality rock in the Farley is established, an analog for other similar limestone units in different locations can be developed.

## **Methodology**

To gather data on the various geologic variables, detailed measured stratigraphic sections were described in eight quarries. Included in these sections were both active and inactive quarries from which KDOT has produced both class 1 and nonclass 1 aggregates from the Farley Limestone. All stratigraphic sections were measured at or near the locations from which KDOT had recently tested aggregates. Also included in the stratigraphic study were descriptions of outcrops and drill cores. These sections helped fill gaps between quarry exposures so that a more accurate stratigraphic reconstruction of the field area was possible. Information obtained includes bedding nature, preliminary lithologic classification, fossil types, and the percentage of the rock volume composed of sparry calcite. Descriptions of outcrops also emphasized determining the percentage of each stratigraphic interval that contained clay-rich zones. Shale beds, concentrated stylocumulates, diffuse stylocumulates, and disseminated argillaceous material were documented. Percentages of the total section that contained each form of argillaceous material were recorded. The different types of clay-rich zones are discussed in greater detail below. Measured stratigraphic sections are in Appendix 1.

After stratigraphic sections were measured and described in the field, samples were collected. For each of the stratigraphic sections, hand samples were collected, and polished slabs and thin sections were made. These slabs and thin sections allowed a more accurate, detailed description of each lithology using the Dunham classification for carbonate rocks (Dunham, 1962). The descriptions include dominant depositional fabric, identification of fossils and other carbonate grains, and a more accurate estimation of the percentage of sparry calcite.

In addition to hand samples, 10 bulk rock samples of 250 pounds each were collected and turned over to the Materials and Research Division of KDOT for physical testing according to their established guidelines and procedures. After initial crushing of these ten samples, three pounds of the crushed aggregate was obtained from KDOT for each sample. This split included both  $\frac{3}{8}$  inch and  $\frac{1}{2}$  inch crushed aggregate. Independent tests conducted on the crushed aggregates included determining acid insoluble residue percentage, grain-size distributions of insoluble residues, x-ray identification of residues, and thin-section petrography to examine lithologies and spar content. Procedures for each of these tests are given in Appendix 2.

### **KDOT Physical Tests**

Ten 250 pound rock samples were obtained from the Farley Limestone in Johnson and Wyandotte counties and were identified as sample numbers KU-1 to KU-10 (Appendix 1, Figures A1.2-A1.10). These samples were then tested by KDOT using the normal testing protocols prescribed by KDOT to determine aggregate durability. Physical test data for samples recently tested by KDOT from the Farley Limestone are also used in the study. These samples are referred to as KDOT-1 to KDOT-20, and stratigraphic locations of these samples are also indicated on the measured sections in Appendix 1. Stratigraphic sections were measured and

described at or near the site of the KDOT sampling, so their test results could be compared directly to field observations.

The following sections summarize the parameters measured by the physical tests conducted by the Materials and Research Division of KDOT. The results of these tests constitute the data that are compared to data on geologic variables.

***Absorption***

Absorption is a measure of porosity and permeability of an aggregate sample and is determined as part of the physical tests conducted by KDOT. The reported value is given as a percentage of weight gain after soaking the aggregate in water for 24 hours. See Appendix 2 for procedures and calculations.

***Modified Freeze-Thaw Test (Soundness)***

The modified freeze-thaw test (soundness) is used as the first cut to determine whether an aggregate will undergo additional testing. The test determines an aggregate's resistance to freezing and thawing and is performed on raw aggregate that has been size graded and weighed. The aggregate is size graded so that only  $1/2$  and  $3/8$  inch aggregates are tested. Following 25 cycles of freezing and thawing, the aggregate is size graded again and reweighed to determine how much mass the original sample has lost. The reported freeze-thaw value is the percentage of the aggregate's original mass that is retained after 25 cycles of freezing and thawing. If the modified freeze-thaw value is 0.85, the value reported in this study would be 85 percent. This indicates the sample lost 15 percent of its mass due to degradation from freezing and thawing. At present, KDOT requires a minimum modified freeze-thaw value of 0.85 to continue with testing.

### ***L.A. Wear Test***

The L.A. wear test examines the resistance to degradation by abrasion and impact of the limestone aggregates using the ASTM Test C131-89. It is done by size grading the aggregates, weighing them, and tumbling them in a large rotating drum with several large steel balls. Following the test, the aggregate is resized and weighed again. The value reported indicates the percentage of the original mass lost due to size reduction from degradation by abrasion and impact. This test is not typically useful in classifying aggregates relative to durability.

### ***Expansion***

Expansion percentages are determined as part of ASTM Test C666-92 Procedure B. It is accomplished by making three concrete beams out of the limestone aggregate to be tested and a standard cement mix. Two pins are placed in the beams, and after the beam is cured a precise measurement of the distance between the pins is measured. The beam is subjected to cycles of freezing and thawing; at periodic intervals the beam is examined and the distance between the pins is remeasured. The value reported is a percentage of expansion over the original measurement. KDOT currently uses an average of 0.02 percent expansion for the three beams as the maximum expansion limit allowed for class 1 aggregate. See Appendix 2 for procedures and calculations.

### ***Durability Factor***

Durability factor is used to indicate an aggregate's durability and resistance to freezing and thawing. The durability factor is determined using ASTM Test C666-92 Procedure B. The value is related to the percent change in the fundamental transverse frequency of the beams, which is reported as the relative dynamic modulus of elasticity. The modulus of elasticity is a ratio of stress to strain in the elastic region and is an overall measurement of stiffness of a



material. The durability factor measures the change in stiffness of the beams after a specified number of cycles of freezing and thawing. Currently, KDOT requires a durability factor of at least 95 to qualify an aggregate as class 1. See Appendix 2 for procedures and calculations.

### **Lithologic Parameters**

The following sections summarize the specifics of lithologic parameters that were compared to the results of the KDOT physical tests.

#### ***Lithology***

Lithology was determined by examination of outcrops, hand samples and thin sections. Aspects of lithology considered include depositional fabric (Dunham textural classification), matrix type, fossils, and grain types. Comparing lithology to KDOT physical tests allows for identification of lithologies that might consistently produce durable aggregates. Lithologic examination also allows conclusions concerning the importance of micrite and microspar versus coarser cement (sparry calcite). Although these lithologic properties are qualitative in nature, there is potential for the identification of characteristics that are important in aggregate durability.

#### ***Spar Content***

Accumulations of coarse spar (clear, crystalline calcite) constitute 10 to 60 percent of the limestones in the Farley. These spar accumulations resulted from either cementation of pore space or neomorphism of micrite matrix. In the Farley Limestone, sparry cement is found in fractures, in molds, and in original pore spaces between or within grains. Neomorphic spar fabrics are also common in the Farley Limestone and dominated by microspar and pseudospar fabrics with crystals defined by Folk (1965) to be in the range of 4 to 50 micrometers in size.

### Bulk Spar Percentage

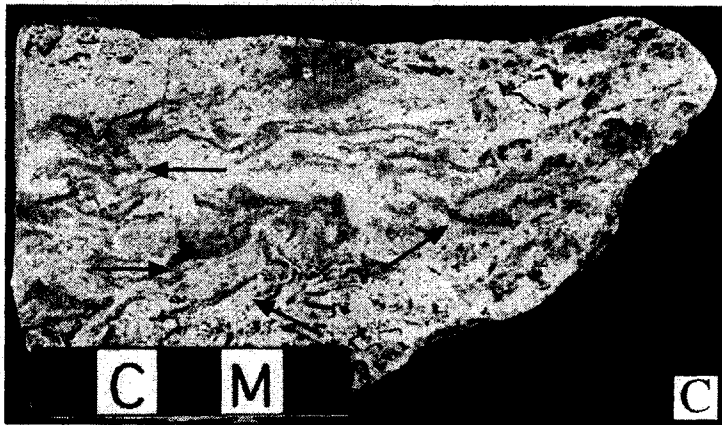
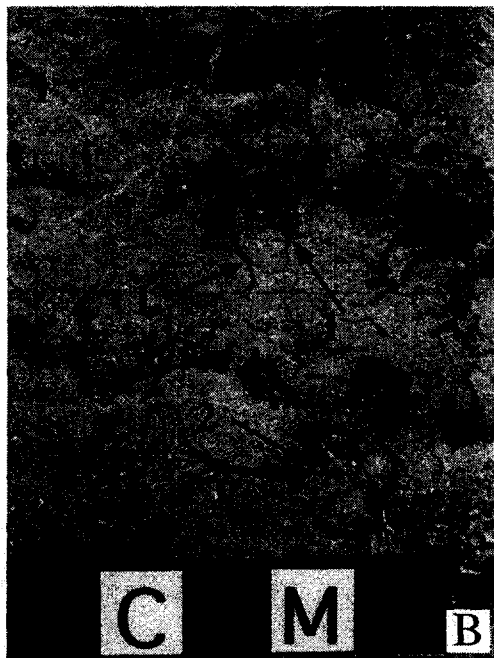
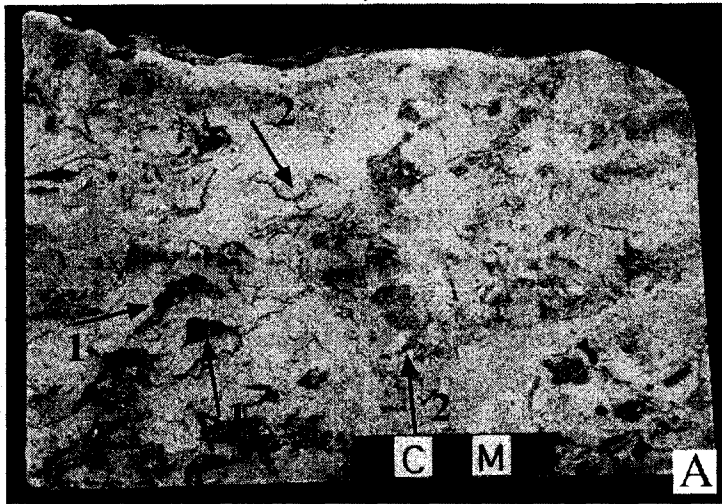
For the purpose of this paper, bulk spar percentage is defined as the percentage of the rock composed of visible, coarsely crystalline material including fracture fillings, spar-filled fossil molds, replaced fossils, and any spar-filled interparticle porosity (Figure 3.1). Estimates of spar content were made from examination of quarry outcrops and from cut and polished hand samples. Any visible accumulation of spar larger than approximately 0.5 mm was considered in the estimate. The value reported is an estimate of the total percentage of the rock volume that is composed of spar.

### Average Spar Crystal Size and Crystal Form

By examining thin sections made from hand samples of each rock subjected to KDOT physical tests, average spar crystal size for each sample was determined. Because 80 to 90 percent of micrite matrix in the rocks of the Farley Limestone was recrystallized to microspar or pseudospar, those crystals finer than 50 micrometers are considered matrix and are not included in the estimates of average crystal size. Also noted during examination of thin sections were various types and shapes of spar present in the rocks. Table 3.1 is a summary of how the spar was classified and described.

### Spar Percentage of Crushed Aggregates (Aggregate Spar)

As defined for this paper, spar percentage of crushed aggregates, referred to as aggregate spar, refers to the percentage of rock composed of spar following crushing and sorting of the original rock. This estimate includes only spar coarser than 50 micrometers. Any spar finer than 50 micrometers is considered matrix and therefore is



**Figure 3.1.** Hand samples showing different types of spar accumulations found in the rocks of the Farley Limestone. (A) Phylloid algal wackestone with spar in shelter pores (1) and phylloid algal molds (2). (B) Phylloid algal wackestone with spar dominantly in fractures (1) and phylloid algal molds (2). (C) Phylloid algal packstone with spar found almost exclusively in phylloid algal molds (arrows).

not included in this percentage. Whereas the bulk spar percentage discussed above is determined from outcrops and hand samples, the aggregate spar percentage was estimated following petrographic examination of splits of aggregate samples subjected to KDOT physical tests in order to deal with differences before and after crushing. Because this property is obtained from crushed aggregates, data were only available for those 10 samples for which crushed aggregates were available (KU-1-KU-10).

**Table 3.1.** Table of spar characteristics observed in the rocks of the Farley Limestone.

Spar Type	Crystal Shape	Crystal Size	Boundary Shape
Sparry Cement	<p>Equant: crystals have essentially equal length and width</p> <p>Bladed: length to width ratios are between 1.5:1 and 6:1</p> <p>Fibrous: length to width ratio is greater than 6:1</p>	Wide range of crystal sizes ranging from approximately 50 microns to several millimeters.	Intercrystalline boundaries of equant crystals are typically planar with even contacts. Irregular boundaries are present in small (under 70 microns) equant crystals and on some bladed crystals.
Neomorphic Spar	Exclusively equant crystals	<p>Microspar: equant crystals of 5-10 microns.</p> <p>Pseudospar: equant crystals of 10-50 microns</p>	Neomorphic spar is typically found in mosaics of microspar or pseudospar with crystal boundaries of an irregular nature.

### *Clay Percentage and Type*

All data concerning clay percentages and forms for all rocks studied were compiled from field observations and laboratory testing.

### Total Percentage of Clay-Rich Strata

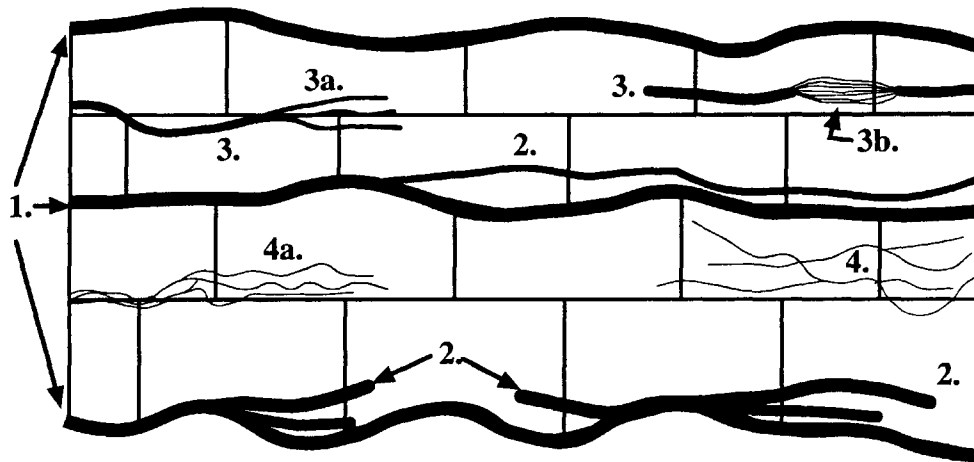
The total percentage of clay-rich strata is an estimate of the total thickness of the stratigraphic interval that contains any type of clay-rich zone. To calculate this value,

estimates of the thickness of individual beds that contained any clay-rich material were made. From these estimates of clay content of individual beds, a total percentage of clay-rich strata was calculated for each stratigraphic interval.

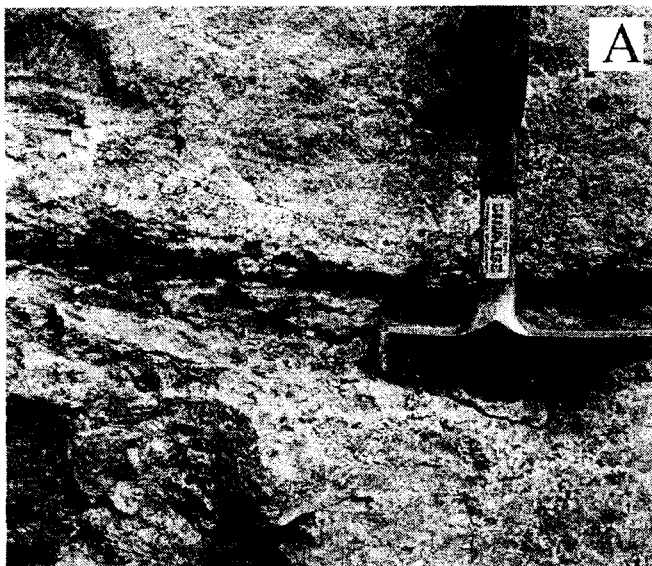
### Clay Distribution

Clay is typically distributed within a stratigraphic interval as shale beds, concentrated stylocumulates, diffuse stylocumulates, and disseminated material. Commonly it is found in concentrated clay-rich seams or stylocumulates defining bedding planes or within individual beds (Figures 3.2, 3.3). Shale beds and concentrated stylocumulates were identified by their size, shape, and relationship to the surrounding carbonate. The concentrated stylocumulates are typically  $\geq 5$  mm thick and are dominantly planar to slightly undulose with uniform thicknesses along their lengths. The seams generally have sharp to slightly gradational contacts with surrounding carbonate and commonly contain fossil material. Concentrated stylocumulates and shale strata are easily identified because they can be removed from the surrounding carbonate with a hammer or pick or by crushing the rock. This is possible because there is little carbonate within the clay-rich area and it is easily separated from the surrounding limestone. Therefore, this occurrence of clay generally does not become a part of the aggregate because it is crushed into fine particles.

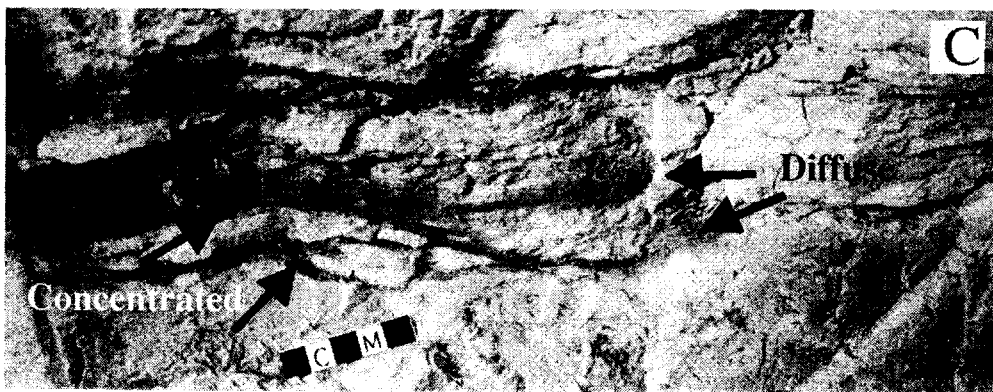
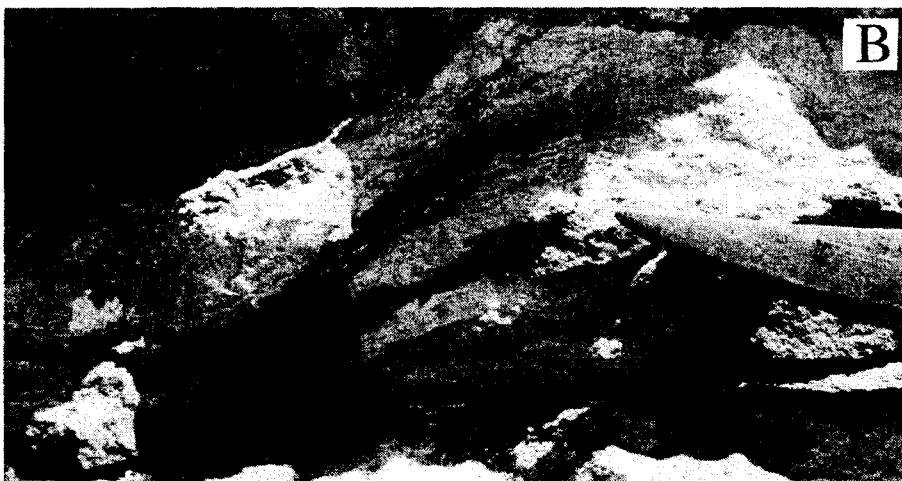
Some clays are in diffuse stylocumulates spread out within limestone beds (Figures 3.2 & 3.4). These diffuse stylocumulates are composed of numerous subparallel microstylolites and have a wispy to patchy appearance commonly dying out into the surrounding limestone. Because the diffuse stylolites are composed of numerous microstylolites spread throughout the limestone, they cannot easily be separated from the surrounding limestone with a pick or by crushing the rock. Because



**Figure 3.2.** Hypothetical illustration of two limestone beds with various forms of clay distributed within them (1). Concentrated stylocumulates or thin shale beds are typically located along bedding planes and may branch into surrounding limestones (2). Concentrated stylocumulates also occur within limestone beds (3). These often branch into slightly more diffuse stylocumulates near their ends (3a) or have zones of diffuse stylocumulates within them (3b). Diffuse stylocumulates also occur as thin wisps or stringers of clay-rich material within limestones (4), and may have a horsetail appearance (4a).



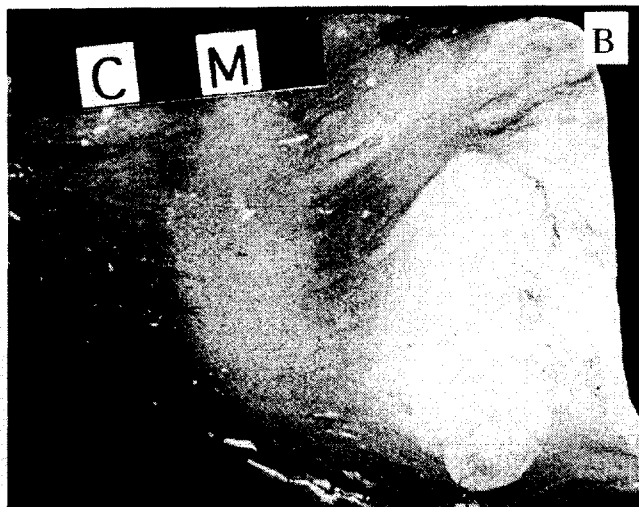
**Figure 3.3.** Photos of concentrated stylocumulates as they appear on outcrop. (A) Thin shale bed located between bedding planes. (B) Concentrated stylocumulate that branches into thinner and slightly more diffuse stylocumulates from left to right. (C) Concentrated stylocumulate that becomes more and more diffuse from left to right. The clay on the left would likely separate from the limestone in crushing whereas that on the right would likely remain in the aggregate after crushing.





A

**Figure 3.4.** (A) Photo of thin, diffuse stylocumulates on outcrop. The irregular pattern, thinness and distribution throughout the limestone would likely cause these clay-rich zones to become part of the aggregate following crushing of the rock.



(B) Hand sample of argillaceous skeletal wackestone (locality SRS) showing the stringy, and wispy nature of the diffuse stylocumulates. These wisps of clay-rich material will not be separated from the limestone when the rock is crushed.



**Figure 3.5.** Photo of a bed of phylloid algal wackestone with completely disseminated argillaceous material throughout its thickness. This form of clay is recognized by the bluish-gray color it imparts to the rock. Due to the disseminated nature of the clay, it will become part of the aggregate following crushing of the rock.



of its diffuse nature and distribution throughout limestone beds, this occurrence of clay generally will be retained in the crushed aggregates

Clay also occurs as completely disseminated argillaceous material in limestone. In these occurrences there are no visible discrete seams or stylolites. Instead, this clay distribution is typically recognized in outcrops by the bluish-gray color the disseminated clay imparts to the rocks (Figure 3.5). Like diffuse stylolites, argillaceous material that is completely disseminated throughout the limestone cannot be separated from the limestone and will become part of the crushed aggregate.

### ***Insoluble Residues***

Data on insoluble residue percentages of aggregate samples KU-1 to KU-10 were determined by the author, whereas percent insoluble residue for aggregate samples KDOT-1 to KDOT-20 were determined by the Materials and Research Division of KDOT as part of their testing protocol. Other data concerning insoluble residues, including grain size distributions and compositions, were determined by the author for samples KU-1 to KU-10 only. See Appendix 2 for sample preparation techniques and procedures for collecting insoluble residue data.

### **Percent Insoluble Residue**

Percent insoluble residue represents the weight percent of aggregate composed of acid insoluble residue determined by digesting crushed aggregate samples in dilute hydrochloric acid, weighing the filtered residues, and calculating the total percentage by weight.

### **Insoluble Residue Grain Sizes & Aggregate Clay Percentage**

Grain size distributions of the insoluble residues were determined for each aggregate sample tested for this study (KU-1 to KU-10). This was accomplished by weighing the residues,

dispersing them in water, and sieving them. Following sieving, the mass of each fraction retained on the sieves and the mass of the fine fraction that passed through the finest sieve was determined and a percentage of the original sample was calculated for each grain size.

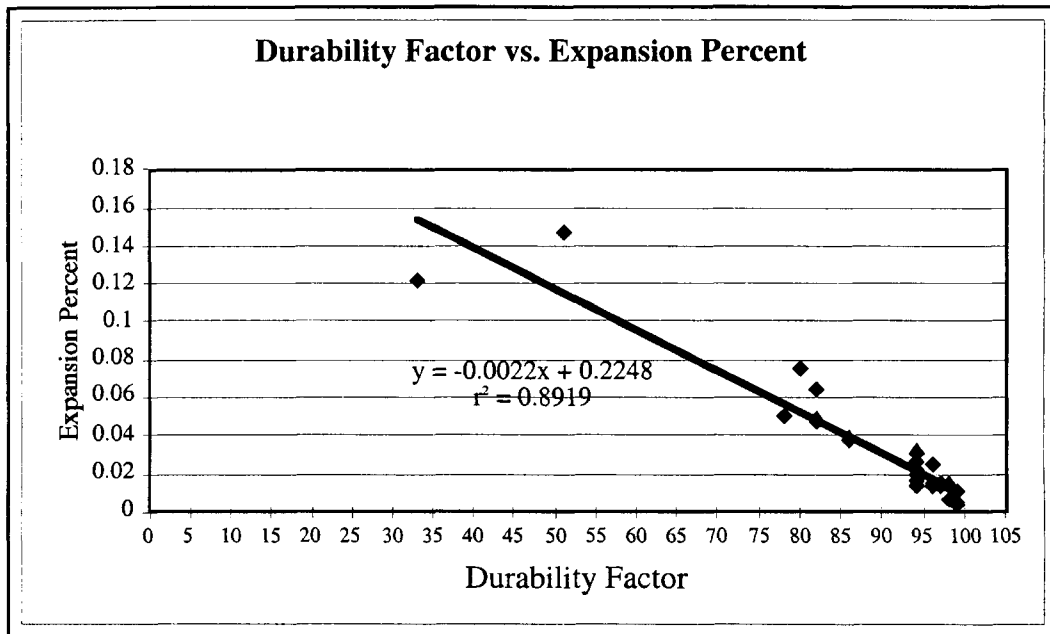
Using the percentage of each sieved residue composed of clay-sized material, a value was calculated that represents the weight percentage of the original aggregate mass composed of clay-sized material. This value is referred to as the aggregate clay percentage. Insoluble residue grain size data were not available for samples taken by KDOT.

#### Insoluble Residue Composition

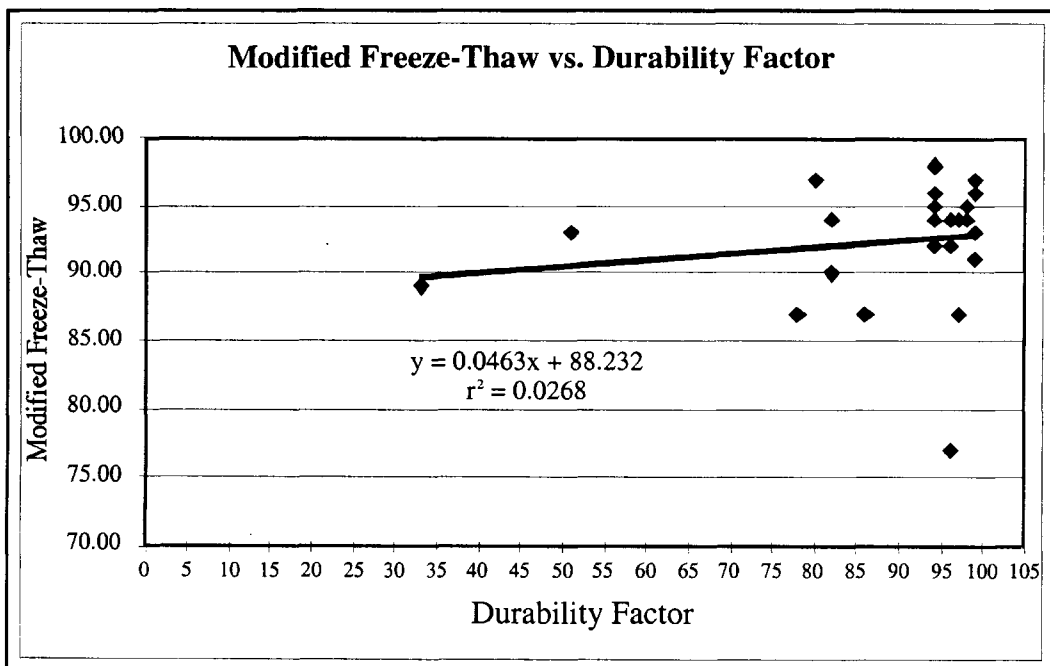
Mineralogical compositions of insoluble residues of samples KU 1 to KU-10 were determined using x-ray diffractometry. These data were not available for samples taken by KDOT.

#### **Results**

In order to evaluate the hypotheses outlined at the beginning, data concerning the geologic variables must be evaluated relative to the results of the KDOT physical tests. Durability factor is the most important measurement in determining if an aggregate is a class 1 aggregate. For this reason, geologic variables are compared to the results of ASTM Test C666-92, Procedure B, which KDOT uses to determine durability factor. Other important test results used in KDOT's determination of whether an aggregate qualifies as class 1 include the expansion percentage and the modified freeze-thaw (soundness) ratio. Therefore, some geologic variables were also compared to these results and correlations are discussed where applicable. Because durability factor is so highly correlated to expansion percentage (Fig. 3.6), it is apparent that in most cases only one of these variables need be compared to lithologic



**Figure 3.6.** XY plot illustrating the relationship between durability factor and expansion percentage (n = 25).



**Figure 3.7.** XY plot showing the relationship between durability factor and modified freeze-thaw (soundness) value (n = 30).

parameters. Alternatively, because the results of the modified freeze-thaw test essentially do not correlate to durability factor (Fig. 3.7), the soundness test may either be reflecting an influence of different variables or may suggest that the soundness test is in need of further evaluation.

To compare most data to the durability factor, simple XY scatter plots were compiled. Then, using simple linear regression, any possible correlations or trends were examined. Although the regression data are not meant to represent rigorous statistical testing, they provide the means to simply evaluate trends useful for indicating those variables that may play a significant role in aggregate durability. In the future, as more comprehensive data are accumulated, these data may be conducive to multivariate statistical analysis. For other, more qualitative data such as lithology, spar types, and clay form, comparisons were made by categorizing the data into classes and compiling histograms.

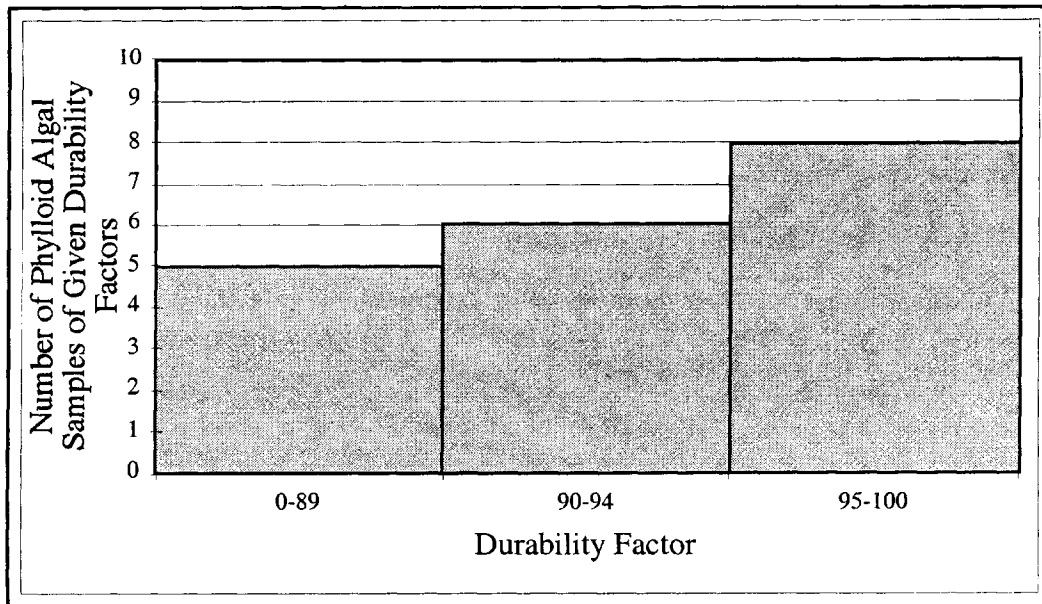
### *Lithology*

The rocks tested for this study (samples KU-1 to KU-10) and other recent KDOT tests (samples KDOT-1 to KDOT-20) are of six different lithologies (Table 3.2). Of the 30 aggregates examined in the study, 25 had durability-factor data. Nineteen of those 25 aggregates are phylloid-algal lithologies. Of those 19, eight have durability factors of at least 95, six have durability factors of 90 to 94, and only five fall within the 0 to 89 range (Figure 3.8).

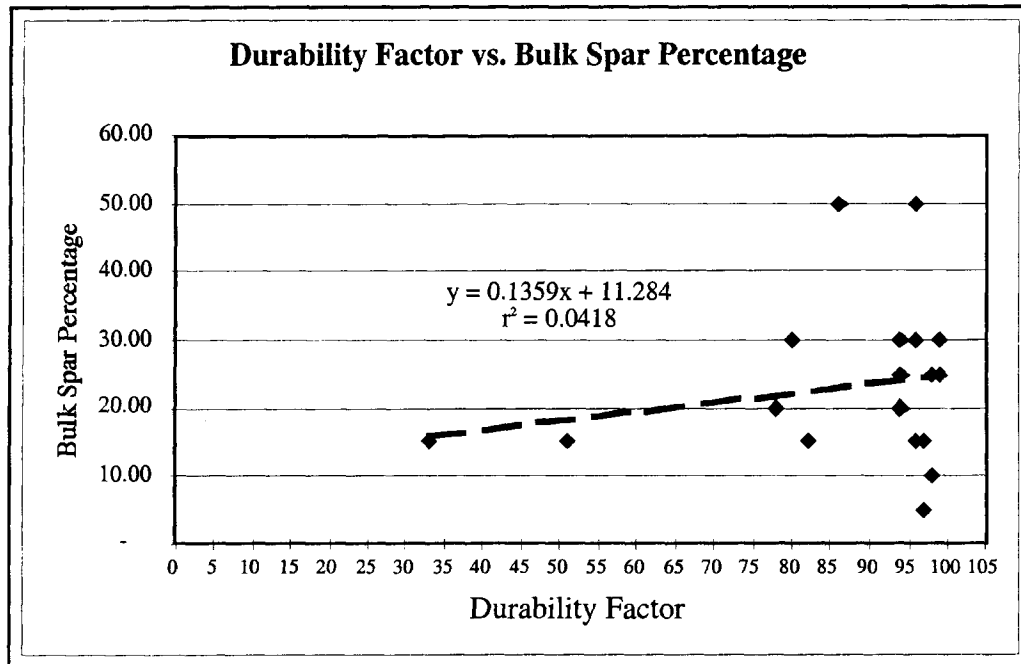
Coarser grained, micrite-poor lithologies such as skeletal grainstone (KU-3) and skeletal, peloidal packstone (KU-7) have durability factors of at least 95. Finer grained, micrite or microspar matrix-rich lithologies such as skeletal wackestone (KU-8) and phylloid algal wackestone (KU-5) also have durability factors of at least 95. Therefore, it does not appear possible to predict durability based exclusively on the

**Table 3.2.** Information regarding lithology of each aggregate source. Information includes locality and stratigraphic unit from which each sample was taken, lithology, matrix or cement type and dominant grain type. Also given are durability factors for each aggregate (NC= not calculated).

Lab. #/Sample #	Sample Source	Lithology	Dominant Matrix or Cement	Dominant Grain Type(s)	Dblty Factor
97-3685/KU-1	SRS L. Frly	Argil. Sk. Wckstn	Pseudospar & Microspar	Skeletal Fragments (Bryozoan, Crinoid, Brachiopod)	NC
97-3686/KU-2	SRS U. Frly	Phyl. Algal Wckstn	Micrite & Microspar	Phylloid Algae	94
97-3687/KU-3	SRO L. Frly	Skel. Grnstr	Equant Cement	Skeletal Frags., Quartz Grains, Peloids	97
97-3688/KU-4	SRBS L. Frly	Oolite	Isopach., Micrite, Eqnt Cement	Ooids, Peloids, Skeletal Fragments	98
97-3689/KU-5	SRBS U. Frly	Phyl. Algal Wckstn	Peloidal Micrite & Microspar	Phylloid Algae, Bryozoans	99
97-3690/KU-6	RQ U. Frly	Phyl. Algal Pckstn	Peloidal Micrite & Microspar	Phylloid Algae	96
97-3858/KU-7	SRS U. Frly	Pel. Sk. Pckstn	Equant Cement	Micritized Peloids, Skel. Frags (Crinoids, Brachs)	96
97-4058/KU-8	HM L. Frly	Skel. Wckstn	Micrite & Microspar	Fusulinids, Brach. & Bryozoan Frags.	97
97-4059/KU-9	HM U. Frly	Phyl. Algal Wckstn	Peloidal Micrite & Microspar	Phylloid Algae	99
97-4060/KU-10	HM U. Frly	Osagia, Brach Wckstn	Micrite & Microspar	Osagia, Brach Frags, Phylloid Algae, Ooids	82
95-0634/KDOT-1	SRS U. Frly	Phyl. Algal Wckstn	Peloidal Micrite	Phylloid Algae	98
95-634-P/KDOT-2	SRS L. Frly	Phyl. Algal Wckstn	Microspar & Micrite	Phylloid Algae Frags, Bryozoans, Brachs, Crinoids	94
93-4579/KDOT-3	SRO U. Frly	Phyl. Algal Wckstn	Peloidal Micrite	Phylloid Algae, Bryozoans	78
93-4579/KDOT-4	SRO U. Frly	Phyl. Algal Wckstn	Peloidal Micrite	Phylloid Algae, Bryozoans	86
94-0607/KDOT-5	SRBS M. Frly	Mixed Lith.	Equant Cement & Micrite	Peloids, Ooids, Skel. Frags.	82
94-0607/KDOT-6	SRBS U. Frly	Phyl. Algal Wckstn	Peloidal Micrite	Phylloid Algae, Bryozoans	80
94-2268/KDOT-7	HM U. Frly	Phyl. Algal Wckstn	Peloidal Micrite	Phylloid Algae	99
94-2268/KDOT-8	HM U. Frly	Phyl. Algal Wckstn	Peloidal Micrite	Phylloid Algae	99
94-2268/KDOT-9	HM U. Frly	Phyl. Algal Wckstn	Peloidal Micrite	Phylloid Algae	98
94-2268/KDOT-10	HM L. Frly	Phyl. Algal Wckstn	Microspar & Micrite	Phylloid Algae, Peloids, Skel. Frags.	94
94-2268/KDOT-11	HM L. Frly	Sk. Wckstn	Micrite & Microspar	Fusulinids, Bryozoan & Brach. Frags.	NC
93-4579/KDOT-12	SRO M. Frly	Sk. Grnstr	Equant Cement	Skel. Frags., Quartz Grains, Peloids	NC
95-634-P/KDOT-13	SRS L. Frly	Mixed Lith.	Equant Cement	Peloids, Crinoid Frags, Skel Frags.	NC
81-0083/KDOT-14	LQ L. Frly	Arg. Phyl. Algal Wckstn	Micrite & Microspar	Phylloid Algae, Brachiopods	33
81-0083/KDOT-15	LQ L. Frly	Arg. Phyl. Algal Wckstn	Micrite & Microspar	Phylloid Algae, Brachiopods	51
81-0083/KDOT-16	LQ U. Frly	Phyl. Algal Wckstn	Peloidal Micrite	Phylloid Algae	94
81-0083/KDOT-17	LQ U. Frly	Phyl. Algal Wckstn	Peloidal Micrite	Phylloid Algae	94
97-2114/KDOT-18	OAQ U. Frly	Phyl. Algal Wckstn	Peloidal Micrite	Phylloid Algae	96
97-2114/KDOT-19	OAQ U. Frly	Phyl. Algal Wckstn	Peloidal Micrite	Phylloid Algae	94
97-2114/KDOT-20	OAQ U. Frly	Phyl. Algal Wckstn	Peloidal Micrite	Phylloid Algae	NC



**Figure 3.8.** Histogram showing the number of samples of phylloid-algal limestone within durability-factor categories.



**Figure 3.9.** XY Plot showing relationship of durability factor to bulk spar percentage (n = 25). The weak relationship suggested is that as bulk spar percentage increases, durability increases.

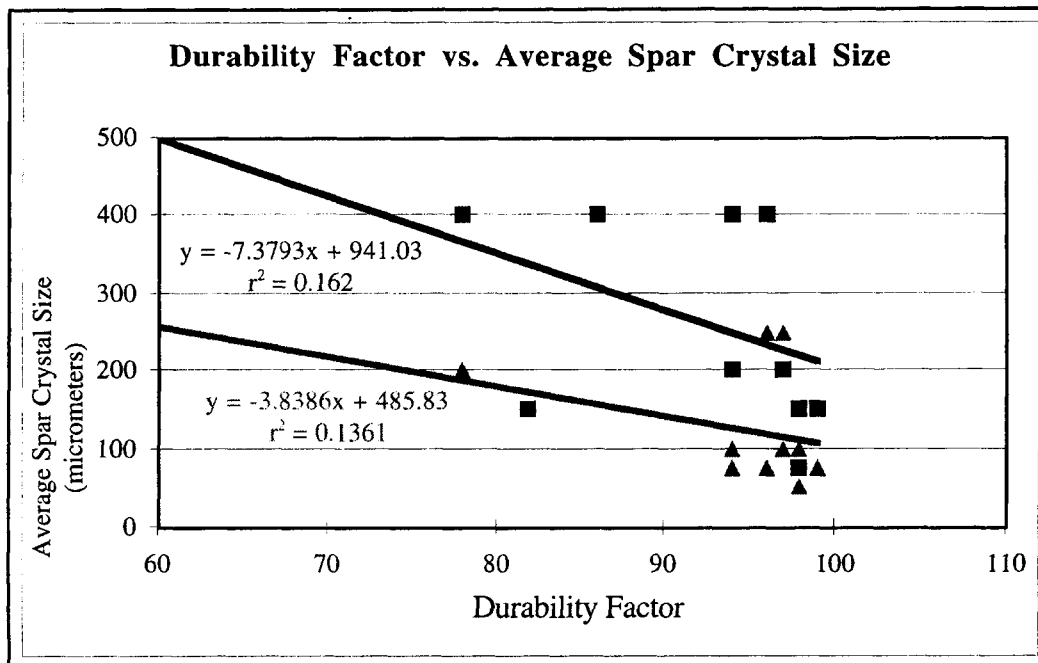
variation in Dunham-classified lithologies in the Farley Limestone. Instead, the results of durability testing indicate that both matrix-rich lithologies such as phylloid-algal wackestone and skeletal wackestone-packstone and matrix-poor lithologies such as skeletal grainstone produce durable aggregates. This indicates that aggregate quality is largely controlled by factors other than lithologic composition. It does seem, however, that matrix-rich lithologies such as phylloid-algal wackestone and skeletal wackestone-packstone generally produce durable aggregates.

### ***Bulk Spar Percentage***

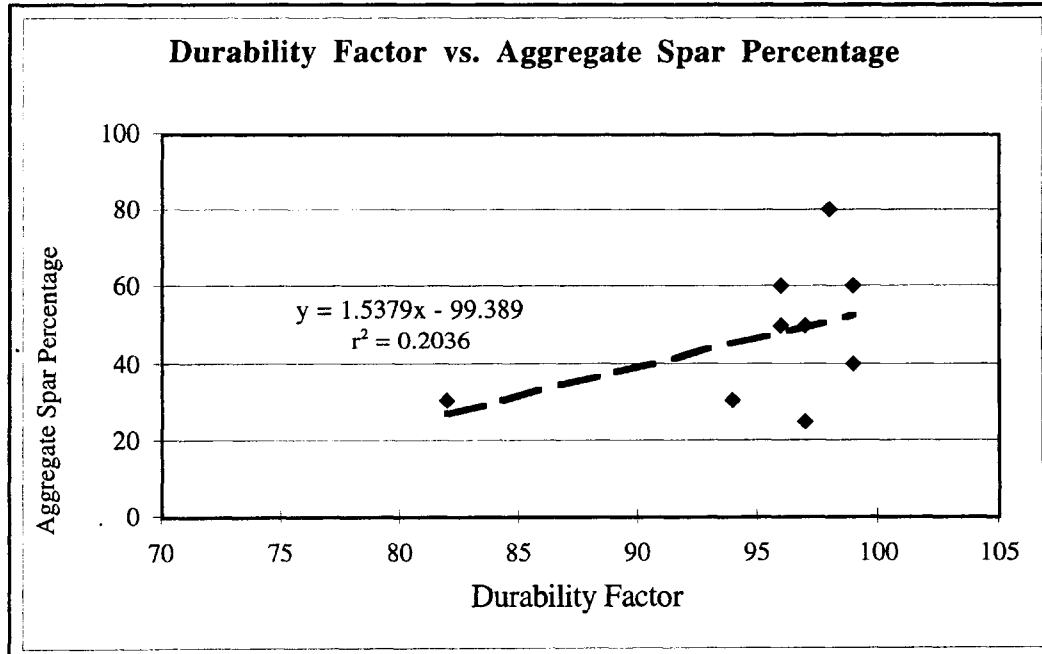
The relationship between bulk spar percentage and durability factor is shown in Figure 3.9. Although the statistical correlation is weak, using the data to evaluate the trend visually is useful. The possible relationship suggested by the regression line is the higher the bulk spar percentage the higher the durability factor, but the fit is so weak we must conclude that, within this data set, there is no real relationship between bulk spar percentage and durability. It is possible, however, that within a larger data set with greater variance a stronger correlation may be established.

### ***Average Crystal Size***

The relationship between average crystal size and durability factor is illustrated in Figure 3.10. This variable was evaluated by determining the average crystal size for each aggregate and then dividing the data into two classes: (1) average crystal size in spar-rich aggregates ( $\geq 25$  percent bulk spar) and (2) average crystal size in spar-poor aggregates ( $< 25$  percent bulk spar). As with the durability factor-bulk spar percentage relationship, the correlations are weak. The regression lines for both classes vaguely suggest that as average crystal size decreases, durability increases. Although the correlations are weak, they are stronger than the correlation between bulk spar percentage and durability factor.



**Figure 3.10.** XY plot showing the relationship between average crystal size (in micrometers) and durability factor. Triangles represent spar-poor samples (n = 12) and squares are spar-rich samples (n = 12).



**Figure 3.11.** XY Plot comparing the total aggregate spar percentage to durability factor (n = 9). The regression line suggests a weak relationship; the higher the aggregate spar percentage the higher the durability.



### ***Aggregate Spar Percentage***

Comparison between durability factor and aggregate spar percentage (Fig. 3.11) shows a slightly stronger correlation than in the other comparisons of bulk spar percentage and average crystal size. Although the plot shows that one data point dominates the correlation, the fit of the regression line suggests that the higher the percentage of aggregate spar, the higher the durability. We must, however, conclude that within this data set, there is no useful correlation. But again, examination of this variable within the context of a larger data set with greater variance may illustrate a more useful correlation.

### ***Total Percentage of Clay-Rich Strata and Distribution of Clay***

Comparing the total percentage of clay-rich strata to durability factor provides one of the stronger correlations. The fit of the regression line in Figure 3.12 suggests that the lower the total percentage of clay-rich strata the higher the durability factor. The correlation between outcrop clay percentage and expansion percentage also produces a relatively strong correlation and suggests that the higher the outcrop clay percentage the higher the expansion (Figure 3.13). These two plots compare the total clay percentage, including shale beds, concentrated stylocumulates, diffuse stylocumulates, and disseminated argillaceous material, to durability factor and expansion percentage. Because shale beds and concentrated stylocumulates are likely to be removed from the limestone during quarrying and crushing, however, correlations between the total percentage of clay-rich strata and durability factor and expansion percentage are not the best representations of the actual aggregate composition. Instead it would be more beneficial to evaluate the impact of only those occurrences of clay that become a part of the aggregate.

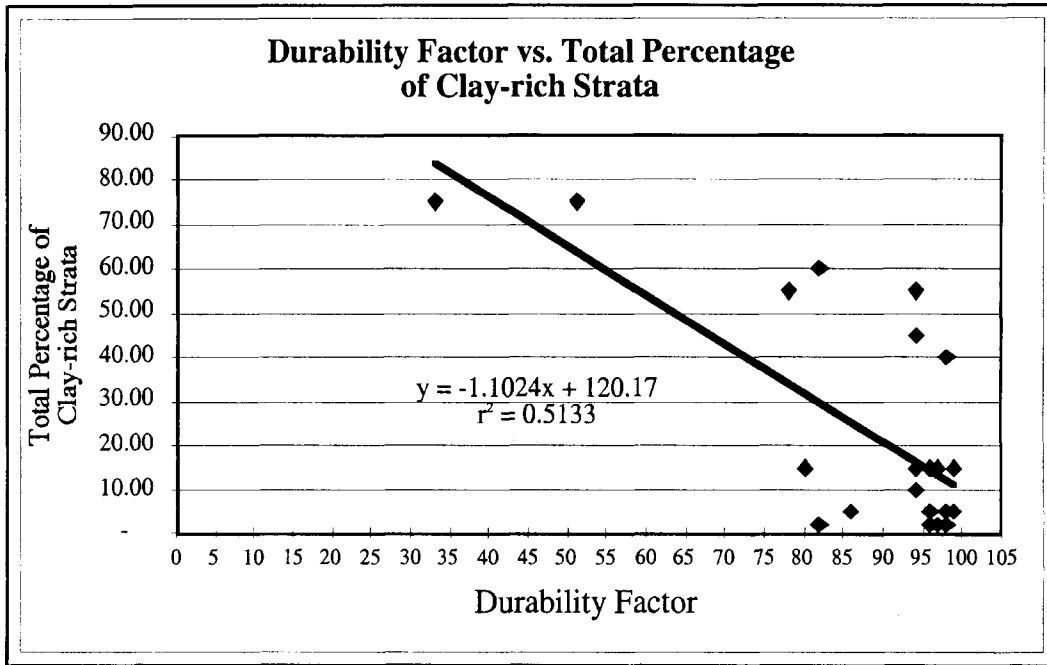
For this reason, a separate estimate was made of the percentage of the strata that contains only diffuse stylolites. Additionally, because the number of samples that

contained enough disseminated clay to be detectable in outcrop is low, disseminated material was also included in this estimate so that the value is a total percentage of diffuse and disseminated clay. These values offer the closest approximations of the actual composition of the aggregate and best illustrate the impact of clay and its distribution on aggregate durability. When the percentage of strata that contains both diffuse and disseminated clay is compared to durability factor, the suggested correlation is stronger than that between total percentage of clay-rich strata and durability factor (Figure 3.14). Additionally, if the percentage of rock that contains diffuse stylolites and disseminated argillaceous material is compared to expansion percentage, another relatively good correlation is suggested (Figure 3.15).

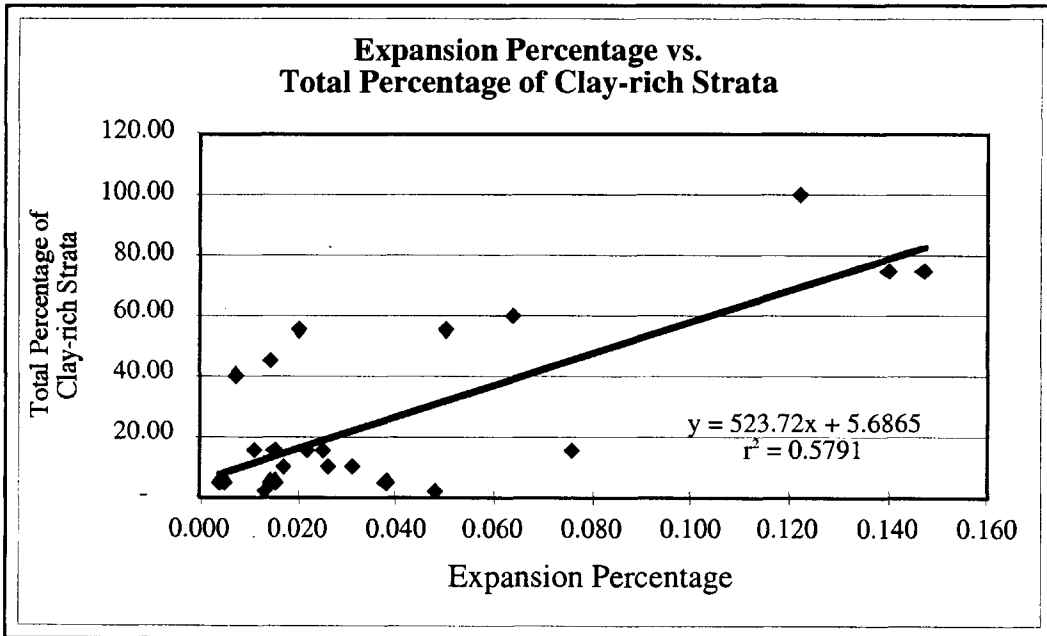
#### ***Percent Insoluble Residue***

Evaluation of insoluble residue data suggests possible trends and relationships, but the correlation is relatively weak. The relationship observed between total percent insoluble residue and durability factor suggests that the lower the insoluble residue percentage the higher the durability factor (Figure 3.16). A similar, slightly stronger correlation exists between expansion percentage and insoluble residue percentage (Figure 3.17). These are the relationships we would expect to see based on the relationship of durability factor and expansion to percent clay. The fact that the correlations related to insoluble residue percentage are considerably weaker than those related to total clay percentage creates a possible contradiction if it is assumed that the bulk insoluble residue percentage should be a reflection of the total percentage of clay-rich strata.

The bulk insoluble residue percentage of the aggregates is not a direct measure of the amount of clay in the rocks. Instead the insoluble residue percentage is a measure of not only the amount of clay in the rocks but also includes things such as quartz, feldspar and organic residue. Therefore, rocks appear to contain no clay can in fact



**Figure 3.12.** XY plot comparing durability factor to total outcrop clay percentage (n = 25). This percentage includes concentrated stylocumulates, diffuse stylolites, and disseminated argillaceous material.



**Figure 3.13.** XY plot comparing expansion percentage to total outcrop clay percentage (n = 26). This percentage includes all three forms of clay.

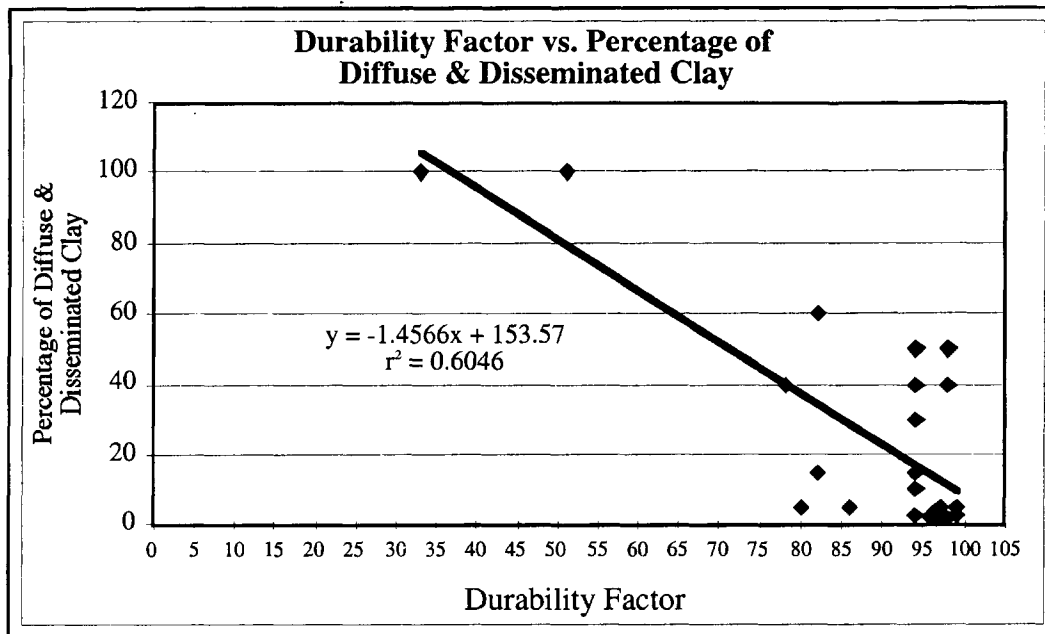


Figure 3.14. XY plot comparing durability factor to the percentage of rock that contains only diffuse stylolites and disseminated argillaceous material (n = 25).

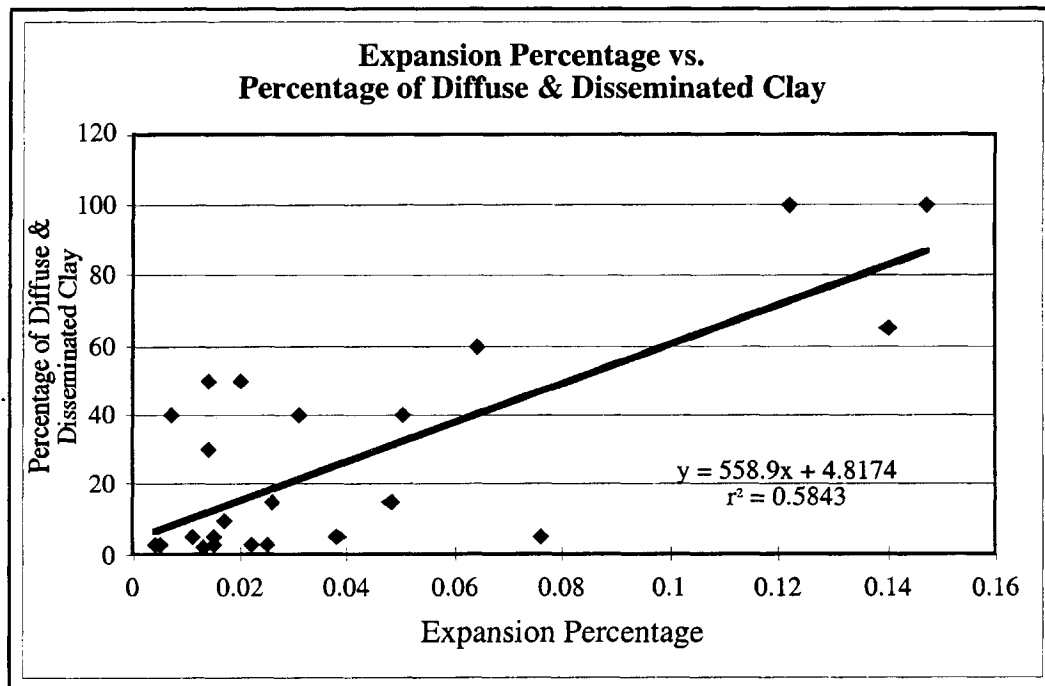
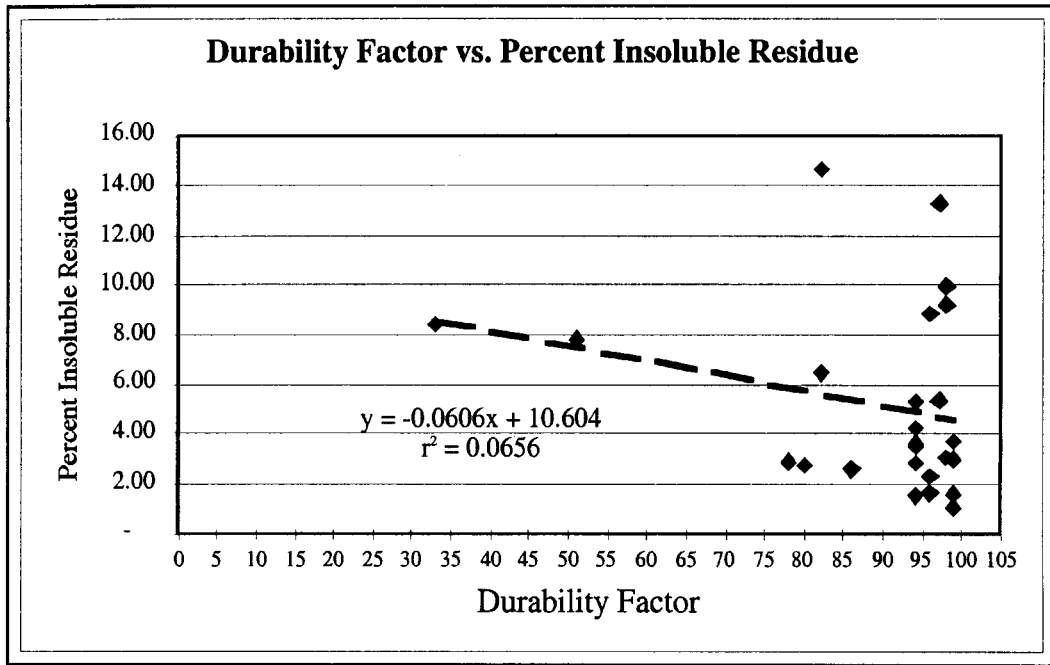
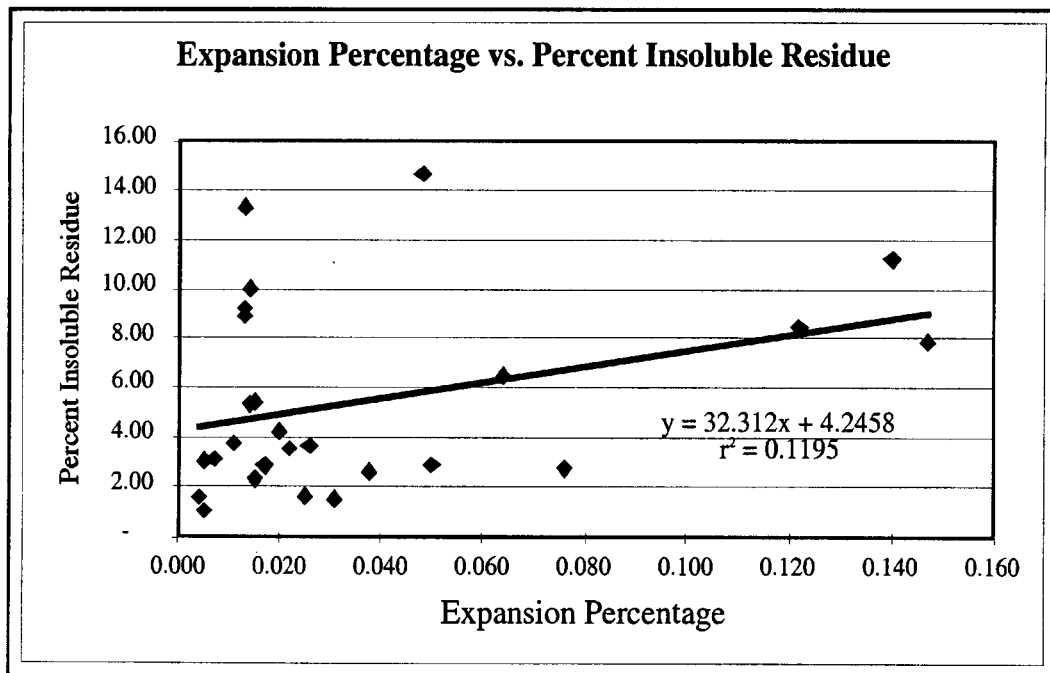


Figure 3.15. XY plot comparing expansion percentage to the percentage of rock that contains only diffuse stylolites or disseminated argillaceous material (n = 26).



**Figure 3.16.** XY plot showing the relationship between durability factor and percent insoluble residue (n = 25).



**Figure 3.17.** XY plot showing the relationship between expansion percentage and percent insoluble residue (n = 26).

have significant amounts of insoluble residue. For example, samples KU-3 and KU-4 have low total clay percentages (2 percent) but relatively high insoluble residue percentages (9.22 percent and 13.32 percent respectively). This indicates that some lithologies that have little to no clay visible on outcrop may contain insoluble materials other than clay, such as quartz, feldspar or organic residue. Furthermore, because insoluble residue percentages are calculated by weight percent, if there is abundant quartz or feldspar in the residue, the insoluble residue percentage is skewed towards the high side because these minerals are heavy relative to clay minerals.

The difference in correlations between insoluble residue percentage and total percentage of clay-rich strata indicates that the presence of minerals such as quartz and feldspar have a much less negative impact on durability factor than do clay minerals. This suggestion is further discussed and supported in the following section.

#### ***Insoluble Residue Composition & Aggregate Clay Percentage***

All residues examined contain quartz and feldspar, and all but one residue contains illite/mica. Other clay minerals in residues include smectite and kaolinite (Table 3.3). Comparison of residue mineralogy with durability factor and expansion percentage, although not a quantitative comparison provides useful information.

Of those aggregates that have durability factors below 95 (KU-2, KU-10) or had testing terminated due to poor performance (KU-1), all contain three detectable clay minerals: illite, smectite, and kaolinite (Table 3.3). Additionally, these aggregates that contain three identified clays in their insoluble residues also have the highest expansion percentages (Table 3.3). There is also an apparent relationship between durability and the aggregate clay percentage in those aggregates that contain the three detectable clay minerals. The aggregate that contains the three clays and has the highest aggregate clay percentage (9.73 percent) is KU-1. This aggregate performed so poorly that testing was

terminated due to degradation and no durability factor was calculated. There was however, an expansion percentage calculated for this aggregate and it was much higher than those expansion percentages calculated for the other aggregates (Table 3.3).

**Table 3.3.** Composition of each insoluble residue for which x-ray diffractometry data were obtained. Also shown are the calculated durability factors (NC = not calculated) and expansion percentages for each of the ten aggregates, as well as the calculated aggregate clay percentages.

Lab. #/Sample #	Quartz	Feldspar	Illite/Mica	Smectite	Kaolinite	Durability Factor	Expansion %	Agg. Clay %
97-3685/KU-1	X	X	X	X	X	NC	0.14	9.73
97-3686/KU-2	X	X	X	X	X	94	0.02	3.64
97-3687/KU-3	X	X	X			97	0.013	6.44
97-3688/KU-4	X	X	X			98	0.013	7.4
97-3689/KU-5	X	X	X			99	0.011	3.18
97-3690/KU-6	X	X	X	X		96	0.015	1.97
97-3858/KU-7	X	X	X		X	96	0.013	8.04
97-4058/KU-8	X	X	X		X	97	0.015	3.87
97-4059/KU-9	X	X				99	0.005	3.02
97-4060/KU-10	X	X	X	X	X	82	0.064	5.8

The seven remaining aggregates have durability factors of at least 95. Of these seven, three (KU-6, KU-7, KU-8) contain a combination of only two detectable clay minerals in the residues, illite and smectite or illite and kaolinite. Although these aggregates have similar expansion percentages, a connection may exist between the presence of smectite and lower durability. Aggregate KU-6 contains smectite but has a relatively low percentage of aggregate clay (1.97 percent), whereas aggregates KU-7 and KU-8 contain higher aggregate clay percentages (8.04 percent and 3.07 percent respectively) and contain no smectite. Although, aggregate clay percentages do not indicate the percentage of smectite exclusively, it is reasonable to infer that smectite is present in higher proportions (as are the other clay minerals) in aggregates with higher aggregate clay percentages. This suggests that the presence of smectite, even in small quantities, may negatively impact durability more than the presence of other clay minerals in higher quantities.

Three aggregates (KU-3, KU-4, KU-5) contain only one detectable clay mineral, and one aggregate (KU-9) contains no detectable clay minerals. These aggregates all have the highest durability factors (97 or higher) and the lowest expansion percentages. Two of these four aggregates contain high aggregate clay percentages (6.44 percent and 7.4 percent). Apparently having only illite or lacking smectite or kaolinite indicates the potential for high durability as long as some clay percentage is not exceeded, but this critical percentage is unknown at this time.

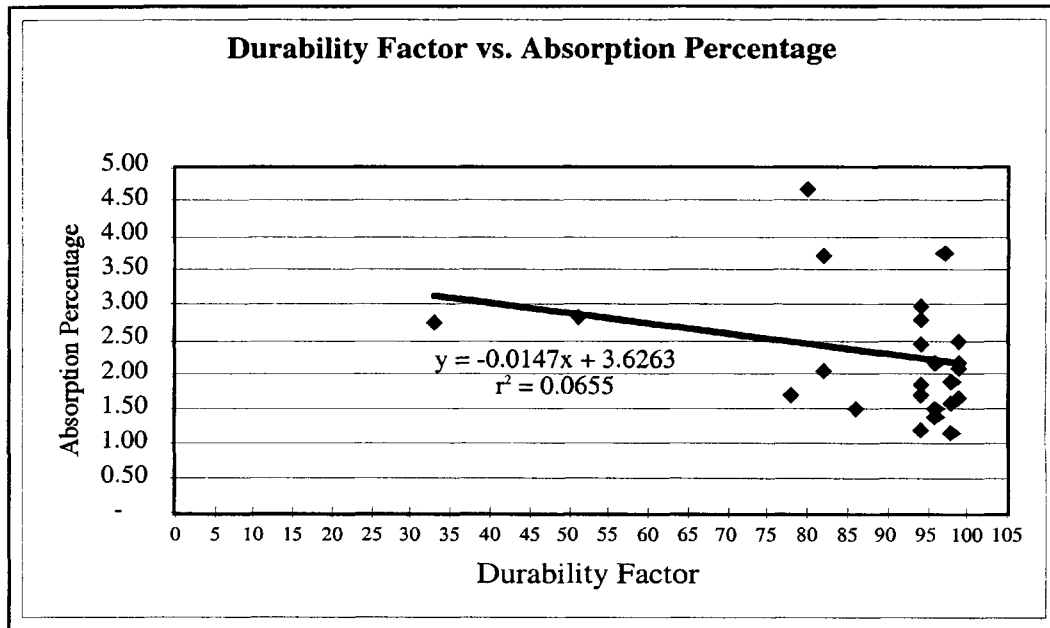
### ***Absorption***

The absorption value is a measure of the porosity and permeability of an aggregate. The correlations between durability factor and absorption are weak or nonexistent (Fig. 3.18), and the correlation between expansion percentage and absorption is only slightly stronger (Figure 3.19). The fit of the regression lines suggest that the lower the absorption percentage the higher the durability factor and the lower the expansion percentage, but the correlations are so weak that, within this data set, we must conclude that there is no relationship between absorption and durability or expansion.

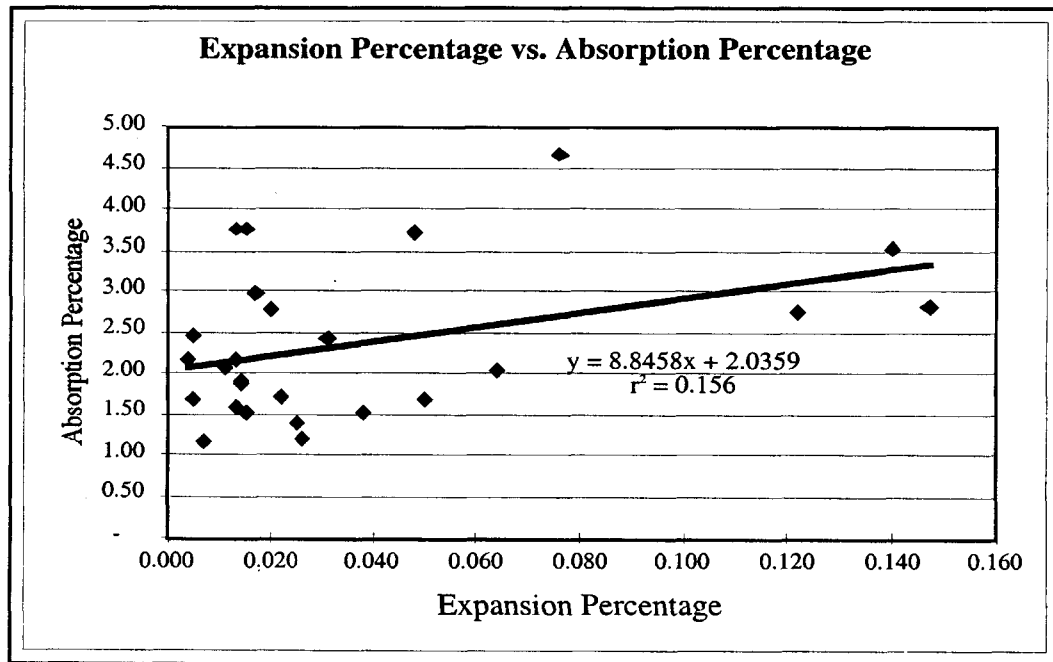
### **Discussion**

KDOT requires class 1 aggregates to meet three specifications: (1) a modified freeze-thaw ratio of 0.85 (85 percent) or greater; (2) a durability factor of 95 or higher; and (3) an expansion percentage of 0.02 percent or lower. Therefore, determining which geologic variables seem to have a direct affect on these three physical properties is important in recognizing what KDOT recognizes as durable aggregate. Because the correlations examined between modified freeze-thaw value and the geologic properties were all weak to nonexistent, the following discussion will concentrate on the comparisons that were made to durability factor and expansion percentage.





**Figure 3.18.** XY plot showing the relationship between durability factor and absorption percentage (n = 25).



**Figure 3.19.** XY plot showing the relationship between expansion percentage and absorption percentage (n = 26).

Of the lithologies examined micrite or microspar matrix-rich lithologies as well as sparry cement-rich lithologies attain class 1 status. Therefore, it seems unlikely that the presence of micrite or microspar matrix in the rocks preferentially produces higher durability aggregates than does the presence of abundant sparry cement. The hypothesis that micrite-rich phylloid-algal lithologies produce durable aggregates seems to be largely supported however. Additionally, other micrite or microspar matrix-rich lithologies such as skeletal wackestone-packstone also commonly produce durable aggregates. Because there are exceptions to these trends and because cement-rich lithologies such as oolite also produce durable aggregates, textural classification cannot be used to confidently predict aggregate durability.

The effect of coarse spar on durability is difficult to establish based on the data collected for this study. The correlation between bulk spar percentage and durability suggests that the more coarse spar present the higher the durability. Alternatively, the correlation between average crystal size and durability suggests that finer average crystal sizes yield higher durability aggregates. Because the correlations are weak for this data set, it is impossible to conclude with certainty that the amount or coarseness of spar present in the rocks has any impact, positive or negative.

In their report on aggregate durability, Wallace and Hamilton (1982) determined that the insoluble residue percentage was significant in predicting aggregate durability. For this reason they included percent insoluble residue value in the Pavement Vulnerability Factor (PVF) calculation that they used to initially identify durable aggregates until physical testing was completed. The correlations between durability factor and percent insoluble residue in my study show no strong correlation. The weak trend suggests that the lower the percent insoluble residue the higher the durability factor and the lower the expansion percentage. Therefore, the hypothesis that high amounts of insoluble residue in the rocks has a negative affect is not refuted. Because

the correlations are weak and both class 1 and nonclass 1 aggregates contain variable percentage of insoluble residue, support for the hypothesis is tenuous at best, and it is clear that variables other than insoluble residue percentage must be involved.

Of the hypotheses examined, those related to the abundance, distribution, and mineralogy of clay in the rocks and insoluble residues produce the strongest correlations. The most accurate indicator of durability seems to be the total percentage of strata that contain diffuse stylocumulates plus disseminated argillaceous material. These occurrences of clay are most likely to become part of the aggregate following crushing and sorting. The relationship observed suggests that those rocks with low percentages of diffuse stylocumulates and disseminated argillaceous material are likely to qualify as class 1 aggregate. Furthermore, those rocks dominated by concentrated stylocumulates and clay beds with little diffuse stylocumulates and disseminated argillaceous material are also likely to produce durable aggregates. Therefore, the hypotheses regarding the presence of concentrated and diffuse stylocumulates as well as disseminated argillaceous material are supported.

As mentioned previously, the main cause of d-cracking is thought to be the expansion and contraction of aggregates caused by freezing and thawing of water entrapped in the aggregate. Given this cause of d-cracking and the information presented regarding clay minerals, it is reasonable to believe that the presence of some clay minerals in the aggregates would negatively impact aggregate durability.

Of the three clay minerals detected in the aggregates examined, smectite is likely to have the most negative impact on aggregate durability. The outstanding characteristic of the smectite group of clays is their capacity to absorb water molecules, thus producing marked expansion of

the structure (Klein & Hurlbut, 1993). This characteristic explains why those aggregates that contain larger amounts of smectite also exhibit the greatest expansion percentages (Table 3.3). Similarly, because expansion is so closely related to the durability factor (Fig. 3.6), the presence of smectite is likely to cause a reduction in durability. Clearly smectite must be present in the aggregates in enough abundance to impact negatively durability. Determining the exact threshold for the amount of smectite that negatively impacts durability will require further work.

### **Conclusions**

All limestone textural classifications may produce class one aggregate and the presence of abundant micrite or microspar matrix or abundant sparry cement has no apparent impact on durability. Micrite or microspar matrix-rich lithologies such as phylloid algal wackestones and packstones and skeletal wackestones and packstones, however, are commonly good sources of durable aggregates.

Other geologic properties such as bulk spar percentage, spar size, insoluble residue percentage and grain size produce suggestive trends when related to durability and expansion. These factors do not, however, seem to be reliable indicators of durability.

Of the geologic parameters examined in this study, those related to the abundance, distribution, and mineralogy of clay seem to be the most significant. The strongest correlations between geologic properties and physical test results are related to the total clay percentage, clay distribution, and composition of insoluble residues. The more clay observed in outcrops (total percentage of clay-rich strata) the lower the durability and the higher the expansion percentage. Limestones that contain clay only in concentrated stylocumulates or shale beds are likely to produce class 1 aggregate because the clays and shales are crushed too finely to become part of

the aggregate. Limestones with diffuse stylocumulates and disseminated clay are less likely to produce class 1 aggregates.

A further indicator of durability is the composition of the insoluble residues. If the residues contain three clay minerals (illite, kaolinite, and smectite) the durability is likely to decrease. Limestones without detectable clay minerals are likely to produce durable aggregates. Furthermore, if even a small amount of smectite is present in the residues, there is a higher likelihood of failure due to the expansive properties of this group of clay minerals.

## **Chapter 4: Conclusions & Implementation**

## Sedimentology & Sequence Stratigraphy

Ten individual lithofacies were identified in the Lane-Island Creek shales and the Farley Limestone: (1) phylloid algal limestones, (2) skeletal wackestone-packstone, (3) peloidal, skeletal packstone, (4) sandy, skeletal grainstone-packstone, (5) oolite, (6) *Osagia*-brachiopod packstone, (7) fossiliferous siltstone, (8) laminated to lenticular-bedded siltstone, (9) organic-rich mudstone and coal, and (10) blocky mudstone. Depositional environments were interpreted for each of these lithofacies.

A sequence-stratigraphic framework was developed for the Lane-Island Creek shales and the Farley Limestone using interpreted lithofacies and their distributions and correlations. This sequence-stratigraphic framework includes the evaluation of the main controls of the distribution of lithofacies. It seems that controlling factors of two different types interacted to cause the complex lateral and vertical distribution of lithofacies. Fluctuating sea-level caused large-scale changes in depositional architecture. Evidence for relative sea-level rise and fall was used to identify related packages of strata, sequence boundaries and other significant surfaces such as marine flooding surfaces. Local factors such as depositional topography and source direction and distribution of siliciclastics interacted further to control the lateral and vertical distribution of lithofacies.

Within the sequence-stratigraphic framework of the Lane-Island Creek shales and the Farley Limestone, several features are important because they have the potential for affecting the interpretation of other similar units in the Pennsylvanian of Kansas.

Most past work concerning the phylloid-algal limestones of the Midcontinent Pennsylvanian suggests that the algae typically constructed thick mounds or banks thereby producing significant depositional topography (Harbaugh, 1959, 1960; Heckel & Cocke, 1969; Crowley, 1969; Arvidson, 1990). We suggest, however, that some phylloid-algal limestones,

especially those in the lower Farley, did not construct topography but rather tended to eliminate it by accumulating in the depositional lows.

The distribution of siliciclastics within the Island Creek Shale and lower Farley Limestone is also significant. Many of these siliciclastics seem to have been deposited preferentially in topographically low areas. In this way, these siliciclastic units are recognized more as valley fills than as traditional delta lobes or complexes. The distribution of siliciclastics in depositional lows diminished depositional topography in places rather than create it. This point is important in considering the framework of other similar Pennsylvanian units; putative deltaic units may have filled depositional lows along the upper surfaces of limestones instead of building positive relief on flat limestone platforms.

Finally, sequence boundaries and other genetic surfaces are not always coincident with boundaries between lithostratigraphic units. For example, a flooding surface that indicates initial sea-level rise may be located within a shale unit and not necessarily at the boundary between the shale and the overlying limestone. For this reason it is always important to consider the lithostratigraphic boundaries separately from the sequence-stratigraphic surfaces and sequence boundaries.

Establishment of a sequence-stratigraphic framework such as that developed herein allows the understanding of relative sea-level history. This understanding of relative sea-level history allows other factors such as paleotopography and sediment dispersal to be evaluated. The methodology and results of this study provide a good model that can be used to evaluate other, similar Pennsylvanian units of the Midcontinent, such as the Argentine Limestone, the Spring Hill Limestone, and the Captain Creek Limestone as well as many others.



## **Geologic Properties Affecting Quality of Limestone Aggregates**

Chapter 3 outlined geologic parameters thought to have a significant impact on the durability and quality of limestone construction aggregates. These parameters include lithologic fabric, amount and coarseness of spar, percent insoluble residue, amount and distribution of clay-rich zones, and the mineralogy of the insoluble residues. Data on these variables were compared to the results of the physical tests used by KDOT to test aggregate durability.

Based on the aggregates tested for this study, lithologic classification is not a reliable indicator of durability. Several different lithologies produced both durable and poor aggregates. Furthermore, the abundance of micrite-rich matrix or amount of sparry cement made little difference in durability. Micrite-rich lithologies such as phylloid-algal wackestone and skeletal wackestone-packstone, however, generally produce durable aggregates. Although possible relationships were suggested for other parameters such as spar content and crystal size as well as insoluble residue percentage, the correlations were weak to nonexistent within the data set used for this study. Therefore, no definitive conclusions can be drawn concerning these variables. Further study of these parameters and evaluation of a larger data set with greater variance, however, may produce stronger correlations and more definitively support or refute the hypotheses presented in this paper.

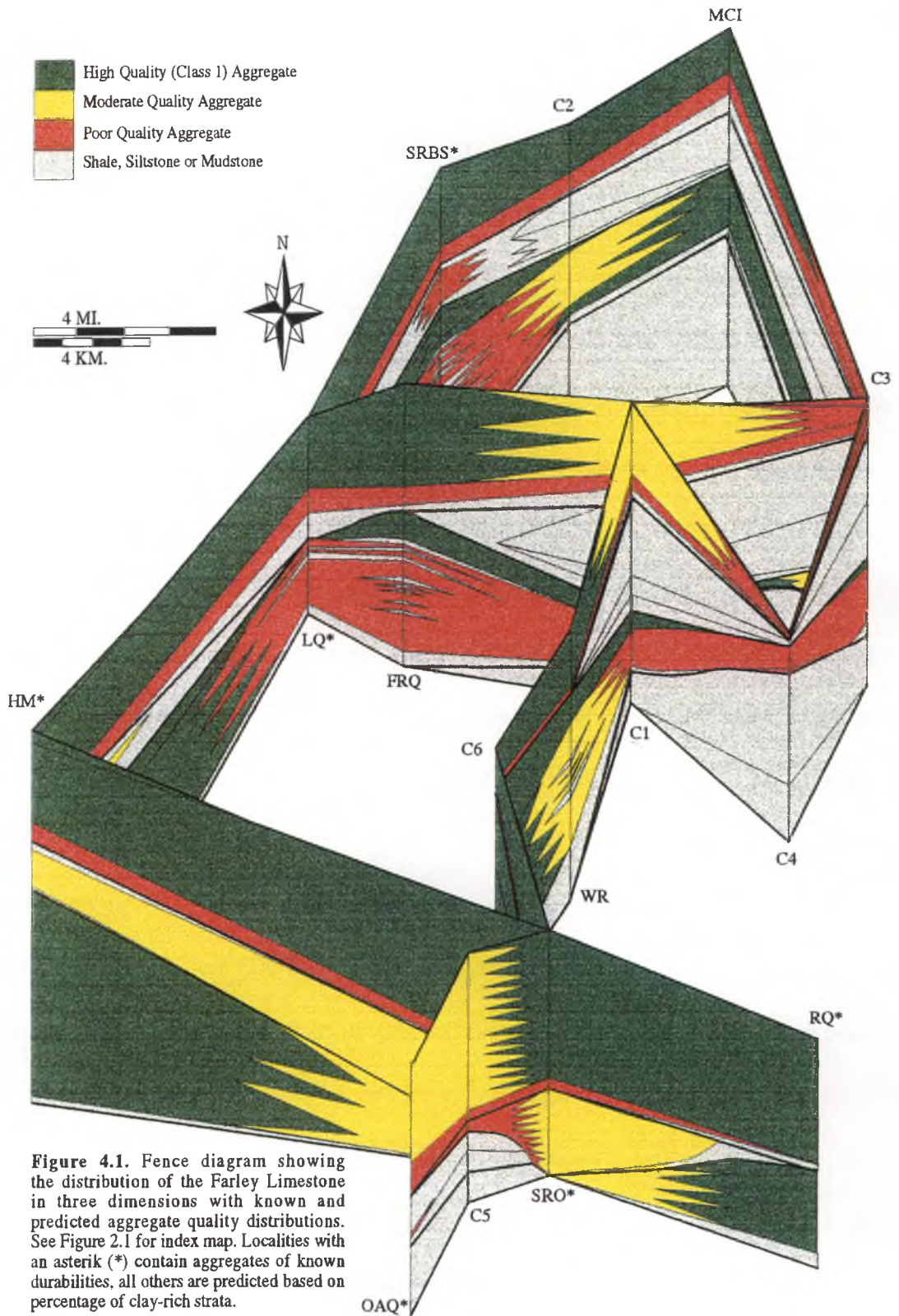
The most significant correlations observed were between durability and the amount, distribution, and mineralogy of clay. The data indicate that the higher the total percentage of clay-rich strata present in the rocks, the lower the durability factor and the higher the expansion percentage. Furthermore, if three different clay minerals are present in the insoluble residues, durability is likely to decline. Smectite seems to have the most significant impact, which is likely to be due to its expansion properties upon absorption of water. Thus, even small amounts of smectite are likely to have a negative impact on aggregate durability; at this time the critical threshold of smectite content is unknown.

### **Predicting the Distribution of Class 1 Aggregate**

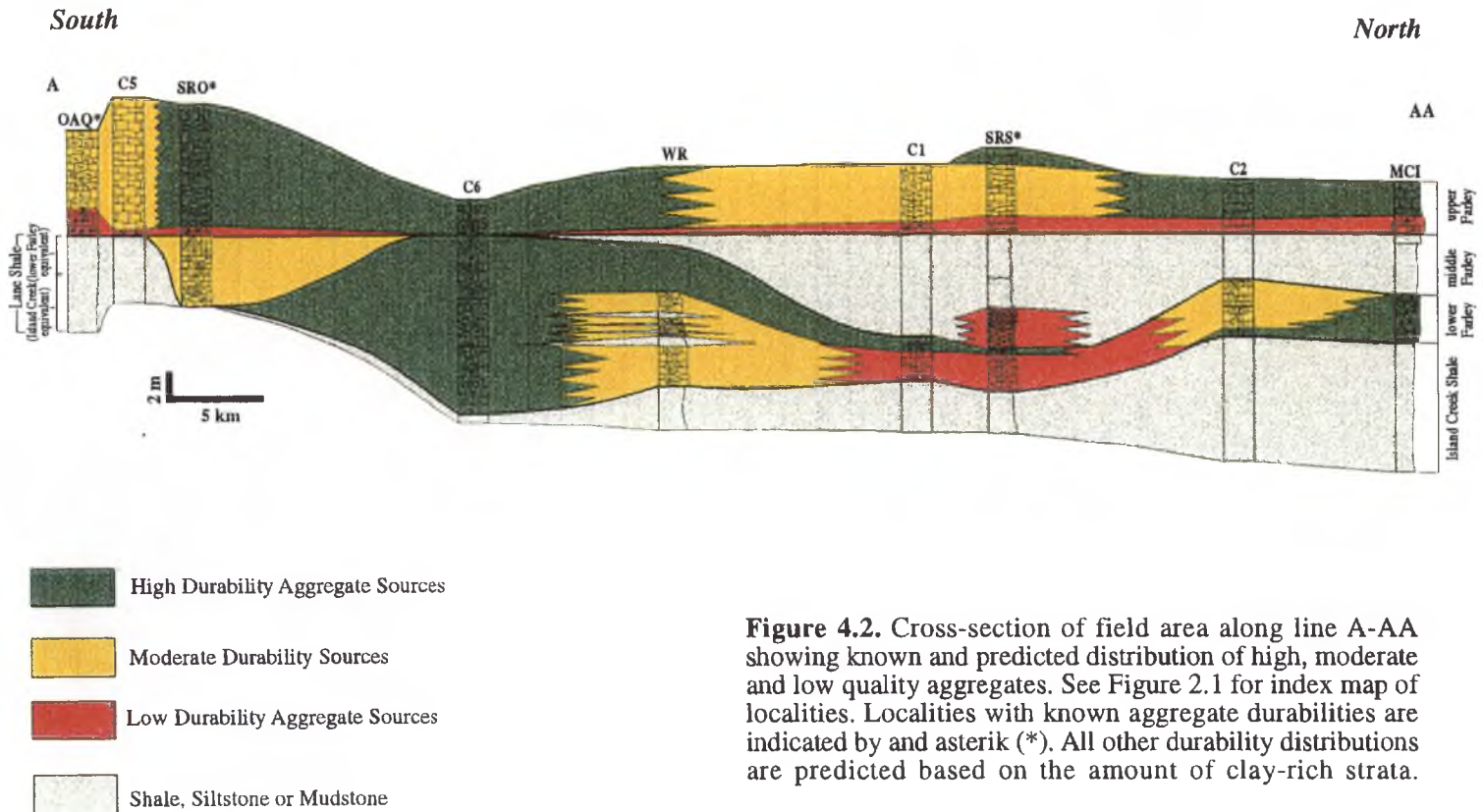
Chapter 2 discussed the lithofacies of the Farley Limestone and illustrated that a complex interaction of factors determined the final lateral and vertical distribution of the lithofacies. Chapter 3 outlined and discussed possible geologic variables that impact aggregate durability. Therefore, to predict the distribution of class 1 aggregate within a limestone unit and then maintain production from the high-quality resources, the information presented in chapters 2 and 3 must be integrated.

As facies change laterally and vertically so do the geologic properties that have an impact on quality of aggregate. As discussed previously, the property that seems to have the greatest impact on the lateral variability of carbonate facies is depositional topography. This topography, the relative sea-level history, and the direction of the source area of the siliciclastics were the most important factors in controlling the distribution of fine siliciclastics within the Farley Limestone. Because, the distribution of fine siliciclastics has the most negative impact on aggregate quality, understanding the controls of fine-siliciclastic distribution results in the understanding of the distribution of durable aggregates.

To show the distribution of class 1 aggregate and nonclass 1 aggregate, the results of KDOT physical tests and known distribution of clay-rich limestone can be integrated with the stratigraphic cross-sections presented in Figures 2.30 to 2.34. The new integrated cross-sections are presented in Figures 4.1 to 4.5. To compile these cross-sections, aggregate quality was determined from KDOT physical test results where possible (indicated by a \* in the locality name). In other areas where there was no physical test data, durability predictions were made from the amount of clay-rich

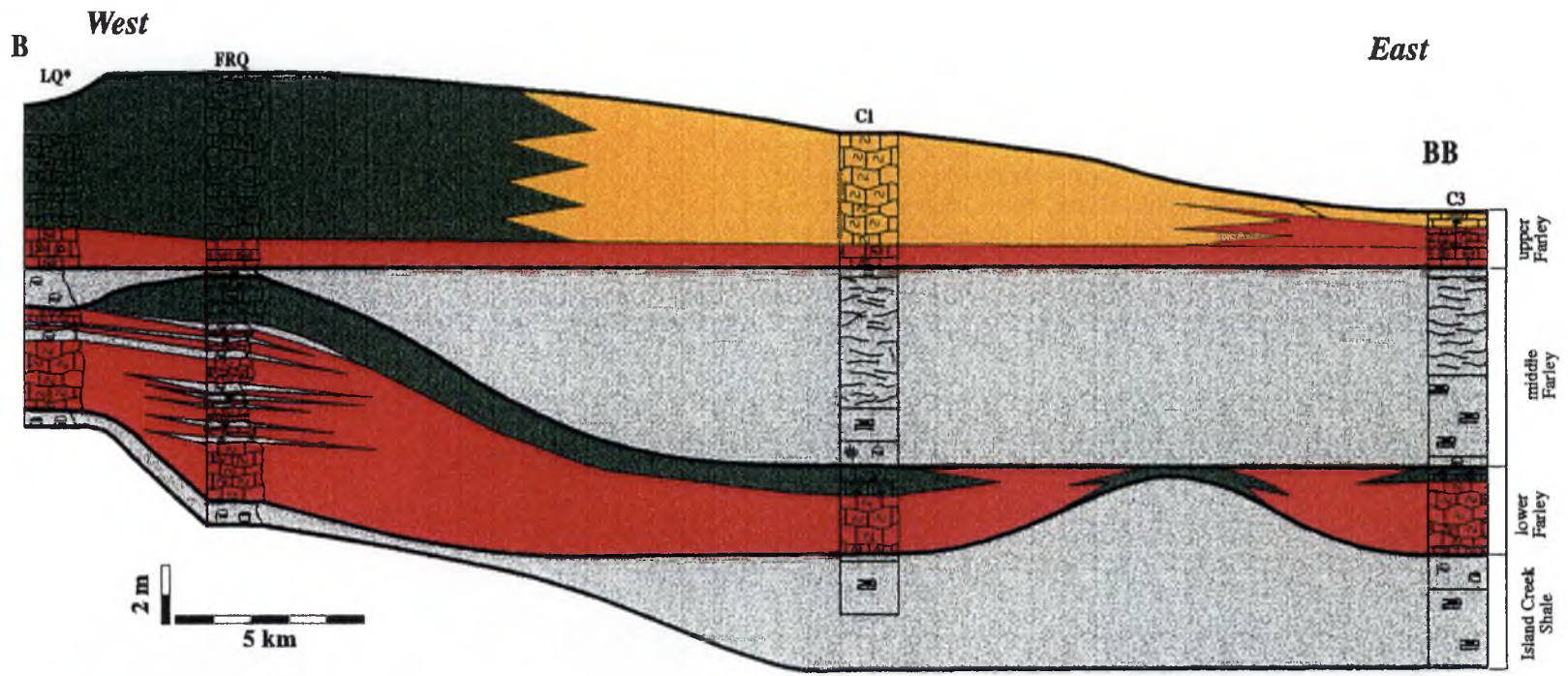


**Figure 4.1.** Fence diagram showing the distribution of the Farley Limestone in three dimensions with known and predicted aggregate quality distributions. See Figure 2.1 for index map. Localities with an asterik (\*) contain aggregates of known durabilities, all others are predicted based on percentage of clay-rich strata.



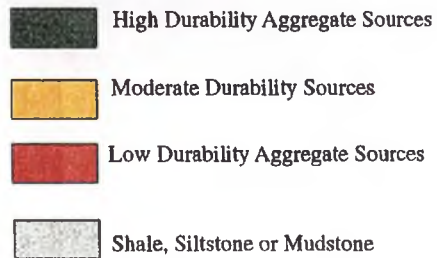
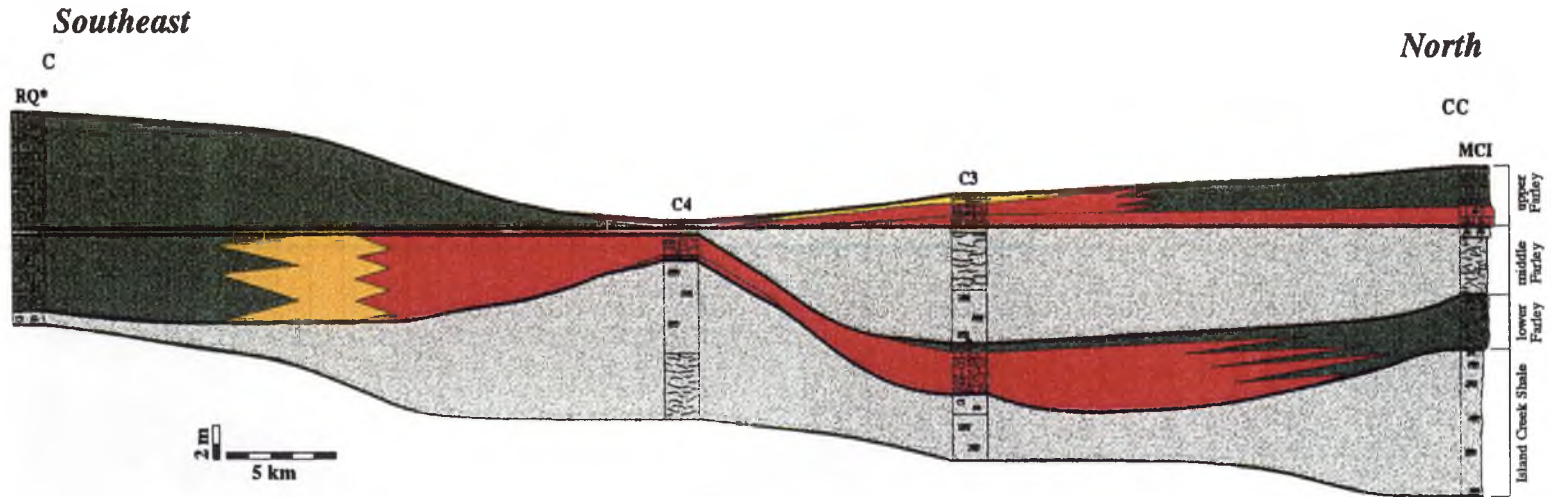
**Figure 4.2.** Cross-section of field area along line A-AA showing known and predicted distribution of high, moderate and low quality aggregates. See Figure 2.1 for index map of localities. Localities with known aggregate durabilities are indicated by and asterik (\*). All other durability distributions are predicted based on the amount of clay-rich strata.



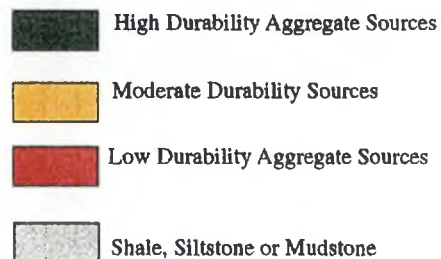
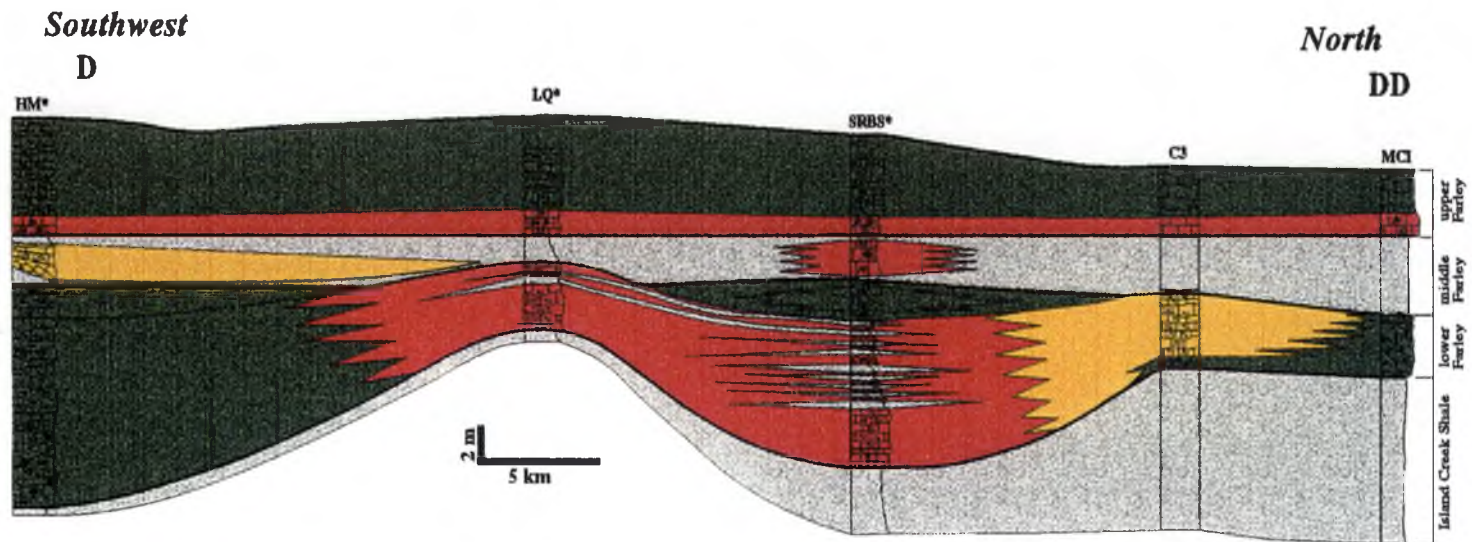


- High Durability Aggregate Sources
- Moderate Durability Sources
- Low Durability Aggregate Sources
- Shale, Siltstone or Mudstone

**Figure 4.3.** Cross-section of field area along line B-BB showing known and predicted distribution of high, moderate and low quality aggregates. See Figure 2.1 for index map of localities. Localities with known aggregate durabilities are indicated by and asterik (\*). All other durability distributions are predicted based on the amount of clay-rich strata.



**Figure 4.4.** Cross-section of field area along line C-CC showing known and predicted distribution of high, moderate and low quality aggregates. See Figure 2.1 for index map of localities. Localities with known aggregate durabilities are indicated by an asterisk (\*). All other durability distributions are predicted based on the amount of clay-rich strata.



**Figure 4.5.** Cross-section of field area along line D-DD showing known and predicted distribution of high, moderate and low quality aggregates. See Figure 2.1 for index map of localities. Localities with known aggregate durabilities are indicated by and asterik (\*). All other durability distributions are predicted based on the amount of clay-rich strata.

rock. Three classes were developed for the integrated cross-sections. The known high-durability aggregates have been tested by KDOT to have durability factors of 95 or greater. The rocks that include that class and that we predict to produce relatively high-durability aggregates are those with low clay content. We arbitrarily chose 30 percent or less of total clay-rich strata as the class commonly producing durable aggregates. We chose 30-40 percent total clay-rich strata aggregates to represent moderate-quality aggregates and those with greater than 40 percent clay-rich strata to represent poor-quality aggregates. These durability categories clearly are not absolute; they are merely chosen to represent lateral variability in limestone quality. For example, some limestones with less than 30 percent total clay in them may fail to make class 1 or, alternatively, some limestones with more than 30 percent clay may produce class 1 aggregates. Instead, the estimations of clay content outlined provide a relatively accurate means to evaluate what the durability is most likely to be.

Good geologic reasons explain the aggregate distribution outlined. We showed that the phylloid-algal limestones of the lower Farley Limestone thicken into the depositional lows such as those found at localities SRBS, FRQ, WR, and C6 (Figures 4.1-4.5). We also concluded that phylloid-algal limestones commonly produce durable aggregates. Normally one might consider that it would be beneficial to quarry operators to locate operations in paleotopographic depositional lows that potentially hold thick accumulations of phylloid algal facies. However, the siliciclastics of the lower Farley also seem to have been deposited preferentially in paleotopographic lows. In some places this has produced successions of alternating siltstone and phylloid-algal facies like those found at localities SRBS, FRQ, and WR (Figures 4.1-4.5). These interbedded limestones contain a high abundance of disseminated argillaceous material and diffuse stylocumulates that were shown to have a negative impact on quality of aggregate. Therefore, the thick successions of phylloid-algal limestones found in the northwest part of the



field area should produce poor aggregate. Farther to the south and southeast, where the interbedded siltstones become less abundant, the clay content of the phylloid-algal limestones decreases. Therefore, at localities such as C6 in the center of the field area, there is a thick succession of phylloid-algal limestone that would be likely to produce high-quality aggregate.

Class 1 aggregate is produced from nearly the entire Farley Limestone stratigraphic interval at localities HM and RQ. These localities are located at the southeastern and southwestern corners of the field area and, as illustrated in Figure 4.5, are located farthest from the sources of siliciclastic material. Furthermore, the rocks in these areas were interpreted to have been deposited in topographic low areas that resulted from both paleotopography and regional depositional dip. Therefore, the conditions of depositional topography and distance from siliciclastic input were favorable for the formation of high-quality limestone aggregates in these areas.

Most of the higher energy facies such as oolite and peloidal, skeletal packstone produce class 1 aggregates. This is likely related to the relatively low clay content in these high-energy facies. Therefore, it is important to understand what controls the distribution of these facies. Some of these high-energy facies in the Farley Limestone are located on or immediately adjacent to paleo highs. Locality MCI in the north and C6 in the center of the field area both contain thick accumulations of high-energy facies along paleo highs in the lower Farley. Alternatively localities HM and SRBS contain thinner accumulations of high-energy facies in slight paleo lows in the lower Farley. Although only two of these localities (HM, SRBS) produce confirmed class 1 aggregate, the characteristics of the rocks in the other localities are favorable for high-quality aggregate. These examples show that it is important to understand the paleotopography of a unit in order to better locate and maintain production from durable aggregate sources.

Establishing a record of sea level fluctuation could also be helpful in the location of sources of high-quality aggregates. For example in the Farley, during times of high relative sea level, the sources of fine siliciclastics would have been shifted distally thereby decreasing the input of fine siliciclastics. Therefore, the rocks deposited during relative sea-level highstands would contain lower percentages of fine siliciclastics, and likely would produce aggregates of higher quality.

In the Farley Limestone, therefore, locating high-quality aggregates requires more than simply locating thick successions of limestone. Having an understanding of the conditions under which the rocks of the Farley Limestone were originally deposited would likely aid in the location and maintenance of class 1 aggregate resources. The most important conditions to understand seem to be paleotopography and source direction and distribution of siliciclastics and relative sea level. Furthermore, it seems likely that the application of these same ideas to other limestone units of similar origin such as the Argentine Limestone, the Spring Hill Limestone and other units of the Pennsylvanian of Kansas will assist in locating high-quality limestone construction aggregates.

### **Implementation**

There are several methods available that would allow KDOT geologists and quarry operators to collect and use stratigraphic and geologic data in order to locate and maintain production from sources of class 1 aggregate.

Exploration for class 1 aggregate can be enhanced by understanding the regional context and rock properties of an individual rock unit. KDOT geologists and quarry operators could take exploratory drill cores and characterize the geologic properties of lithofacies, abundance of clay-rich zones, spar content, percent insoluble residue, and mineralogy of the residues. This would allow KDOT geologists or quarry operators to construct detailed stratigraphic profiles of existing

and potential quarry sites with emphasis on determining paleotopography and source direction and distribution of siliciclastics. Then, as was done in this study, two- and three-dimensional reconstructions of the area can be compiled and used to predict the distribution of class one aggregate. Although not perfectly accurate, these models would provide a tool for decision making regarding future quarry production and locations of new quarries.

Once quarrying has begun, it is important to maintain production of class 1 aggregate as units are quarried. If changes in clay content can be identified during lateral production of a stratigraphic unit, then quarrying can be halted or can proceed in another direction while KDOT physical tests are run. KDOT and quarry personnel could be trained to measure stratigraphic sections or identify increases in diffuse stylocumulates or disseminated clay.

Geophysical tools also may be useful. One such tool is the gamma-ray log, which measures the natural gamma radiation of the rocks and can be used to discriminate clay-rich limestones from clean limestones. The higher levels of radiation in shale are caused by the absorption of thorium by clay minerals, the potassium content of clay minerals (principally illite), and uranium fixed by associated organic material (Doveton, 1994). This is useful in the location of durable aggregates because gamma-ray logs give an indication of the amount of clay contained within a limestone unit. Furthermore, the measurement is relatively simple to obtain using either a hand-held scintilometer at the outcrop, or a gamma-ray logging tool in a borehole.

Standard gamma-ray logging records only the sum of all gamma rays which is useful in differentiating shale and clay from other rock types. Spectral gamma-ray logging, however, allows estimations of the separate contributions of the individual isotopes, which can then be used to estimate clay mineral volumes and types (Doveton, 1994). As was illustrated previously, the presence of clay, especially some types of clay minerals, has a significantly negative impact

on aggregate durability. Therefore, the ability to locate not only clay-rich limestones but to also identify the clay minerals and percentages could be very useful in avoiding non-class 1 aggregates. For this reason, spectral gamma-ray logging is potentially a very powerful tool.

Ground penetrating radar (GPR) is another geophysical tool that could be useful in the search for class 1 aggregates. GPR detects differences in the dielectric permittivity of the rocks in the subsurface. This electrical property of the rocks is controlled mainly by the water content and is often a function of the amount and type of clay present in the rocks. Therefore GPR could be used to create a three-dimensional picture of the rocks in the subsurface, showing distributions of clay-rich and clay-poor strata. A study is currently underway (Franseen & Martinez, in press) to test the applicability of GPR to the class 1 aggregate problem.

The location and maintenance of sources of class 1 aggregates is an important problem to address. The use in both state and local construction projects of the best, most durable aggregates available is economically important. This study represents an initial step in producing a set of geologic criteria that can be used to identify limestones that are likely to produce class 1 aggregates. Furthermore, this study has shown that by understanding the regional and local controls on the distribution of carbonate lithofacies the chances of locating and maintaining sources of class 1 aggregates are greatly enhanced. Future study will be useful not only in continuing to test my conclusions but also in applying the concepts to other similar limestone units from which class 1 aggregates are produced.

## References

- Arvidson, R.S., 1990, Stratigraphy, carbonate petrology, diagenesis, and trace element cement geochemistry of the Wyandotte limestone (Upper Pennsylvanian), Miami County, Kansas: Unpub. Master's Thesis, University of Iowa, 213 p.
- ASTM, 1995, Annual Book of ASTM Standards: Section 4, Construction: vol. 04.02, Concrete and Aggregates, Publication Code Number: 01-040295-07.
- Ball, S.M., Pollard, W.D., and Roberts, J.W., 1977, Importance of phylloid algae in development of depositional topography- reality or myth? *in* Reef and Related Carbonates, Ecology, and Sedimentology: American Association of Petroleum Geologists, Studies in Geology, No. 4, p. 239-259.
- Best, C.H., 1974, D-cracking in PCC pavements—cause and prevention: Manhattan, KS: Department of Applied Mechanics, Kansas State University: Report No. KSU-EES-2472.
- Bukovatz, J.E., Crumpton, C.F., Worley, H.E., 1973, Study of d-cracking in Portland cement concrete pavements: Report 1, Field Phase: Topeka, KS: State Highway Commission of Kansas, Planning and Development Department, Research Division.
- Bukovatz, J.E., and Crumpton, C.F., 1981, Study of d-cracking in Portland cement concrete pavements: V. 2- Laboratory Phase: Topeka, KS: Kansas Department of Transportation, Planning and Development Department, Research, Development and Implementation Section: Report No. FHWA-KS 81-2.
- Clarkson, E.N.K., 1993, Invertebrate Paleontology and Evolution: London, Chapman & Hall, 434 p.

- Crowley, D.J., 1969, Algal-bank complex in the Wyandotte Limestone (Late Pennsylvanian) in Eastern Kansas: Kansas Geological Survey, Bulletin 198, 52 p.
- Crumpton, C.F., Wojakowski, J., Wallace, H., and Hamilton, L.D., 1994, Study of d-cracking in Portland cement concrete pavement: V. 4—Petrographic phase and final report: Topeka, KS: Kansas Department of Transportation, Division of Operations, Bureau of Materials and Research: Report No. FHWA-KS-94/3.
- Cunningham, K.J. and Franseen, E.K., 1992, Conglomeratic Limestones of the Upper Pennsylvanian Captain Creek Limestone and their Association with the Lower Sequence Boundary of the Stanton Depositional Sequence, Northwestern Johnson County, Kansas: Kansas Geological Survey Open-file Report 92-51 47 p.
- Doveton, J. H., 1994, Geologic log interpretation: Society of Economic Paleontologists and Mineralogists Short Course No. 29, 169 pp.
- Dunham, R.J., 1962, Classification of carbonate rocks according to depositional texture *in* Classification of Carbonate Rocks- A Symposium: American Association of Petroleum Geologists, Memoir, no. 1, p. 108-121.
- Enos, P., Herman, D., Watney, L., and Franseen, E., 1989, Stop 4: I-70/I-435 Interchange: Bonner Springs Shale and Plattsburg Limestone *in* Watney, W.L., French, J.A., and Franseen, E.K., eds. Sequence stratigraphic interpretations and modeling of cyclothems in the Upper Pennsylvanian (Missourian), Lansing and Kansas City groups in eastern Kansas: Guidebook of the Kansas Geological Society, 41st Annual Fieldtrip, p. 115-125.
- Feldman, H.R., Franseen, E.K., Fahr, T.R. and Maples, C.G., 1990, Geology and Sedimentology of the Hamilton Lagerstätte *in* Cunningham, C.R., and Maples C.G., eds., 1990 Society of Vertebrate Paleontology Upper Paleozoic of

- Eastern Kansas Excursion Guidebook, Kansas Geological Survey Open-file Report 90-24, p. 37-41.
- Folk, R.L., 1965, Some aspects of recrystallization in ancient limestones *in* Pray, L.C., and Murray, R.C., eds., Dolomitization and Limestone Diagenesis: A Symposium: Society of Economic Paleontologists and Mineralogists, Special Publication, No. 13, p. 14-48.
- Ginsburg, R.N., 1960, Ancient analogues of recent stromatolites: International Geological Congress, Report of the 21st Session Norden, Pt. 22, p. 26-35.
- Golubic, S., Perkins, R.D., and Lukas, K.J., 1975, Boring microorganisms and microborings in carbonate substrates *in* Fray, R.W., ed., The Study of Trace Fossils: A Synthesis of Principles, Problems, and Procedures in Ichnology: New York, Springer-Verlag, p. 229-259.
- Harbaugh, J.W., 1959, Marine bank development in Plattsburg limestone (Pennsylvanian), Neodesha-Fredonia area, Kansas: Kansas Geological Survey, Bulletin 134, p. 289-331.
- 1960, Petrology of marine bank limestones of Lansing group (Pennsylvanian), Southeast Kansas: Kansas Geological Survey, Bulletin 142, p. 189-234.
- 1964, Significance of marine banks in Southeastern Kansas in interpreting cyclic Pennsylvanian sediments: Kansas Geological Survey, Bulletin 169, p. 199-203.
- Harris, J., 1985, Stop 2: Intersection of K-7 and K-32 Highways, East Edge of Bonner Springs: Wyandotte Limestone Stratigraphy *in* Watney, W.L., Kaesler, R.L., and Newell, K.D., eds., Recent Interpretations of Late Paleozoic Cyclothems: Proceedings of the 3rd Annual Meeting and Field Conference, Mid-Continent Section, Society of Economic Paleontologists and Mineralogists, p. 31-33.

- Harris, P.M., 1984, Cores from a Modern Carbonate Sand Body: The Joulters Ooid Shoal, Great Bahama Bank *in* Harris, P.M. ed., Carbonate Sands—A Core Workshop: Society of Economic Paleontologists and Mineralogists Core Workshop No. 5, p. 429-464.
- Heckel, P.H., 1972, Recognition of ancient shallow marine environments *in* Rigby, J.K., and Hamblin, W.K., eds., Recognition of Ancient Sedimentary Environments: Society of Economic Paleontologists and Mineralogists, Special Publication, No. 16, p. 226-286.
- 1977, Origin of phosphatic black shale facies in Pennsylvanian cyclothems of Mid-continent North America: American Association of Petroleum Geologists, Bulletin, v. 61, p. 1045-1068.
- 1980, Paleogeography of eustatic model for deposition of Mid-continent Upper Pennsylvanian cyclothems *in* Fouch, T.D., and Magathan, E.R. eds., Paleozoic Paleogeography of West-Central United States: Society of Economic Paleontologists and Mineralogists, West-Central United States Paleogeography Symposium 1, Rocky Mountain Section, p. 197-214.
- 1983, Diagenetic model for carbonate rocks in Mid-continent Pennsylvanian eustatic cyclothems: *Journal of Sedimentary Petrology*, v. 53, No. 3, p. 733-759.
- 1984, Factors in Mid-continent Pennsylvanian limestone deposition *in* Hyne, H.J., ed., Limestones of the Mid-Continent: Tulsa Geological Society, Special Publication, No. 2, p. 25-50.
- Heckel, P.H., and Cocke, J.M., 1969, Phylloid algal-mound complexes in outcropping Upper Pennsylvanian rocks of Mid-continent: American Association of Petroleum Geologists, Bulletin 53, p. 1058-1074.



- Hinds, H., and Greene, F.C., 1915, The stratigraphy of the Pennsylvanian series in Missouri: Missouri Bureau of Geology and Mines, v. 13, 2nd series, p. 75-102.
- Johnson, J. H., 1946, Lime-secreting algae from the Pennsylvanian and Permian of Kansas: Geological Society of America, Bulletin, v. 57, p. 1087-1120.
- 1963, Pennsylvanian and Permian algae: Quarterly of the Colorado School of Mines, v. 58, no. 3, 211 p.
- Kansas Department of Transportation, 1990, Standard Specifications for State Road and Bridge Construction. Topeka, Kansas.
- Klein, C., and Hurlbut, C.S., 1993, Manual of Mineralogy, 21st Edition, John Wiley & Sons: New York, 681 p.
- Kobluk, D.R., and Risk, M.J., 1977, Micritization and carbonate-grain binding by endolithic algae: American Association of Petroleum Geologists, Bulletin, v. 6, p. 1069-1082.
- Konishi, K., and Wray, J.L., 1961, *Eugonophyllum*, a new Pennsylvanian and Permian algal genus: Journal of Paleontology, v. 35, p. 659-666.
- Matheny, J. Paul, Longman, M. W., 1996, Power Desert Creek Reservoirs in the Paradox Basin: examples of phylloid algae filling depositional lows related to salt dissolution in Longman, M.W., & Sonnenfeld, M.D., eds., Paleozoic Systems of the Rocky Mountain Regions. Rocky Mountain Section, Society of Economic Paleontologists and Mineralogists, p. 267-282.
- Moore, D.G., and Scruton, P.C., 1957, Minor internal structures of some recent unconsolidated sediments: American Association of Petroleum Geologists, Bulletin, v. 41, p. 2723-2751.

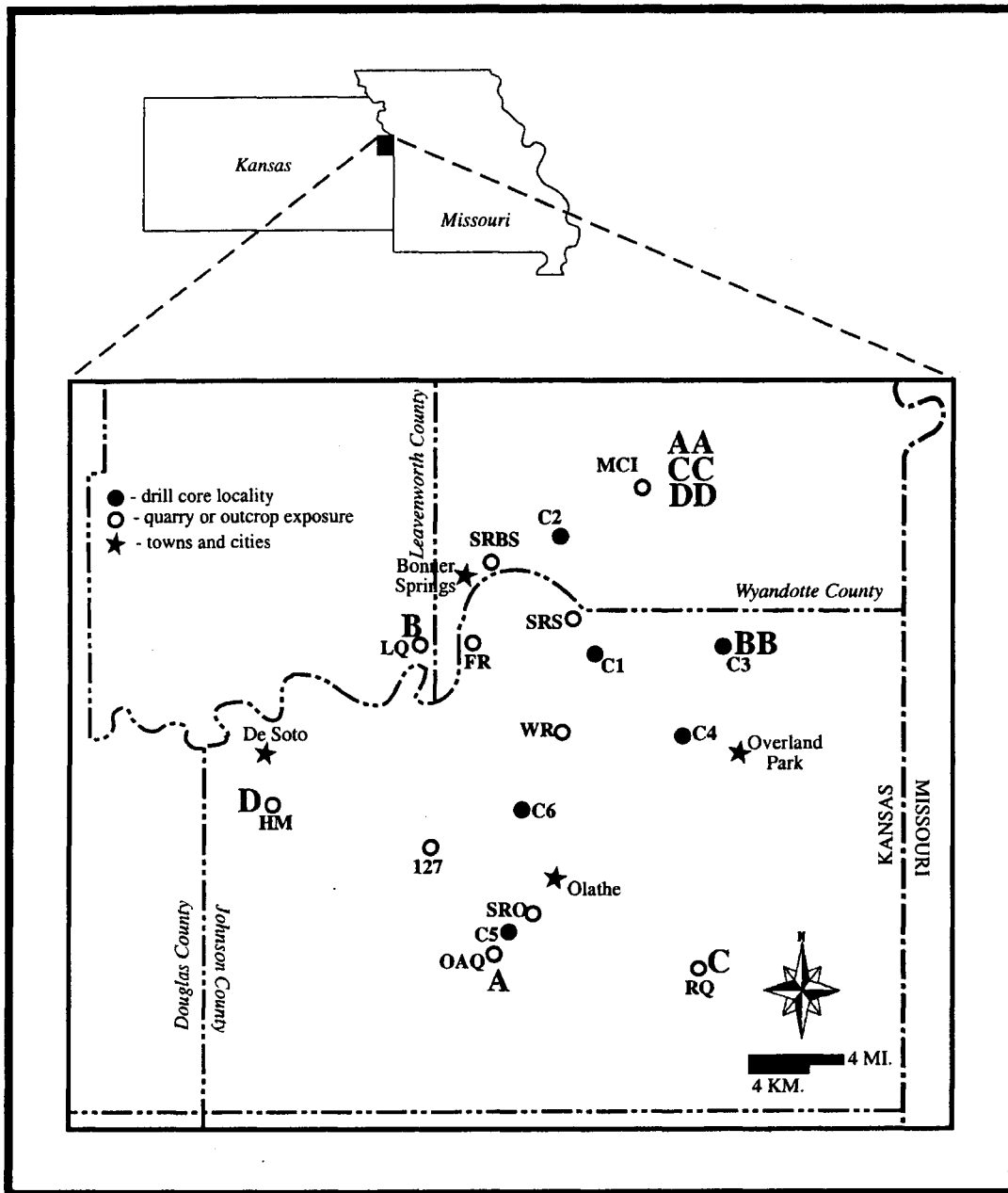
- Moore, R.C., 1932, A reclassification of the Pennsylvanian system in the northern Mid-Continent region, Guidebook, Sixth Annual Field Conference: Kansas Geological Society, p. 79-97.
- 1935, Stratigraphic classification of the Pennsylvanian rocks of Kansas: Kansas Geological Survey, Bulletin 22, p. 116-124.
- 1949, Divisions of the Pennsylvanian system in Kansas: Kansas Geological Survey, Bulletin 83, 203 p.
- Newell, N., 1935, Geology of Johnson and Miami counties, Kansas: Kansas Geological Survey, Bulletin 21, p. 55-181.
- O'Connor, H.G., 1971, Geology and ground-water resources of Johnson County, northeastern Kansas: Kansas Geological Survey, Bulletin 203, 68 pp.
- Ramsbottom, W.H.C., 1978, Carboniferous *in* McKerrow, W.S., ed., The Ecology of Fossils: Massachusetts, The MIT Press, p. 146-183.
- Reineck, H.E., and Singh, I.B., 1975, Depositional Sedimentary Environments: New York, Springer-Verlag, 439 p.
- 1980, Depositional Sedimentary Environments—With Reference to Terrigenous Clastics: Springer-Verlag, Berlin, 439 p.
- Retallack, G.C., 1990, Soils of the Past: Boston, Unwin Hyman, 520 p.
- Shepard, F.P., 1964, Criteria in modern sediments useful in recognizing ancient sedimentary environments *in* VanStraaten, L.M.J.U., ed., Developments in Sedimentology: Deltaic and Shallow Marine Deposits, v. 1, p. 1-25.
- Tedesco, L.P., and Wanless, H.R., 1989, Role of burrow excavation and infilling in creating the preserved depositional fabric of Pennsylvanian phylloid mounds of southeastern Kansas *in* Watney, W.L., French, J.A., and Franseen, E.K., eds. Sequence stratigraphic interpretations and modeling of cyclothems in the Upper Pennsylvanian (Missourian), Lansing and Kansas City groups in eastern

- Kansas: Guidebook of the Kansas Geological Society, 41st Annual Fieldtrip, p. 115-125.
- Tucker, M.E., 1991, *Sedimentary Petrology: An Introduction to the Origin of Sedimentary Rocks*: Oxford, Blackwell Scientific Publications, 260 p.
- Tsien, H.H., 1985, Algal-bacterial origin of micrites in mud mounds *in* Toomey, D.F., and Nitecki, M.H. eds., *Paleoalgology, contemporary research and applications*: Springer-Verlag, Berlin, p. 290-296.
- Wallace, H.E., and Hamilton, L.D., 1982, An Investigation of Kansas Limestones as they Pertain to the "D-Cracking" Phenomena: Unpublished paper presented to D-Cracking Workshop, Overland Park Kansas, February, 17 & 18: Kansas Department of Transportation, 19 p.
- Watney, W.L., 1980, Cyclic sedimentation of the Lansing-Kansas City groups in northwestern Kansas and southwestern Nebraska: Kansas Geological Survey, Bulletin 220, 72 p.
- Watney, W.L., French, J. A., Franseen, E.K., 1989, Sequence stratigraphic interpretations and modeling of cyclothems in the Upper Pennsylvanian (Missourian), Lansing and Kansas City groups in eastern Kansas: Guidebook of the Kansas Geological Society, 41st Annual Fieldtrip, 211 p.
- Watney, W.L., and Heckel, P.H., 1994, Revision of the stratigraphic nomenclature and classification of the Marmaton, Pleasanton, and Kansas City groups in Kansas: Kansas Geological Survey, Open File Report 94-34, p. 1-18.
- Wilson, J.L., 1970, Depositional facies across carbonate shelf margins: Gulf Coast Association of Geological Societies Transactions, v. 20, p. 229-233.
- Wilson, J.L., and Jordan, C., 1983, Middle Shelf Environment, *in* Scholle, P.A., Bebout, D.G., and Moore, C.H., eds., *Carbonate Depositional Environments*: American Association of Petroleum Geologists, Memoir 33, p. 297-344.

Wray, J.L., 1964, *Archeolithophyllum*, an abundant calcareous alga in limestones of the Lansing Group (Pennsylvanian), southeastern Kansas: Kansas Geological Survey, Bulletin 170, pt. 1, 13 p.

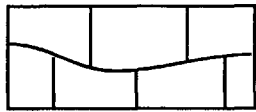
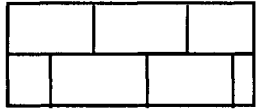
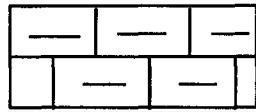
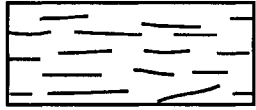
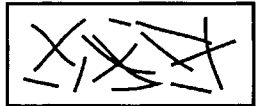
----- 1968, Late Paleozoic phylloid algal limestones in the United States: 23rd International Geological Congressional Report, Prague.



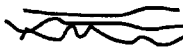



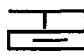



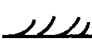






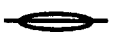








**Appendix 1: Measured Stratigraphic Sections**



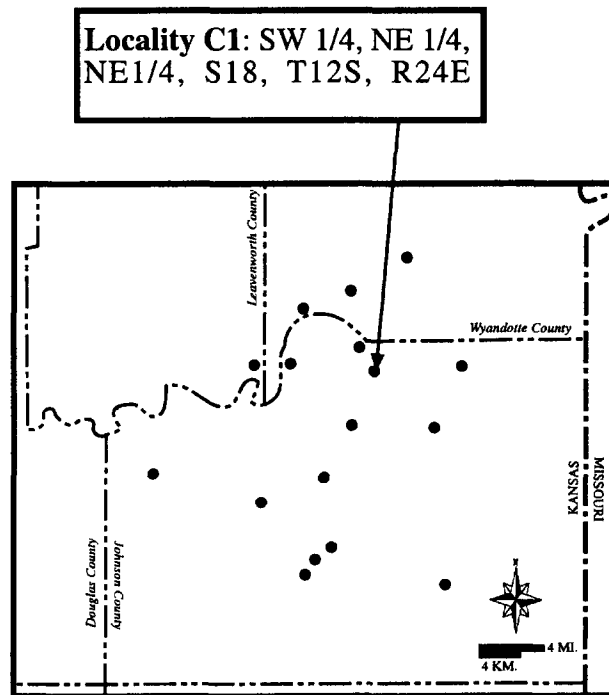
**Figure A1.1.** Index map showing location and type of field localities and major towns for reference. This appendix includes measured stratigraphic sections for each locality shown on this map.

# Lithologic Symbols

	Wavy-Irregular Bedded Limestone
	Even-Massive Bedded Limestone
	Argillaceous Limestone (Diffuse Stylocumulates)
	Calcareous Siltstone (Fossiliferous or Laminated)
	Non-calcareous, Blocky Mudstone

	Shale Parting		Fenestrate Bryozoans
	Concentrated Stylocumulates		Ramosse Bryozoans
	Interlaminated Sandstone-Siltstone		Productid Brachiopod
	Interlaminated Limestone-Shale		Spiriferid Brachiopod
	Lenticular Bedding		Brachiopod (General)
	Ripple Cross-Lamination		Rugose Coral
	Geopetal Structures		Crinoid Ossicles
	Plant Fragments (General)		Gastropod
	Plant Fragments (Leaves)		Fusulinids
	Plant Fragments (Roots)		Shell Fragments
	Phylloid Algae		Peloids
	<i>Osagia</i>		Ooids
	Encrusters (General)		Coated Grains

**Locality C1:** Core section. Drilled inside the exit ramp loop that leads from Interstate 435 North to Shawnee Mission Parkway West. Described portion includes all the Farley Limestone and most of the Island Creek. Measured section starts at the base of the core and continues upward. Also included in the core is most of the Vilas Shale, the entire Plattsburg Limestone and the entire Bonner Springs Shale. These units were not described in detail for this study.





Rock Unit(s): IC. Shale + Fanley Ls

Thickness	Lithology & Weathering Profile	Fossils & Grains	Sed. Struct & Diag. Feat.	Rock Name (Dunham)	Cement	Color	Sample No.	Photo No.	Additional Remarks
10cm		<p> </p>	<p> </p>	Phylloid Algal Wavestone	Graptolite, Fed. + Fossils all contain coarse spar. (102020)			<p> </p>	Ab. brown mottling + fractures. Fractures filled w/ spar
		<p> </p>		Arg. Fusulinid/ Sh. Pecten					
		<p> </p>		Fossiliferous Siltstone					Calcareous, blocky
10cm +			<p> </p>	Laminated, Lenticular Siltstone					Wavy lamination Slightly micaceous Non-fossiliferous Non-calcareous

Date 2/10/98

Location Core # SMP / J=485

Page 1 of 4

1: 20cm

Rock Unit(s): Farley LS

Thickness	Lithology & Weathering Profile	Fossils & Grains	Sed. Struct & Diag. Feat.	Rock Name (Dunham)	Cement	Color	Sample No.	Photo No.	Additional Remarks
10m				Blacky Mudstone					Micaceous Non fossiliferous Non calcareous
99cm				Laminated-Lenticular Siltstone					Unfossiliferous
(200)				Fossiliferous Siltstone					
54cm				Blocky Skeletal Bedstone	Little to no coarse grain			1-70	
5cm				as below				1-70	

Date 2/10/99

Location Cox # SMP/I-485

Page 2 of 4

Rock Unit(s): Fairy LS

Thickness	Lithology & Weathering Profile	Fossils & Grains	Sed Struct & Diag Feat	Rock Name (Dunham)	Cement	Color	Sample No.	Photo No.	Additional Remarks
100cm		N#A B	AB-M	Mottled Phylloid Algal Wackestone	Spur = (~20%)			H0	Gray mottling seems to form above or around phylloid algae
60cm		N#A A.B.	M	Phylloid Algal Wackestone	Ab. spur (~25-35%)			H3	Shelter Porosity & fractures filled w/ spur
42cm		N#B		Argillaceous Phyl. Algal Wack.	Phyllofretches base spur (~6%)			H4A	Marker Bed *
10cm		N#B #		Oolitic Wack.					

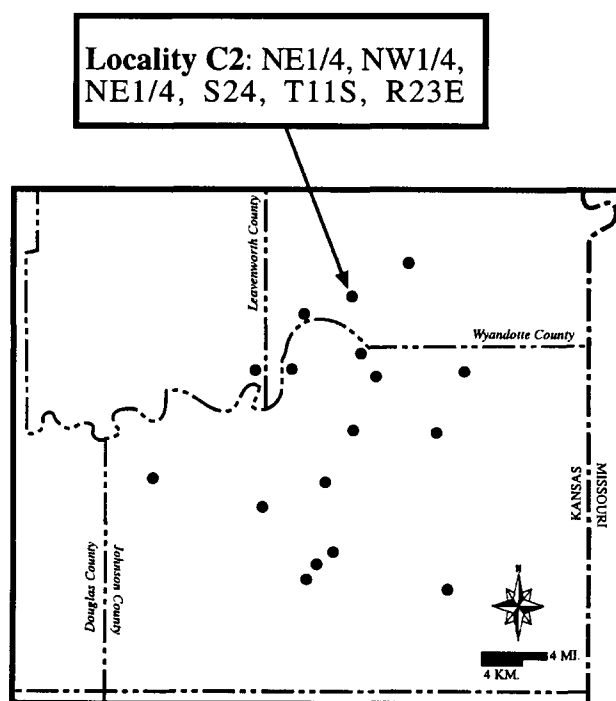
Date 2/10/91

Location Cove #1 S.M.P/I-435

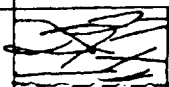
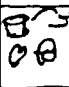
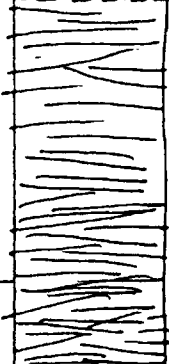
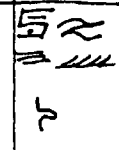
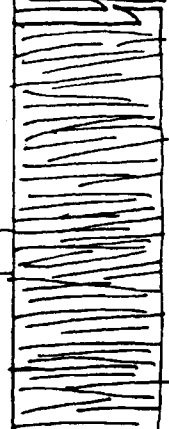
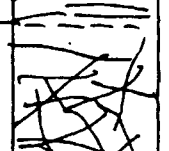

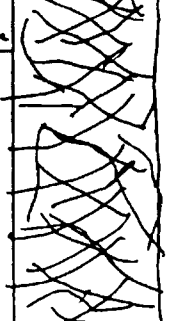

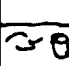
Page 3 of 4



**Locality C2:** Core section. Drilled between the southbound lanes of Interstate 435 and the southbound onramp from Kansas Avenue. Includes a small portion of the Bonner Springs Shale, the entire Farley Limestone, and Island Creek Shale with the upper few centimeters of the Argentine Limestone. Measured section starts at the base of the core and continues upward.



Rock Unit(s): Island Creek Sh. / Arg. Top

Thickness	Lithology & Weathering Profile	Fossils & Grains	Sed. Struct & Diag. Feat.	Rock Name (Dunham)	Cement	Color	Sample No.	Photo No.	Additional Remarks
				Foss: <u>Wierus</u> <u>Siltstone</u>					Very calcareous. Obviously fossilif.
				Laminated Lenticular Siltstone					Interbedded fine sand & silt. Wavy-discont. lens Sand is slightly calcareous Sand 90 higher @ top (~50%)
276									
		4 ft + G-m		Blocky Mudstone					Non-calcareous
156									
30 cm				St. Crinoidal PK-siltstone					Argentine Top

Date 3/9/89

Location Cox #2 Kansas Ave / I435

Page 1 of 3

1:20cm

Rock Unit(s): Fasley LS

Thickness	Lithology & Weathering Profile	Fossils & Grains	Sed. Struct & Diag Feat	Rock Name (Dunham)	Cement	Color	Sample No.	Photo No.	Additional Remarks
8cm		☉☉☉☉	☉ M	Phylloid Alg Wackestone	Sparsely phyll. brkds (~15%)			42A	Brachiopods. found here
		☉☉☉☉	☉	Cryst. Wacke Fossil. F.					Mudcrack Bed
46cm		☉☉☉☉		Blocky Mudstone					Calcareous Stromatolites
			☉☉☉☉ M	Laminated limestone siltstone					Sandstone at base from thin clayey beds (1-2cm)
		☉☉☉☉		Fossil. Calcareous					
35		☉☉☉☉		Pebbled, Skeletal Pktm	No coarse spar visible			42D	
47		☉☉☉☉		Argillaceous Phyl. Alg Wacke	Coarse spar = ~5%			43C	
8cm		☉☉☉☉	☉☉☉☉ M	Phylloid Alg Wackestone	Coarse spar in phyl. + graptolite (~20%)			43B	At. brachiopods w/ graptolite common Conc. stromatolites
15cm		☉☉☉☉		Caliche Transition				43A	

Date 8/1/91

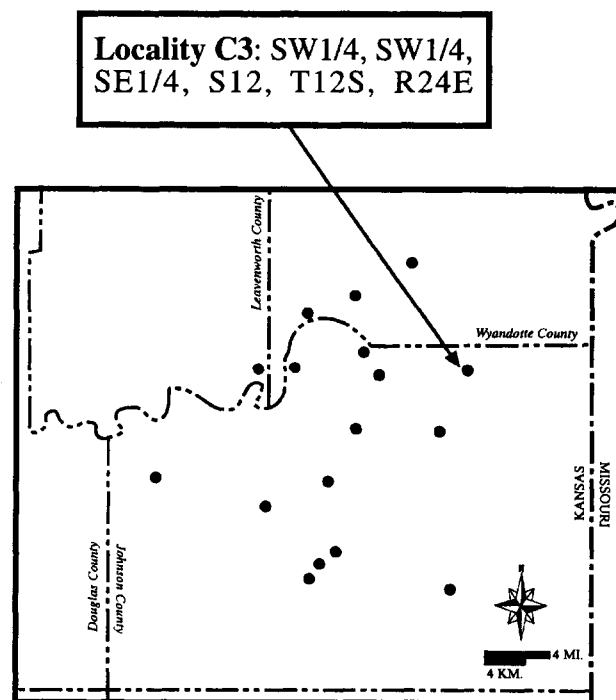
Location D435/KS Ave - Cont 2

Page 2 of 3





**Locality C3:** Core section. Drilled between the southbound lanes of Interstate 35 and the southbound offramp leading to Shawnee Mission Parkway. Includes a small portion of the Bonner Springs Shale, the entire Farley Limestone, and Island Creek Shale with the upper few centimeters of the Argentine Limestone. Measured section starts at the base of the core and continues upward.



Rock Unit(s): Tr. Coast Fanlyls

Thickness	Lithology & Weathering Profile	Fossils & Grains	Sed. Struct & Diag. Feat.	Rock Name (Dunham)	Cement	Color	Sample No.	Photo No.	Additional Remarks
2m			SR	Laminated siltstone					Inter laminated
1.5m		○ ○ ○ ○ ○ ○		Oolitic peloidal siltstone	None visible		53C		23cm karst cavity. Drill bit dropped & lost correlation Textured surface
12		○ ○ ○ ○ ○ ○		Oolitic peloidal siltstone	None visible		53B		
25		○ ○ ○ ○ ○ ○		Oolitic peloidal siltstone	None visible		53A		Sharp contact
50		○ ○ ○ ○ ○ ○	○ S ○ M	Phyl. Argil. Wackestone	Coarse grain in phyls, breccias & fractures (~20%)				
30cm		○ ○ ○ ○ ○ ○	○	Argillaceous Phylloid Argil. Wackestone	No visible coarse grain				
		○ ○ ○ ○ ○ ○	S	Fossilif. Siltstone			54B		Calcareous
190cm			SR SR SR	Laminated Lenticular Siltstone			45A		Interlaminated silty-sandy siltstone Circular to elliptical sand lenses are barren fills & they are also Some carbonated lenses. Faint ripples visible Borrowed often disturbed laminations
40cm		○ ○ ○ ○ ○ ○		Phyl. Argil. Wackestone					Argentine Top

Date 7/19/88

Location TR/SMP G-3

Page 1 of 2

1.20m

Rock Unit(s): Fairley ls

Thickness	Lithology & Weathering Profile	Fossils & Grains	Sed. Struct & Diag. Feat.	Rock Name (Dunham)	Cement	Color	Sample No.	Photo No.	Additional Remarks
				Arg. shale					Bonne Springs shale
2cm		~80 02		Skolither Pictum			51B 51A		Sharp contact
3cm		no #		Phyl. Myp limestone	Carra-sponic pith, brachi (185-200)				
3cm		no #	⊙	Onchite Pictum			52A		Marked
17cm		φ φ φ		Blocky Mudstone					Non calcareous Massive
17cm				Laminated, Lenticular Siltstone			53A		Tribolam. silt + sand Non-calcareous Massive No fossils Fossiliferous thin beds Much fewer burrows

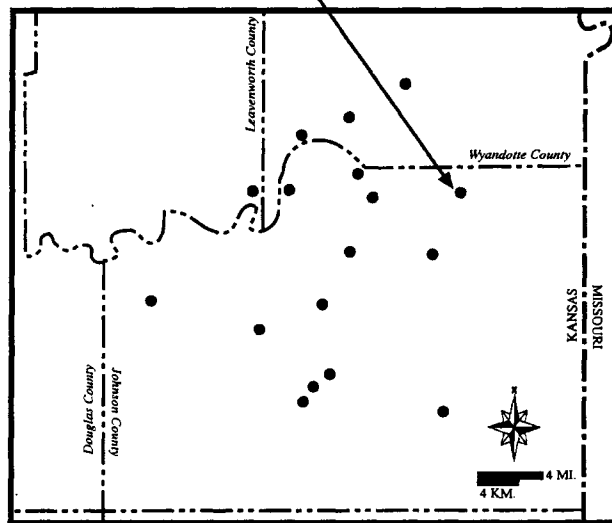
Date 3/9/78

Location I-35/S.M.P. - Cor #3

Page 2 of 2

**Locality C4:** Core section. Drilled in the west shoulder along the northbound onramp leading from 95th Street onto US Highway 169. Includes the entire Farley Limestone, the Island Creek Shale and the upper 2 meters of the Argentine Limestone. Measured section starts at the base of the core and continues upward.

**Locality C4: SW1/4, SE1/4,  
SE1/4, S35, T12S, R24E**



Rock Unit(s): Argentine, Is. Creek

Thickness	Lithology & Weathering Profile	Fossils & Grains	Sed. Struct & Diag. Feat.	Rock Name (Dunham)	Cement	Color	Sample No.	Photo No.	Additional Remarks
64cm				Laminated, Lenticular Siltstone					Interlam. Non-alcareous
150cm				Blocky Mudstone			62A		Occasional sand lens, Ab. plant material Body fossils present but rare Island Creek
86cm				Phyllonitic Algal Wackestone	as below				Shale partings in this section shows depth in them, as well as limestone  ↑ Argentine ↓
19cm				Siltstone					Thick, shale seen thinner than shale below
82cm				Phyllonitic Algal Wackestone	Consistent & somewhat not ab. (~10%)				Prominent shale partings
20cm									

Date 3/10/98

Location US 19 / 13th St. Core #4

Page 1 of 2

1:20cm

Rock Unit(s): Is Creek, Farley Ls

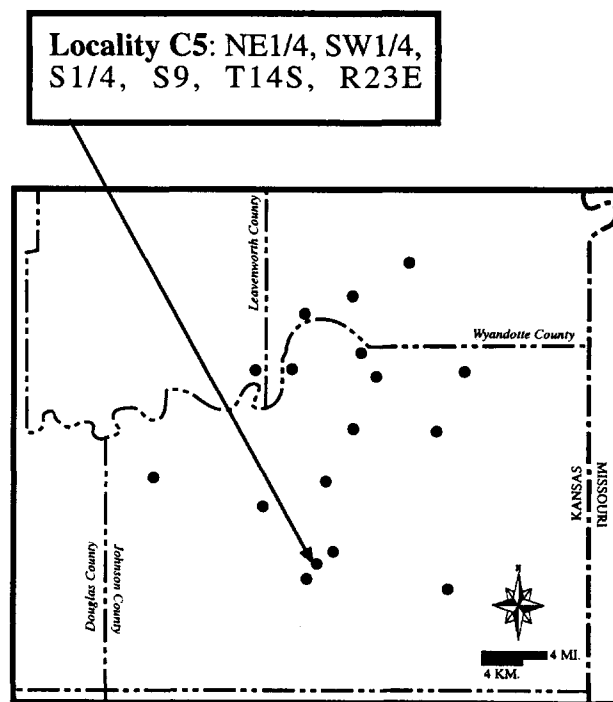
Thickness	Lithology & Weathering Profile	Fossils & Grains	Sed. Struct & Diag. Feat.	Rock Name (Dunham)	Cement	Color	Sample No.	Photo No.	Additional Remarks
									Bonnet Springs Shale
15cm				Pellucid St. Pk. sh.	No coarse sp.				
1cm			B R	Lamin. Shale					
59cm				Phys. H. sh. Wksh.	Sp. ~ 20%				No encrusting Lithoclasts @ top Mottled @ top
1cm				St. Pellucid Pk. sh.	No coarse sp.		6-15		Arg @ base top
									Argil @ base as below
2+				as below					

Date 2/10/98

Location USG 190' @ Corn #4

Page 2 of 2

**Locality C5:** Core section. Drilled inside the Johnson County Aggregate Quarry, in the southwest portion of the quarry. Includes the entire Farley Limestone, the Island Creek Shale and the upper few centimeters of the Argentine Limestone. Measured section starts at the base of the core and continues upward.



Rock Unit(s): Argentine Bl. Farley LS

Thickness	Lithology & Weathering Profile	Fossils & Grains	Sed Struct & Diag. Feat.	Rock Name (Dunham)	Cement	Color	Sample No.	Photo No.	Additional Remarks
12' 2"		20#	AA → A.B.	Phylloid Bed Wackestone	Sp. = -15-20		7B		Slightly mottled Ab. phylloid known pieces Shale partings thru rd. face
48"		20#		Oncolite Wackestone	Little to no coars sp.		72A		Marker Bed
103"		20#	AA →	Fossilif. Shale					
		20#		Organic Rich Mudstone		↑ lighter Dk gray- Black			
				Coal seam					
				Lam. Siltstone					
36"		20#							Argentine LS

Date 9/11/98

Location To City Agg Quarry - 6005

Page 1 of 2

1:20" scale



Rock Unit(s): Farley

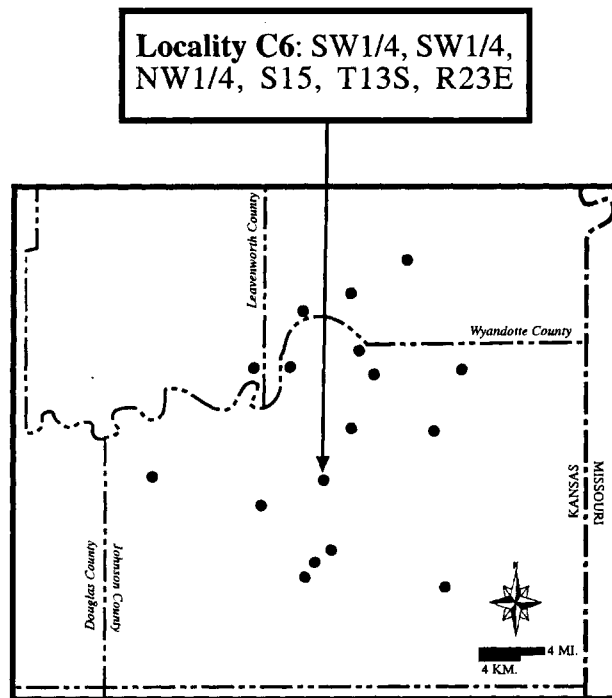
Thickness	Lithology & Weathering Profile	Fossils & Grains	Sed. Struct & Diag. Feat.	Rock Name (Dunham)	Cement	Color	Sample No.	Photo No.	Additional Remarks
		20# 30#	3 AR M	Mottled Prayed Royal Wheaton			7-18	7-18	No shell porosity Filled w/ spar. Gray mottled found above phyls. Also brecciated fractures are common & filled w/ spar
36cm									
20cm				ashlar			7-1A		

Date 3/1/98

Location To City Agg Quarry Cret

Page 2 of 2

**Locality C6:** Core section. Drilled in the west shoulder along Kansas Highway-7, just south of the 111th Street/College Boulevard exit ramp. Includes the entire Farley Limestone, the Island Creek Shale and the upper 1.5 meters of the Argentine Limestone. Measured section starts at the base of the core and continues upward.



Rock Unit(s): Argentine - Farley Ls

Thickness	Lithology & Weathering Profile	Fossils & Grains	Sed. Struct & Diag. Feat.	Rock Name (Dunham)	Cement	Color	Sample No.	Photo No.	Additional Remarks		
				as above							
		no #	○	st. - Phys. Al. d. Waleshire ↑ Arg. oxidation underneath					Marker Bed Oolitic - other nodules		
45cm		# 10 # 11 # 12 # 13 # 14 # 15 # 16 # 17 # 18 # 19 # 20 # 21 # 22 # 23 # 24 # 25 # 26 # 27 # 28 # 29 # 30 # 31 # 32 # 33 # 34 # 35 # 36 # 37 # 38 # 39 # 40 # 41 # 42 # 43 # 44 # 45 # 46 # 47 # 48 # 49 # 50 # 51 # 52 # 53 # 54 # 55 # 56 # 57 # 58 # 59 # 60 # 61 # 62 # 63 # 64 # 65 # 66 # 67 # 68 # 69 # 70 # 71 # 72 # 73 # 74 # 75 # 76 # 77 # 78 # 79 # 80 # 81 # 82 # 83 # 84 # 85 # 86 # 87 # 88 # 89 # 90 # 91 # 92 # 93 # 94 # 95 # 96 # 97 # 98 # 99 # 100		Bloody silty - sandy shale (Fac. lens)						Fossiliferous (plant stems) seen by large impressions	
10cm		# 101 # 102 # 103 # 104 # 105 # 106 # 107 # 108 # 109 # 110 # 111 # 112 # 113 # 114 # 115 # 116 # 117 # 118 # 119 # 120 # 121 # 122 # 123 # 124 # 125 # 126 # 127 # 128 # 129 # 130 # 131 # 132 # 133 # 134 # 135 # 136 # 137 # 138 # 139 # 140 # 141 # 142 # 143 # 144 # 145 # 146 # 147 # 148 # 149 # 150 # 151 # 152 # 153 # 154 # 155 # 156 # 157 # 158 # 159 # 160 # 161 # 162 # 163 # 164 # 165 # 166 # 167 # 168 # 169 # 170 # 171 # 172 # 173 # 174 # 175 # 176 # 177 # 178 # 179 # 180 # 181 # 182 # 183 # 184 # 185 # 186 # 187 # 188 # 189 # 190 # 191 # 192 # 193 # 194 # 195 # 196 # 197 # 198 # 199 # 200		Sketched, Pebbled Granular	No cement seen visible except in one large fracture	Mid- light grey				Porous; high rock as to other lithologies (~10-15%) Overall fine-grained, well sorted. Thin layer of s.l.c. fossil material (shert)	
5cm		# 201 # 202 # 203 # 204 # 205 # 206 # 207 # 208 # 209 # 210 # 211 # 212 # 213 # 214 # 215 # 216 # 217 # 218 # 219 # 220 # 221 # 222 # 223 # 224 # 225 # 226 # 227 # 228 # 229 # 230 # 231 # 232 # 233 # 234 # 235 # 236 # 237 # 238 # 239 # 240 # 241 # 242 # 243 # 244 # 245 # 246 # 247 # 248 # 249 # 250 # 251 # 252 # 253 # 254 # 255 # 256 # 257 # 258 # 259 # 260 # 261 # 262 # 263 # 264 # 265 # 266 # 267 # 268 # 269 # 270 # 271 # 272 # 273 # 274 # 275 # 276 # 277 # 278 # 279 # 280 # 281 # 282 # 283 # 284 # 285 # 286 # 287 # 288 # 289 # 290 # 291 # 292 # 293 # 294 # 295 # 296 # 297 # 298 # 299 # 300		shaly, shale w/ crinoids						Fossiliferous?	
20cm		# 301 # 302 # 303 # 304 # 305 # 306 # 307 # 308 # 309 # 310 # 311 # 312 # 313 # 314 # 315 # 316 # 317 # 318 # 319 # 320 # 321 # 322 # 323 # 324 # 325 # 326 # 327 # 328 # 329 # 330 # 331 # 332 # 333 # 334 # 335 # 336 # 337 # 338 # 339 # 340 # 341 # 342 # 343 # 344 # 345 # 346 # 347 # 348 # 349 # 350 # 351 # 352 # 353 # 354 # 355 # 356 # 357 # 358 # 359 # 360 # 361 # 362 # 363 # 364 # 365 # 366 # 367 # 368 # 369 # 370 # 371 # 372 # 373 # 374 # 375 # 376 # 377 # 378 # 379 # 380 # 381 # 382 # 383 # 384 # 385 # 386 # 387 # 388 # 389 # 390 # 391 # 392 # 393 # 394 # 395 # 396 # 397 # 398 # 399 # 400	# 301 # 302 # 303 # 304 # 305 # 306 # 307 # 308 # 309 # 310 # 311 # 312 # 313 # 314 # 315 # 316 # 317 # 318 # 319 # 320 # 321 # 322 # 323 # 324 # 325 # 326 # 327 # 328 # 329 # 330 # 331 # 332 # 333 # 334 # 335 # 336 # 337 # 338 # 339 # 340 # 341 # 342 # 343 # 344 # 345 # 346 # 347 # 348 # 349 # 350 # 351 # 352 # 353 # 354 # 355 # 356 # 357 # 358 # 359 # 360 # 361 # 362 # 363 # 364 # 365 # 366 # 367 # 368 # 369 # 370 # 371 # 372 # 373 # 374 # 375 # 376 # 377 # 378 # 379 # 380 # 381 # 382 # 383 # 384 # 385 # 386 # 387 # 388 # 389 # 390 # 391 # 392 # 393 # 394 # 395 # 396 # 397 # 398 # 399 # 400		mottled Sketched Phys. - Algal Waleshire  (Arg. in places)	Zone of cement seen throughout (15-25% density)					Fairly sparse fauna Argentine Ls

Date 3/25/98

Location K-7/III<sup>rd</sup> St Case # 10

Page 1 of 3

(: 20 cm

Rock Unit(s): Fairley LS

Thickness	Lithology & Weathering Profile	Fossils & Grains	Sed. Struct & Diag Feat	Rock Name (Dunham)	Cement	Color	Sample No.	Photo No.	Additional Remarks
20cm		● ● ● S	}	Pale dol Pale-granitic ?	Very little cement seen - only in small lenses (5-10%)		8-10 8-11 8-2A		Next to dol in road ... a more a massive ledge; In Possible rest beds on Kaplan wgs
37cm ↓		2 ● ● # ● ●	A.B. # ● >	Skeletal, Phyl-Algal Wackestone	Coarse gran throughout, at up. inconsistent distribution up to 25% in places. (Average is ~15%)				Stylonematites throughout significant clay lenses throughout  Arylaceras in places

Date 3/25/98

Location K-7/111<sup>m</sup> St Cor #B

Page 2 of 3

Rock Unit(s): Farley Ls

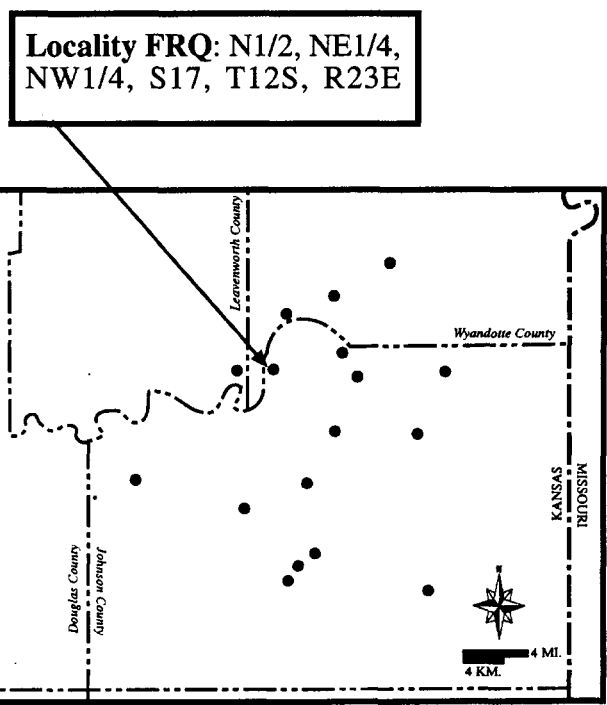
Thickness	Lithology & Weathering Profile	Fossils & Grains	Sed. Struct & Diag. Feat.	Rock Name (Dunham)	Cement	Color	Sample No.	Photo No.	Additional Remarks
83cm		2 # ① ②	A.B. 3	Bacteroid, Skeletal/ Phyt.-Kgd Wackestone	Spore on fracture, phyl. & trace (~15%)		8-1F		
6cm		③		Sandy-silty shale					
16cm		④ ⑤		oolite			8-1G		
				as below			8-1D		

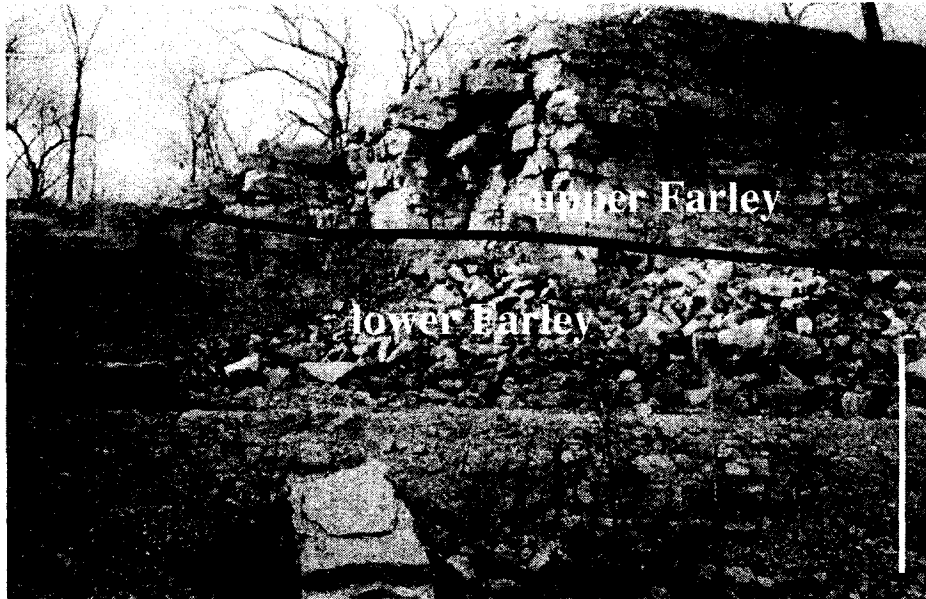
Date 3/25/98

Location K-7/111<sup>th</sup> St Cor # 10

Page 3 of 3

**Locality FRQ:** Quarry section. Measured in an abandoned quarry on Frisbie Road. (Frisbie Road is closed but accessible). Section was measured along the north wall of the quarry. This was the only easily accessible exposure. Includes entire Island Creek Shale and all but the very upper portion of the Farley Limestone. The Argentine Limestone is exposed but was not measured in detail.





**Figure A1.2:** Outcrop photo of abandoned quarry exposure along Frisbie Road in Johnson County. Black line indicates the level of a thin shale that is the middle Farley Shale and divides the section into the three members of the Farley Limestone. Scale bar is 1.5 meters.

Rock Unit(s): Farley LS

Thickness	Lithology & Weathering Profile	Fossils & Grains	Sed. Struct & Diag. Feat.	Rock Name (Dunham)	Cement	Color	Sample No.	Photo No.	Additional Remarks
60cm		~ 9 ~ 10		Bedded, Skeletal Packstone			FR-3		Single massive, bed
200cm		~ 10 # A		Phyl. Algal Wackestone - Fossil. Shale			FR-2b		Upper shale same as well cemented & more calcareous  Lower shale are darker w/ more @ & #
100cm		~ 10 # A	●	Phylloid Algal Wackestone	Coarse spar in fossils & phyl. large brachs filled w/ coarse spar (+1-2mm) (~15-20%)		FR-1		Ledge steps back ~20 ft.  Horizon 5' large, more ab. brachs filled w/ coarse spar.
40cm		@ # @		Fossiliferous Siltstone					

Date 2-23-99

Location Frederic Road Quarry

Page 1 of 2

1:20 cm



Rock Unit(s): Farley Ls

Thickness	Lithology & Weathering Profile	Fossils & Grains	Sed Struct & Diag. Feat	Rock Name (Dunham)	Cement	Color	Sample No.	Photo No.	Additional Remarks
15cm		20A #B	AR	Phylloid Algal Wackestone			R20		Clean of shale.  Irregularly bedded wavy & fractured  Top is weathered; soil profile sits directly on top of Farley
20									
60									
30									
40									
48									
38									
16									
24cm									
53cm									
			Org. skeletal Wackestone						
			Fossilif. Siltstn						
			as below						

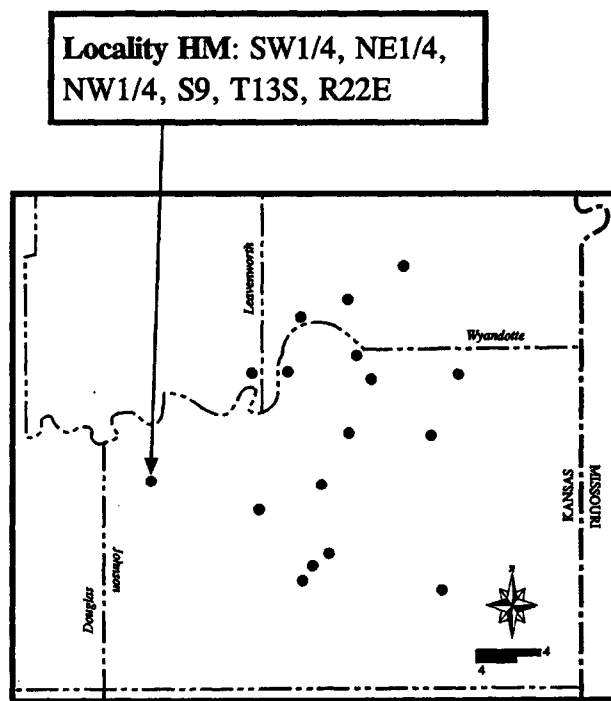
Date 2-23-98

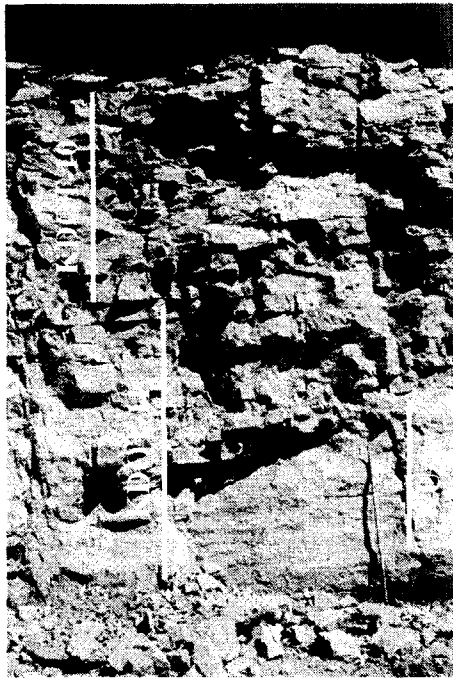
Location Fristone Road Quarry

Page 2 of 2

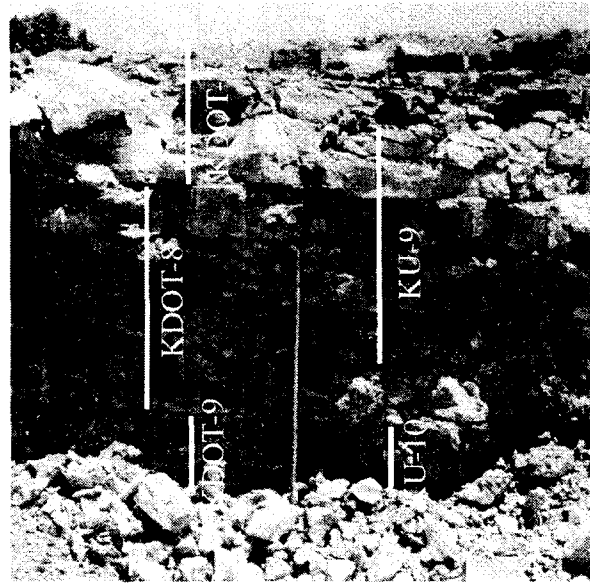
1:20 cm

**Locality HM:** Quarry section. Measured in an active quarry operated by Hunt-Midwest Mining Company. Quarry is located south of 95th Street in DeSoto, KS. Section was measured along the east wall of the quarry in the southeast corner. Measured section includes the Island Creek Shale and a complete Farley Limestone Section. The Argentine Limestone and the Bonner Springs Shale are also well exposed in this quarry. Aggregate samples KU-8, KU-9, KU-10 as well as KDOT-7, 8, 9, 10, 11 are from this quarry.





(A)



(B)



(C)

**Figure A1.3:** Outcrop photos showing exposures measured in the Hunt-Midwest Sunflower quarry in DeSoto Kansas, Johnson County. The staff in each photo is 1.5 meters for scale. (A) Lower Farley outcrop with locations from which aggregate samples were collected for physical testing. In the case of the KDOT samples, this indicates the stratigraphic level from which the samples were taken but not the exact location. (B) Upper Farley outcrop with aggregate sampling locations indicated. (C) Middle Farley showing medium-scale cross-bedding.

Rock Unit(s): Laura Farley

Thickness	Lithology & Weathering Profile	Fossils & Grains	Sed. Struct & Diag Feat	Rock Name (Dunham)	Cement	Color	Sample No.	Photo No.	Additional Remarks
190 cm +		BON J	○	Skeletal Wackestone	Coars. spar 15 not ab. Fills occasional voids & replaces fossils  ~ 15% of rock is coars. spar		KU-11		Fusulinids common Appear as one massive bed ~200cm thick. Is broken by concentrated shale partings but these are not bedding planes. Thin shale seams are slightly discon. up & down  Clay occurs in cement. Seams up to 8-10cm thick & in wavy strings through the layer.  Wavy only ~15-20% contains clay.  Base has ab. disseminated shale i.e. gradational contact
10cm		FOSS		Fossiliferous Siltstone			KU-8		Fossiliferous Siltstone

Date 1:10pm

Location Swiflowery Quarry (HMO) Dept

Page 1 of 5

Rock Unit(s): Lower Farley

Thickness	Lithology & Weathering Profile	Fossils & Grains	Sed Struct & Diag. Feat.	Rock Name (Dunham)	Cement	Color	Sample No.	Photo No.	Additional Remarks
17cm+		20 # 1	A.B. ⊙	Phylloid Algal Wackestone	Ab. fine spine from phyla. Coarse spn fbb fractures. (~20%)				Very little d. fine clay (15%)
15cm									
9cm		20 # 2	⊙ A.B.	Phylloid Algal Wackestone	Spn in fractures & replacing bryozoan phyla. (20-25%) Xst size is 1/2mm		K207-10		Staly seams at bedding plane. Each bed has a small amount of clay diffu into surrounding LS @ bedding plane ~10-15% hr d. fine clay in it.
22cm									
36cm									
16cm									
5cm				Silt seam					Laterally continuous (variable thickness)
33cm		20 # 3	⊙ A.B.	Phylloid Algal Wackestone	Spn more abundant due to more fossils r phylloid alge (10-25%) Size is 1/2mm		K207-11		Relatively clean of clay except @ bedding planes r few con together sides ~5% calcareous clay.
30cm									
19cm+				see below					cont. from P3 1

Date \_\_\_\_\_

Location Swallow, DeSoto, KS

Page 2 of 5

Rock Unit(s): Lower-Middle Farley

Thickness	Lithology & Weathering Profile	Fossils & Grains	Sed. Struct & Diag. Feat.	Rock Name (Dunham)	Cement	Color	Sample No.	Photo No.	Additional Remarks
30cm				Shale					Middle Farley Shale
Not to scale		⊙ ⊙ ⊙ ⊙ ⊙ ⊙ ⊙ ⊙ ⊙	///	X-bedded Skeletal Pack Granular	No coarse cement Fine spar fills most interparticle space (~25-45%)				Large scale x-bedding Shale below produces r-swell. Pachydictya common Sandy-silty (ft 2 sand)
15cm		⊙ ⊙ ⊙ ⊙ ⊙		Pebbly Skeletal Packstone	Little to no coarse spar (~5%) Fine spar (~5%)		HA-7		Densely packed; Fine grain (~2mm) Shal @ bedding plane
25cm		⊙ ⊙ ⊙ ⊙ ⊙ ⊙ ⊙ ⊙ ⊙	⊙	Relict Skeletal Packstone	Fine spar (~1mm) is abundant (~40-60%) Recept. fossil frag - other		HA-6 KDOT-10		No major clay present Spar fills all interparticle pore space. Coarse ground than bed above. Thicker bedded than below.
5cm		⊙ ⊙ ⊙ ⊙ ⊙	⊙ A.B.	Phylloid Algal Wackestone	Spar fills fractures & replaces fossils & phyllo. (~4mm) (~20-30%)		HA-5 HA-4		Mottled appearance Very little clay - only than changes @ bedding plane (~5%)
11cm		⊙ ⊙ ⊙ ⊙ ⊙	⊙	Phyl. Algal Wackestone as below	More coarse spar (1-5mm) ~25%		HA-4		Very little clay (~5%) cont. from pg 2

Date \_\_\_\_\_ Location Southwestern Desoto KS Page 3 of 5

Rock Unit(s): Upper Farley


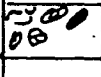
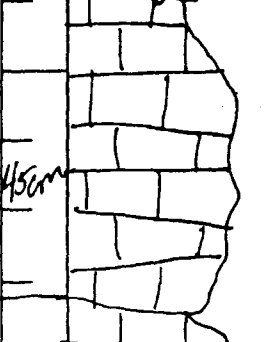
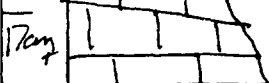
Thickness	Lithology & Weathering Profile	Fossils & Grains	Sed Struct & Diag Feat	Rock Name (Dunham)	Cement	Color	Sample No.	Photo No.	Additional Remarks
38cm		U ⊕ A ⊕ # ⊕		Phylloid Algal Wackestone	Coarse spon not abundant. Fills vugs & repletes basins & phyls. Faint in large (1cm+) vugs in some fossils (n 25%) Fine spon also present (n 15%)		S-3 A-3 S-2 S-1 A-2		Irregularly bedded Large vugs filled w/ very large calcite spher. Other vugs filled w/ dolomite (bragoo) and spherulite?
35cm									Most large brachs are lined w/ coarse spher of calcite or dolomite. Some very coarse; several cm. Phyl. density is variable.
45cm									The coarsest spon found in vugs & fossils will likely crush out. Shale/dog only found in some at bedding plane. No diff. dog anywhere. (S-2)
35cm									
47cm				Phyl Algal Wackestone ↑ Coarse Wackestone	Coarse spon phyls and other fossils (n 15%)			Marker Bed	
				Shale/dog Wackestone			A-10 A-11 A-12	A-10 A-11 A-12	A-10 A-11 A-12

Date \_\_\_\_\_

Location Sunflower Quarry

Page 4 of 5

Rock Unit(s): \_\_\_\_\_

Thickness	Lithology & Weathering Profile	Fossils & Grains	Sed. Struct & Diag. Feat.	Rock Name (Dunham)	Cement	Color	Sample No.	Photo No.	Additional Remarks
5-10				Almond Shale Pebbles			516 517		Sharp contact along upper bed. Variable thickness & bedding. Faint all along exposure. Hard sand?
45cm				as below			5-7 KNOT-7		Color becomes mottled @ top
17cm									

Date \_\_\_\_\_

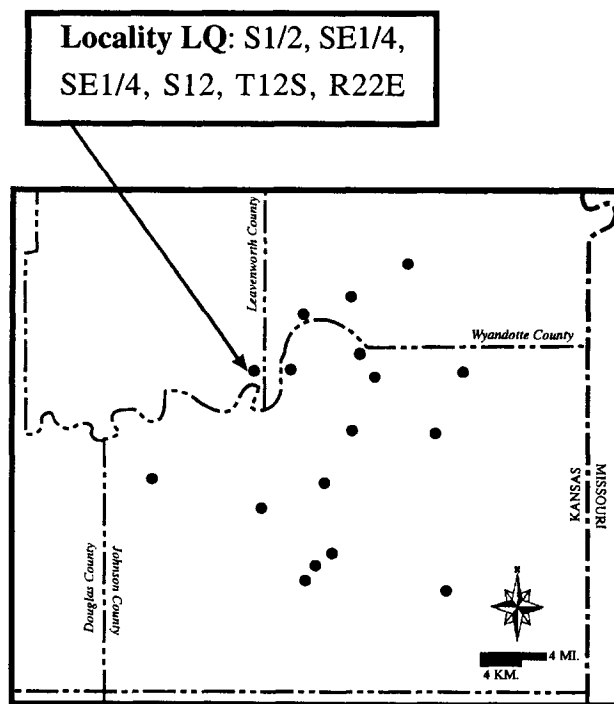
Location Sunflower Quarry

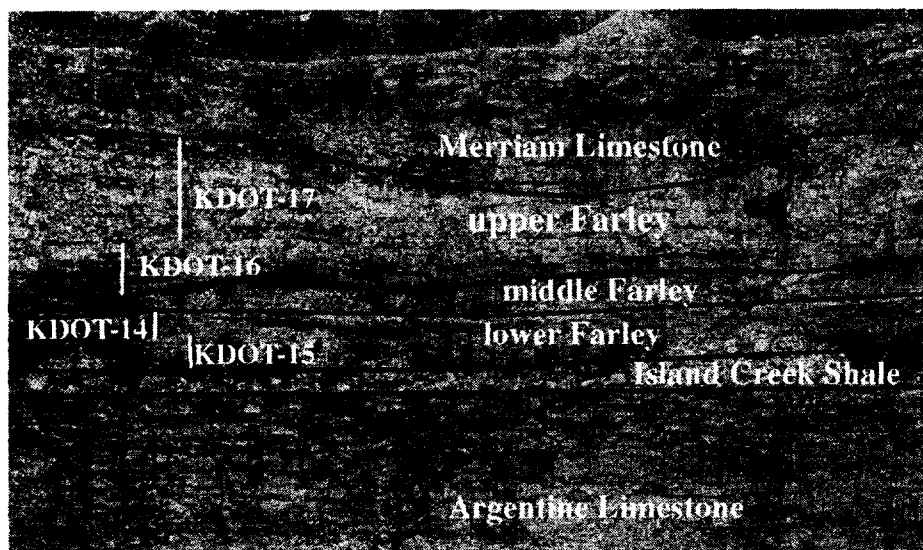
Page 5 of 5



**Locality LQ:** Quarry section. Measured in the inactive quarry on Loring Road west of Bonner Springs in Leavenworth County. The Farley Limestone is accessible in the upper portion of the quarry. Follow quarry roads up around to the northeast. Argentine Limestone is exposed at the level of the quarry pond and the Island Creek Shale and Farley Limestone is accessible by climbing. The upper portions of the Farley were only reachable with a ladder and some was out of reach completely.

This section contains aggregate samples KDOT 14-17





**Figure A1.4:** Outcrop photo of exposure in the inactive Loring quarry. Members of the Farley are outlined as are the surrounding units. Note that the Bonner Springs Shale is absent in this location. Aggregate sample locations are also noted.

Rock Unit(s): Is. Creek + Farley

Thickness	Lithology & Weathering Profile	Fossils & Grains	Sed. Struct & Diag. Feat.	Rock Name (Dunham)	Cement	Color	Sample No.	Photo No.	Additional Remarks
57+		⊕ # N		Phyl. Algal Wackestone	Very little coarse grain ( $\leq 5\%$ )		L-3		
3				Fossilif. Siltstone					
5		N ⊕ #		Phyl. Algal Wack.					
8		N ⊕ #		Phyl. Algal Wackestone					
18		⊕ #		Fossilif. Siltstone					
32		N ⊕		Phyl. Algal Wackestone	Less grain than below $\sim 5-10\%$		L-2		Large phylloid algal
10		N ⊕ ⊕ ⊕	⊕	Phyl. Algal Wackestone	Coarse grain $\leq .5mm$ $\sim 15\%$		L-1		Shale content in these phyl. wackestones is red high. However, its fully disintegrated gray matrix a black line, especially near the top & in the interbedded nature.
52		N ⊕ ⊕ ⊕	⊕	Phyl. Algal Wackestone	Coarse grain in phyls. & brechs ( $\pm .5mm$ and) $\sim 15\%$		L-1		Well preserved branches w/ internal structure
12		N ⊕ ⊕ ⊕	⊕	Phyl. Algal Wackestone					
15		⊕ ⊕ #		Fossiliferous Siltstone					
26cm									

10cm

Date 12/5/97

Location Loring Quarry

Page 1 of 2

1:10cm

Rock Unit(s): Farley LS

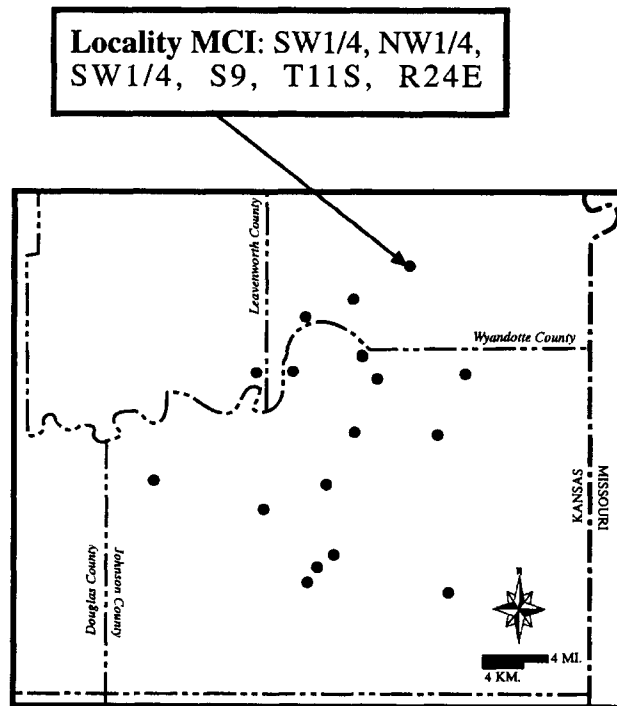
Thickness	Lithology & Weathering Profile	Fossils & Grains	Sed Struct & Diag Feat	Rock Name (Dunham)	Cement	Color	Sample No.	Photo No.	Additional Remarks
25		N# @	A.B. ○	Phyl. Algal Wackestone	Spumose ch. in cracks & fossils (~25-30%)		L5		Continues up out of reach.  Large shallow pores + fractures filled w/ coarse spar.
28									
60cm		@ N#		Osagia, Brachiopod Wackestone	Coarse spar in cracks & other fossils (~10-15%)		KDUT-15		Osagia very ab. as are Composita  Encrusts more ab. @ the base.
60cm		@ # @		Fossilif. Siltstone			F		skeletal structure @ very base  Most fossiliferous near the top Calcareous throughout
3cm									

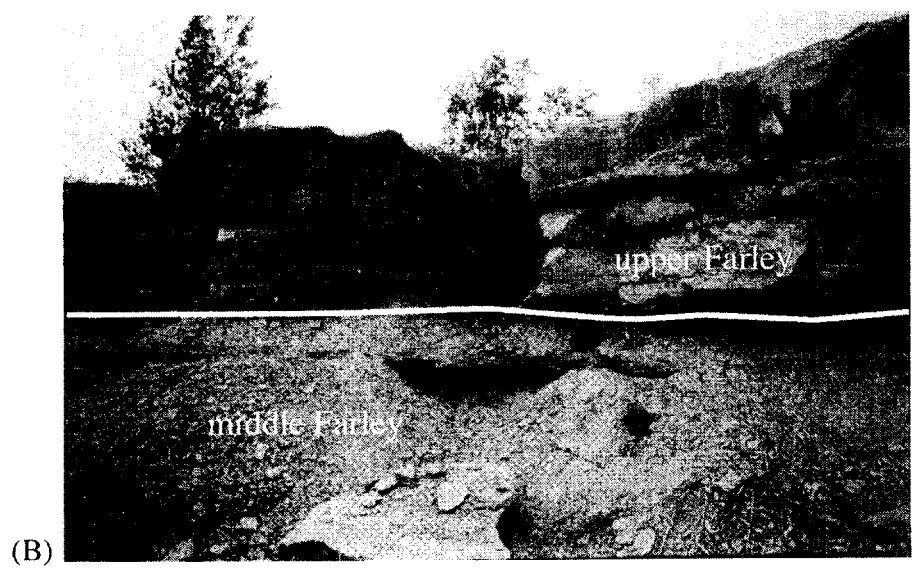
Date 12/5/97

Location Loring Quarry

Page 2 of 2

**Locality MCI:** Roadcut/outcrop. Located north of Interstate 70 in Wyandotte County. Measured section was compiled from two localities. The Farley Limestone was measured from the outcrop located at the Motor Carrier Inspection Station on I-70. The Island Creek was measured approximately 1 mile to the west along the north side of the 78th Street westbound exit ramp.





**Figure A1.5:** Outcrop photos of locality MCI. (A) Lower Farley is composed of single massive bed of cross-bedded oolite. (B) Middle Farley is a member composed exclusively of siltstone whereas the upper Farley is dominantly phylloid algal wackestone to packstone.

Rock Unit(s): Fairley

Thickness	Lithology & Weathering Profile	Fossils & Grains	Sed Struct & Diag. Feat.	Rock Name (Dunham)	Cement	Color	Sample No.	Photo No.	Additional Remarks
2cm		#0~		Phys. bedded Wackestone					
6cm+		#0~ B~		Organic Bedded Wackestone					Marker Bed
		00		Platy-arenaceous facies siltstone					
				Blocky Non-laminar Mudstone					Reddish streaks & color mottling
				covered					
		#00A 00~	/// Conchoidal Porosity	X-bedded Oolitic Grainstone					Large whole bryozoan fronds separating the top surface along with abundant other structural  Single massive bed
16cm									
2cm									

Date 10/21/57

Location Metro Center Ings Station I-70

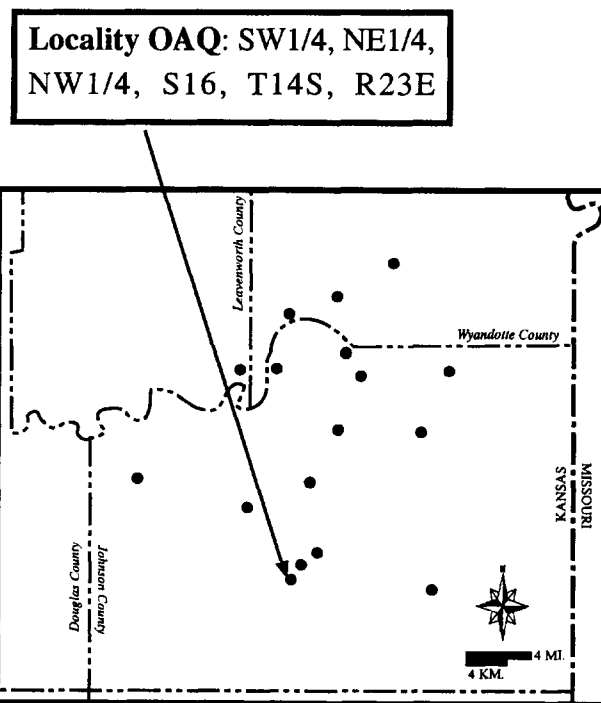
Page 2 of 3

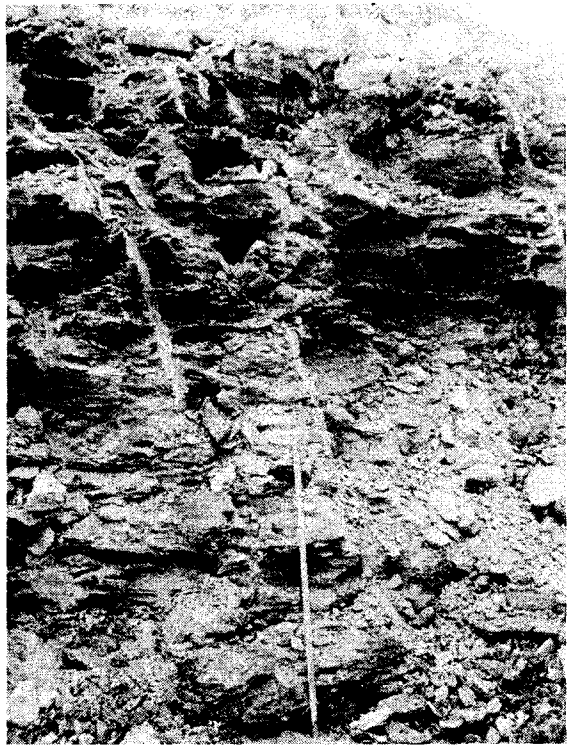
1:20 cm





**Locality OAQ:** Quarry section. Measured in an active quarry operated by Olathe Aggregate Company. Quarry is located in Olathe west of Lone Elm Road on 158th Street. Section measured was located in the southeast corner of the quarry. Measured section includes the Farley Limestone, Lane Shale and Bonner Springs Shale. The Argentine Limestone was not yet exposed in this quarry except for the upper surface. Aggregate samples KDOT-18, 19, & 20 are from this quarry.



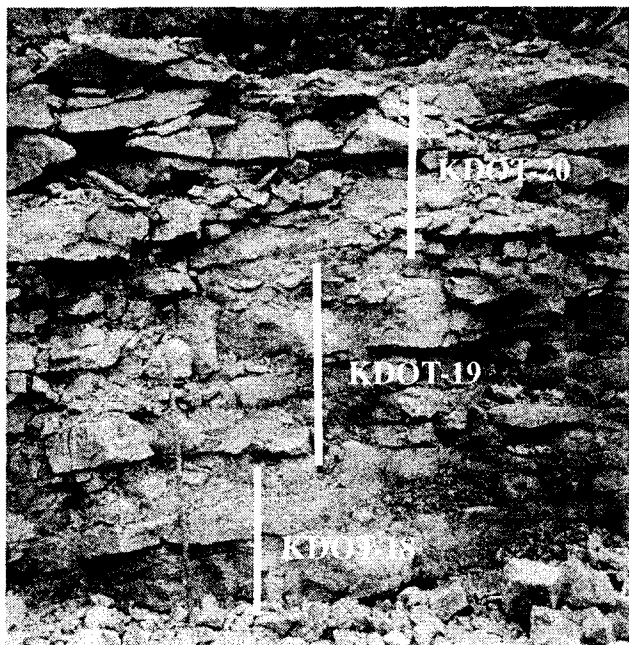


**Figure A1.6.** Outcrop photos of quarry exposure in the Olathe Aggregate Quarry. Section was measured in the southeast corner of the quarry.

(A) Thick outcrop of siltstone facies makes up the Island Creek, lower Farley and middle Farley equivalent units here. This is the Lane Shale located in the south of the field area.

(B) Upper Farley outcrop with locations from which aggregate samples were taken marked.

(A)



(B)

Rock Unit(s): Essex Valley

Thickness	Lithology & Weathering Profile	Fossils & Grains	Sed Struct & Diag Feat.	Rock Name (Dunham)	Cement	Color	Sample No.	Photo No.	Additional Remarks
				Dr. mudstone Coal Seam		Black			Dark, organic rich shale
200 cm				Laminated, lenticular Siltstone		Med - Dr Gray			Plant material common Notable lack of body fossils. Darkens in color up towards the coal seam. Ripple laminated lenses of fine sand.

Date 8/6/97  
 1:10 pm

Location Clinton Co. Quarry

Page 1 of 4

Rock Unit(s): Essex Creek in Valley

Thickness	Lithology & Weathering Profile	Fossils & Grains	Sed. Struct & Diag Feat	Rock Name (Dunham)	Cement	Color	Sample No.	Photo No.	Additional Remarks	
4cm		~ @ #								
10cm		~ @	A.B.	Phy. Algal Wadsworth	Sp. replaced Fills phyllid algal nodules Fract. ls. (~150-152)		DA4		* Marker Bed  Clay ab. @ base but less ab. upwards  (~30% has d. Frond)	
		⊕ # ⊕ ⊙	Osgood Wadsworth					DA3		
		⊕ ⊕ ⊙	St. Pishin							
10cm		~ @ ⊕ ⊕ ⊕ ⊙		Fossilif. S. Hudson		DL Gray			At least material Fossil. fragments	
								DA2		
10cm		~ ⊕		Compacted Skeletal Pisces	No coarse cement				Compacted shell debris - skeletal intraclasts; shells have flat like into shell; very cherty	
6cm								DA1		

Date 8/6/97

Location Chatham Ag. Co. Quarry

Page 2 of 4

Rock Unit(s): Grey - S




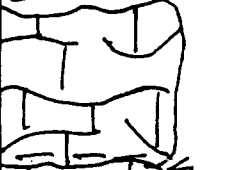

Thickness	Lithology & Weathering Profile	Fossils & Grains	Sed Struct & Diag Feat	Rock Name (Dunham)	Cement	Color	Sample No.	Photo No.	Additional Remarks
2cm+		N # ①	A.B.	Phylloid Algal Wackestone					Beats are separated by thin, concentrated shale seams that diffuse above and below ~9% of clay per bed = 5-10%
5cm		N # ②	A.B.	Phylloid Algal Wackestone	Sp. Filled fractures & fossils & molds (1-2-3%)		OA-7		Spavis shows but not overly coarse In all cases no det. sizes greater than 1-2mm were observed
26		N # ③	A.B.	Phylloid Algal Wackestone					
30		N # ④	A.B.	Phylloid Algal Wackestone				OA-6	
23		N # ⑤	A.B.	Phylloid Algal Wackestone				OA-5	
34cm		N # ⑥	A.B.	Phylloid Algal Wackestone					

Date 8/6/97

Location Clayton Aggs Co Quarry

Page 3 of 4

Rock Unit(s): Fairly - by Bower

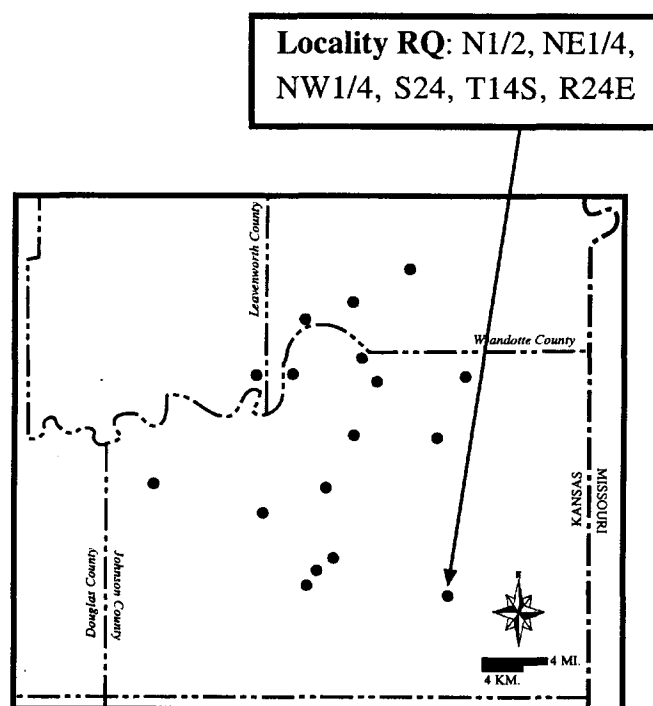
Thickness	Lithology & Weathering Profile	Fossils & Grains	Sed. Struct & Diag. Feat.	Rock Name (Dunham)	Cement	Color	Sample No.	Photo No.	Additional Remarks
52m				Staly Conglomerate					Large clasts of what appear to be phys. chert Wadestone.  Makes thick massive beds topping the Fairly.  Clasts pack into a hardened, clayey matrix
28									
25		N# 8	A-B.	Phyllite Bed Wadestone	or below				as below.
22		N# 8	A-B.	Phyllite Bed Wadestone					

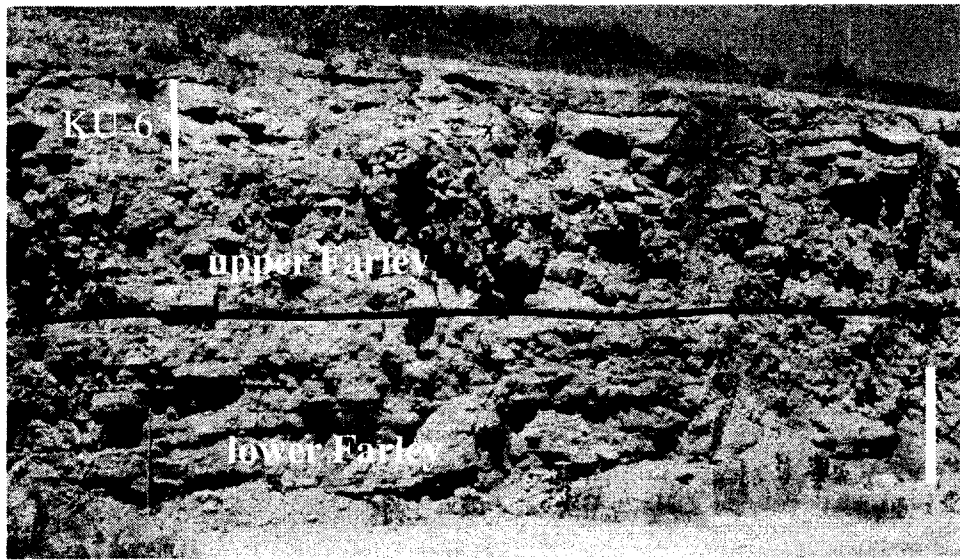
Date 9/6/97

Location Obatah Agg Co. Quarry

Page 4 of 4

**Locality RQ:** Quarry section. Measured in an active quarry operated by Reno Construction Company. Quarry is located on 161st Street and Switzer Road. Section was measured in the northeast corner of the quarry just south of 161st Street. Measured section includes a complete Farley Limestone and Island Creek Shale section. The Argentine Limestone is well exposed in this quarry as well. The Bonner Springs Shale is absent here.





**Figure A1.7:** Outcrop photo of exposure measured in the Reno West quarry. Middle Farley is represented by a thin shale seam at the level of the black line in the photo. Aggregate sample KU-6 was collected from the interval indicated. Scale bar is 1.5 meters.



Rock Unit(s): Facies 25

Thickness	Lithology & Weathering Profile	Fossils & Grains	Sed Struct & Diag Feat.	Rock Name (Dunham)	Cement	Color	Sample No.	Photo No.	Additional Remarks
10cm		N # 8	⊙	Phyl. Algal Wackestone	Spn. in phyl. (~20%)				
32cm		N # 8	⊙	Phyl. Algal Wackestone	Ab. coarse spn spn. near base. Changes w/ height (50-15%) Spn. size is variable (2.3mm)				Phyls. most ab. @ base Ab. shatter possibly f. but w/ coarse spn.
17cm		N 8	A.B	Phyl. Algal Wackestone	Highly recryst. ~70% fine spn & microspn		RW7		Ab. shatter possibly f. but w/ spn below phyls. No visible clay.
16cm		N # 8	A.B	Phyl. Algal Wackestone	Very little visible spn. All present is fine (1mm) (~15%)		RW6		Ab. silty stringers. Not concentrated accumulation Typically found around bedding plane. (~20%)
11cm									
14cm									
28cm									
1cm				Blocky-lam Siltstone					Well cemented calcareous
46cm		⊙ # 8 ~		Shaly Wackestone	Fine-med spn (1mm) (~5-10%)		RW5		Mica concentrations & stringy shale (shaly wackest.) (~20-35%)
10cm									Cont. from pg 1

Date \_\_\_\_\_

Location Reno West Quarry

Page 2 of 4

Rock Unit(s): Fairley LS

Thickness	Lithology & Weathering Profile	Fossils & Grains	Sed. Struct & Diag Feat.	Rock Name (Dunham)	Cement	Color	Sample No.	Photo No.	Additional Remarks
20+		# @ B Y N		Skeletal Wackestone	Fine-mud spar in fossils (<1cm) (~10%)				Ab. d. fluxe & conc. shale seams (~25%)
3cm		# @ B	AB	Skeletal Wackestone	Med-coarse spar in brown and greyish (<1cm) (~5%)		Rw3		Ab. silty diffuse stylolites ~25-30% has d. fluxe clay in it
2cm		# @ B		Skeletal Wackestone	Spar only visible in fossils & @ crinoids (~5%)				Ab. large crinoid stems Very little clay material Some @ base (~5%)
1cm		# @ B		Skeletal Wackestone	Spar only visible in fossils & @ crinoids (~5%)				Ab. large crinoid stems Very little clay material Some @ base (~5%)
5cm		# @ B		Skeletal Wackestone	Spar only visible in fossils & @ crinoids (~5%)				Ab. silty material diffused @ base. indistinct (~50% has oleg. nit)
17c.		# @ B		Skeletal Wackestone (Argillaceous)	Spar only visible in fossils & @ crinoids (~5%)				Blocky to slightly platy. Ab. crinoid stems of all sizes.
3cm		# @ B		Fossiliferous Siltstone					

Date 7/2/97

Location Reno West Quarry

Page 1 of 4

1:10cm

Rock Unit(s): Fairy LS


Thickness	Lithology & Weathering Profile	Fossils & Grains	Sed Struct & Diag Feat	Rock Name (Dunham)	Cement	Color	Sample No.	Photo No.	Additional Remarks
14cm +		~#⊙ □ ▽	A.B.	Phylloid Algal Wacke - Packstone	Ab. coarse med coarse spar Replace phyls Shale part is rare. Spar replaced - phyls or a few fossils.		RW1		Very clean LS w/ little to no clay material. (< 1%) No shale between bedding planes Phyls are densely packed w/ ab. shaly porosity & autoclastic brecciation.
3cm									
3cm									
3cm									
13cm									
18cm									
22cm									
23cm									
3cm +									

Date \_\_\_\_\_

Location Reno West Quarry

Page 3 of 4

Rock Unit(s): Facey S

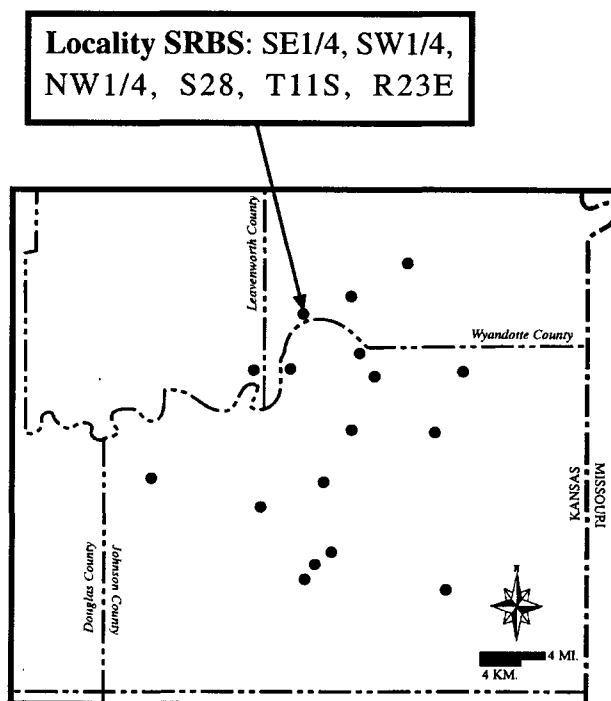
Thickness	Lithology & Weathering Profile	Fossils & Grains	Sed. Struct & Diag. Feat.	Rock Name (Dunham)	Cement	Color	Sample No.	Photo No.	Additional Remarks
4m				dol below					

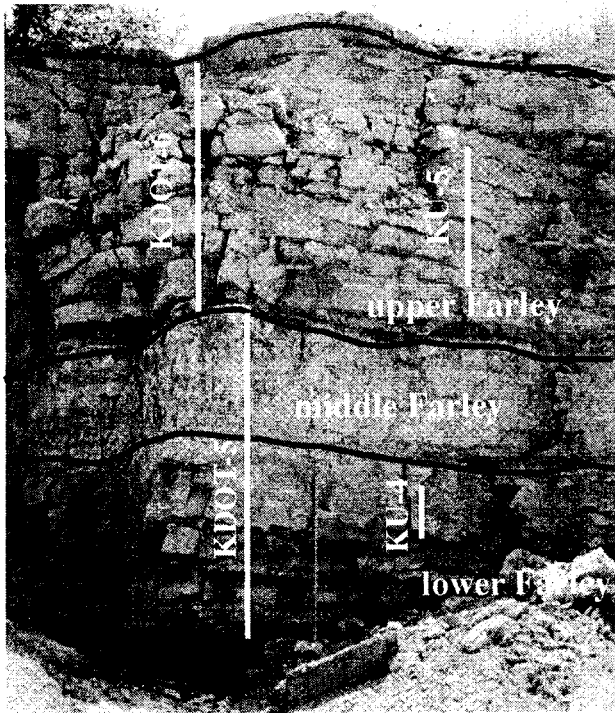
Date \_\_\_\_\_

Location Reno West Quarry

Page 4 of 4

**Locality SRBS:** Quarry section. Measured in active quarry operated by Shawnee Rock Company. Quarry is located along Kansas Highway 32 just east of Kansas Highway 7. Section was compiled from two localities within the quarry. The middle and upper Farley sections were measured in what was the southwest corner of the quarry. This section has since been covered for reclamation. The lower Farley and Island Creek Shale were measured in an active section of the quarry in an area approximately 500 feet north of the rock crusher. This quarry contains full sections of the Argentine Limestone, Bonner Springs Shale and the Merriam and Spring Hill Limestones in addition to the Farley. Aggregate samples KU 4 & 5 as well as KDOT 5 & 6 are from this quarry.

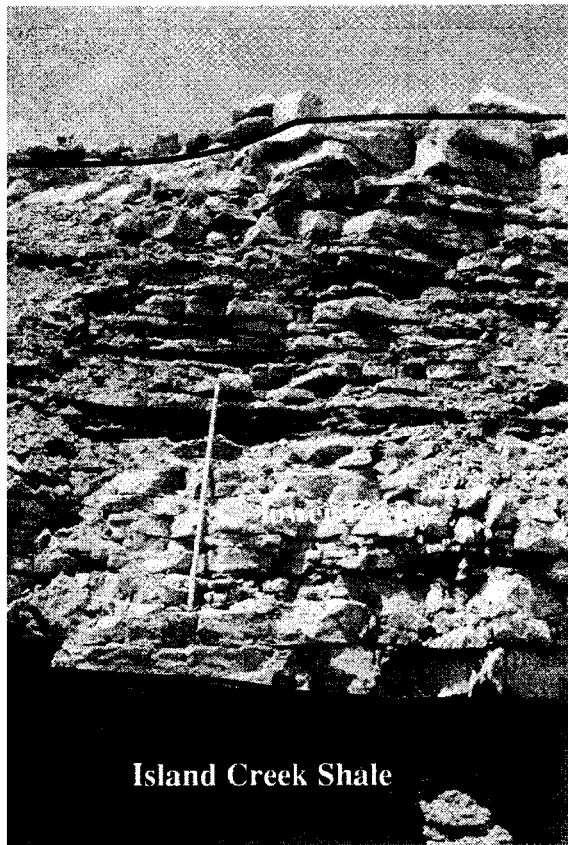




(A)

**Figure A1.8:** Outcrop photos of measured sections from Shawnee Rock Company's Bonner Springs quarry. Measuring staff in each photo is 1.5 meters for scale.

(A) Upper portion of the lower Farley in addition to the middle and upper Farley members. The middle Farley here is dominated by a thick bed of limestone, and not the normal shale as in other localities. Locations from which aggregate samples KU 4 & 5 as well as KDOT 5 & 6 were taken are marked.



(B)

(B) Island Creek Shale interval and the majority of the lower Farley limestone. The lower Farley here includes a thick section of interbedded limestone and siltstones.

Island Creek Shale

Rock Unit(s): Lower Farley

Thickness	Lithology & Weathering Profile	Fossils & Grains	Sed. Struct & Diag Feat	Rock Name (Dunham)	Cement	Color	Sample No.	Photo No.	Additional Remarks
9cm		#							
44cm		~ ⊕	⊕ ⊖	Phylloid-stygal Wackestone	Spore replaced phyls + fossils + fill structure (~15%)				Shale clay concentrated in pockets + seams throughout. (~80% contains clay)
15cm		~ ⊕ ⊖	⊕	Phylloid-stygal Wackestone	Spore replaced phyls + fossils. Fills irregular shaly pores (~15-20%)				Shale across bedding planes diffuse up + down into ls (~5-10%) Most phylloids very fragmented
20cm				Wackestone					Fewer phyls + more large cracks near top
3cm									
27cm		~ ⊕ ⊖	⊕ ⊖	Phylloid-stygal Wackestone	Some spore replaced phyls + fossils (~10%)	Greenish Gray			Some diffuse clay seams @ top of polite + in white (~10%) Distinct upward lithology change
10cm		⊕ ⊖		Oolite	No coarse spore visible - oolite	Med-dark gray			Conchoidal dark nuclei (6% of base has clay)
162cm		# ⊕		Fossiliferous shale					Island Creek shale

Date 6/24/97

Location Shawnee Rock #2 Banner zone 115

Page 1 of 2

1:10cm

Rock Unit(s): Lower Farley

Thickness	Lithology & Weathering Profile	Fossils & Grains	Sed. Struct & Diag. Feat.	Rock Name (Dunham)	Cement	Color	Sample No.	Photo No.	Additional Remarks
7cm		#	○						
7cm		#	○						
4cm		#	○						
22cm		#	○						
15cm		#	○						
15cm		#	○						
15cm		#	○						
10cm		#	○						
7cm		#	○						
8cm		#	○						
6cm		#	○						
6cm		#	○						
12cm		#	○						
		#	○	Fossiliferous Siltstone					Comb. Temp. 1

Date 6/24/97

Location Skaneateles Park #2 Banner Springs, KS

Page 2 of 2



Rock Unit(s): Farley LS

Thickness	Lithology & Weathering Profile	Fossils & Grains	Sed Struct & Diag Feat	Rock Name (Dunham)	Cement	Color	Sample No.	Photo No.	Additional Remarks
40cm +				Skeletal Wackestone (Mudstone?)	Very finely recryst. Microspar + micrite matrix (spar = ~5%)				Very blocky nature. Abundant ext. fractures clean of clay content. Mostly micrite matrix
18cm				Siltstone Peloidal, Skeletal Packstone	Spar content is mostly recryst. (~15%)		BS-11		Mud cover ground the oxide below Thickness varies laterally No clay No clay present Large fenestrate bypasses in some places Small ooid size. Very little micrite present.
55cm				Oolitic Peloidal Packstone	Highly recryst. w/ very fine spar. Some spar not visible (~25%) All spars much less than 5um		BS-3		
23cm				Peloidal, Skeletal Packstone	Sil. matrix is mostly recryst. Finespar (sil. mat) (~15-20%)		BS-2		Sil. debris concentrated in pockets Spar same @ base edge (~10%) Alternating siltstone/LS succession
10cm				Foss. Siltstone					
10cm				Phylloid Algal Wackestone	Spar replace phylloid fossils (~10-15%)				
6cm				Foss. Siltstone Phylloid Algal Wackestone	As above (~10-15%)		BS-1		LS beds are argillaceous throughout + some have shale lamination at their
3cm				Foss. Siltstone					
3cm				Phylloid Algal Wackestone	As above (~10-15%)				
7cm +				Foss. Siltstone					

Date 6/30/97

Location Snowflake Rock #2, Bonner Springs, KS

Page 1 of 3

Rock Unit(s): Facey - 2 - 100m

Thickness	Lithology & Weathering Profile	Fossils & Grains	Sed. Struct & Diag. Feat.	Rock Name (Dunham)	Cement	Color	Sample No.	Photo No.	Additional Remarks
15m +									Shale partings between bedding planes.
24m		~ @ #	⊙ A.S.	Phyl. Algal Wackestone	Med-coarse sp. found around phyl beds in shallow part Fills + replace fossils - (3mm)		K005-5		Shale diffused up & down from bedding planes. Mostly concentrated near top (~5-10%)
24m		~ @ #	⊙ A.S.	Phyl. Algal Wackestone	(~25-30%) sp. also found in bacteria fabric.		B5-20		A.S. autochthon (compacted) brecciation Only about 5% of sp. is in large shallow part or beds. Most is in thin fractures & phylloid edges
24m		~ @ #	⊙ A.S.	Phyl. Algal Wackestone					
53m		~ @ # ~ @ # ~ @ #	⊙	Phylloid-Algal Wackestone	Sp. coarse around band the base (53mm) Coarse sp. fills beds (~20%)		B5-7		Transitional Marker Bed A.S. large whole beds
11m				Osgia, Brach Wackestone			B5-6		Clay only diffused near bedding plane (~10%)
11m				siltstone			B5-5		Blocky texture; laterally persistent
48cm +				as above	Small amount of very fine sp. (~5%)		B5-4		

Date \_\_\_\_\_

Location near 100m 2 Bonnet Springs St

Page 2 of 3

Rock Unit(s): \_\_\_\_\_

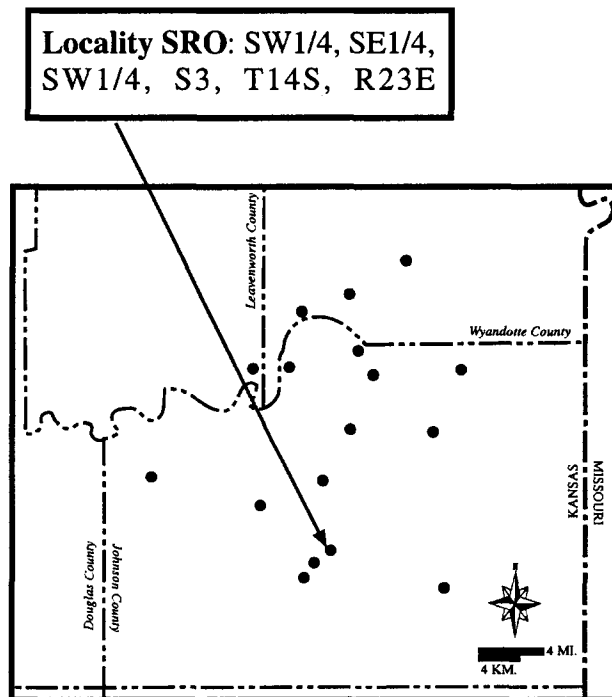
Thickness	Lithology & Weathering Profile	Fossils & Grains	Sed. Struct & Diag. Feat.	Rock Name (Dunham)	Cement	Color	Sample No.	Photo No.	Additional Remarks
57cm		~#	AB V	Phyf. Algal Wackestone	Some fine gr. (silica) fracture (~10%)		B510		St. debris in pockets. Clay around bedding planes. (± ~5%) in carbonate seams.
46cm		~#	AB x	Phyf. Algal Wackestone	Sp. silty fossils + fractures (± 2%) (~15-20%)		B59		St. debris in fine fill.
19cm		~#	AB	Phyf. Algal Wackestone	as low		B58		as below

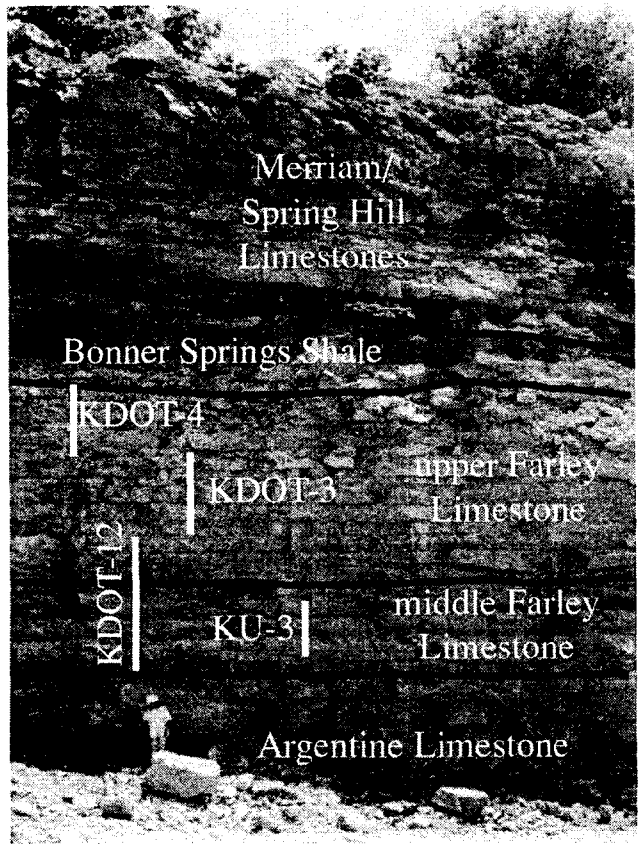
Date \_\_\_\_\_

Location Shawnee Rock #2, Bonner, Ind. age

Page 3 of 3

**Locality SRO:** Quarry section. Measured in an active quarry operated by Shawnee Rock Company. Quarry is located in Olathe west of Lone Elm Road on 151st Street. Section measured was located on the south wall of the quarry. Measured section includes only the Farley Limestone but the Argentine Limestone and the Bonner Springs Shale were both briefly examined here also. The Lane-Island Creek Shale is missing at this locality. Aggregate samples KU-3 and KDOT-3, 4 and 12 are from this quarry.





**Figure A1.9:** Outcrop photo of Shawnee Rock Company's Olathe quarry. The lower Farley Limestone is missing in this location. The Bonner Springs Shale shows significant thickness variation due to downcutting by the overlying Merriam Limestone.

Rock Unit(s): Farley/Argentine LS

Thickness	Lithology & Weathering Profile	Fossils & Grains	Sed. Struct. & Diag. Feat.	Rock Name (Dunham)	Cement	Color	Sample No.	Photo No.	Additional Remarks
15cm				Flat-bedded sandy, skeletal granitoid					
35cm				Cross-bedded sandy, skeletal granitoid	or below				
12cm				Cross-Bedded Sandy, Skeletal Peck-Granitoid	Coarse spon found in fossils. Spon fills most interstitial space. (± low-)				Coarse granitoid. Mostly skeletal fragments with some whole fossils + some nodules. Silt + fine sand content is high. Qtz. sand is abundant. Accounts for ~ 80% of grains under microscope. Cross bedding is large-scale + looks like channels in some places.
5cm				Purple Argill. Limestone	No coarse spon filling voids + fossils (not sig)				This bed is the upper part of the Argentine

KDOT-3

02

01

Date 6/26/17

Location Shawnee Rock #336.46 KS

Page 1 of 4

1:10am

Rock Unit(s): Foley LS

Thickness	Lithology & Weathering Profile	Fossils & Grains	Sed. Struct & Diag. Feat.	Rock Name (Dunham)	Cement	Color	Sample No.	Photo No.	Additional Remarks
40cm		~ ② ③		Phyll. Mg. L. Wackestone	Sparingly in phyl. beds (~15-20%)				This bed contains disseminated clay throughout most of its thickness. ~80-90% has some clay in it.
69cm		~ # ②		Phyl. Mg. L. Wackestone	Very little coarse spar. Replace fossils or phyl. (~15-20%)		04		Concentrated seams + disseminated clay present here. ~55-60% has clay in it.
3cm		~ ② ② ③	○	Phyl. Mg. L. Wackestone Oolite, Barred wackestone Sh. Packstone	Coarse spar fills bed + replaces phyl. (~10%)				Marker Bed. Contains calc. spherulites + large fossil fragments. Color change vertically. Thin shale bed at base (2-4cm).
34cm		# ② ③ ① ② ③		Bioclastic Spar. oolite Sandy skeletal Groundmass	Little to no visible coarse spar. Fine spar. fill most interparticle pore space (~40%)		03		
10cm		# ② ③ ① ② ③	≡	Flat-bedded, massive Skeletal oolite					
16cm		# ② ③ ① ② ③	≡						

Date 1/24/57

Location Shawnee Rock #3, Olathe, KS

Page 2 of 4

Rock Unit(s): Farley Limestone

Thickness	Lithology & Weathering Profile	Fossils & Grains	Sed. Struct & Diag. Feat.	Rock Name (Dunham)	Cement	Color	Sample No.	Photo No.	Additional Remarks
22cm +		N <sup>o</sup> #			APA med coarse zone present in fossils & phyls				This upper section of phyl algal wackestone is significantly different than that below.
35cm			m		Free zone present in dark mottled area.				Has a distinctly mottled appearance due to veins of dark cement zone running through the beds.
16cm			m	Phylloid	Overall, med fine cement very abundant.				Contains much less disseminated clay. Only has considerable zones along bedding planes
3cm			m	Algal	Coarse = ~20% Fine = ~80% Dol = ~20%		06		
27cm			m	Wackestone					
17cm			m						
42cm		N <sup>o</sup> #	⊖	Phylloid Algal Wackestone	Coarse zone (phyllo-ferri- & phyls. (~15-20%))			05	~30% contains clay. Bryozoa none obs.
10cm +		N <sup>o</sup> #							Cont. from pg 2

Date 6/26/17

Location Shannon Rock #3, Olathe, KS

Page 3 of 4



Rock Unit(s): Fairley -S

Thickness	Lithology & Weathering Profile	Fossils & Grains	Sed. Struct & Diag. Feat.	Rock Name (Dunham)	Cement	Color	Sample No.	Photo No.	Additional Remarks
42cm		~#		Phylloid Algal Wackestone	Spars only in phylloid algal (~15%)		08		Abt concentrated clay seams ~40% less clay in it
3cm		#		Stylolite LS					Thin stylolite (block)
45cm		~#		Phylloid Algal Wackestone	as below		07		as below
46cm									

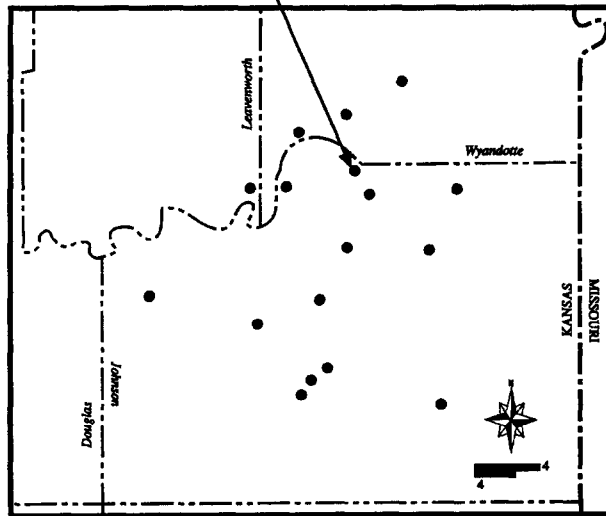
Date 6/20/57

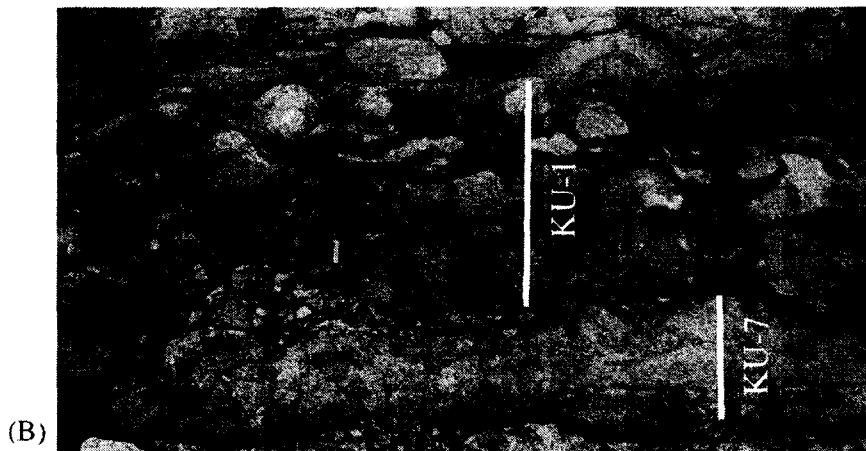
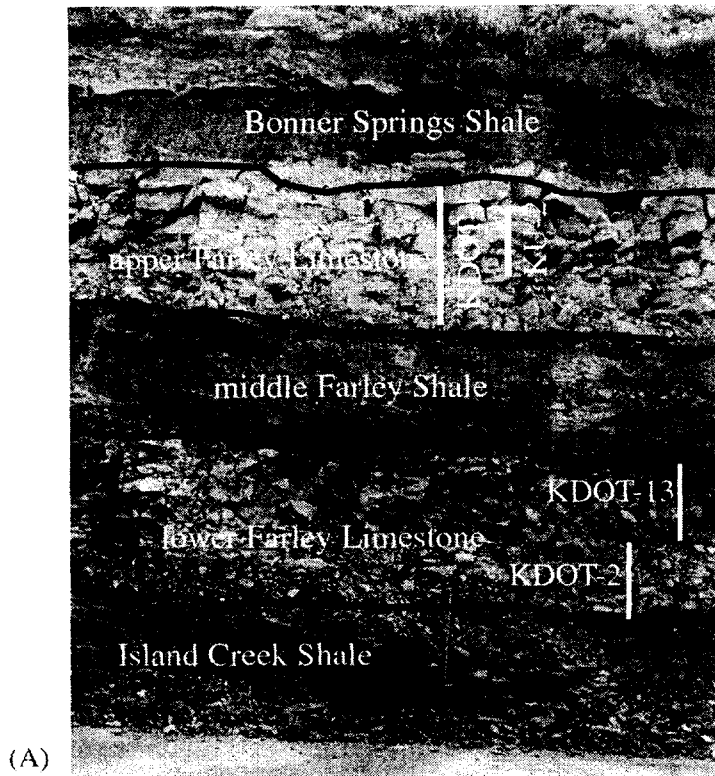
Location Shawnee Rock #3 Okla KJ

Page 4 of 4

**Locality SRS:** Quarry section. Measured in active quarry/landfill operated by Shawnee Rock Company and Deffenbaugh Disposal. Section was measured in area of the quarry referred to by quarry employees as 120 acres. This is in the southeast portion of the quarry to the southeast of the south guard shack. If entering the quarry along the south road, turn left at the stop sign located before the guard shack and follow the quarry access road. Units exposed in this area included partial Argentine Limestone, and full sections of the Island Creek Shale, Farley Limestone and Bonner Springs Shale. Aggregate samples KU-1, 2 & 7 as well as KDOT-1, 2 & 13 are from this quarry.

**Locality SRS: C, SE1/4, SW1/4,  
S6, T12S, R24E**





**Figure A1.10:** Outcrop photos of measured section from Shawnee Rock Company's Shawnee quarry. (A) Photo of entire Farley section as well as Island Creek Shale and Bonner Springs Shale. Locations of aggregate samples are indicated. (B) Close-up of a portion of the lower Farley Limestone with locations from which aggregate samples were taken indicated.

Rock Unit(s): Lower Farley LS

Thickness	Lithology & Weathering Profile	Fossils & Grains	Sed Struct & Diag Feat	Rock Name (Dunham)	Cement	Color	Sample No.	Photo No.	Additional Remarks
35m		# 0 0 0 0 0		Stylolite-rodular Argillaceous Skeletal Limestone	Large (4-12cm) spar-filled vugs & veins Spar size < than Spar content is very high. Comp. spar ~ 25%	Dr gray - Barns Blue	1-KD 01-1		Fossil fragments conc. in stylolites around nodules. Some in nodules Ab. vugs & vugs filled w/ coarse spar Matrix is microspar Clay (at bottom) ~ 20%
20cm		0 0 0 0		Productid/ Blotid, Skeletal Biotin	Med spar in Productid Rampant (~15-20%)		SH-6 SH-7	A-29	Coarse spar in matrix. Pebbles of study material (~12) V. highly porous. Comp. spar in matrix
4cm				Siltstone					
4cm		0 0 0 0	0	Phylloid Algal Limestone	Med spar (10%) Less sparse finer than below		SH-2		Shale is disconformable fine bedding planes. 20% fossil content, deep water All phylloid content is fragmented small Higher ratio of brachiopods & bryozoa
23m		0 0 # 0 0 0 0 0	0 0 0 0	Phyl. Algal Limestone	Ab. coarse & fine spar (10-15%)		SH-1		~ 40% contains diffuse clay
3cm				Siltstone					Undulating shale bed
14cm		0 0 # 0		Phyl. Algal Limestone	sp ~ 20%				Waxy concentrated clay seams ~ 40%
35cm		0 0 # 0	0 0	Phyl-Algal Limestone	Med. spar filling brachiopods & replacing phyl. algal (~15%)				~ 60% diffuse clay at base (transitional gradal contact)
10cm						Med light Gray (N6)			1.5m & 1.2m high massive non-fossiliferous bluish gray shale




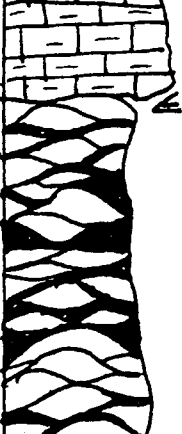
Date 6/11/97

Location Shawnee Rock #1, Shawnee, KS

Page 1 of     

1:10m

Rock Unit(s): Lower Farley

Thickness	Lithology & Weathering Profile	Fossils & Grains	Sed. Struct & Diag. Feat.	Rock Name (Dunham)	Cement	Color	Sample No.	Photo No.	Additional Remarks
10cm		FOF	U	St. Westmore	Highly recy'd (50-60%)	Black gray			Fingering matrix w/ large white trash fossils
20cm		FOF	U	St. Westmore	Highly recy'd. (50-60%)	Black gray			Argillaceous ls. Plant frags - burrows ab. No glaucosphaerids but completely amorphous (disseminated)
15cm		FOF	U	St. Westmore	Highly recy'd. (50-60%)	Black gray	SN-5		
40cm				as below			SN-1		Continued from p. 1

Date 6/11/97

Location Shannon Rock #1, Shannon, KS

Page 2 of

Thickness	Lithology & Weathering Profile	Fossils & Grains	Sed. Struct & Diag. Feat.	Rock Name (Dunham)	Grain Size	Color		Sample No.	Photo No.	Additional Remarks
						Fresh	Weathered			
				(Slightly laminated - lenticular) Siltstone		Dk Gray  Green Gray		58	Micaceous throughout: much more so towards the base. Fossiliferous @ top 10cm  Top ~25cm much more calcareous overall cemented. Prominent horizon of calcareous concretions/nodules.  Obvious lack of any body fossils or impressions.  Calcareous throughout but only very slightly.	

Date 4/1/67

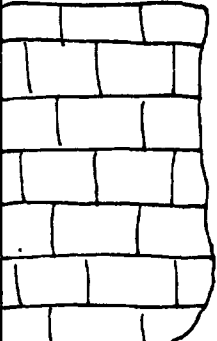

Location Shawnee Rock #1

Page 1 of 1

1:20 cm



Rock Unit(s): Upper Fordy LS

Thickness	Lithology & Weathering Profile	Fossils & Grains	Sed. Struct & Diag. Feat.	Rock Name (Dunham)	Cement	Color	Sample No.	Photo No.	Additional Remarks
49m		R*DB e		Peloidal, skeletal Packed	Little to no coarse spar Spar mostly fine crystalline (micro?)		64-4	B-3	Top surface has large boulders on it. Dominantly peloids & laminae Massive but contains along outcrop Very clean ~5% clay content
32m		~P B O	(P)	Phyl. Algal Wackestone	Very little spar. No dolomite? coarse fossils lining beds.	Tannish Brown/ Orange	54-3	B-3	Phyl. Alg. coated w/ dolomite Mottled porosity ~35% carbonate & fine clay

Date 6/17/97

Location Shawnee Rte #1, Shawnee, KS

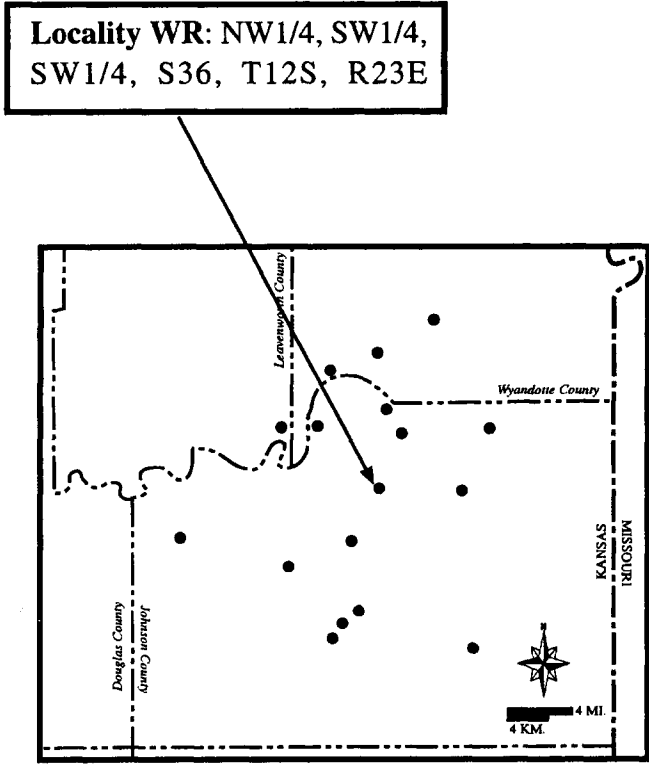
Page 2 of 2





**Figure A1.11:** Photo of outcrop located near the intersection of Woodland Road and 95th Street in Johnson County. The Farley Limestone outcrop here is not a complete section. Only the lower half is present.

**Locality WR:** Road cut along Woodland Road just south of 95th Street in Johnson County. Go north from K-10 on Woodland Road past the intersection of 95th Street. The roadcut is on the east side of the road and includes the Argentine Limestone, Island Creek Shale, and a partial Farley Limestone section.



Rock Unit(s): Fairley Ls

Thickness	Lithology & Weathering Profile	Fossils & Grains	Sed Struct & Diag Feat	Rock Name (Dunham)	Cement	Color	Sample No.	Photo No.	Additional Remarks
	Covered or Missing								
13		no #	AB	Phy. Alg. Wackestone	Sp. in bands breaks up (15-25%)				
28									
22								WR-4	
21					Fossilif. Siltstn				
15			no #		Phy. Alg. Wackestone				
9					Fossilif. Siltstn				
13			no #		Phy. Alg. Wack.				
10					Fossilif. Siltstn				
12			no #		Phy. Alg. Wack.				
28					Fossilif. Siltstn				
18		no #	AB	Phy. Alg. Wackestone	Ab. coarse spec. Fills shelled pores or replaces phg.			WR-3	
50				Phy. Alg. Wackestone	(15-20%)			WR-2	
20									
20									
25cm								WR-1	
45cm				Blocky fossiliferous Siltstone					

Date 11/5/97

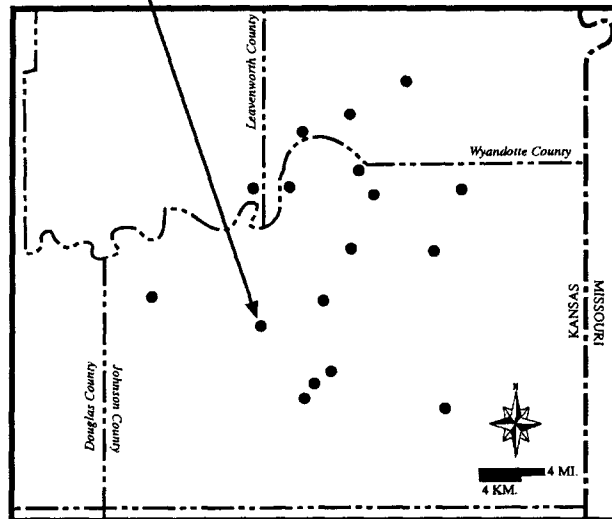
Location Woodland Road / 95th St

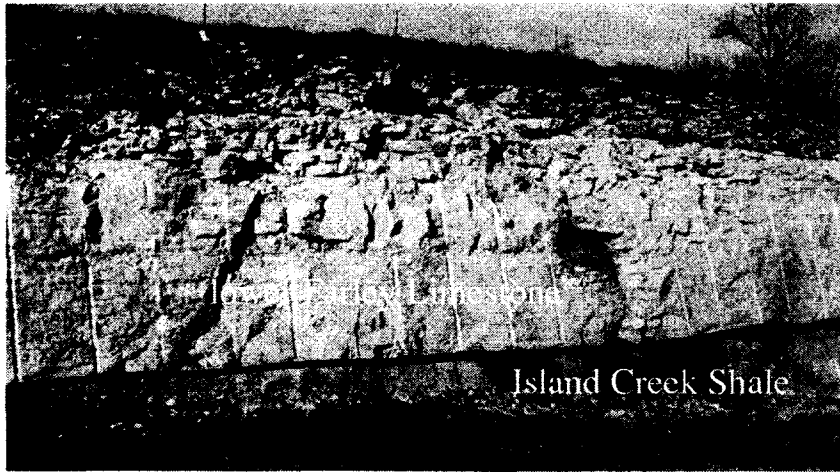
Page 1 of 1

1:20 cm

**Locality 127:** Roadcut along 127th Street in Johnson County. Go east from the intersection of 127th Street and Gardner Road in eastern Johnson County approximately 1.5 miles. Roadcut is on the north side of the road and includes Argentine Limestone, Island Creek Shale, and a partial section of the Farley Limestone.

**Locality 127: SW1/4, SE1/4,  
SE1/4, S19, T13S, R23E**





**Figure A1.12:** Outcrop photo of roadcut along 127th Street in Johnson County. The Farley Limestone section at this locality is incomplete, only the lower portion is present.

Rock Unit(s): Isle Rock & Farley

Thickness	Lithology & Weathering Profile	Fossils & Grains	Sed Struct & Diag Feat	Rock Name (Dunham)	Cement	Color	Sample No.	Photo No.	Additional Remarks	
20cm		~ @ #	m	Phylloid Algal Wackestone	as below				More ab. Fe with staining.	
12cm		~ @ #	o o	Phylloid Algal Wackestone	More more coarsely textured (~25-30%)			1272	Massively bedded Stylonulites more distinct Noticeably more coarsely crystalline	
35		~ @ #	o z	Phylloid Algal Wackestone	Coarser grained fossils, facies similar to previous (~5-10%)				Stylonulites, shale lenses Some chert present	
25		~ @								
45		~ @ #						1271		
45		~ @ #								
72cm		~ @ #		Fossiliferous Siltstone						
100m				Argentine LS					~ 8-10m thick	

Date 2-23-98

Location 127<sup>th</sup> St. Outcrop

Page 1 of 3

1:20cm

Rock Unit(s): Fairley LS

Thickness	Lithology & Weathering Profile	Fossils & Grains	Sed. Struct & Diag. Feat.	Rock Name (Dunham)	Cement	Color	Sample No.	Photo No.	Additional Remarks
									Top well weathered
		No. 1 # 2		Phylloid Algal Wackestone	Abn. coarse spongy phyllo-fossils smaller on shaly part (127-302)		1275	Thinly bedded than below; slightly wavy	
15		UR#		Phyl. Algal Wackestone	Spongy below - perhaps slightly less		1274		ab. Fe-rich staining
20								1273	
30									

Date 2-23-77

Location 127<sup>th</sup> St. Outcrop

Page 2 of 2

**Appendix 2: KDOT Physical Tests & Other Laboratory Procedures**



## **KDOT Physical Test Procedures and Calculations**

Guidelines presented below are reproduced from two sources. Information about ASTM testing is from the Annual Book of ASTM Standards (ASTM, 1995) and information pertaining to KDOT test methods is from the 1990 edition of the Standard Specifications for State Road and Bridge Construction, (Kansas Department of Transportation, 1990).

### **KDOT Modified Soundness Test for Aggregates**

#### ***Description***

This test, known as the “Modified Freeze and Thaw” test, shall be used to determine the soundness characteristics of Durability Classed Aggregate (Class 0 and 1).

#### ***Sample Preparation***

Preliminary preparation shall include removal of all material retained on the 3/4 “ mesh sieve and that passing the 3/8” mesh sieve, and the removal of all mud, clay lumps or sticks. The material shall not be washed. Shale and shale-like material, coal, asphalt coated pieces, rotten stone, soft or friable particles and other foreign material shall not be removed prior to testing. The material shall then be oven dried to a constant mass at a temperature of  $230 \pm 9^{\circ}$  F. Final preparation shall consist of screening oven dried material over 3/4”, 1/2” and 3/8” mesh sieves to meet the following grading.

<u>Individual Sieves</u>	<u>Cumulative Weight Retained (gms)</u>
3/4”	0
1/2”	2,500
3/8”	5,000

### ***Procedure***

After sieving, the material shall be placed in an open top container, covered with a No. 16 mesh sieve cloth and submerged in tap water maintained at a temperature from 70° to 80° F for a period of  $24 \pm 4$  hours. The sample shall then be tested in accordance with subarticle 1117(s)(4.2) and (4.3). One freezing period and one thawing period shall be considered one cycle. After the sample has been subjected to 25 cycles of freezing and thawing it shall be washed over a No. 12 sieve and oven dried to a constant mass at a temperature of  $230^{\circ} \text{ F} \pm 9^{\circ} \text{ F}$ . The sample shall then be screened over a 1/2" and 3/8" mesh sieve.

### ***Calculation***

(1) The cumulative percentage of material retained on each sieve (3/4", 3/8", No. 4 and No. 8) before testing shall be computed and recorded. (2) The cumulative percentage of material retained on each sieve at the end of the test shall be computed and recorded. (3) The sum of the cumulative percentages of aggregate retained on the sieves after 25 cycles of freezing and thawing shall be divided by the sum of the cumulative percentages of aggregates retained on the same screens before testing. The value obtained shall be known as the freeze-thaw loss ratio.

## **KDOT Determination of Specific Gravity and Absorption**

### ***Description***

This test method covers the procedures for determining the specific gravity and absorption of Durability Classed Aggregates.

### ***Sample Preparation***

Select a portion of the aggregate by splitting or quartering. The minimum weight of the sample, all of which passes the 3/4" sieve and is retained on the 3/8" sieve, shall be separated as shown below.

<u>Individual Sieve Size</u>	<u>Weight (grams)</u>
Passing 3/4" and retained on 1/2"	2800
Passing 1/2" and retained on 3/8"	2800

Thoroughly wash the sample over the No. 12 sieve to remove dust and other adherent coating. Dry the sample to a constant weight in the oven. Combine the two fractions to provide a sample meeting the following guidelines.

<u>Sieve Size</u>	<u>Cumulative Weight Retained (grams)</u>
3/4"	0
1/2"	2250
3/8"	4500

### ***Procedure***

Immerse the sample in water and stir vigorously. Soak for a period of  $24 \pm 4$  hours. Remove the sample from the water and bring it to a dampened absorbent cloth. For the purpose of this test, saturates surface-dry condition of the aggregate has been reached when the particle surface appears to be moist but not shiny.

Weigh the sample immediately after obtaining the saturated surface-dry condition. All weights used in this test shall be to the nearest one gram. Immediately

after obtaining the saturated surface-dry weight, immerse in water, stir to remove any entrapped air and weigh. The water temperature shall be  $75^{\circ} \pm 10^{\circ}$  F. Dry the sample at a constant weight at a temperature of approximately  $230^{\circ}$  F. Cool the sample to room temperature and weigh.

### ***Calculation***

(1) Bulk Specific Gravity =  $A/(B-C)$

(2) Bulk Specific Gravity: Saturated Surface-Dry Basis =  $B/(B-C)$

(3) Apparent Specific Gravity =  $A/(A-C)$

(4) Absorption (%) =  $100 \times [(B-A)/A]$

Where: A = Weight in grams of oven-dry sample in air  
B = Weight in grams of saturated surface-dry sample in air  
C = Weight in grams of saturated sample in water

## **ASTM C666: Standard Test Method for Resistance of Concrete to Rapid Freezing and Thawing: Procedure B**

### ***Scope***

This test method covers the determination of the resistance of concrete specimens to rapidly repeated cycles of freezing and thawing in the laboratory. The procedure is intended for use in determining the effects of variation in the properties of concrete on the resistance of the concrete to the freezing-and-thawing cycles.

### ***Significance and Use***

As noted in the scope, the procedure described in this test method is intended to determine the effects of variations in both properties and conditioning of concrete in the resistance to freezing and thawing cycles. Specific applications include the ranking of

coarse aggregates as to their effect on concrete freeze-thaw durability, especially where soundness of the aggregate is questionable.

It is assumed that the procedures will have no significantly damaging effects on frost-resistant concrete which may be defined as (1) any concrete not critically saturated with water (that is, not sufficiently saturated to be damaged by freezing) and (2) concrete made with frost-resistant aggregates and having an adequate air-void system that has achieved appropriate maturity and thus will prevent critical saturation by water under common conditions.

If as a result of performance tests, described in this test method, concrete is found to be relatively unaffected, it can be assumed that it was either not critically saturated, or was made with "sound" aggregates, a proper air-void system, and allowed to mature properly.

### ***Apparatus***

The freezing-and-thawing apparatus shall consist of a suitable chamber or chambers in which the specimens may be subjected to the specified freezing and thawing cycle, together with the necessary refrigerating and heating equipment and controls to produce continuously, and automatically, reproducible cycles within the specified temperature requirements.

The apparatus shall be arranged so that, except for necessary supports, each specimen is completely surrounded by air during the freezing phase of the cycle and by water during the thawing phase. Rigid containers which have the potential to damage specimens, are not permitted.

### ***Freezing-and-Thawing Cycle***

Conformity with the requirement for the freezing-and-thawing cycle temperature measurements are based on measurements of control specimens of similar concrete in which suitable temperature-measuring devices are embedded.

The nominal freezing-and-thawing cycle shall consist of alternately lowering the temperature of the specimens from 40 to 0° F and raising it to 40° F in not less than 2 nor more than 5 hours. Not less than 20% of the time shall be used for thawing. At the end of the cooling period the temperature at the centers of the specimens shall be 0° ± 3° F, and at the end of the heating period the temperature shall be 40° ± 3° F with no specimen at any time reaching a temperature lower than -3° F nor higher than 43° F. The time required for the temperature at the center of any single specimen to be reduced from 37 to 3° F shall be not less than one half of the length of the cooling period, and the time required for the temperature at the center of any single specimen to be raised from 3 to 37° F shall not be less than one half of the length of the heating period. For specimens to be compared to each other, the time required to change the temperature at the centers from 35 to 10° F shall not differ by more than one-sixth of the length of the cooling period for any single specimen and the time required to change the temperature at the centers of any specimens from 10 to 35° F shall not differ by more than one-third of the length of the heating period for any single specimen.

The difference between the temperature at the center of a specimen and the temperature at its surface shall at no time exceed 50° F. The period of transition between freezing and thawing phases of the cycle shall not exceed 10 minutes.

### *Procedure*

Immediately after the specified curing period bring the specimen to a temperature within  $-2^{\circ}\text{F}$  and  $+4^{\circ}\text{F}$  of the target thaw temperature that will be used in the freeze-thaw cycle and test for fundamental transverse frequency, weigh, determine the average length and cross section dimensions of the concrete specimen and determine the initial length comparator(optional) with the length change comparator. Protect the specimens against loss of moisture between the time of removal from curing and the start of the freezing-and-thawing cycles.

Start freezing-and-thawing test by placing the specimens in the thawing water at the beginning of the thawing phase cycle. Remove the specimens from the apparatus, in a thawed condition, at intervals not exceeding 36 cycles of exposure to the freezing-and-thawing cycles, test for fundamental transverse frequency and measure length change (optional) with the specimens within the temperature range, weigh each specimen, and return them to the apparatus. To ensure that the specimens are completely thawed and at the specified temperature place them in a tempering tank or hold them at the end of the thaw cycle in the freezing-and-thawing apparatus for a sufficient time for this condition to be attained throughout each specimen to be tested. Protect the specimens against loss of moisture while out of the apparatus and turn them end-for-end when returned. Return the specimens either to random positions in the apparatus or to positions according to some predetermined rotation scheme that will ensure that each specimen that continues under test for any length of time is subjected to conditions in all parts of the freezing apparatus.

Continue each specimen in the test until it has been subjected to 300 cycles of freezing-and-thawing or until its relative dynamic modulus of elasticity reaches 60% of the initial modulus, whichever comes first, unless other limits are specified. For the

optional length change test, 0.10% expansion may be used as the end of test. Whenever a specimen is removed because of failure, replace it for the remainder of the test with a dummy specimen.

Each time the specimen is tested for fundamental frequency and length change make a note of visual appearance and make special comment on any defects that develop. When it is anticipated that specimens may deteriorate rapidly, they should be tested for fundamental transverse frequency and length change (optional) at intervals not exceeding 10 cycles when initially subjected to freezing and thawing.

When the sequence of freezing and thawing must be interrupted store specimens in a frozen condition.

### **Calculation**

*Relative Dynamic Modulus of Elasticity* - Calculate the numerical values of relative dynamic modulus of elasticity as follows:

$$P_c = (n_1^2/n^2) \times 100$$

Where:  $P_c$  = relative dynamic modulus of elasticity, after  $c$  cycles of freezing and thawing, percent  
 $n$  = fundamental transverse frequency at 0 cycles of freeze-thaw  
 $n_1$  = fundamental transverse frequency after  $c$  cycles of freeze-thaw

*Durability Factor* - Calculate the durability factor as follows:

$$DF = PN/M$$

Where:  $DF$  = durability factor of the tested specimen  
 $P$  = relative dynamic modulus of elasticity at  $N$  cycles, percent  
 $N$  = number of cycles at which  $P$  reaches a specified minimum value for discontinuing the test or the specified number of cycles at which the exposure is to be terminated, whichever is less  
 $M$  = specified number of cycles at which the exposure is to be terminated

*Length Change in Percent (Expansion)* - Calculate the length change as follows:

$$L_C = \frac{(l_2 - l_1)}{L_g} \times 100$$



Where:  $L_c$  = length change of the test specimen after C cycles of freeze-thaw, %  
 $l_1$  = length comparator reading at 0 cycles  
 $l_2$  = length comparator reading after C cycles  
 $L_g$  = the effective gage between the innermost ends of the gage studs

### **ASTM C131: Standard Test Method for Resistance to Degradation of Small-Size Coarse Aggregate by Abrasion and Impact in the Los Angeles Machine**

#### ***Scope***

This test method covers a procedure for testing sizes of coarse aggregate smaller than 1 1/2" for resistance to degradation using the Los Angeles testing machine.

#### ***Summary of Test Method***

The Los Angeles test is a measure of degradation of mineral aggregates of standard gradings resulting from a combination of actions including abrasion or attrition, impact, and grinding in a rotating steel drum containing a specified number of steel spheres, the number depending upon the grading of the test sample. As the drum rotates, a shelf plate picks up the sample and the steel spheres, carrying them around until they are dropped to the opposite side of the drum, creating an impact-crushing effect. The contents then roll within the drum with an abrading and grinding action until the shelf plate impacts and the cycle is repeated. After the prescribed number of revolutions, the contents are removed from the drum and the aggregates portion is sieved to measure the degradation as percent loss.

#### ***Significance and Use***

The Los Angeles test has been widely used as an indicator of the relative quality or competence of various sources of aggregate having similar mineral compositions. The results do not automatically permit valid comparisons to be made between sources distinctly different in origin, composition or structure. Specification limits based on this

test should be assigned with extreme care in consideration of available aggregate types and their performance history in specific end uses.

***Procedure***

Place the test sample and the charge in the Los Angeles testing machine and rotate the machine at a speed of 30 to 33 rpm for 500 revolutions, discharge the material from the machine and make a preliminary separation of the sample on a sieve coarser than the 1.70 mm (No. 12). Wash the material coarser than the 1.70 mm sieve, oven dry at 221 to 230°F to substantially constant weight and weigh to the nearest 1 gram.

***Calculation***

Express the loss (difference between the original weight and the final weight of the test sample) as a percentage of the original weight of the test sample. Report this value as the percent lost.

*The following tests and procedures were performed by the author, using laboratory equipment provided by the University of Kansas Department of Geology.*

#### **Determination of Percent Insoluble Residue**

1. Obtain crushed aggregate sample and split into two fractions (one of 3/8 inch and one of 1/2 inch aggregate) of 50 grams each. Dry in oven at approximately 150° overnight.
2. Digest in 10% hydrochloric acid (HCl) by placing in large beaker and adding acid in 100 ml increments until all reaction ceases. Allow to sit for several hours to ensure reaction is complete.
3. Filter residue and solution through filter paper capable of retaining clay size particles.
4. Remove residue from filter as completely as possible. (Save filters)
5. Allow sample to dry at room temperature for 48-72 hours or place in oven at approximately 90 degrees C for 4-5 hours.
6. Weigh samples and record weights.
7. Weigh filter papers with remaining residues and record. Also weigh several empty, dry filter papers and average weight to subtract as standard.
8. Store samples in airtight, labeled vials for later use.
9. Calculate percentage of original 100 gram sample that is insoluble residue

#### **Sample Preparation of Insoluble Residues for X-Ray Diffraction Study**

1. Place approximately 1 gram of insoluble residue in plastic test tube. Also place equal amount of Calgon (commercial soap that contains sodium hexametaphosphate) in tube for dispersion.

2. Add 7-10 ml of water to tube and agitate in mechanical shaker for 10 minutes to separate clays from coarser particles.
3. After dispersion is accomplished, immediately centrifuge sample for 4-5 minutes to accomplish particle size separation.
4. Decant liquid into new tubes making sure to keep careful track of which tubes correspond to original sample and decanted sample. Save silt and sand sized fraction and keep wet by adding 5 ml of water to tube. The decanted fraction obtained in this step contains the clay size sediment fraction for x-ray identification.
5. Centrifuge clay sample for additional 15 minutes to settle out coarsest clay particles.
6. Using an eye-dropper, apply a small sample of the clay slurry to a ceramic tile cut to fit into sample holder of x-ray diffractometer.
7. Allow tile to dry so that clay is still damp but not dry enough to crack or peel.
8. Run x-ray diffractogram while sample is still damp.
9. Index and identify component minerals from resultant diffractogram.
10. From silt and sand sized slurry obtained from step 4, make a new ceramic tile with coarser fraction of sediment and run additional x-ray pattern to facilitate additional identifications.

### **Preparation of Aggregate Thin Sections for Petrographic Examination**

1. Obtain enough small cardboard boxes to hold one of each sample. Those boxes used in this study were 3 inch by 2 inch sample boxes.
2. Fill the sample boxes with equal amounts of washed and oven dried, 1/2 inch and 3/8 inch aggregate.

3. Pour clear modeling resin over aggregates to fill empty space and bond the aggregates together for cutting. Allow to dry according to instructions for the resin.
4. Using a suitable rock saw, cut the base from the boxes to provide a smooth surface for thin section preparation.
5. Polish the bottom surface on a rotating polishing wheel so that it is flat and will evenly adhere to a glass slide.
6. Mount the aggregate box to a glass slide and prepare as a normal thin section.

#### **Insoluble Residue Grain Size Separations**

1. Dry insoluble residue sample or a fraction thereof in oven at approximately 150° F overnight.
2. Weigh samples to the nearest .05 gram and record the weights as the original weight.
3. Place sample into large jar or bottle that can be tightly sealed. To the sample add approximately 1-2 grams of Calgon (commercial soap containing sodium hexametaphosphate) and approximately 100-150 ml of water.
4. Agitate bottle or jar by hand or using a mechanical shaker for a minimum of 5 minutes.
5. Wash the residue through stacked sieves of 500 microns, 250 microns, 125 microns and 63 microns to achieve grain size separations.
6. Place the sieves with the residues into an oven at approximately 125° F for 10-15 minutes.
7. Carefully remove all residues from each sieve being as quantitative as possible and weigh. Record each weight as a mass retained on each sieve. For example: Retained on 125 micron sieve = 1.25 grams.

8. Total the masses retained on each sieve. The difference between the original mass and the total of each fraction is the portion of the sample finer than 63 microns (finer than silt-sized sediment).

Lab. #/Sample #	Durability Factor	Modified Freeze/Thaw	Absorption %	Expansion %	LA Wear	% AIR
97-3685/KU-1	NC	81	3.53	0.14	30	11.22
97-3686/KU-2	94	95	2.78	0.02	29	4.22
97-3687/KU-3	97	87	3.76	0.013	41	13.32
97-3688/KU-4	98	94	1.58	0.013	24	9.22
97-3689/KU-5	99	91	2.08	0.011	29	3.72
97-3690/KU-6	96	94	1.53	0.015	28	2.32
97-3858/KU-7	96	77	2.18	0.013	27	8.87
97-4058/KU-8	97	94	3.76	0.015	34	5.37
97-4059/KU-9	99	93	2.47	0.005	31	3.02
97-4060/KU-10	82	94	2.04	0.064	25	6.47

**Table A2.1.** Results of KDOT physical testing for samples KU-1-10. See Appendix 2 for procedures and calculations. (% AIR = Percent Acid-Insoluble Residue; NC = Not Calculated)

Lab. #/Sample #	Durability Factor	Modified Freeze/Thaw	Absorption %	Expansion %	LA Wear	% AIR
95-0634/KDOT-1	98	95	1.18	0.007	24	3.10
95-634-P/KDOT-2	94	92	1.87	0.014	NC	5.30
93-4579/KDOT-3	78	87	1.69	0.05	27	2.89
93-4579/KDOT-4	86	87	1.52	0.038	24	2.59
94-0607/KDOT-5	82	90	3.72	0.048	41	14.69
94-0607/KDOT-6	80	97	4.67	0.076	35	2.75
94-2268/KDOT-7	99	96	1.67	0.005	23	1.06
94-2268/KDOT-8	99	97	2.16	0.004	28	1.60
94-2268/KDOT-9	98	95	1.90	0.014	29	9.99
94-2268/KDOT-10	94	94	1.20	0.026	25	3.64
94-2268/KDOT-11	NC	81	3.26	NC	31	8.70
93-4579/KDOT-12	NC	84	2.76	NC	30	7.91
95-634-P/KDOT-13	NC	75	3.73	NC	NC	9.48
81-0083/KDOT-14	33	89	2.76	0.122	NC	8.47
81-0083/KDOT-15	51	93	2.82	0.147	NC	7.85
81-0083/KDOT-16	94	92	2.44	0.031	NC	1.53
81-0083/KDOT-17	94	98	2.97	0.017	NC	2.86
97-2114/KDOT-18	96	92	1.39	0.025	25	1.64
97-2114/KDOT-19	94	96	1.71	0.022	27	3.54
97-2114/KDOT-20	NC	83	1.99	NC	28	1.84

**Table A2.2.** Results of KDOT physical testing for samples KDOT-1-20. See Appendix 2 for procedures and calculations. (% AIR = Percent Acid-Insoluble Residue; NC = Not Calculated)



Lab. #/Sample #	% > 5 mm	% .25 - .5 mm	% .12 - .25 mm	% .06 - .12 mm	% < .06 mm
97-3685/KU-1	3.33	3.80	4.51	2.38	85.99
97-3686/KU-2	0	6.38	5.11	4.26	84.25
97-3687/KU-3	0.50	1.06	17.02	32.98	48.4
97-3688/KU-4	0	0	4.4	15.38	80.22
97-3689/KU-5	0	0	4	14.4	81.6
97-3690/KU-6	0	0	9.09	6.06	84.85
97-3858/KU-7	0	0	3.26	6.09	90.65
97-4058/KU-8	8.33	6.25	4.16	9.17	72.08
97-4059/KU-9	0	0	0	0	100
97-4060/KU-10	0	0	0	10.32	89.68

**Table A2.3.** Grain-size distributions for insoluble residues of samples KU-1-10. Data is given as a percentage of the total residue that is composed of 5 grain size categories.

Lab. #/Sample #	Bulk Spar %	Avg. Crystal Size	Total Agg. Spar %
97-3685/KU-1	10.00	70	25
97-3686/KU-2	25.00	400	30
97-3687/KU-3	5.00	75	50
97-3688/KU-4	10.00	100	80
97-3689/KU-5	30.00	200	40
97-3690/KU-6	50.00	150	60
97-3858/KU-7	15.00	50	50
97-4058/KU-8	15.00	75	25
97-4059/KU-9	25.00	150	60
97-4060/KU-10	15.00	75	30
95-0634/KDOT-1	25.00	400	
95-634-P/KDOT-2	20.00	250	
93-4579/KDOT-3	20.00	250	
93-4579/KDOT-4	50.00	400	
94-0607/KDOT-5	15.00	75	
94-0607/KDOT-6	30.00	200	
94-2268/KDOT-7	25.00	150	
94-2268/KDOT-8	25.00	150	
94-2268/KDOT-9	25.00	75	
94-2268/KDOT-10	20.00	150	
94-2268/KDOT-11	15.00	75	
93-4579/KDOT-12	5.00	100	
95-634-P/KDOT-13	20.00	75	
81-0083/KDOT-14	15.00	100	
81-0083/KDOT-15	15.00	100	
81-0083/KDOT-16	30.00	200	
81-0083/KDOT-17	20.00	200	
97-2114/KDOT-18	30.00	400	
97-2114/KDOT-19	30.00	400	
97-2114/KDOT-20	30.00	250	

**Table A2.4.** Data concerning bulk spar percentage, average spar crystal size and aggregate spar percentage. See Chapter 3 for a definition of each category.

Lab. #/Sample #	Clay %	Dif./Diss. Clay %
97-3685/KU-1	75.00	65
97-3686/KU-2	55.00	50
97-3687/KU-3	2.00	2
97-3688/KU-4	2.00	2
97-3689/KU-5	15.00	5
97-3690/KU-6	5.00	3
97-3858/KU-7	2.00	2
97-4058/KU-8	15.00	5
97-4059/KU-9	5.00	3
97-4060/KU-10	60.00	60
95-0634/KDOT-1	40.00	40
95-634-P/KDOT-2	45.00	30
93-4579/KDOT-3	55.00	40
93-4579/KDOT-4	5.00	5
94-0607/KDOT-5	2.00	15
94-0607/KDOT-6	15.00	5
94-2268/KDOT-7	5.00	3
94-2268/KDOT-8	5.00	3
94-2268/KDOT-9	5.00	50
94-2268/KDOT-10	10.00	15
94-2268/KDOT-11	15.00	5
93-4579/KDOT-12	2.00	2
95-634-P/KDOT-13	60.00	55
81-0083/KDOT-14	100.00	100
81-0083/KDOT-15	75.00	100
81-0083/KDOT-16	10.00	40
81-0083/KDOT-17	10.00	10
97-2114/KDOT-18	15.00	3
97-2114/KDOT-19	15.00	3
97-2114/KDOT-20	15.00	30


**Table A2.5.** Data regarding total percentage of clay-rich strata (Total Clay %) and percentage of strata that contains diffuse and disseminated clay (Dif./Dissem. Clay %).

# K - TRAN

KANSAS TRANSPORTATION RESEARCH  
AND  
NEW - DEVELOPMENTS PROGRAM



A COOPERATIVE TRANSPORTATION RESEARCH PROGRAM BETWEEN:

KANSAS DEPARTMENT OF TRANSPORTATION 

THE KANSAS STATE UNIVERSITY 

THE UNIVERSITY OF KANSAS 